

Remote Sensing of Grassland Variables Across Seasons and Using Multiple Spectral Devices

Craig Michael Pearce MEdSci

**This thesis is submitted for the degree of Doctor
of Philosophy**

August 2023

Lancaster Environment Centre

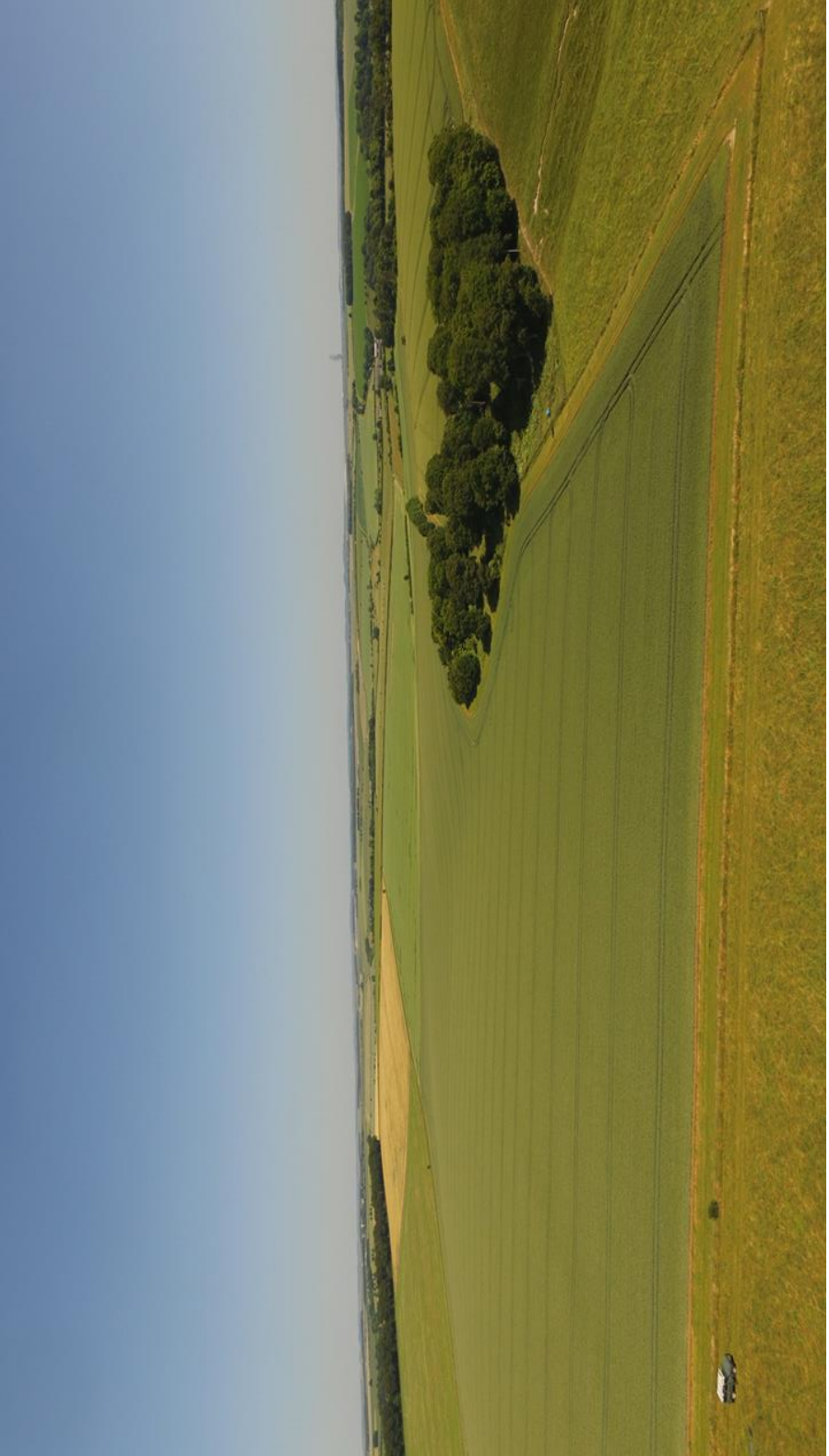
Graduate School of the Environment



**UK Centre for
Ecology & Hydrology**



**ROTHAMSTED
RESEARCH**



“Success is the ability to go from one failure to another without loss of enthusiasm.”

Winston Churchill

Declaration

This thesis has not been submitted in support of an application for another degree at this or any other university. It is the result of my own work and includes nothing that is the outcome of work done in collaboration except where indicated. Many of the ideas in this thesis were the product of discussions with my supervisory team and other collaborators; Dr. France Gerard, Prof. Alan Blackburn, Mr. Charles George, Prof. Paul Harris, Dr. Douglas Kelley, and Dr. Simon Smart.

Craig Pearce MEdSci (Hons)

Lancaster University, UK

Acknowledgements

Firstly, thanks goes to all of my supervisors for the practical support, insight and exchange of ideas over the course of the PhD. I am indebted to Charles George for his practical and moral support, especially during some character-building fieldwork campaigns. Thanks also goes to everyone at UKCEH who supported me including all of the senior scientists, support staff and people in the CCS team who are too many to mention in person here. I also want to thank everyone at Natural England who supported us, especially Colin Newlands and Simon Hope for their warm welcome and for the fascinating insights into their work. I hope this work will prove beneficial to Natural England in the future.

I have been lucky to have met many amazing people at UKCEH. Particularly my office buddies Doug Kelley and Emma Barton for enriching my PhD experience by being good friends and mentors, and being there whether times were good or tough. I am indebted to Helen Cunnold who was always there to help during difficult times. It has also been great to have met many other PhD students, too many to acknowledge personally. I will particularly miss our mass gatherings at pubs, restaurants and house parties.

I have also been lucky to have worked with great people since. Particular thanks goes to Trevor Thomas for being a great friend and mentor, and for having faith in me to have the ability to support your amazing research. I would also like to thank Jean-Charles Gordon for giving me the opportunity to work within an amazing team doing exciting work.

I would finally like to thank my family and close friends for being there. I would like to thank Vince Sin and Curtis Thorpe in particular for their valued friendship. Hopefully we will go on more adventures with the rest of the team again soon. I am especially grateful to Mark Searle, it is strange to think that so many amazing things that have happened over the last ten years can be linked to one conversation we had whilst dog walking. You were there at a time when few others were and you had belief when few others did, I will always be grateful to you.

Abstract

In the UK, the regeneration and conservation of semi-natural grasslands is important, especially for grasslands protected by legislation such as UK Biodiversity Action Plan (BAP) priority habitats or Sites of Special Scientific Interest (SSSIs). As such, monitoring grassland condition is necessary, but conventional methods of measuring grassland condition are time consuming and limited in their spatial coverage. This thesis tested if remote sensing can provide a more cost- and time-effective solution to measuring grassland condition as defined by the Common Standards Monitoring (CSM).

A field spectroscopy experiment was designed to explore the potential link between grassland spectral reflectance, plus a metric representing a traditional measure of grassland condition referred to as CSM-condition. Partial least squares regressions were used to evaluate the relationship between grassland multi-spectral reflectance and a range of condition-related grassland variables; between the condition related grassland variables and CSM-condition and between the grassland multi-spectral reflectance and CSM-condition. The evaluation tested the relationships across grassland types, seasons and spectral devices used; and between grassland variable observations made in terms of mass or % cover.

When analysing data collected at patch level during the summer; the mass of bryophytes, dead material and graminoids plus the % cover of forbs can be predicted to a moderate level of accuracy (R^2 values of >0.5 and $nRMSE <100$) when analysing data from all seven grasslands. When analysing data from all Parsonage Down NNR grasslands; the mass of bryophytes, the % cover of live material, % cover-based live:dead ratio and CSM-condition could be predicted to a high level of accuracy (R^2 values of >0.7 and $nRMSE <100$). Moisture content plus the % cover of dead material, forbs and gram:forb ratio were all predicted to a moderate level of accuracy as well as CSM-condition predicted by grassland variable values. When using data from all Ingleborough NNR grasslands; the % cover of forbs and biomass plus the mass of bryophytes, dead material and live material could be predicted to a moderate level of accuracy. When using patch level data collected across three seasons; the % cover of dead material, live material and live:dead ratio plus the mass of graminoids could be predicted when using three seasons of data collected on one grassland, or for all three Parsonage grasslands, to at least a moderate level of accuracy although

some models trained with % cover data had a high accuracy. Forbs (mass and % cover) plus the mass of gram:forb ratio, live material and live:dead ratio could be predicted to at least a moderate level of accuracy for some grasslands.

When using data from all grasslands collected in one season the mass of a range of grassland variables could be predicted to a moderate level of accuracy for the spring and autumn months but not when using % cover data. Using CROPSCAN and SVC data produced similar results, with slightly stronger results from the CROPSCAN, but using data from the Rikola camera produced weaker results. When the results of trained PLSR models were extrapolated to field level, the projected predicted grassland variable values from models trained with CROPSCAN MSR 16R data looked promising but the results have not been externally validated using a separate data set. The most important spectral bands for predicting grassland variables and CSM-condition were NIR and SWIR with the red edge (647nm) and 470nm also having some importance. The most important grassland variables for predicting CSM-condition were depended on whether the grassland variable was mass-based or % cover-based. When using mass data; graminoid:forb ratio mass and live:dead ratio mass were consistently important. When using % cover data; forbs cover, graminoids cover and live:dead ratio cover were consistently important.

Overall, the results suggest that some of the condition-related variables considered in this thesis are predicted with reasonable accuracy and precision at patch level (i.e. R^2 values of >0.5 and $nRMSE <100$), but producing reliable results requires a sufficient quantity of data to train the statistical models (at least 30 quadrats of samples), particularly if the results are to be extrapolated to field level as additional data are required for the external validation of the results. Grassland variable prediction success varied with number of sites considered and with season with no clear consistent pattern. Also, none of the grassland variables could be consistently predicted strongly across all the different grasslands or seasons.

This has implications for any land manager who wishes to emulate the methods in this thesis. The results suggest that this thesis provides a more cost- and time-effective solution for capturing grassland condition; but anyone emulating these methods would have to carefully choose the variables, grassland types and seasons to collect data and would have to collect a sufficient quantity of data for model training, testing and evaluation. A consequence of adopting, or refining, the approach in this thesis could be more effective monitoring (and therefore timely intervention where necessary) of UK Biodiversity Action Plan (BAP) priority habitats and Sites of

Special Scientific Interest (SSSIs). Refining this approach could include testing different modelling approaches and focusing further work on the successful aspects of this research such as key grassland and wavelength variables.

1 Table of contents

2	Declaration	iii
3	Acknowledgements	iv
4	Abstract	v
5	Table of contents	viii
6	List of tables	xii
7	List of figures	xiii
8	Abbreviations, Acronyms and Notations	xviii
9	Chapter 1 - Introduction	1
10	1.1. Background	1
11	1.2. Research aims.....	2
12	1.3. Thesis structure	3
13	Chapter 2 - Literature Review	5
14	2.1. The conventional approach to measuring grassland condition <i>in situ</i>	5
15	2.2. Remote sensing platforms used in grassland condition studies	9
16	2.2.1. Field radiometry (hand-held spectral devices)	13
17	2.2.2. Uncrewed Aerial Vehicles (UAV) and crewed aircraft remote sensing.....	13
18	2.2.3. Satellite remote sensing	15
19	2.3. Remote sensing approaches for grassland condition-related variables.....	18
20	2.3.1. Biomass, height and % vegetation cover.....	20
21	2.3.2. Leaf area index (LAI), plant area index (PAI) and green area index (GAI) ...	22
22	2.3.3. Fraction of absorbed photosynthetically active radiation (FAPAR).....	25
23	2.3.4. Normalised difference vegetation index (NDVI)	26
24	2.3.5. Specific leaf area (SLA).....	28
25	2.3.6. Leaf dry matter content (LDMC)	29
26	2.3.7. Leaf water content (LWC)	31
27	2.3.8. Dead matter and % bare ground cover.....	32
28	2.3.9. Species richness, indicator species and invasive species	34
29	2.3.10. Biochemical variables.....	35
30	2.4. Summary and conclusions.....	36
31	Chapter 3 – Methods	38
32	3.1. Definition of grasslands and UK grasslands.....	38
33	3.2. Study sites	39
34	3.3. Data collection	45

35	3.3.1. Fieldwork plan and sampling strategy	47
36	3.3.2. Quadrat sampling	48
37	3.3.3. Grassland reflectance	52
38	3.3.3.1. Spectral devices	52
39	3.3.3.2. Spectral data collection.....	54
40	3.4. Data pre-processing	57
41	3.4.1. Grassland condition: converting a qualitative measure into a quantitative	
42	gradient.....	57
43	3.4.2. Processing response data before model training.....	60
44	3.4.2.1. Test for normality	60
45	3.4.2.2. Transformation of response variables	61
46	3.4.3. Grassland reflectance	62
47	3.4.3.1. CROPSCAN data processing	62
48	3.4.3.2. ASD data processing	63
49	3.4.3.3. SVC data processing	63
50	3.4.3.4. Rikola VNIR imagery processing	64
51	3.4.3.5 Scaling of reflectance data.....	66
52	3.5. Analytical methods.....	66
53	3.5.1. Testing for significant difference of grassland variables between grassland	
54	sites	67
55	3.5.2. Partial least squares regression	69
56	3.5.2.1. Variable Importance in Projection	74
57	3.5.2.2. Model fit and validation	74
58	3.5.2.3. Confidence intervals (CIs).....	76
59	3.5.2.4. Coefficient of variation	76
60	3.6. Summary of the main chapters	77
61	3.6.1. Varying sample information within and across sites	79
62	3.7. Summary of the methods.....	79
63	Chapter 4 - Assessing the condition of semi-natural grasslands using CROPSCAN	
64	field radiometry at patch level (1m ²).....	81
65	4.1. Predictor correlation matrices.....	81
66	4.2. Grassland site characteristics.....	85
67	4.3. Predicting grassland variables and condition using PLSR.....	87
68	4.4. Stability and consistency between model runs using the same response	
69	variable	94
70	4.5. VIP analysis for spectral band and grassland variable selection.....	95

71	4.6. Comparison of PLSR models trained with actual data and PLSR models	
72	trained with random data.....	102
73	Chapter 5 - Assessing seasonal effects on the condition of calcareous semi-natural	
74	grasslands using CROPSCAN field radiometry at patch level (1m ²)	107
75	5.1. Grassland site characteristics.....	107
76	5.2. Predicting grassland variables and CSM-condition using PLSR.....	110
77	5.2.1. Mass-based grassland variable data	110
78	5.2.2. Cover-based grassland variable data.....	115
79	5.2.3. Predicting CSM-condition with spectral data or grassland variables	119
80	5.3. Stability and consistency between model runs using the same response	
81	variable	119
82	5.4. VIP analysis for spectral band and grassland variable selection.....	121
83	5.4.1. Mass and cover data	121
84	5.4.2. Grassland variables predicting condition.....	128
85	5.5. Comparison of PLSR models trained with actual data and PLSR models	
86	trained with random data.....	130
87	Chapter 6 - Comparison of patch level (1m ²) spectral data from different devices and	
88	an assessment using field level (200x1m) CROPSCAN data when predicting	
89	condition-related grassland variables on calcareous semi-natural grasslands	135
90	6.1. Grassland site characteristics.....	135
91	6.2. Predicting grassland variables and condition using PLSR.....	137
92	6.2.1. Predicting mass-based grassland variable data.....	137
93	6.2.2. Predicting cover-based grassland variable data.....	137
94	6.2.3. Predicting CSM-condition using grassland variables.....	138
95	6.3. Comparing observed and predicted values	141
96	6.4. Extrapolating predicted grassland variables and condition using CROPSCAN	
97	data as predictors	141
98	6.5. Stability and consistency between model runs using the same response	
99	variable	150
100	6.6. VIP analysis for spectral band selection	152
101	6.7. Comparison of PLSR models trained with actual data and PLSR models	
102	trained with random data.....	155
103	Chapter 7 – Discussion.....	158
104	7.1. Effectiveness of using PLSR in a RS of grassland condition study	158
105	7.2. The use of mass- or cover-based variables for condition assessment	160
106	7.3. Predicting grassland variables and CSM-condition	163
107	7.3.1. Predicting grassland variables and CSM-condition using spectral data as	
108	predictors	163

109	7.3.2. Predicting CSM-condition using grassland variables	170
110	7.4. Extrapolating predicted grassland variables.....	171
111	7.5. Choice of spectral bands	175
112	7.6. Practical implications of RS condition monitoring of grasslands	178
113	7.7. Study limitations	181
114	7.8. Potential research opportunities.....	183
115	Chapter 8 - Conclusion.....	185
116	References and Bibliography.....	188
117	Appendix	210
118	Correlation matrices	210
119	Chapter 4 full results	216
120	Chapter 5 full results	220
121	Chapter 6 full results	226
122	Observations vs. predictions – Chapter 4.....	229
123	Observations vs. predictions – Chapter 5.....	233
124	Observations vs. predictions – Chapter 6.....	238
125	Extrapolating predicted grassland variables and condition using Rikola data as	
126	predictors	243
127		
128		
129		
130		
131		
132		
133		
134		
135		
136		
137		
138		
139		

140 List of tables

141 Table 2.1: Overview of widely available RS platforms.

142 Table 2.2: Specifies the number of papers discussed in Section 2.3 (with total number
143 of references for each section in parentheses) and also some characteristics of those
144 papers, such as which RS platforms were used and whether the metric in question
145 was used as a predictor or response in models. Note that multiple spectral devices
146 are often used in RS studies, in particular data from at least one hand-held device
147 and at least one airborne device (UAV, aircraft or satellite). Also note that some
148 studies used a metric as a response variable and as a predictor of other metrics.

149 Table 3.1: The environmental characteristics of the two locations chosen for data
150 collection ascertained using information provided by Natural England and by
151 conducting a desk study (BGS UKSO, 2017; Edina®, 2017).

152 Table 3.2: The characteristics of the seven study sites using information provided by
153 Natural England or gained from the desk study (BGS UKSO, 2017; Edina®, 2017).
154 The NVC for each grassland was ascertained by entering species abundance data
155 into MAVIS software (Smart et al., 2016).

156 Table 3.3: Variables used in this study, listing whether mass and/or % cover data
157 were used to establish them and at which NNR locations they were collected. In the
158 context of this thesis, moisture content refers to leaf wet mass - leaf dry mass).

159 Table 3.4: Summary of multispectral and hyperspectral devices used in the field.

160 Table 3.5: Provides information related to how the NVC of each quadrat (and
161 therefore each grassland) was determined. This includes the alphanumerical
162 identification code of the criteria that was applied, criteria within that classification that
163 were applied, and criteria that it was not possible to apply because of a lack of data.

164 Table 3.6: Summarises some of the characteristics of the data sets used in the main
165 chapters of this thesis. This includes where data were collected, which season, which
166 spectral devices were used and the scale of the data collection.

167

168

169 **List of figures**

170 Figure 1.1: Schematic of the attributes of each of the main chapters of this thesis,
171 highlighting how each of the chapters are different from each other.

172 Figure 2.1: Conventional grassland data being collected on a quadrat at Over Pasture
173 (Ingleborough NNR).

174 Figure 2.2: A Matrice 600 UAV being prepared for launch at Scar Close Moss at
175 Ingleborough NNR.

176 Figure 2.3: Grasslands representing a gradient of structural heterogeneity from
177 simple to complex: a) monoculture grassland, b) semi-improved grassland (Top Cow
178 Pasture, Ingleborough NNR), c) semi-improved calcareous grassland (100 Acre,
179 Parsonage NNR), d) semi-natural calcareous grassland (Castle Down, Parsonage
180 NNR), e) semi-natural limestone pavement grassland (Scar Close Moss,
181 Ingleborough NNR), f) semi-natural acid mire grassland (Scar Close Moss,
182 Ingleborough NNR).

183 Figure 3.1 The boundaries and locations of transects 1 to 3 at Parsonage Down
184 NNR. Note that data were collected at this location across three seasons.

185 Figure 3.2: Site boundaries and locations of transects for Grasslands 4 to 7 at
186 Ingleborough NNR.

187 Figure 3.3: Schematic showing the sampling strategy for data collection (using Castle
188 Down as an example). The yellow line represents the 200m transect and the dark
189 blue squares represent the quadrats. The white squares represent the spatial
190 reference panels and the other grey and black squares represent calibration panels.
191 The green lines are the UAV flight path and the blue rectangle in the background
192 represents the area covered by the UAV-mounted Rikola camera.

193 Figure 3.4: An overhead view showing how each quadrat was sampled by destructive
194 sampling.

195 Figure 3.5: A grass sample separated into its constituent parts (clockwise from top-
196 left): dead material, graminoids, other, forbs and bryophytes.

197 Figure 3.6: An overhead view showing how each quadrat was sampled using two
198 hand-held spectrometers (blue = CROPSCAN, red = SVC/ASD).

199 Figure 3.7: Schematic of overarching approach used to establish if remote sensing
200 can be used to determine grassland condition and to identify which spectral bands
201 and which grassland variables are particularly suited for condition monitoring using
202 remote sensing.

203 Figure 3.8: Schematic showing the partial least squares regression (PLSR) approach
204 developed to establish if spectral data can be used to determine grassland condition
205 (A) and to identify which spectral bands (B) and which grassland variables (C) are
206 particularly suited for condition monitoring using spectral remote sensing. R^2 ,
207 normalised root mean square error (nRMSE) and variable importance in projection
208 (VIP) are used to evaluate and compare model performance.

209 Figure 4.1: Correlation matrices between predictors used in PLSR modelling a)
210 spectral bands from CROPSCAN, b) spectral bands from Rikola VNIR camera, c)
211 mass data, d) % cover data where $n = 30$ (data from Parsonage grasslands).
212 Correlation coefficients that are not statistically significant ($\alpha \geq 0.05$) are
213 blanked out.

214 Figure 4.2: Boxplots of grassland variables (mass in g and cover in %) for the seven
215 grassland sites. The boxplot colours summarise the unpaired two-sample Wilcoxon
216 test results between grassland types: A grassland variable was considered
217 significantly different between two grasslands if $p < 0.05$; the boxplot of each grassland
218 site is coloured according to the number of sites from which it is significantly
219 different.

220 Figure 4.3: Absolute numbers of quadrats of each level of condition per grassland
221 according to the UKCSM criteria and grassland NVC classifications for each of the
222 seven grassland sites. Sites 1 to 3 are for Parsonage Down NNR (names in green)
223 and Sites 4 to 7 are for Ingleborough NNR (names in red). Good condition means
224 that $>80\%$ UKCSM criteria are met, intermediate is 60-80% of criteria met and bad is
225 $<60\%$ criteria met.

226 Figure 4.4: Plots for results of 426 PLSR regressions, each of which represent the
227 median R^2 and nRMSE values of 1000 model runs, where (i) spectral data (either
228 FULL or VNIR) were used to predict grassland variables (coloured dots) and CSM
229 based condition (black dot) and (ii) grassland variables were used to predict CSM

230 based condition (white dot). Panels a and b show results for mass based analysis; c
231 and d for % cover based analysis.

232 Figure 4.5: % coefficient of variation (CV) plots for the R^2 and nRMSE results of the
233 site specific PLSR models grouped per treatment (% cover - left; mass - right) and
234 spectral input data (full spectrum - top; VNIR - bottom).

235 Figure 4.6: VIP plots showing which combinations of spectral bands (predictors) and
236 which responses (grassland variables on x axis and CSM-condition on y axis) are
237 most important in the PLSR models trained in this study.

238 Figure 4.7: VIP plot showing which grassland variables are most important in
239 predicting CSM-condition using either mass or % cover data from analysing
240 grasslands individually or collectively for one or both locations.

241 Figure 4.8: Comparison of the median values of iterated model runs using actual
242 response data and 44 or 999 model runs (dependent on whether grasslands were
243 analysed individually or collectively) using randomised response data. The plot shows
244 the ranking of the actual model out of the maximum iterated runs (either 45 for
245 individual grasslands or 1000 for collective grasslands), where high rankings (e.g.
246 >950 for the 95% level) are sought.

247 Figure 5.1: Boxplots of the mass or % cover values of grassland variables for the
248 three grassland sites. The boxplot colours summarise the unpaired two-sample
249 Wilcoxon test results between grassland types and seasons: a grassland variable
250 was considered significantly different between two grasslands if $p < 0.05$; the boxplot
251 of each grassland site is coloured according to the number of different site-season
252 combinations from which it is significantly different.

253 Figure 5.2: Median results of iterated model runs where spectral data were used to
254 predict CSM-condition and mass-based grassland variables for each of the three
255 seasons ($n = 10$ or 30) and for all seasons ($n = 30$ or 90). Also included are the
256 results of predicting CSM-condition using grassland variables as predictors.

257 Figure 5.3: Median results of iterated model runs where spectral data were used to
258 predict CSM-condition and cover-based grassland variables for each of the three
259 seasons ($n = 10$ or 30) and for all seasons ($n = 30$ or 90). Also included are the
260 results of predicting CSM-condition with grassland variables data.

261 Figure 5.4: % coefficient of variance (CV) for the R^2 and nRMSE results of the site
262 specific PLSR models grouped per treatment and spectral input data.

263 Figure 5.5: VIP plots showing which combinations of spectral bands (predictors) and
264 which responses (grassland variables on x axis and CSM-condition on y axis) are
265 most important in the study PLSR models where a) PLSR models trained with FULL
266 spectral data and mass-based variables and b) PLSR models trained with VNIR
267 spectral data and mass-based variables.

268 Figure 5.6: VIP plots showing which combinations of spectral bands (predictors) and
269 which responses (grassland variables on x axis and CSM-condition on y axis) are
270 most important in the study PLSR models where a) PLSR models trained with FULL
271 spectral data and cover-based variables and b) PLSR models trained with VNIR
272 spectral data and cover-based variables.

273 Figure 5.7: VIP plot showing which grassland variables are most important in
274 predicting CSM-condition using either mass- or cover-based grassland variables from
275 analysing grasslands individually or collectively or for one or all seasons.

276 Figure 5.8: Rankings of the median values of iterated model runs using actual mass
277 response data and also iterated model runs using randomised response data, where
278 rankings >95% level are considered significant for the actual model fit.

279 Figure 5.9: Rankings of the median values of iterated model runs using actual %
280 cover response data and iterated model runs using randomised response data,
281 where rankings >95% are considered consistently superior to randomised models.

282 Figure 6.1: Boxplots of the grassland variable values for the three grassland sites.
283 The boxplot colours summarise the unpaired two-sample Wilcoxon test results
284 between grassland types where the colour represents the number of sites from which
285 each grassland variable is significantly different ($p < 0.05$).

286 Figure 6.2: Median results of iterated model runs where spectral data from three
287 different devices were used to predict CSM-condition and mass-based grassland
288 variables for all grasslands collectively ($n = 30$) or single sites ($n = 10$).

289 Figure 6.3: Median results of iterated model runs where spectral data from three
290 different devices were used to predict CSM-condition and cover-based grassland
291 variables for all grasslands collectively ($n = 30$) or single sites ($n = 10$).

292 Figure 6.4(a-g): Projections of predicted grassland variable values derived from
293 PLSR models trained with CROPSCAN spectral data.

294 Figure 6.5: % coefficient of variation (CV) for the R^2 and nRMSE results of the site
295 specific PLSR models grouped per treatment and spectral input data from different
296 spectral devices.

297 Figure 6.6: VIP plots showing which regions of spectral data from three different
298 devices and which responses (grassland variables on x axis and CSM-condition on y
299 axis) are most important in the study PLSR models where mass-based grassland
300 variables are used as response data.

301 Figure 6.7: VIP plots showing which regions of spectral data from three different
302 devices and which responses (grassland variables on x axis and CSM-condition on y
303 axis) are most important in the study PLSRs where % cover-based grassland
304 variables are used as response data.

305 Figure 6.8: Rankings of the median values of the iterated model runs using actual
306 mass response data and 999 model runs using randomised mass response data,
307 where rankings >95% are considered significant for the actual model fit.

308 Figure 6.9: Rankings of the median values of the iterated model runs using actual %
309 cover response data and iterated model runs using randomised % cover response
310 data, where rankings >95% are considered significant for the actual model fit.

311

312

313

314

315

316 **Abbreviations, Acronyms and**

317 **Notations**

318 ASD - Analytical Spectral Device

319 BAP - Biodiversity Action Plan

320 CSM – Common Standards Monitoring

321 CV - Coefficient of variation

322 EM - Electromagnetic spectrum

323 ENVI - Environmental Visualisation software

324 ES – Ecosystem service(s)

325 EVI - Enhanced vegetation index

326 EWT – Equivalent water thickness

327 FAPAR - Fraction of absorbed photosynthetically active radiation

328 FOV - Field of view

329 GAI – Green area index

330 JNCC - Joint Nature Conservation Committee

331 LAI - Leaf area index

332 LDMC – Leaf dry matter content

333 LWC - Leaf water content (%)

334 MODIS - Moderate Resolution Imaging Spectroradiometer

335 NDVI – Normalised difference vegetation index

336 NDWI – Normalised difference water index

- 337 NIR - Near infrared spectral domain (701-1400nm)
- 338 NNR - National Nature Reserve
- 339 nm - Nanometre
- 340 nRMSE - Normalised root mean square error
- 341 NVC - National Vegetation Classification
- 342 OLS - Ordinary Least Squares Regression
- 343 PCA - Principal component analysis
- 344 PAI – Plant area index
- 345 PLSR - Partial least squares regression
- 346 RE - Red edge spectral region (650-810nm)
- 347 RMSE - Root mean square error
- 348 RS - Remote sensing
- 349 SLA – Specific leaf area
- 350 SPOT - *Satellite Pour l'Observation de la Terre*
- 351 SSSI - Site of Special Scientific Interest
- 352 SVC - Spectra Vista Corporation
- 353 SWIR - Shortwave infrared spectral domain (1401-2500nm)
- 354 VIP - Variable importance of prediction
- 355 VIs - Vegetation indices
- 356 VIS - Visible spectral region (390-700nm)
- 357 VNIR - Visible to near infrared regions of the electromagnetic spectrum
- 358 VSWIR - Visible to shortwave infrared regions of the electromagnetic spectrum

359 Chapter 1 - Introduction

360 1.1. Background

361 A report by the Food and Agricultural Organisation highlights the global extent of
362 grasslands and their socio-economic importance. For example, an estimated one
363 billion people depend on livestock as a source of income and food including
364 approximately 70% of the world's rural poor (Neely et al., 2009). Despite their
365 importance; grasslands face encroachment, degradation and fragmentation due to
366 increasing population, urbanisation and industrial development (Reid et al., 2005).
367 Grasslands are also subject to degradation or loss through overgrazing, intensive
368 management practices and climate change (Ali et al., 2016; Bullock et al., 2011;
369 Möckel et al., 2014; Neely et al., 2009). Grassland degradation results in reduced
370 ecosystem services, increased carbon emissions, increased soil erosion, increased
371 fertiliser use, increased likelihood of eutrophication of adjacent water bodies and
372 biodiversity loss (Bullock et al., 2011; Dusseux et al., 2014; Möckel et al., 2014; Neely
373 et al., 2009; Smith et al., 2009; Smith et al., 2016).

374 Although the loss in extent of semi-natural grasslands has slowed over the last ten
375 years in the UK, agricultural improvement since 1945 has resulted in the loss of
376 approximately 90% of semi-natural grasslands. This loss, primarily attributed to
377 agricultural improvement through arable crop planting or fertiliser use, has caused a
378 reduction in the wide range of ecological and recreational services that grasslands
379 offer. Relative to agriculturally improved land, the services that semi-natural
380 grasslands offer include reduced emissions of methane and nitrous oxide, improved
381 effectiveness as a carbon sink, improved water infiltration and storage plus improved
382 species richness with the ecosystem services that increased biodiversity offers. As
383 part of the effort to preserve these ecosystem services, 2% of UK grassland areas
384 were designated a Biodiversity Action Plan (BAP) priority habitat for their high
385 biodiversity (Bullock et al., 2011) which has since been encompassed in the UK Post-
386 2010 Biodiversity Framework (JNCC and DEFRA 2012).

387 For the purpose of facilitating grassland regeneration and conservation, this research
388 was conducted within the context of providing landowners with a framework (Xu and
389 Guo, 2015) to create spatial-temporal data analysis projections that provide cost- and

390 time-effective grassland condition information. Such a framework would provide
391 landowners with the means to identify impending land management issues and
392 facilitate effective intervention. In addition, improved condition monitoring is
393 considered particularly important in the UK, especially if predictions that farmlands
394 will need to be worked more intensely and/or sustainably in the future become reality
395 (Baulcombe et al., 2009; Garnett and Godfray, 2012; Godfray and Garnett, 2014;
396 Pywell et al., 2015). There are few studies that directly attempt to understand how the
397 remote sensing (RS) of grassland condition on semi-natural grasslands can be
398 achieved as they often focus on experimental and/or relatively structurally
399 homogeneous grasslands.

400

401 **1.2. Research aims**

402 The primary aim of this research is to assess the link between condition-related
403 grassland variables (including a metric referred to as CSM-condition, explained in
404 Section 3.4.1) with grassland spectral reflectance through field and drone spectro-
405 radiometry at a range of spatial-temporal scales. The focus of achieving this aim is on
406 grassland condition within the context of ecosystem services (ES) and on a range of
407 grassland types that exist within the UK. this thesis is focused on how RS techniques
408 could be deployed to address some of the limitations of establishing grassland
409 condition using traditional techniques by addressed the following questions:

- 410 1. Can grassland condition-related variables form the basis for RS-based
411 approaches to monitoring grassland condition? Which grassland variables are
412 the most suitable and are they suitable for all different types of grasslands?
- 413 2. Can grassland condition be determined accurately across seasons using
414 remote sensing techniques?
- 415 3. Is it possible to upscale models trained with field radiometry data from patch
416 level (1m^2) to field level using data collected with a CROPSCAN or a UAV?

417 Related to these are the following detailed questions:

- 418 4. Can PLSR models trained using spectral reflectance data predict grassland
419 variables or CSM-condition with an acceptable level of accuracy (i.e. $R^2 > 0.5$)

- 420 and nRMSE<100)? Can CSM-condition be predicted with an acceptable level
421 of accuracy using grassland variable data?
- 422 5. Will using mass or % cover of grassland variables impact on the relationship
423 between grassland variables and spectral reflectance?
- 424 6. Does utilising reflectance data recorded across a wider spectral range (i.e.
425 including SWIR spectral values), instead of across the visible and near-
426 infrared (NIR) spectrum, lead to more successful monitoring of grassland
427 condition using remote sensing?
- 428 7. Does the choice of radiometry instruments affect the relationship between
429 grassland variables and reflectance?
- 430 8. Which spectral reflectance bands are the strongest predictors of each
431 grassland variable including CSM-condition and which grassland variables are
432 the strongest predictors of CSM-condition?

433

434 **1.3. Thesis structure**

435 This thesis is presented according to the requirements to attain a PhD at Lancaster
436 University and consists of eight chapters. Chapter 1 (this chapter) introduces the
437 thesis, including the research context and research aims. Chapter 2 provides a
438 literature review that encompasses many approaches to establishing grassland
439 condition, both conventional and by using RS methods. Chapter 3 describes and
440 discusses the research methods. This includes a detailed description of sampling
441 strategy and the analytical processes applied to captured data sets.

442 There are three main chapters to this thesis which have been summarised in Figure
443 1.1, all of which explore particular aspects of the RS of grassland condition. Chapter
444 4 investigates the ability to predict condition-related grassland variables on seven
445 semi-natural grasslands; three grasslands at Parsonage Down NNR and four
446 grasslands at Ingleborough NNR using data collected in summer. This work directly
447 addresses issues around conducting RS studies of grassland condition on a range of
448 different types of structurally heterogeneous semi-natural grasslands. Chapter 5
449 investigates the relationship between reflectance and condition-related grassland

450 variables across the growing seasons, focussing on the three sites at Parsonage
 451 Down NNR. This work directly addresses questions regarding which time of the year
 452 is most effective for collecting data to calibrate a PLSR model that will have the most
 453 predictive power, or whether calibrating a PLSR with data from three seasons gives it
 454 more predictive power than using data collected from just one season. The results of
 455 Chapters 4 and 5 raised questions about the importance of different regions of the
 456 EM spectrum in predicting grassland variables. Chapter 6 investigates the value of
 457 SWIR data by comparing the predictive power of different PLSR models trained with
 458 reflectance spectra from three different spectral devices that collect spectral data in
 459 slightly different spectral regions, numbers of bands and spectral resolution. As this
 460 research would only be useful to landowners if results could be upscaled to field
 461 level, Chapter 6 also explores the ability of PLSR models trained with data collected
 462 at patch level (1m²) to predict grassland variable values at field level (200x1m).
 463 Chapter 7 discusses the results presented in the previous three chapters. Chapter 8
 464 concludes the thesis by providing key findings, potential future research plus
 465 considerations that should be taken when using the methods described in this thesis.

Chapter 4	Chapter 5		Chapter 6	Chapter 6
Assessing the condition of semi-natural grasslands using CROPSCAN field radiometry at patch level	Assessing seasonal effects on the condition of calcareous semi-natural grasslands using CROPSCAN field radiometry at patch level	Chapters	Comparison of patch level spectral data from different devices when predicting condition-related grassland variables on calcareous semi-natural grasslands	An assessment using field level (200x1m) CROPSCAN data when predicting condition-related grassland variables on calcareous semi-natural grasslands
Parsonage Down NNR Ingleborough NNR	Parsonage Down NNR	Field locations	Parsonage Down NNR	Parsonage Down NNR
Summer	Spring Summer Autumn	Seasons	Summer	Summer
CROPSCAN	CROPSCAN	Spectral devices	CROPSCAN SVC Rikola	CROPSCAN
1m ²	1m ²	Scale	1m ²	200x1m

466
 467 *Figure 1.1: Schematic of the attributes of each of the main chapters of this thesis,*
 468 *highlighting how the thesis chapters are different from each other.*

469 Chapter 2 - Literature Review

470 2.1. The conventional approach to measuring 471 grassland condition *in situ*

472 The term “grassland condition” has multiple interpretations, which will influence the
473 metrics used to define it. For land managers such as commercial farmers, grassland
474 condition may refer to grassland productivity, grass nutrient content or the number of
475 grazing animals that can be supported (Badgery et al., 2020; Bullock et al., 2011;
476 Marsett et al., 2006; Schils et al., 2013). A report by Schils et al. (2013) explains that
477 a range of destructive and non-destructive methods (including RS techniques) can be
478 used to quantify grassland productivity. Broadly speaking; conventional methods of
479 productivity measurements focusses on dry matter yield, grassland density or just
480 grassland height. Grassland productivity can also be indirectly quantified by
481 quantifying animal products or the number of grazing animals, e.g. by quantifying
482 fodder milk units or fodder units intensive beef production. Other studies may use
483 linked grassland variables such as biomass to estimate productivity. For example, Ni
484 (2004) used destructive sampling to estimate biomass and then used modelling
485 techniques to estimate net primary productivity (using biomass and other variables
486 such as climate) on a range of grasslands in northern China. Fliervoet (1987) used
487 grass cuttings to establish biomass and leaf area index on fifteen different grassland
488 types in Holland. These grasslands were then divided into four different levels of
489 productivity using data collected on leaf size and inclination in a principal components
490 analysis. Bai et al. (2001) used grass cuttings, ruler measurements of grass height, %
491 cover estimates of grassland variables and % cover estimates of species abundance
492 to quantify multiple grassland variables and then used these variables to examine the
493 relationship between biodiversity, productivity and herbivory. First, species biomass
494 data were used to quantify grassland condition where grassland condition refers to
495 productivity. Then, the link between condition and the height, mass and/or % cover of
496 the following grassland variables was assessed using canonical correspondence
497 analysis (CCA): biomass, live material, graminoids, forbs, bryophytes, dead material
498 and bare soil. One conclusion of the study was that an increase in quantity in all of
499 these variables except the bryophyte-based variables and bare soil was linked with
500 better grassland condition in relation to better productivity.

501 Other land managers, particularly those who have a legal obligation to protect or
502 improve the ecosystem services (ES) value of the grasslands that they manage, may
503 instead consider grassland condition from this perspective (Bullock et al., 2011).
504 Ecosystem services are broadly defined as a range of goods and services provided
505 by nature and these services can be categorised as provisioning services (e.g. food),
506 regulating services (e.g. flood control), cultural services (e.g. recreation) or supporting
507 services which refers to any services that supports the other three categories such as
508 nutrient cycling (Lamarque et al., 2011). Studies on ecosystem services usually focus
509 on a specific aspect of this broad remit (Plantureux et al., 2016). The main focal
510 points of these studies according to Rodríguez-Ortega et al. (2014) are gene pool
511 protection (including biodiversity), climate regulation (including carbon sequestration)
512 and also grassland aesthetic value (including cultural value). Zhao et al. (2020) stated
513 that carbon sequestration, preventing water erosion of the soil and above-ground
514 biomass (productivity) are the most frequently mentioned ecosystem services in the
515 380 papers and 32 book chapters that were reviewed but 33 different ecosystem
516 services were mentioned at least once.

517 Some authors linked different ecosystem services by showing that some ecosystem
518 services can have a positive impact on others, referred to as complementarity. Tilman
519 et al. (2006) conducted a decade-long study on experimental grasslands and found
520 that ecosystem stability (and therefore the provision of ecosystem services including
521 productivity) improved with increased biodiversity. Craven et al. (2016) conducted a
522 meta-analysis using data collected on 16 grasslands across North America and
523 Europe to assess whether more biodiverse grasslands are more resilient to the
524 negative effects of fertilisation and drought regarding their ecosystem service value.
525 This study was conducted in the context that greater biodiversity increases the
526 functioning of ecosystems. It was found that the positive effects of biodiversity on
527 above-ground productivity are robust to the effects of fertilisation and drought. Reich
528 et al. (2012), using two experimental grasslands for data collection including the
529 Cedar Creek experiment used by Tilman et al. (2006), found that the negative impact
530 of biodiversity loss on biomass and productivity becomes greater over time.

531 In the EU, some areas that provide ecosystem services such as biodiversity,
532 aesthetic or recreational value are chosen to become part of the Natura 2000 network
533 of conservation sites. This includes some types of grasslands which can be
534 designated as special areas of conservation (SACs) and as special protection areas
535 (SPAs) if threatened bird species inhabit them. For example, grasslands labelled as

536 "(6210) semi-natural dry grasslands and scrubland facies on calcareous substrates
537 (*Festuco-Brometalia*)" are a part of the Natura 2000 network because of their
538 relatively high plant biodiversity, their recreational value and also because of their
539 protected bird and Orchid species. Each classification of grassland has a system of
540 conservation and monitoring specific to it, which takes into consideration the biggest
541 threats to those grasslands. For example, some of the biggest threats to the
542 aforementioned *Festuco-Brometalia* grasslands are related to natural afforestation
543 and therefore a focal point of the overall strategy for monitoring and conservation is
544 the prevention of shrub species from succeeding over grass species. Monitoring of
545 these grasslands to ensure that the management strategy is working focuses on plant
546 species counts, although these species counts can be expanded to include insect
547 and bird species (Calaciura and Spinelli, 2008; Silva et al. 2008).

548 Within the context of ecosystem services in the UK, the conventional approach to
549 monitoring grassland condition is detailed in the Common Standards Monitoring
550 (CSM) guidance with National Vegetation Classification (NVC) standards being
551 provided for each classified grassland type. The NVC standards recommend
552 identifying grassland communities primarily using species abundance data and
553 information on environmental variables. CSM guidance discusses the use of a
554 number of generic primary and secondary attributes (or criteria), plus some criteria
555 specific to each NVC grassland type, as a means of establishing grassland condition.
556 Primary attributes refer to characteristics chosen for community identification whilst
557 secondary attributes relate to sward structure; height, litter and bare ground.
558 Secondary attributes are highly variable and easily reversible through cutting or
559 grazing and are therefore considered less reliable than primary attributes (JNCC,
560 2004; 2006).

561 The primary attributes consist of grass:herb ratio (a.k.a. graminoid:forb ratio),
562 grassland extent, positive and negative indicator species plus other indicators of local
563 distinctiveness such as transitional zonation and rare species. Diversity and
564 productivity are considered too time consuming to be regularly or effectively
565 monitored, hence indicator species are chosen as primary attributes (JNCC, 2004).
566 Noss (1990) warned that focusing on indicator species alone may prevent the
567 discovery of some environmental trends, which may explain why CSM guidance also
568 includes other criteria such as environmental variables. Grasslands that do not meet
569 the criteria specific to their NVC category are considered to be in unfavourable
570 condition (JNCC, 2004; 2006).

571 Although the studies discussed in this section generally did not use RS techniques,
572 they provide evidence that there is a link between some ecosystem services such as
573 biomass, productivity and biodiversity. A RS of grassland condition study still requires
574 some data gathering on condition-related grassland variables which requires a
575 fieldwork campaign (see Figure 2.1) even if collecting these data is time consuming
576 and limited in its spatial coverage. Furthermore, the CSM guidelines make
577 assumptions about which criteria best reflect grassland condition and how effective
578 they are at capturing changes in condition over space and time.

579



580

581 *Figure 2.1: Conventional grassland data being collected on a quadrat at Over Pasture*
582 *(Ingleborough NNR).*

583

584 **2.2. Remote sensing platforms used in** 585 **grassland condition studies**

586 Studies investigating the use of RS for grassland condition primarily used devices
587 mounted on UAVs or satellites, sometimes in conjunction with hand-held devices and
588 destructive samples, with relatively few studies exclusively using hand-held devices
589 or using devices mounted on crewed aircraft. The wide variety of devices deployed is
590 reflected in the range of spatial scales used in these studies, which ranged from leaf
591 level to regional level. There are also several considerations to make when deploying
592 spectral devices. Readings can be taken at nadir only (e.g. Schile et al., 2013) or
593 multiple directions (e.g. Cole et al., 2014). Some devices have a dual field of view,
594 where readings can be taken of incoming radiation as well as the target. These
595 devices can display or utilise downwelling illumination readings, making it easier to
596 make an informed decision on whether the illumination is adequate for RS data
597 collection, and may automatically calculate reflectance values of the target based on
598 downwelling illumination. Readings taken in low illumination conditions can lead to a
599 reduced signal to noise ratio, especially in the SWIR part of the spectrum (Roelofsen
600 et al., 2014) and electro-optical satellite imagery can be obscured by clouds.
601 Therefore, it is common practice to collect data with spectral devices in clear sky
602 conditions and within two hours of solar maximum (e.g. Guo et al., 2005; Yao et al.,
603 2013) as solar zenith angle can have an impact on results (Ishihara et al., 2015) or to
604 choose satellite imagery with as little cloud cover as possible. Even when spectral
605 data are collected in clear sky conditions, short-term changes in irradiance and
606 atmospheric conditions will affect the observed spectral data. The only way to
607 account for this is by converting readings into reflectance. This requires concurrent
608 observations of downwelling (i.e. irradiance) and upwelling radiation (i.e. reflected
609 radiance) or measurements taken intermittently between the target (such as
610 vegetation) and a reference calibration panel (Dusseux et al., 2014). Drone or crewed
611 aircraft imagery collected across areas which include reference panels placed on the
612 ground, and collected in conjunction with other ground-based spectral devices, can
613 achieve the same purpose.

614 Within the context of grassland condition, each device and supporting platform has
615 advantages and disadvantages relative to others when taking into consideration
616 important aspects such as spatial resolution, spatial coverage and spectral
617 information. Table 2.1 summarises the comparison between the main types of

618 platforms used to support spectral devices; the main types of platforms being hand-
619 held, uncrewed aerial vehicles (UAVs), crewed aircraft and satellites. There is an
620 overlap in some metrics between platforms, for example the most expensive and
621 heaviest hand-held devices (e.g. ASD FieldSpec Pro) can be more expensive and
622 heavier than the cheapest and lightest drones (e.g. DJI Parrot), and the most
623 expensive and heaviest aircraft (e.g. NASA Ikhana drone) can be more expensive
624 and heavier than the cheapest and lightest satellites (e.g. Dove nanosatellites by
625 Planet Labs Inc.).

626 Table 2.1: Overview of widely available RS platforms

System	No of spectral bands	Spatial resolution	Repeat frequency	Spatial coverage	Flight time	Portability	Government regulations	Size of team	Platform cost	Image cost to customer
Satellite	Few-multi spectral RGB, NIR, SWIR, TIR	Low to very high (km - cm)	1-16 days, determined by satellite orbit and constellation number	From global to user defined ~10,000 km ² areas	Years	N/A	N/A	Very high	Very high	Free to very high
Crewed aircraft	Few-hyperspectral RGB, NIR, SWIR	High (meters)	Single or more repeat visits determined by user	< 10,000 km ²	Hours	Low	High	High	High-very high	Free to high
UAS	Few-multi spectral RGB & NIR	High-very high (m-cm)	Single or more repeat visits determined by user	meters-hectares	Minutes -hours	Low-high	High	Low-high	Low-high	Free to high
Hand-held	Few-hyperspectral RGB, NIR, SWIR	High-very high (m-cm)	Single or more repeat visits determined by user	Samples of <5m ²	N/A	High	Low	Low	Low-med	N/A

627 Relative to other platforms; the strongest advantages of using hand-held devices are
628 their portability and, in the case of devices such as the Analytical Spectral Device
629 FieldSpec Pro (referred to as ASD from now on), their ability to collect hyperspectral
630 data along a relatively wider range of the electromagnetic (EM) spectrum. One of the
631 biggest disadvantages of hand-held devices is their reduced spatial coverage over
632 most UAVs, aircraft or satellite imagery as they can only take spot measurements.
633 Anderson and Gaston (2013) and Von Beuren et al. (2015) explored the advantages
634 and disadvantages of UAV data collection compared to other platforms. Despite small
635 drone-mounted cameras having less functionality, for example because these
636 devices collect data on fewer spectral wavelengths, they are much more flexible to
637 deploy making it easier to collect data at a higher spatial-temporal resolution than
638 crewed aircraft or satellites. UAV platforms are also becoming more cost effective
639 and therefore more accessible. Spatial coverage, which varies subject to the size of
640 the UAV (Anderson and Gaston, 2013), is improved when compared to using hand-
641 held devices but not when compared to crewed aircraft (except for the largest UAVs
642 or satellite imagery). UAV-mounted multi-spectral cameras are generally limited to
643 the visible and NIR part of the EM spectrum and are expensive. Although aircraft
644 have the advantage of rapidly collecting hyperspectral imagery over a relatively large
645 area, crewed aircraft have much greater asset, maintenance and storage costs plus
646 asset deployment is more challenging. Furthermore, with the exception of the largest
647 UAVs and satellites, a greater quantity and expertise of crew is required for
648 operations. Satellite mounted sensors can collect relatively large swaths of imagery
649 anywhere on Earth including regions that may be inaccessible due to terrain or
650 conflict (Geerken et al., 2005). Also, some optical sensors cover a relatively wide
651 region of the EM spectrum (e.g. Landsat-8 covers VIS to TIR range of EM spectrum)
652 although satellites generally use broader bands than hand-held devices.
653 Furthermore, satellite imagery from government-owned satellites are often made
654 freely and easily accessible to the general public but access to commercial imagery
655 can be costly. Satellite data generally have a low spectral and spatial resolution
656 compared to data from hand-held devices and drone-mounted cameras (Lillesand et
657 al., 2015) and the number of available spectral bands is predetermined and limited
658 when compared to hyperspectral hand-held devices and UAV-mounted multi spectral
659 devices.

660

661 **2.2.1. Field radiometry (hand-held spectral devices)**

662 Field radiometry studies that use hand-held devices have been used in proof of
 663 concept studies plus these data are often used for the purpose of calibrating or
 664 evaluating satellite, aircraft or UAV derived data products. Within the context of
 665 vegetation condition studies, hand-held devices such as the CROPSCAN MSR 16R
 666 or ASD FieldSpec Pro have been used to collect reflectance data on different
 667 vegetation types (e.g. Dusseux et al., 2014), bare soil and litter (Asner et al., 2000) or
 668 lichens and exposed rock (Veen et al., 2006). Data may be collected on target
 669 patches in the field or on samples (such as leaf cuttings) in a laboratory (e.g. Asner,
 670 1998). Within the context of grassland condition studies, spectral data from hand-held
 671 devices have been collected for calibration purposes or to utilise as predictors of
 672 above ground biomass (Psomas et al., 2011), biochemical variables (e.g. nitrogen
 673 content) (Roelofsen et al. 2014; Polley et al. 2022), vegetation indices (e.g. Yang
 674 and Guo, 2014) or a combination of at least some of the aforementioned categories
 675 of variables (Asner, 1998; Asner et al., 2000).

676 Relative to each other; hand-held devices can also offer very different spectral
 677 ranges, spectral coverage, spatial coverage and portability. Hyperspectral devices
 678 such as the ASD provide superior spectral range (350-2500nm), spectral coverage
 679 (data collected on most wavelengths in this range) and spectral resolution
 680 (bandwidths of 3nm) but are expensive. On the other hand, data collection with a
 681 CROPSCAN MSR 16R is easy relative to devices such as the ASD FieldSpec Pro
 682 and SVC HR-1024i as these devices need regular calibration whilst the CROPSCAN
 683 MSR 16R collects upwelling and downwelling radiation simultaneously. Furthermore,
 684 the CROPSCAN MSR 16R is relatively lightweight, portable and robust with a longer
 685 battery life making it relatively quick and easy to collect data in the field.

686

687 **2.2.2. Uncrewed Aerial Vehicles (UAV) and crewed aircraft** 688 **remote sensing**

689 Anderson and Gaston (2013) described the four main categories of UAV platform
 690 which are primarily delineated by size: large UAVs (payload ~200-1100kg), medium
 691 (payload ~50kg), small and mini (payload ~5-30kg), and micro and nano (payload
 692 <5kg). Larger UAVs have the advantages of being able to carry a larger payload, fly
 693 to a higher altitude and have a longer flight time. On the other hand, larger drones

694 have higher running and setup costs. Larger drones also have greater logistical
695 challenges such as asset storage and operation (Anderson and Gaston, 2013). The
696 same advantages and disadvantages of using a large UAV also applies to using
697 crewed aircraft.

698



699

700 *Figure 2.2: A custom-built Matrice 600 UAV being prepared for launch at Scar Close*
701 *Moss at Ingleborough NNR.*

702

703 UAV-mounted sensors are being utilised for environmental monitoring in a wide
704 variety of applications including grassland condition (see review by Salamí et al.,
705 2014). UAV RS of grassland condition studies usually focus on particular grassland
706 variables (particularly biomass, e.g. Capolupo et al. (2015)) but can include
707 biochemical variables (e.g. Polley et al. 2022) and species composition (e.g. Lu et al.,
708 2009) which usually includes the deployment of small rotary drones (<10kg). Small
709 drone platforms are becoming increasingly common in RS studies. Although UAV
710 based RS studies have become more commonplace since 2015, replacing crewed
711 aircraft-based RS studies, organisations such as the Natural Environment Research
712 Council Airborne Research Facility (NERC-ARF) and National Aeronautics and
713 Space Administration (NASA) have been operating for decades (since 1971 in the

714 case of NASA and 1983 in the case of NERC-ARF) and currently still deploy aircraft-
715 mounted hyperspectral sensors for environmental monitoring. These aircraft have
716 been utilised for a wide range of Earth Science related studies including studies on
717 grassland condition such as studies on grassland species diversity in relation to
718 invasive species (Gholizadeh et al., 2019), estimating LAI on grasslands (Atzberger
719 et al., 2015; Punalekar et al. 2018), predicting equivalent water thickness on different
720 vegetation types (e.g. Li et al. 2008) and studies encompassing multiple structural
721 and biochemical grassland variables (Schweiger et al., 2017). Asner et al. (1998,
722 2000) conducted aircraft RS studies on semi-arid grasslands, shrublands and
723 transition zones (succeeding from grasslands to shrublands) to attribute vegetation
724 variables with the variation of wavelengths in the 400-2500nm spectral region.

725

726 **2.2.3. Satellite remote sensing**

727 Satellite imagery has been used in a wide range of applications which includes
728 vegetation condition monitoring and specifically the monitoring of grassland condition.
729 Some of the earliest remote sensing studies (Jordan, 1969) used vegetation indices
730 derived from satellite data with coarse spatial and spectral resolution relative to
731 satellite data available today. Satellite sensors with a relatively low spatial resolution,
732 such as the Moderate Resolution Imaging Spectroradiometer (MODIS) on the Terra
733 and Aqua satellite platforms, often have the advantage of a relatively high temporal
734 resolution. For example; MODIS collects data with a spatial resolution of 250m-
735 1000m for 36 spectral bands, depending on wavelength, and a revisit rate of 1-2
736 days) (Maccherone, 2021) and are freely available online. Various studies utilised
737 vegetation indices, where these indices were in some way related to grassland
738 condition, from MODIS satellite products. Wang et al. (2020) and Xu et al. (2013)
739 calculated NDVI from calibrated radiance values for their studies which focused on
740 estimating grassland productivity. Lyu et al. (2020) used Normalized Difference
741 Vegetation Index (NDVI) and Enhanced Vegetation Index (EVI) satellite products
742 provided by NASA to assess grassland degradation in their study, where their
743 methods linked both productivity and ES to grassland degradation. Gao et al. (2006)
744 also focused their study on grassland degradation, but instead used three different
745 NDVI-derived satellite products; MODIS NDVI 10-day product, Advanced Very High
746 Resolution Radiometer (AVHRR) 10-day product and Satellite Pour l'Observation de
747 la Terre (SPOT)-Vegetation 10-day composite NDVI product. Other studies used

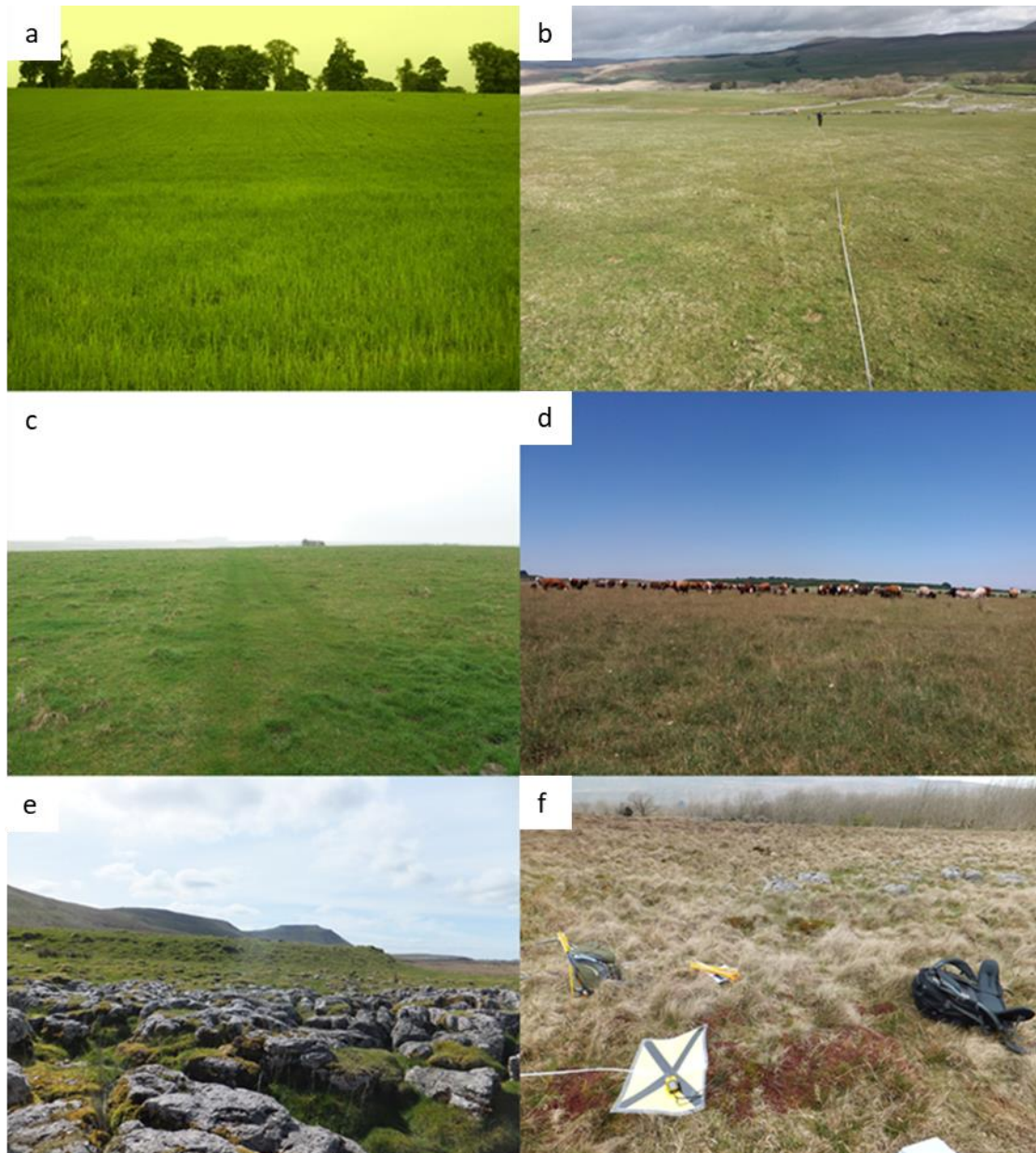
748 other satellite products to establish grassland productivity. For example, Zhao et al
749 (2014) used MODIS eight-day net photosynthesis and gross primary productivity
750 (GPP) satellite products in their above ground biomass estimate study.

751 In contrast, satellites can also have a relatively high spatial resolution at the expense
752 of temporal resolution unless they form part of a large satellite constellation such as
753 Skysat satellites (Planet Labs, 2021). For example, Sentinel-2 is a two constellation
754 satellite system that collects data on the VIS-SWIR parts of the EM spectrum with a
755 spatial resolution of 10-60m (depending on wavelength) and revisit rate of ~5 days
756 whilst Landsat-8 is a one constellation satellite that collects data on the VIS-TIR parts
757 of the EM spectrum with a spatial resolution of 15-100m (also depending on
758 wavelength) and a revisit rate of 16 days. Gu and Wylie (2015) estimated grassland
759 productivity for central Nebraska at a 30m scale using two satellite products; 30-m
760 Landsat 8 Level 1T (terrain-corrected) imagery and the 250m MODIS NDVI product.
761 Xu et al (2014) used Landsat-8 OLI imagery and Landsat-7 Enhanced Thematic
762 Mapper Plus imagery in their study to estimate the dead material component of
763 grasslands in Grasslands National Park, Canada.

764 It is important that the spatial resolution of satellite imagery is appropriate to the study
765 being conducted. A spatial resolution of 10-300m may be adequate for an effective
766 study of large rangeland areas or homogeneous grasslands, but could be too coarse
767 for studying the condition of fragmented or structurally heterogeneous grasslands
768 (examples of different levels of structural heterogeneity provided in Figure 2.3) (Ali et
769 al., 2016; Dabrowska – Zielinska et al., 2015; Lausch et al., 2016) or for a species-
770 focused RS of grassland condition study (e.g. Wang et al. 2018a). For example,
771 alkaline grasslands that exist within base rich flushes could only be distinguished
772 from surrounding acid grassland by using high spatial resolution imagery as they are
773 less than 10m wide (Smart, S. pers. comm. 12th December 2016). Resolution that is
774 too coarse can lead to irregularities with ground truthing when averaging of *in-situ*
775 data is required during up-scaling (Ali et al., 2016; Dabrowska – Zielinska et al., 2015;
776 Lausch et al., 2016). Alternatively, higher spatial resolution satellite data (such as
777 sub-meter scale imagery from commercial Pleiades satellites) can provide solutions
778 related to low spatial resolution (e.g. Mirik and Ansley) but access to these images
779 can be expensive and will also have a lower temporal resolution (Ali et al., 2016;
780 Chopping et al., 2008). Commercial satellite companies such as Planet Labs seek to
781 overcome the issue of spatial vs. temporal resolution by launching large
782 constellations of relatively small and inexpensive satellites referred to as

783 “microsatellites” or “nanosatellites” (Planet Labs, 2021). It should also be noted that a
 784 lack of data collected with other spectral devices within the study area specifically for
 785 the purpose of validation may still mean a relatively high amount of error in the results
 786 of a RS study (Loew et al., 2017).

787



788

789 *Figure 2.3: Grasslands representing a gradient of structural heterogeneity from*
 790 *simple to complex: a) monoculture grassland, b) semi-improved grassland (Top Cow*
 791 *Pasture, Ingleborough NNR), c) semi-improved calcareous grassland (100 Acre,*
 792 *Parsonage NNR), d) semi-natural calcareous grassland (Castle Down, Parsonage*
 793 *NNR), e) semi-natural limestone pavement grassland (Scar Close Moss,*

794 *Ingleborough NNR*), f) *semi-natural acid mire grassland (Scar Close Moss,*
 795 *Ingleborough NNR)*.

796

797 **2.3. Remote sensing approaches for grassland** 798 **condition-related variables**

799 Many approaches have been taken to monitor grassland condition using remote
 800 sensing techniques, targeting a wide range of condition-related variables and using
 801 various analytical techniques. A grassland condition study may compare the results
 802 of predicting multiple condition-related variables (e.g. Kahmen and Poschlod, 2008;
 803 Schweiger et al., 2017) or focus on specific variables (e.g. Pasolli et al., 2015). Some
 804 focussed on capturing the process of habitat degradation through land use change
 805 (Boyle et al., 2014), others on species diversity or invasive species (Boyle et al.,
 806 2014; Lausch et al., 2018), grassland variables such as biomass (e.g. Schweiger et
 807 al., 2017) or through the use of at least one of many metrics referred to as spectral
 808 traits by Lausch et al. (2018). To predict these variables, the full of spectral range of
 809 data collected by at least one spectral device may be used in analysis. Alternatively,
 810 specific bands or a combination of bands may be used to predict condition-related
 811 variables instead (e.g. Davidson et al., 2006).

812 Some studies used grassland variables or “spectral traits” to correlate, predict or
 813 validate other grassland variables or spectral traits. For example; Wylie et al. (2002)
 814 used a combination of destructive samples and spectral data to make modelled
 815 estimates of FAPAR as well as LAI and biomass for the North American Great Plains
 816 region, then assessed the relationship of these metrics with NDVI. Destructive
 817 samples and multispectral data collected with a CROPSCAN MSR 16R were used to
 818 derive FAPAR, LAI and biomass, then these metrics were regressed against NDVI
 819 which was projected for the region using spectral data from the Landsat Thematic
 820 Mapper. Wylie et al. (2002) found that there was a strong correlation between NDVI
 821 and all three metrics ($R^2 > 0.9$) showing that they have a strong relationship.

822 The rest of this chapter further explores the wide variety of RS of grassland condition
 823 studies that have been conducted so far focussing on the metrics that are most
 824 commonly used:

- 825 • Biomass, height and % cover
- 826 • Leaf area index (LAI), plant area index (PAI) and green area index (GAI)
- 827 • Fraction of absorbed photosynthetically active radiation (FAPAR)
- 828 • Normalised difference vegetation index (NDVI)
- 829 • Specific leaf area (SLA)
- 830 • Leaf dry matter content (LDMC)
- 831 • Leaf water content (LWC)
- 832 • Dead matter and bare ground
- 833 • Species richness, indicator species and invasive species
- 834 • Biochemical variables

835

836 *Table 2.2: Specifies the number of papers discussed in Section 2.3 (with total number*
 837 *of references for each section in parentheses) and also some characteristics of those*
 838 *papers, such as which RS platforms were used and whether the metric in question*
 839 *was used as a predictor or response in models. Note that multiple spectral devices*
 840 *are often used in RS studies, in particular data from at least one hand-held device*
 841 *and at least one non-terrestrial device (UAV, aircraft or satellite). Also note that some*
 842 *studies used a metric as a response variable and as a predictor of other metrics.*

Metrics	Number of references	Hand-held	UAS	Crewed aircraft	Satellite	Predictor	Response
Biomass, height and % cover	5 (17)	3	1	0	4	0	5
LAI, PAI and GAI	6 (22)	5	0	1	4	0	5
FAPAR	4 (6)	3	0	0	2	0	3
NDVI	6 (12)	1	0	0	6	6	0

SLA	3 (12)	2	0	0	1	3	0
LDMC	3 (10)	1	2	1	1	0	3
LWC	3 (3)	2	0	0	2	0	3
Dead matter and bare ground	3 (14)	2	0	0	3	0	3
Species richness, indicator species and invasive species	5 (10)	2	1	3	1	1	4
Biochemical variables	4 (9)	4	2	1	0	0	4

843

844 **2.3.1. Biomass, height and % vegetation cover**

845 Many studies have focused on or incorporated biomass, grass height and/or other
846 productivity measures into their study to establish grassland condition with respect to
847 ecosystem services (e.g. Homolová et al., 2014) or grassland productivity (Bullock et
848 al., 2011; Schils et al., 2013) and have used one of these grassland variables to help
849 determine another. For example, productivity can be determined by weighing
850 destructive samples taken from a defined area which is then combined with grass
851 height measurements to derive biomass (Bai et al., 2001; Psomas et al., 2011).
852 Alternatively, the mass of destructive samples from a defined area alone is used (e.g.
853 Schweiger et al., 2017).

854 Changes in biomass can be related to the degradation of grassland condition and
855 associated socio-economic and ecological impacts (Gao et al., 2006; JNCC, 2004;
856 Lyu et al., 2020; Psomas et al., 2011). Changes in grassland variables related to
857 biomass such as % vegetation cover and height can also be related to reduced
858 condition. Grass height can be an indicator of degradation (Spagnuolo et al., 2020),
859 undergrazing or overgrazing, all of which negatively impact biodiversity (JNCC, 2004;
860 2006). The % cover of graminoids and forbs, plus the associated graminoid:forb ratio,
861 are grassland variables that are related to biomass as a greater % cover of these
862 variables means more biomass. Changes in the cover of graminoid species may
863 impact on bryophyte species (Ingerpuu et al., 2005) which are linked to good
864 condition for some grassland types (JNCC, 2004). Few RS studies of grassland
865 condition have separated graminoid from forb biomass, but Schweiger et al. (2017)
866 used PLSR to predict these variables plus a range of other grassland variables using
867 airborne imaging spectroscopy data as predictors. The PLSR models produced R^2
868 results of >0.5 but model performance deteriorated to $R^2 <0.2$ after external
869 validation. Grazing regime (Bai et al., 2001), soil depth, slope and aspect all also
870 have an influence on biomass quantity (Harzé et al., 2016).

871 Most studies of biomass were conducted at field or regional level; although data
872 collected by satellites or aircraft are often used, an increasing number of studies are
873 conducted using data collected by a UAV. Tucker et al. (1985) used 1km and 4km
874 spatial resolution data from NOAA-6 and NOAA-7 plus ground measurements with a
875 hand-held radiometer and grass clippings to establish the biomass of an area of
876 grassland in the Senegalese Sahel. Zhao et al. (2014) estimated the biomass of the
877 Xilingol grassland using MODIS eight-day PSNnet (net photosynthesis) 1km spatial
878 resolution product and destructive samples collected at 1205 field survey data points
879 for months of July and August for the years 2005-2012. Four different regression
880 analyses, each using a different function, were used to predict biomass using the
881 PSNnet values as predictors and the mass of grass cuttings as a response. All four
882 regression models produced R^2 values of 0.55-0.65. Psomas et al. (2011) collected
883 biomass samples and spectral data, using a field spectro-radiometer (i.e. ASD), on
884 grasslands that represented a moisture gradient. These data sets were utilised to
885 predict above-ground biomass at patch level ($1m^2$), then the results were upscaled
886 using either VIs as predictors in ordinary least squares regression or using selected
887 bands used as predictors in multiple linear regression using hyperspectral data
888 collected by the Hyperion EO-1 satellite. The strongest models for predicting biomass
889 at patch level used selected (by branch-and-bound variable searching algorithm)

890 combinations of bands in multiple linear regression which produced R^2 values of
891 0.51-0.86. Marcett et al. (2006) used Landsat 30m spatial resolution imagery (plus
892 ground truthing using a LI-COR LAI-2000 hand-held device) to quantify biomass,
893 height and vegetation cover for managed rangelands in the USA. Vegetation cover
894 was established using the Soil Adjusted Total Vegetation Index (SATVI), plus
895 biomass and height were estimated using a near infrared (NIR) band although the
896 authors believe that a high forb cover (30%) reduced the accuracy of the results.
897 Capolupo et al. (2015) also targeted a wider range of grassland variables when they
898 compared the results of PLSR and multiple vegetation indices (VI) to establish which
899 was best in estimating biochemical and structural grassland variables. UAV-acquired
900 hyperspectral images were collected over two seasons (in May and October) on
901 experimental grassland plots near Kleve, Germany. The results for using VIs as
902 predictors in linear regression models produced R^2 results <0.5 for all grassland
903 variables. Using spectral data collected for one season in PLSR produced R^2 results
904 $\Rightarrow 0.7$ for grass height and fresh matter yield. The predictive power of the PLSR
905 models increased when data from two seasons were used in the same model, where
906 the results of predicting most grassland variables were >0.7 , with all three structural
907 variables (height, fresh matter yield and dry matter yield) being more strongly
908 predicted with R^2 results >0.8 .

909

910 **2.3.2. Leaf area index (LAI), plant area index (PAI) and green** 911 **area index (GAI)**

912 A review by Weiss et al. (2004) has covered how LAI is defined, the theoretical
913 background behind the RS approach to measuring LAI and the reasons for using LAI
914 in a grassland condition study. Shen et al. (2014) covers a range of methods and also
915 reasons for measuring LAI. Because of the extensive information provided in these
916 reviews, only a summary of LAI is provided in this thesis. The way that leaf area
917 index (LAI) is defined, measured and and/or calculated has changed over time. LAI is
918 traditionally defined as leaf area density over canopy height but can also be defined
919 as half the total developed area of leaves per unit ground horizontal surface area
920 (Weiss et al., 2004). LAI is a common choice for grassland condition RS studies
921 because LAI (plus leaf angle distribution and leaf water content) is considered to be
922 one of the dominant controls on canopy reflectance data for dense canopies (Asner,
923 1998; Roelofsen et al., 2015).

924 LAI is related to canopy biomass, grassland density, stress (in the context of LAI, this
925 refers to increased bare ground), growth or productivity, grassland structural
926 heterogeneity (a proxy for biodiversity), management practices (Dusseux et al., 2014;
927 Haboudane et al., 2004; He et al., 2007; Möckel et al., 2014; Yang and Guo, 2014;
928 Zhang et al., 2020) and water content (Davidson et al., 2006; Sibanda et al., 2019).
929 Because of this, other important calculations linked to grassland condition can be
930 derived from LAI. For example, Anderson et al. (2004) stated that there is a linear
931 relationship between LAI and vegetation water content and Davidson et al. (2006)
932 utilised LAI when calculating canopy level equivalent water thickness (EWT).

933 *In situ* approaches of capturing LAI during data collection are summarised by Weiss
934 et al. (2004) and a range of traditional and RS methods of data collection are
935 discussed by Shen et al. (2014). Destructive methods for measuring LAI, such as the
936 conveyor belt method (where LAI is derived by scanning individual leaves placed on
937 a conveyor belt), is time-consuming which results in small sample sizes (Roelofsen et
938 al., 2014). This has encouraged the use of RS techniques to measure LAI (Shen et
939 al. 2014; Weiss et al., 2004).

940 Remote-sensing grassland condition studies have used hand-held devices and/or
941 satellite data to estimate LAI (Shen et al. 2014) and have also renamed and/or
942 redefined LAI as plant area index (PAI) (Asner et al., 2000) or green area index (GAI)
943 (Pasolli et al., 2015). When collecting RS data on the ground using handheld devices,
944 many studies used a LAI-2000 (LICOR, Lincoln, NE) Plant Canopy Analyser to
945 estimate LAI or PAI (Haboudane et al., 2004; He et al., 2007; He and Guo, 2006).
946 Grassland LAI studies have also measured GAI of alpine grasslands using a Li-3100
947 portable leaf area meter (Pasolli et al., 2015) and measured grassland LAI using a
948 combination of destructive sampling and an AT leaf area meter (Curran and
949 Williamson, 1987).

950 Many studies that used LAI also utilised satellite products to conduct large-scale
951 studies, where destructive samples and/or RS data collected at ground level were
952 used for ground-truthing. Pasolli et al. (2015) estimated LAI using Moderate
953 Resolution Imaging Spectroradiometer (MODIS) satellite imagery (with ground truth
954 data from a Li-3100 LICOR hand-held device) for mountain grasslands in the Alps.
955 The accuracy of these measurements (RMSE accuracy of 1.68 m^2) was considered
956 by the authors to be an improvement on previous studies in such difficult terrain, this
957 improvement was attributed to customised MODIS data and an improved algorithm.
958 He and Guo (2006) used SPOT-4 data and ground measurements using a LICOR

959 LAI-2000 hand-held device to map the LAI of mixed prairie grasslands in Grasslands
 960 National Park, Canada. It was found that adjusted transformed soil-adjusted
 961 vegetation index (ATSAVI) was best for estimating LAI for mixed grasslands. ATSAVI
 962 was also found to be the best predictor of LAI on semi-arid environments of low
 963 vegetation cover by He et al. (2007). Both studies defined ATSAVI as:

964

$$965 \quad ATSAVI = \frac{a(\rho_{NIR} - a\rho_{Red} - b)}{a\rho_{NIR} + \rho_{Red} - ab + X(1 + a^2)}, X = 0.08 \quad (eq. 2.2)$$

966

967 where Red refers to a band within the red part of the spectrum and NIR refers to a
 968 band in the NIR part of the spectrum. They have been more broadly defined as
 969 different studies choose to utilise different bands within the red and NIR regions of
 970 the spectrum. Atzberger et al. (2015) compared four different approaches for
 971 estimating grassland LAI; two statistical modelling methods (predictive equations and
 972 VIs, referred to as PEre-adjust and vegetation index respectively) and two radiative
 973 transfer models (RTM) inversion methods (one based on look-up-tables and one
 974 based on predictive equations). Data were collected *in-situ* through destructive
 975 sampling and by using a LAI-2000 hand-held device, plus hyperspectral data were
 976 collected using the HyMap aircraft. All methods produced R² values of 0.75-0.91, but
 977 it was stated that the accuracy and robustness of the statistical models decreases
 978 when fewer samples are used for calibration. Punalekar et al. (2018) combined *in-situ*
 979 LAI (collected with a LAI-2000 hand-held device) and field spectro-radiometry (SVC
 980 HR 2024i) to calibrate an inverted PROSAIL radiative transfer model to estimate LAI
 981 and biomass from 10m Sentinel-2 satellite data on a mixture of pasture and
 982 experimental grasslands. Ordinary least squares (OLS) regression produced R²
 983 results between observed and predicted LAI values ranging from 0.61-0.87 across
 984 three different grasslands. Schweider et al. (2020) compared the ability of a soil-leaf-
 985 canopy radiative transfer model and random forest regression to predict biomass and
 986 LAI using Sentinel-2 imagery with field measurements taken using an ASD
 987 FieldSpec-2 spectroradiometer hand-held device. Biomass was estimated with a
 988 mean R² of 52% (44-66%) and nRMSE of 17% (14-22%). LAI models performed with
 989 a mean R² of 0.62 (0.44-0.81) and nRMSE of 23% with the two modelling producing
 990 similar results.

991 There are direct and indirect methods of establishing grassland LAI and each has
992 practical issues (Shen et al. 2014). Although non-destructive data collection using a
993 hand-held spectral device is more time-efficient than destructive sampling, it has
994 been shown that there is variability in optical LAI measurements taken on the same
995 samples plus non-destructive sampling underestimates LAI (He et al., 2007; He and
996 Guo, 2006). He et al. (2007) compared the accuracy of two different hand-held
997 instruments (LAI 2000 and AccuPAR) with destructive sampling for estimating LAI.
998 He et al. (2007) showed that the lower the LAI of four grassland communities studied,
999 the greater the underestimated percentage of LAI values collected using RS devices
1000 relative to destructive sampling.

1001 He et al. (2007) suggested that this underestimation was due to three reasons.
1002 Firstly, placing a sensor onto grass disturbs it resulting in higher incident light deeper
1003 in the canopy and therefore an underestimation of leaf interception and LAI.
1004 Secondly, the instruments calculate LAI using absorbed radiation to establish the
1005 amount of light intercepted by the canopy, ignoring leaf transmission scattering and
1006 all second-order radiative effects in three-dimensional space. The aforementioned
1007 issues are referred to as radiative error and are believed to contribute to an
1008 underestimation of LAI. Lastly, the measurements are calculated based on an
1009 assumption that there is a random distribution of foliage which may not be true of
1010 some grassland patches.

1011 This underestimation appears to be inconsistent in the literature and therefore cannot
1012 be corrected to match destructive sampling. Furthermore, it would not be practical to
1013 use a RS technique to collect data on heavily grazed grasslands which have blades
1014 that are shorter than the instrument height (Gerard, F. pers. comm. 12th June 2017).
1015 This explains why LAI estimation studies have been carried out on croplands (Bacour
1016 et al., 2002; Haboudane et al., 2004), prairies (He et al., 2007; He and Guo, 2006)
1017 and woodlands (e.g. Chen et al., 1997) which have relatively tall vegetation.

1018

1019 **2.3.3. Fraction of absorbed photosynthetically active radiation** 1020 **(FAPAR)**

1021 The fraction of absorbed photosynthetically active radiation (FAPAR) refers to the
1022 absorbed fraction of the photosynthetically active radiation (PAR) part of the EM
1023 spectrum (considered to be within the 400-700nm range) (Asner et al. 1998). Spectral

1024 data can be used to calculate FAPAR, but satellite products such as the MODIS
1025 LAI/FPAR product can be downloaded with this metric already calculated for the user.
1026 Aside from being used as a metric in estimating variables related to vegetation
1027 condition such as net primary productivity and greenness, FAPAR is also used as a
1028 parameter in climatological (because it is associated with the carbon cycle) and
1029 ecological models (Tao et al. 2016).

1030 Olofsson and Eklundh (2007) exploited the relationship between FAPAR and NDVI
1031 by using NDVI to model FAPAR for various sites in the Scandinavian region which
1032 had a mixed cover of trees, shrubs and grass species. NDVI came from MODIS
1033 satellite data and the modelled FAPAR was validated against ground measurements.
1034 For all sites, the RMSE of mean (%) ranged from 0.33% to 31% with an average of
1035 6.9%. Rossini et al. (2014) used a range of VIs and PAR as variables in their models
1036 to derive gross primary productivity (GPP) on sub-alpine grasslands. The models had
1037 relative root mean square deviation (rRMSD %) values ranging from just under 20%
1038 to over 50%. Schile et al. (2013) estimated the FAPAR on Californian wetlands with a
1039 high % cover of dead material, where FAPAR was used as a proxy for productivity. A
1040 range of unspecified VIs were calculated using data collected at different depths of
1041 the vegetation with a ASD FieldSpec Pro and used as independent variables in
1042 pairwise correlation of FAPAR. The dependent variable (FAPAR) was calculated from
1043 incoming and transmitted photosynthetically active radiation measurements taken in
1044 the field at three different levels (heights) of the vegetation. The findings suggested
1045 that a high % dead material cover had a negative impact on the strength of
1046 correlation between VIs and FAPAR, plus the structure of wetlands (in particular the
1047 very tall vegetation relative to other grassland types) make capturing grassland
1048 variable data difficult. Another drawback to using FAPAR as a condition metric is that
1049 FAPAR satellite products have low spatial resolution (300m or 1km). Some studies
1050 overcame this by calculating FAPAR themselves using higher spatial resolution
1051 satellite imagery.

1052

1053 **2.3.4. Normalised difference vegetation index (NDVI)**

1054 Normalised difference vegetation index (NDVI) is a measure of the difference
1055 between two spectral bands collected on a given space, one wavelength from the red
1056 region of the spectrum and another from the NIR region (Tucker, 1979). Exactly

1057 which wavelengths are chosen, and how wide the bandwidths are, depends on the
1058 spectral device used for data collection. NDVI can be calculated as:

1059

$$1060 \quad \quad \quad (NIR - RED) / (NIR + RED) \quad \quad \quad (eq. 2.1)$$

1061

1062 NDVI is considered to be related to grassland condition as NDVI has been linked to
1063 LAI, biomass, FAPAR and GPP which are used as proxies of condition (Chapungu et
1064 al., 2020; Chen et al., 2009; Corbane et al., 2013; Gu and Wylie, 2015; Wang et al.,
1065 2020). This link has been utilised in land use classification studies (Corbane et al.,
1066 2013; Geerken et al., 2005) and cutting/grazing regime studies (Halabuk et al., 2015).
1067 NDVI is almost always calculated at regional scale using satellite products for
1068 vegetation condition monitoring. Satellite products came from a range of satellites,
1069 but the most common satellite product for most of the studies that focused on using
1070 NDVI and on grassland condition utilised Moderate Resolution Imaging
1071 Spectroradiometer (MODIS) satellite imagery or the vegetation index 16-day global
1072 NDVI product derived from MODIS imagery (e.g. Halabuk et al., 2015; Xu et al.,
1073 2013).

1074 Many studies that used NDVI as a grassland condition-related metric utilised satellite
1075 products to conduct large-scale studies. Xu et al. (2013) calculated NDVI from
1076 MODIS imagery acquired during the May-September period for the years 2003-2008
1077 to use as a proxy to map productivity for all grasslands in China, broken down by
1078 region. Productivity was used as a proxy for grassland condition, where relatively
1079 higher productivity was considered to demonstrate good condition. Gu and Wylie
1080 (2015) also used a MODIS NDVI satellite product (250-m MODIS GSN where GSN
1081 refers to growing season NDVI) where NDVI was used as a proxy to map
1082 productivity, but this time for Nebraska (USA). Gu and Wylie (2015) then used 30-m
1083 Landsat Thematic Mapper (TM) data to downscale their productivity map. Piecewise
1084 regression showed a strong correlation between predicted GSN and actual GSN ($r =$
1085 0.97 , average error = 0.026). On the other hand, some studies found that NDVI was a
1086 weak predictor of biomass. Chen et al. (2009) attempted to estimate biomass on
1087 alpine meadows in China by using a range of narrowband VIs (including NDVI) as
1088 predictors in a PLSR model. The strongest PLSR model ($R^2 = 0.27$) was produced by
1089 using NDVI calculated using 746nm and 755nm wavelengths. Psomas et al. (2011)
1090 tested the ability of a range of VIs (including NDVI) and selected bands to predict
1091 biomass at patch level ($1m^2$) using ASD data (unlike the previous three studies

1092 discussed in this section which did not use any ground truthing), before upscaling the
 1093 results. Although the patch level results, using four variants of NDVI, produced R^2
 1094 values 0.51-0.65, using selected combinations of individual bands in multiple linear
 1095 regressions produced higher R^2 values of 0.51-0.86.

1096 Using NDVI is particularly disadvantageous when calculated on grasslands with a
 1097 relatively high % cover of litter. Xu et al. (2014) explored the relationship between
 1098 NDVI and dead material cover to investigate how changes in dead material alter the
 1099 relationship of total biomass and NDVI using destructive samples and Landsat
 1100 imagery. Positive/negative relationships between total biomass and NDVI only
 1101 existed where dead material consisted of <20% or >80% of total cover. Guo et al.
 1102 (2005) showed how dead litter complicates analyses (e.g. using VIs as predictors in
 1103 models) not designed for heterogeneous landscapes such as mixed prairie
 1104 grasslands. It was found that NDVI is not suitable for biomass estimation whilst leaf
 1105 area index (LAI) had stronger results although LAI could only explain 59.8% variation
 1106 of total biomass. LAI was able to explain 81.5% of variation of plant moisture content
 1107 (absolute difference between wet and dry biomass in this case) compared to 53.2%
 1108 for NDVI. The study site included grazed and non-grazed sites, but the percentage of
 1109 dead material and exact nature of grazing was not specified.

1110

1111 **2.3.5. Specific leaf area (SLA)**

1112 Specific leaf area (SLA) is the one-sided area of a fresh leaf divided by its dry mass,
 1113 where the lamina (leaf blade) is used for area measurements of grass samples which
 1114 are usually oven-dried at 60-80°C for 48-72 hours (e.g. Molinari and D'Antonio, 2014)
 1115 then weighed to ascertain dry mass. SLA has been used in previous traditional and
 1116 RS of grassland condition studies as a lower SLA can be an indicator of reduced
 1117 grass moisture or nutrients (Harzé et al., 2016, Liu et al. 2017) and can also be used
 1118 to calculate other metrics related to grassland condition (Ferreira et al., 2011; He et
 1119 al., 2007). For example, He et al. (2007) calculated LAI from SLA and Ferreira et al.
 1120 (2011) used SLA and biomass values derived from destructive sampling to establish
 1121 equivalent water thickness (EWT). Liu et al. (2017) calculated SLA for four dominant
 1122 grassland genera in Northern China. They also linked SLA to condition-related
 1123 variables such as nitrogen content and also related soil and climatic variables such
 1124 as soil nutrient content, mean annual precipitation and mean annual temperature.

1125 One disadvantage of this approach is that data collection can be time-consuming as
1126 the leaf area of individual grass blades has to be measured using leaf area
1127 measuring software or a ruler (e.g. Harzé et al., 2016) meaning that either proxies are
1128 used or only a small sample set is collected (e.g. Roelofsen et al., 2014; Wellstein et
1129 al. 2017). Proxies and databases have been used to represent SLA in some studies
1130 (e.g. Möckel et al., 2014) to avoid time-consuming data collection. Furthermore, some
1131 studies suggest that the variability of SLA within each grassland and between
1132 different grasslands is relatively high compared to some other spectral traits (Firn et
1133 al., 2019; Harzé et al., 2016).

1134 Another disadvantage is that other variables are more effective and practical for
1135 establishing grassland condition than SLA. Roelofsen et al. (2014) found that specific
1136 leaf area and nutrient-related variables (N and P content) was poorly predicted from
1137 any spectral data whilst leaf dry matter content was more strongly correlated with
1138 spectral data. Smart et al. (2017) found that Leaf Dry Matter Content (LDMC)
1139 predicted above-ground net primary productivity (aNPP) better than SLA and could
1140 be measured *in situ* in a more time-effective manner. Pakeman et al. (2011) tested
1141 whether LDMC, SLA or three biochemical variables (C, N and C:N) could be used to
1142 train a linear regression or exponential model to predict grassland litter
1143 decomposition. It was found that LDMC was the best predictor, although models
1144 trained using LDMC still had weak predictive power (best result of $R^2 = 0.334$).

1145

1146 **2.3.6. Leaf dry matter content (LDMC)**

1147 Leaf dry matter content (LDMC) is defined as the ratio of leaf dry mass to fresh mass
1148 (Garnier et al., 2001) and like SLA, is related to productivity (Ali et al., 2019; Smart et
1149 al., 2017). LDMC can be calculated by weighing vegetation leaves acquired from
1150 destructive sampling before and after oven-drying (Garnier et al. 2001). LDMC has
1151 been linked to other condition-related grassland variables such as biomass (Polley et
1152 al. 2020) and nitrogen content (Polley et al. 2022) and also linked to vegetation
1153 indices such as NDVI (Polley et al. 2020). Studies that used LDMC as a condition
1154 metric were conducted at a range of scales and using a wide range of spectral
1155 devices, but most studies were conducted at field or regional scale and utilised
1156 satellite products.

1157 Roelofsen et al. (2014) collected spectral data on individual leaves in a laboratory
1158 (400-1800nm spectral range of 35 species) and tested the strength of correlation
1159 between these spectral data and a range of structural and biochemical variables.
1160 LDMC had higher r^2 values (0.57-0.58) than other morphological and biochemical
1161 variables which had correlation values $r^2 < 0.3$ except leaf nitrogen content (0.46-
1162 0.66). Ali et al. (2019) compared the performance of PLSR and 11 different VIs to
1163 predict LDMC on wetlands in the Netherlands where Sentinel-2 spectral data were
1164 used as predictors. Using spectral data in PLSR produced the strongest prediction of
1165 LDMC ($R^2 = 0.71$) although four of the eleven VIs produced relatively strong results in
1166 predicting LDMC ($R^2 = 0.67$). Polley et al. (2020) used patch level spectral data
1167 collected by a drone on both semi-natural and monoculture grasslands in PLSR
1168 models to predict LDMC at both leaf level and canopy level. The results of these
1169 models were then extrapolated to field level using spectral data collected from an
1170 aircraft. The PLSR models were reported to explain 62% and 73% of the variance in
1171 LDMC of individual leaves and canopies respectively. It is assumed that these results
1172 are at patch level, it is not made clear how well these models perform when
1173 extrapolated to field level using airborne collected spectral data. It was also found by
1174 using variable importance in projection (VIP) that the red edge and NIR spectral
1175 bands were the strongest predictors of LDMC. Polley et al. (2022) also used patch
1176 level spectral data on semi-natural and monoculture grasslands, this time collected
1177 using a drone and ASD hand-held spectrometer, to predict LDMC using PLSR with a
1178 R^2 value of 0.73. Roelofsen et al. (2014) tested the strength of correlation between
1179 the spectral signature of individual leaves (400-1800nm spectral range of 35 species)
1180 measured in a laboratory and a range of structural and biochemical variables. LDMC
1181 had higher r^2 values (0.57-0.58) than other morphological and biochemical variables
1182 which had correlation values $r^2 < 0.3$ except leaf nitrogen content (0.46-0.66).

1183 There are advantages to using LDMC over SLA, for example LDMC correlates more
1184 closely with spectral data than SLA (Roelofsen et al., 2014). Furthermore, it is easier
1185 to take ground measurements of LDMC and it is a more effective proxy than SLA for
1186 grassland variables such as net primary productivity and litter decomposition
1187 (Pakeman et al., 2011; Smart et al., 2017). LDMC has the disadvantage of being
1188 time-consuming to measure (as measurements of individual blades of grass are
1189 being taken) resulting in a low sample size (Shipley and Vu, 2002) and has high
1190 within-grassland variability (Harzé et al., 2016).

1191

1192 **2.3.7. Leaf water content (LWC)**

1193 Moisture content is defined as the difference in weight (gram or % for absolute or
 1194 relative moisture content respectively) between wet grass sample mass and dry
 1195 grass sample mass and is linked to drought and wildfire risk. Like SLA and LDMC,
 1196 measuring LWC requires oven-drying grass cuttings which are weighed before and
 1197 after oven-drying (Davidson et al., 2006). Davidson et al. (2006) applied VIs, “band
 1198 combinations” and “derivative combinations” with OLS regression to predict absolute
 1199 and relative vegetation water content (AWC and RWC respectively) on a prairie
 1200 grassland–shrubland at patch level using CROPSCAN hand-held spectrometer data.
 1201 “Band combinations” and “derivative combinations” were combinations of bands that
 1202 were potentially the best predictors based on a modified bootstrap approach but
 1203 these bands were not specified by the authors. The results of predicting AWC and
 1204 RWC were then upscaled from patch level (0.5m spatial resolution) to field level (30m
 1205 spatial resolution) to make the spatial resolution comparable to Landsat TM imagery.
 1206 It was found that “band combinations” predicted AWC with high R^2 and RMSEP
 1207 values ($R^2 = 0.8$ and RMSEP = 48.4 at patch level and $R^2 = 0.73$ and RMSEP = 53.1
 1208 at field level) as did some VIs ($R^2 = 0.76$ and RMSEP = 51.7 at patch level and $R^2 =$
 1209 $0.7-0.71$ and RMSEP = 52.6 at field level). RWC predictions were less accurate, but
 1210 once again using band combinations performed best with results of $R^2 = 0.53$ and
 1211 RMSEP = 0.05. Li et al. (2008) used leaf-level data and NASA AVIRIS aircraft
 1212 spectral data to estimate equivalent water thickness (EWT). At leaf level, EWT was
 1213 estimated with R^2 values during calibration and validation >0.99 . When modelling with
 1214 data from AVIRIS, the R^2 values were $R^2 = 0.87$ after calibration and $R^2 = 0.78$ after
 1215 validation. Ferreira et al. (2011) quantified the spatial and temporal variability of
 1216 vegetation (forest, shrubland and grassland) water content in the Cerrado of Brazil
 1217 using EWT. EWT was derived from ground-based measurements of SLA and leaf
 1218 water concentration. EWT was predicted at patch level and then up-scaled using two
 1219 different approaches, one approach used an unspecified regression analysis
 1220 (possibly OLS regression) and Earth Observing-1 (EO-1) Hyperion satellite imagery.
 1221 The other approach applied a different unspecified regression analysis (also possibly
 1222 OLS regression) to the MODIS vegetation index 16-day 250m spatial resolution
 1223 global product. The outcome of extrapolating the results using these two different
 1224 satellite products were compared and the lower spatial resolution (250m) MODIS
 1225 product appeared to give lower canopy EWT values relative to the EO-1 Hyperion
 1226 satellite 30m spatial resolution imagery. As part of a wider study conducted on
 1227 experimental grasslands, Sibanda et al. (2019) used spectral data collected using an

1228 ASD FieldSpec Pro plus data from two hyperspectral satellites (HyspIRI and EnMAP)
1229 to train PLSR and sparse PLSR models to estimate EWT. Models were trained on
1230 each of the twelve experimental grasslands that represented a range of different
1231 fertiliser treatments, and also trained on either HyspIRI or EnMAP data. The results
1232 presented in the figures of the paper are from trained sparse PLSR models as these
1233 apparently outperformed PLSR models. The R^2 values from models trained with
1234 HyspIRI data seemed to range from approximately 0.5-0.9 whilst models trained with
1235 EnMAP data ranged from approximately 0.2-0.7. Wavelengths close to the water
1236 absorption bands in the upper NIR and SWIR regions of the EM spectrum were the
1237 strongest predictors of EWT.

1238

1239 **2.3.8. Dead matter and % bare ground cover**

1240 Dead material, in the context of this thesis, refers to any above-ground necromass
1241 belonging to a floral species whilst bare ground refers to any non-vegetated surface
1242 including bare soil and rock. Dead material can consist of standing senesced plants
1243 or overlying litter (Xu et al., 2014; Yang and Guo, 2014). Dead material is used as an
1244 indicator of disturbance level (Xu et al., 2014) or management intensity as this
1245 variable is influenced by grazing regime, cutting and fire (Franke et al., 2012; Xu et
1246 al., 2014). For example, a build-up of litter can be the result of a lack of hay collection
1247 or undergrazing which can affect species composition (JNCC, 2004; 2006). Particular
1248 species produce relatively large amounts of litter, and the species in question may be
1249 a positive or negative indicator species depending on the grassland type (Gerard et
1250 al., 2015).

1251 Studies (e.g. Möckel et al. 2014) have linked an increased % cover of bare soil with a
1252 reduction in grassland condition. Common Standards Monitoring (CSM) guidance
1253 recommends bare soil cover of <5% for most grassland types although a relatively
1254 higher (unspecified) % cover of bare soil is accepted for certain acid and calcareous
1255 grasslands. A low percentage of bare soil is seen as more beneficial than no bare soil
1256 as it promotes the regeneration of grass from seed, but a relatively high % cover of
1257 bare soil may also be considered unfavourable as undesirable species (such as
1258 invasive or highly competitive species) are more likely to colonise the bare patch
1259 (JNCC, 2004). Möckel et al. (2014) tried to classify different successional phases on
1260 grasslands and used bare soil as an indicator of condition. Their study assumed

1261 gradual degradation (as increased % bare soil cover) for all fields with time plus dead
1262 litter was removed during data collection.

1263 Guo et al. (2005) investigated the relationship between spectral data and *in situ*
1264 grassland measurements on a range of grassland variables in a native mixed prairie
1265 ecosystem, which included study sites that had a relatively high litter content. Data
1266 were collected using two hand-held devices (to collect hyperspectral data and LAI
1267 measurements) on a total of sixty 100m transects. Correlation analysis was run
1268 between biophysical variables and NDVI then LAI respectively with the Jack-knife
1269 used as a validation technique. Regression analysis was used to predict total
1270 biomass and plant moisture content from NDVI and LAI separately. All biophysical
1271 variables except moisture content ($r = 0.729$) had low r values when using NDVI in
1272 analysis. Using LAI produced r values >0.7 for graminoids, dead material and
1273 moisture content. Xu et al. (2014) calculated a range of indices using Landsat 7
1274 imagery to test their potential as predictors to estimate dead cover. The results
1275 suggest that the dead component can be estimated with multispectral images using
1276 Normalized Burn Ratio (NBR) or Normalized Difference Water Index (NDWI), but the
1277 relationships are highly influenced by bare soil and soil crust, i.e. are only significant
1278 when bare soil and soil crust are $<20\%$ of cover.

1279 It has been stated in a number of papers that dead material and bare soil complicate
1280 RS studies of heterogeneous grasslands (Asner, 1998; Asner et al., 2000; He and
1281 Guo, 2006; Schile et al., 2013; Shen et al., 2014; Xu et al., 2014; Yang and Guo,
1282 2014; Zhao et al., 2014). Xu et al. (2014) partly attributed this complication to a
1283 similarity in spectral signature between dead litter, bare soil and soil crust (i.e.
1284 bryophytes), with the only main difference in part of the shortwave infrared region
1285 (~ 2000 nm). Xu et al. (2014) and Yang and Guo (2014) show how different ratios of
1286 bare soil, dead material and green grass within a study site change the shape of the
1287 grassland spectral signature in specific places and in a subtle way. Dead material
1288 also causes an increase in variation of the spectral signature on the same grassland
1289 type (Asner et al., 2000; Xu et al., 2014). Furthermore, it was stated by Asner et al.
1290 (2000) that the presence of dead material could be detected in the spectral signature,
1291 but not quantified.

1292

1293 **2.3.9. Species richness, indicator species and invasive** 1294 **species**

1295 Species richness is the absolute number of species within a defined space, which is
 1296 not to be confused with species abundance which refers to the relative abundance
 1297 (usually captured as % cover) of each species within a defined space. Positive
 1298 indicator species are species considered to be indicative of a particular grassland
 1299 community with negative indicator species being their antithesis. Invasive species are
 1300 described as non-native species that have a negative impact on their new
 1301 environment, where this negative impact could refer to reduced biodiversity for
 1302 example (JNCC, 2004; 2006).

1303 Several studies have associated particular grassland species or communities with
 1304 condition as part of a specific grassland variable study (e.g. Bai et al. (2001) focused
 1305 on biomass), as a proxy for other condition-related variables (e.g. Roelofsen et al.,
 1306 2015), part of a more holistic study (e.g. Homolová et al., 2014) or wider framework to
 1307 label a particular grassland by type or condition (e.g. JNCC, 2004). These studies
 1308 were conducted at a range of scales, with studies utilising spectral data collected
 1309 from a UAV becoming increasingly common.

1310 Wang et al. (2018) used data from multiple ground-level spectral devices and the
 1311 aircraft-mounted AISA Eagle imaging spectrometer to link spectral variation with
 1312 grassland biodiversity in Minnesota, USA. Zaman et al. (2011) used multispectral
 1313 imagery from a UAV to identify the spread of an invasive species (*Phragmites*
 1314 *australis*) in wetlands in Utah, USA. Roelofsen et al. (2015) used indicator species as
 1315 part of a remote sensing study to indicate soil pH and groundwater levels. Schweiger
 1316 et al. (2017) reiterated that indicator species are related to soil biogeochemistry plus
 1317 biochemical and structural grassland variables. Möckel et al. (2014) used indicator
 1318 species as part of a RS study to identify grasslands at different levels of “succession”
 1319 which actually related to management type and degradation. Mansour et al. (2016)
 1320 mapped grassland degradation using SPOT 5 data by using the distribution of
 1321 indicator species as a proxy for degradation. Edaphic factors derived from soil
 1322 samples (including soil chemistry) were used to improve the classification accuracy,
 1323 including edaphic (soil-related) factors was reported to have increased the
 1324 classification accuracy by 13% to 88.60%.

1325 Noss (1990) summarised the ideal indicator species but also stated that one limitation
 1326 to this approach is that it is possible that the indicator species may not indicate

1327 anything about some environmental trends. Xu and Guo (2015) stated that many
 1328 variables are not taken into consideration when only using indicator species in a
 1329 study such as energy flux, nutrient cycle, productivity, diversity or response capacity
 1330 to disturbance. This is possibly because data collection for species richness or
 1331 abundance is also time-consuming, limiting time to collect data on other variables
 1332 (JNCC, 2004). Despite this, the use of indicator species as part of a more
 1333 comprehensive study was still recommended by Noss (1990).

1334

1335 **2.3.10. Biochemical variables**

1336 There are a wide range of biochemical grassland variables used as proxies of
 1337 grassland condition in the literature such as chlorophyll, nitrogen and phosphorus
 1338 which are linked to plant stress (i.e. nutrient deficiency) (Lausch et al., 2018).
 1339 Estimating canopy biochemical variables from remote sensing is usually carried out
 1340 using hyper-spectral reflectance signatures where particular bands or regions of the
 1341 spectral signature are sensitive to changes in a particular chemical, for example the
 1342 chlorophyll absorption peaks within the visible region of the EM spectrum. Destructive
 1343 grass samples are analysed in a laboratory to ascertain the concentration of
 1344 chemicals targeted by a given study (e.g. Asner, 1998). These chemical
 1345 concentration values are then used as response variables in models where hyper-
 1346 spectral data are used as predictors.

1347 Many studies have tried to link spectral data and biochemical variables at different
 1348 scales but most of these studies focus on forests (e.g. Asner et al., 2011; 2015) with
 1349 few studies being conducted on grasslands. Polley et al. (2022) used patch level
 1350 spectral data from a drone and ASD hand-held spectrometer to predict community
 1351 nitrogen levels with a R^2 value of 0.87 using PLSR. Wang et al. (2019) compared the
 1352 ability of PLSR and Gaussian processes regression to predict fifteen different
 1353 grassland biochemical and structural variables on experimental grasslands using
 1354 data from the NASA AVIRIS aircraft. Both modelling approaches predicted all
 1355 variables except lignin and chlorophyll a + b with R^2 values > 0.55 (some with R^2
 1356 values > 0.8). The biochemical variables predicted by models with a moderate to
 1357 strong predicting power included nitrogen, carbon, carbon:nitrogen ratio,
 1358 hemicellulose and cellulose. Capolupo et al. (2015) compared the results of PLSR
 1359 and multiple vegetation indices (VI) to establish which was best in estimating
 1360 biochemical and structural grassland variables. Using spectral data collected in a

1361 PLSR model produced R^2 results $\Rightarrow >0.7$ for grass height and fresh matter yield whilst
1362 all biochemical variables (except potassium content with R^2 results = 0.68) produced
1363 R^2 results <0.6 . Roelofsen et al. (2014) also found that structural variables had a
1364 stronger relationship with spectra than biochemical variables in their study on the
1365 strength of correlation between leaf-level spectral data and multiple structural and
1366 biochemical variables. Apart from leaf nitrogen content (0.46-0.66), LDMC had higher
1367 r^2 values (0.57-0.58) than all other morphological and biochemical variables which
1368 had correlation values $r^2 <0.3$.

1369 A key disadvantage of using biochemical variables in a RS of grassland condition
1370 study is the time and cost required to establish chemical concentrations on a
1371 sufficient number of destructive samples to effectively train a model. Furthermore,
1372 scaling grassland biochemical content from leaf level to canopy level can be affected
1373 by confounding variables as grassland canopy reflectance is strongly influenced by
1374 vegetation structural properties (He and Mui, 2010). This could explain why structural
1375 variables can be more effectively predicted than biochemical variables (Capolupo et
1376 al., 2015; Roelofsen et al., 2014).

1377

1378 **2.4. Summary and conclusions**

1379 Lausch et al. (2018) stated that a holistic approach, referring to taking a multitude of
1380 environmental and management-related variables into consideration, is required for
1381 the effective RS monitoring of grassland condition to capture the non-linear effects of
1382 reduced plant condition. This would increase the likelihood of recognising a reduction
1383 in condition and acting in a more decisive and targeted way to improve plant
1384 condition. Lausch et al. (2018) also accepted that a truly holistic approach, capturing
1385 a wide range of inter-related data types, is not practical due to time and resource
1386 constraints. This means that conducting a RS of grassland condition study means
1387 making difficult decisions on which data sets to collect, including which spectral
1388 devices to use and which grassland variables to focus on. This literature review
1389 explored which spectral devices, condition-related spectral variables or grassland
1390 variables and which framework would be most effective for a RS of grassland
1391 condition study. This review also conducted a process of elimination to understand
1392 which approaches of the RS of grassland condition are both viable and relatively less
1393 explored.

1394 Many RS studies of grassland condition are conducted on experimental grasslands
1395 (e.g. Capolupo et al., 2015) or relatively structurally homogeneous grasslands (e.g.
1396 Zhao et al., 2014). Many of these studies focused on spectral variables related to the
1397 structural or chemical properties of grassland canopies. Some grassland variables,
1398 such as dead material (Yang and Guo, 2014) and bryophytes (Cole et al., 2014) have
1399 received little attention in previous grassland condition studies and data were only
1400 collected over one or two seasons in many of these studies. Very few studies have
1401 been conducted in the UK (Cole et al., 2014), none of which utilised multispectral
1402 imagery collected by a UAV (e.g. Cupolupo et al., 2015). This is despite the
1403 advantages that UAV data collection offers, for example some UK grasslands are
1404 fragmented and the use of UAVs in condition studies, rather than satellite products,
1405 on fragmented grasslands has been suggested by Dabrowska - Zielinska et al.
1406 (2015).

1407

1408

1409

1410

1411

1412

1413

1414

1415

1416

1417

1418

1419 Chapter 3 – Methods

1420 The primary aim of this research is to assess the link between the definition of
 1421 grassland condition used in this thesis (CSM-condition, explained in Section 3.4.1)
 1422 and condition-related grassland variables with grassland spectral reflectance through
 1423 field and drone spectro-radiometry at a range of spatial-temporal scales. Focussing
 1424 on semi-natural grasslands within the UK and within the context of ecosystem
 1425 services (ES), this work addressed the questions specified in Section 1.2 using the
 1426 methods described in this chapter.

1427

1428 3.1. Definition of grasslands and UK grasslands

1429 As grasslands are defined broadly (Reinermann et al., 2020), a definition specific to
 1430 this thesis is provided in this section. This thesis uses the Dixon et al. (2014)
 1431 definition of grasslands as a non-wetland type dominated or co-dominated by
 1432 graminoids and forbs where trees consist of <10% cover and shrubs <25% cover
 1433 although legumes have also been considered in this thesis in line with some other
 1434 grassland studies (e.g. Dabrowska - Zielinska et al., 2015). Graminoids consist of the
 1435 families Poaceae (true grasses), Juncaceae (rushes) and Cyperaceae (sedges)
 1436 whilst forbs are herbaceous flowering plants that do not include grass families
 1437 considered to be graminoids. This thesis uses the standard definition of bryophytes,
 1438 which includes any species considered to be mosses, liverworts or hornworts.

1439 Volume three of British Plant Communities defines different categories of
 1440 mesotrophic (neutral), calcicolous (alkaline), calcifugous (acid) and montane
 1441 grasslands according to the National Vegetation Classification (NVC) system. Volume
 1442 two uses the same system to classify mires and heaths. These subcategories are
 1443 often divided by a change in species presence and abundance as a result of different
 1444 treatment but are also related to environmental variables such as surficial geology.
 1445 An example of this are MG5-MG7 grasslands; where different cutting and/or grazing
 1446 regimes may have led to a difference in species composition but surficial geology and
 1447 fertiliser treatment may have also had an effect (Rodwell, 1991; 1992).

1448

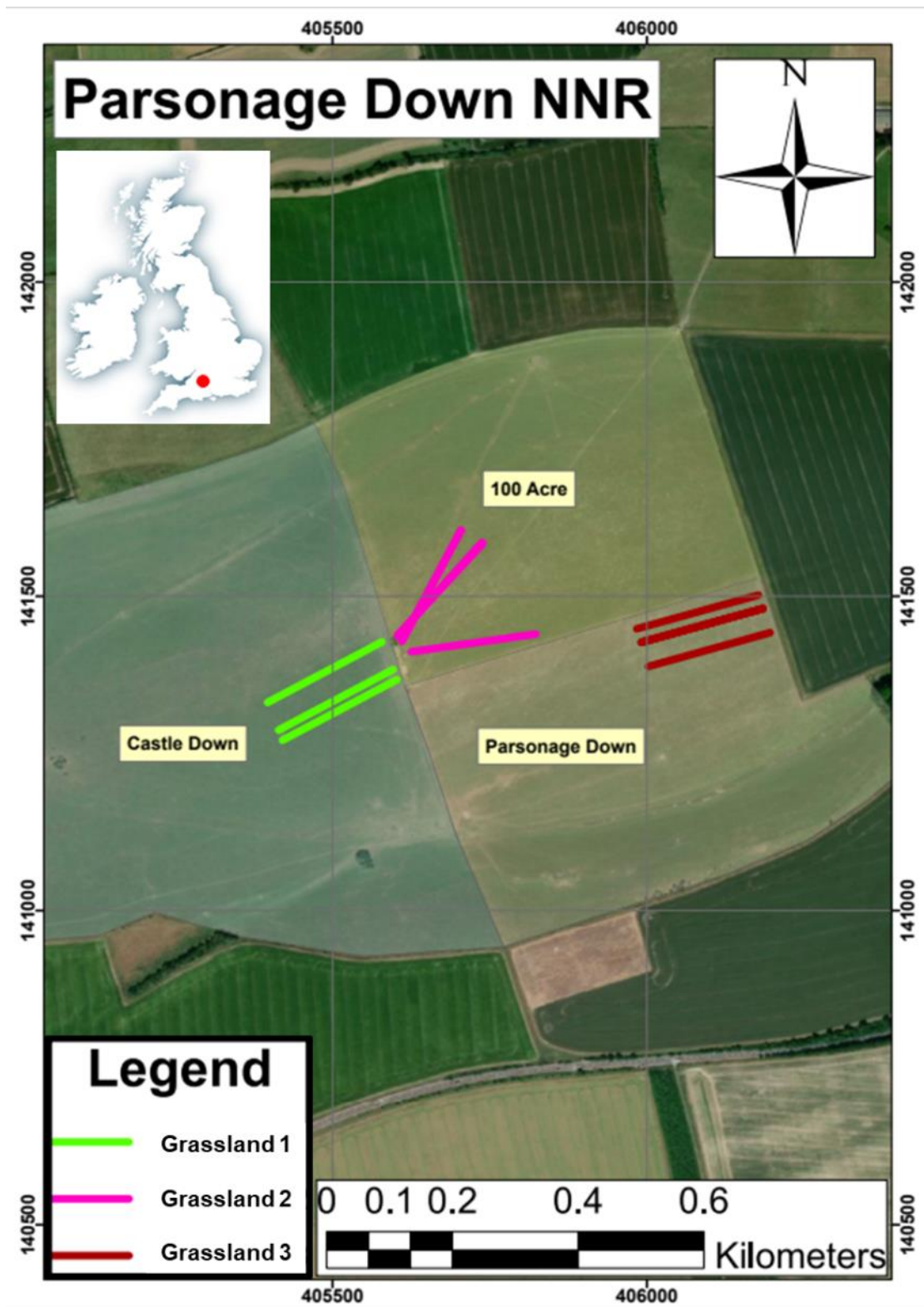
1449 **3.2. Study sites**

1450 Halabuk et al. (2015) stated that the success of grassland studies depends mainly on
1451 site specific conditions, including the grassland types to be studied. Furthermore,
1452 Harzé et al. (2016) conducted a grassland condition study measuring three functional
1453 variables (specific leaf area, leaf dry matter content and plant vegetative height) on
1454 four calcareous grassland species within three populations. The study showed that
1455 for total variability of the considered grassland variables, 0-30% of variance was
1456 attributed to between population differences and 70-100% to within population
1457 differences. These findings were taken into consideration when choosing the study
1458 sites and grassland types. Data were collected on seven temperate semi-natural
1459 grassland sites across two locations in England; three grasslands located in the
1460 Parsonage Down National Nature Reserve (NNR) and four in the Ingleborough NNR.

1461 Parsonage Down NNR is located in the chalk downs of Salisbury Plain, Wiltshire, UK
1462 ($51^{\circ} 10' 42.2159''\text{N}$, $1^{\circ} 54' 38.0528''\text{W}$, Figure 1a). It is a 275-hectare site of special
1463 scientific interest (SSSI) and also part of a working farm managed by Natural
1464 England. Most of the reserve consists of mixed-grazed calcareous grasslands that
1465 represent a range of improvement levels. This location is characterised by chalk
1466 geology with associated alkaline soil and calcareous grasslands which are mixed-
1467 grazed. Calcareous grasslands are a UK Biodiversity Action Plan (BAP) priority
1468 habitat and therefore the monitoring of their condition is mandatory to land managers.
1469 Three grasslands were chosen for data collection that represented varying stages of
1470 improvement located on the same geology and with the same grazing regime,
1471 reducing the possibility of these variables acting as confounding variables (Kahmen
1472 and Poschlod, 2008).

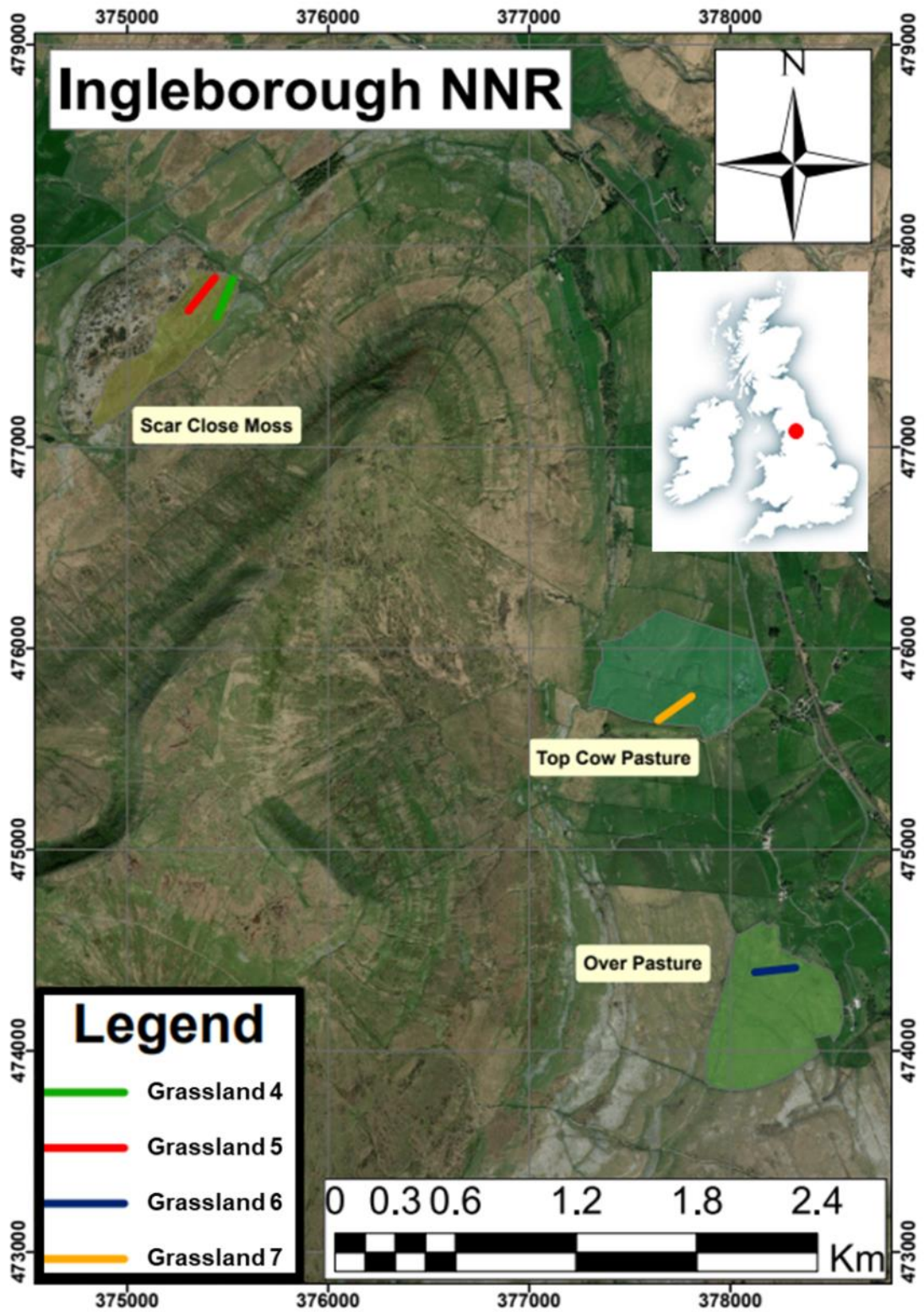
1473 Ingleborough NNR is situated in the south-west of the Yorkshire Dales National Park
1474 in North Yorkshire, UK ($54^{\circ} 11' 44.5452''\text{N}$, $2^{\circ} 21' 0.9432''\text{W}$, Figure 1b). The
1475 reserve covers 1,014 hectares of mountainous karst terrain and contains a range of
1476 vegetation types that are associated with (i) a mixed basic and acidic solid geology
1477 and drift and (ii) a lowland to upland gradient. The area has calcareous, acid, neutral,
1478 improved, semi-improved and reverting grassland plus blanket-bog over gritstone or
1479 drift. A variety of grazing regimes exist; sheep, cattle, mixed and no grazing take
1480 place on different fields. Data were collected on four grasslands that represent a
1481 variety of grassland types and grazing regimes.

1482 Overall, the seven grassland sites were chosen to encompass a range of
1483 management styles, grazing regimes, species composition and grassland structural
1484 complexity. Maps of each location can be seen in Figures 3.1 and 3.2, a summary of
1485 the environmental characteristics of each location is provided in Table 3.1 and a
1486 summary of the environmental characteristics of each study site is provided in Table
1487 3.2.



1488

1489 *Figure 3.1 The boundaries and locations of transects 1 to 3 at Parsonage Down*
 1490 *NNR. Note that data were collected at this location across three seasons.*



1491
1492 *Figure 3.2: Site boundaries and locations of transects for Grasslands 4 to 7 at*
1493 *Ingleborough NNR.*

1494

1495 *Table 3.1: The environmental characteristics of the two locations chosen for data*
 1496 *collection (from information provided by Natural England and by conducting a desk*
 1497 *study (BGS UKSO, 2017; Edina®, 2017).*

Location	Management	Geology	Soil type	Grassland type
Parsonage Down (Wiltshire)	Previously improved mixed grazed grasslands at different levels of reversion	Cretaceous chalk formations (Seaford and Newhaven)	Lime-rich alkaline soil (freely draining)	Chalk grasslands of a range of condition types; improved, reverting, semi-improved and semi-natural
Ingleborough (North Yorkshire)	Previously improved, semi-natural, experimental and rewilding grassland plus peat and limestone pavements – sheep, cow and mixed grazing	Danny Bridge Limestone Formation (limestone), Yoredale Group (LST, MST and SST interbeds) plus till	Peat (poor drainage), acidic loamy peaty soils (high drainage) and rendzinas	A variety of types – acid, alkaline, peat bog, limestone pavement

1498

1499 *Table 3.2: The characteristics of the seven study sites using information provided by*
 1500 *Natural England or gained from the desk study (BGS UKSO, 2017; Edina®, 2017).*
 1501 *The NVC for each grassland was ascertained by entering species abundance data*
 1502 *into MAVIS software (Smart et al., 2016).*

Site	Site Location	Site Name	Grassland type / NVC	Grazing regime	Improvement level & grazing intensity	Grassland structure
1	Parsonage	Castle Down	Chalk grassland / CG2	Mixed grazing	Unimproved	Relatively long grass with tussocks
2	Parsonage	100 Acre	Semi-improved grassland / MG6	Mixed grazing	Relatively improved	Relatively long grass with tussocks
3	Parsonage	Parsonage Down	Semi-improved grassland / MG5	Mixed grazing	Semi-improved	Relatively long grass with tussocks
4	Ingleborough	Scar Close Moss	Alkaline grassland / CG10	Sheep grazing	Unimproved but heavily grazed	Closely cropped by grazing, with intermittent limestone pavement
5	Ingleborough	Scar Close Moss	Acid mire grassland / M19	Sheep grazing	Unimproved and under-grazed	Relatively long grass with tussocks and heather, plus sinkholes
6	Ingleborough	Over Pasture	Alkaline grassland / CG10	Cow grazing	Unimproved	Lightly grazed with a low % cover of limestone

7	Ingleborough	Top Cow Pasture	Sloping semi-improved grassland / MG5	Sheep grazing	Semi-improved and heavily grazed	Closely cropped by grazing, forb dominated in places
---	--------------	-----------------	---------------------------------------	---------------	----------------------------------	--

1503

1504 3.3. Data collection

1505 The literature review revealed that there were few RS studies using the mass of
1506 grassland constituents (e.g. graminoids) as studies that collect destructive samples
1507 usually only measure total biomass (such as Schweiger et al., 2017). However, it was
1508 thought that collecting and utilising data on mass and % cover would have their own
1509 set of advantages and disadvantages. Because bryophytes are sometimes covered
1510 by a canopy of graminoids, collecting destructive samples (i.e. mass data) helped
1511 establish the amount of bryophytes present, which could have an important impact on
1512 reflectance and be missed using the % cover approach. Also, % cover data are
1513 compositional data, i.e. relative rather than absolute values, which are constrained to
1514 0-100%. Some analytical methods (e.g. principle component analysis), particularly
1515 those using untransformed compositional data and assuming that those data can be
1516 projected in Euclidean space, can lead to spurious results as some analyses assume
1517 that the data set values are unconstrained and do not transform data as part of the
1518 analysis (Gupta et al., 2018; Reimann et al., 2012). Furthermore, there is at least
1519 some collinearity in all compositional data because the variables under consideration
1520 will always total 100% and an increase in one variable inevitably means a decrease
1521 in at least one other variable (Dormann et al. 2012). Using grass cuttings provides the
1522 opportunity for establishing biomass, which is often used as a grassland condition
1523 measure, plus other grassland constituents can be measured by separating the grass
1524 samples into their constituent parts before weighing. On the other hand, establishing
1525 mass is far more time consuming than % cover and lacks spatial coverage of the
1526 quadrat relative to % cover data.

1527 The grassland variables in Table 3.3 were chosen as it was thought that these
1528 variables would be influential to changes in the spectral signature; particularly grass
1529 profile (influenced by graminoid:forb ratio), bare soil cover and dead material cover
1530 (Asner et al., 2000; Guo et al., 2010; Xu et al., 2014)(Asner et al., 2000; Guo et al.,

1531 2010; Xu et al., 2014). Furthermore, it was necessary to collect traditional data on
 1532 grassland composition to utilise the criteria for measuring grassland condition
 1533 provided by the CSM documents. Data were not collected on LAI despite this
 1534 approach being taken by a multitude of RS studies on the basis that LAI is
 1535 considered to be a dominant control on canopy reflectance (Asner, 1998; Roelofsen
 1536 et al., 2015) as it was not possible to collect LAI data on very short grasslands
 1537 (<5cm). It is thought that not taking LAI into consideration is not detrimental to this
 1538 thesis as biomass, which is considered, is related to LAI (e.g. Möckel et al. 2014).
 1539 Similar approaches have been used in other RS grassland condition studies where
 1540 collecting data on LAI was not viable, for example Möckel et al. (2014) used changes
 1541 in graminoid and bare soil cover as part of a RS of grassland condition study
 1542 conducted on the island of Öland in Sweden.

1543

1544 *Table 3.3: Variables used in this study, listing whether mass and/or % cover data*
 1545 *were used to establish them and at which NNR locations they were collected. In the*
 1546 *context of this thesis, moisture content refers to leaf wet mass - leaf dry mass).*

Grassland variable	Type	Location
Bare ground	% cover	Ingleborough
Biomass	mass	Both
Bryophytes	% cover, mass	Both
Dead material	% cover, mass	Both
Forbs	% cover, mass	Both
Graminoids	% cover, mass	Both
Graminoid:bryophyte ratio (‘gram:bryo ratio’)	% cover, mass	Both
Graminoid:forb ratio (‘gram:forb ratio’)	% cover, mass	Both
Live material	% cover, mass	Both

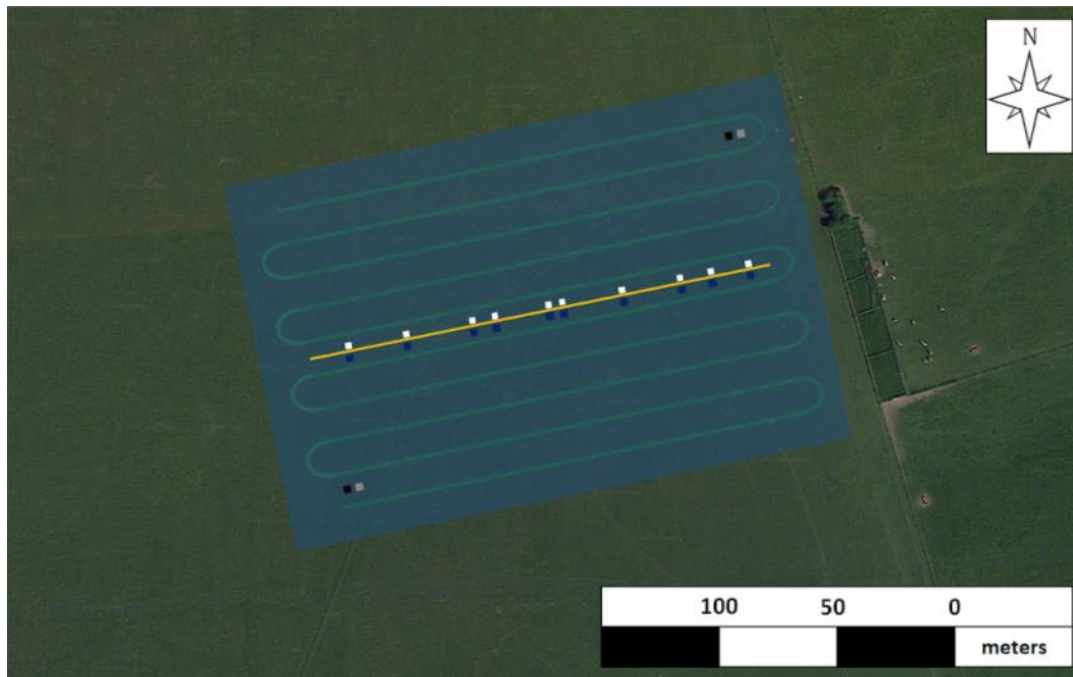
Live material:dead material ratio (‘live:dead ratio’)	% cover, mass	Both
Moisture content i.e. <i>leaf wet mass - leaf dry mass</i>	% mass	Both

1547

1548 **3.3.1. Fieldwork plan and sampling strategy**

1549 On each of the seven chosen grasslands, a 200m transect was set up and ten
1550 quadrats (1m²) placed along it at random (Figure 3.3) where a random integer
1551 generator (<https://www.random.org/>) was used to choose how far along the transect
1552 to place the quadrats. The three Parsonage Down sites were revisited three times
1553 during the 2018 growing season (spring, summer and autumn) on the following dates:
1554 16th – 20th April, 25th – 29th June and 10th – 14th September. Radiometers require
1555 sufficient irradiance (considered to be 400 W/m² in this thesis) to operate which
1556 eliminates the possibility of data collection during the winter (CROPSCAN Inc., 2018).
1557 At the four Ingleborough sites, data were collected during the summer of 2017 (1st –
1558 9th July) (see Section 3.6). Each quadrat was geo-referenced using an eTrex 10
1559 GNSS device giving GPS readings with potential spatial accuracies of 2-3m. For sites
1560 that were revisited during the growing season, reference points (e.g. fence posts) and
1561 photographs were used to relocate quadrats precisely. To locate the quadrats
1562 accurately on the drone collected imagery, laminated white A4 sheets (large enough
1563 to be visible on the drone imagery) were placed directly opposite the quadrat at a
1564 distance of 60cm from bottom-left quadrat corner.

1565



1566

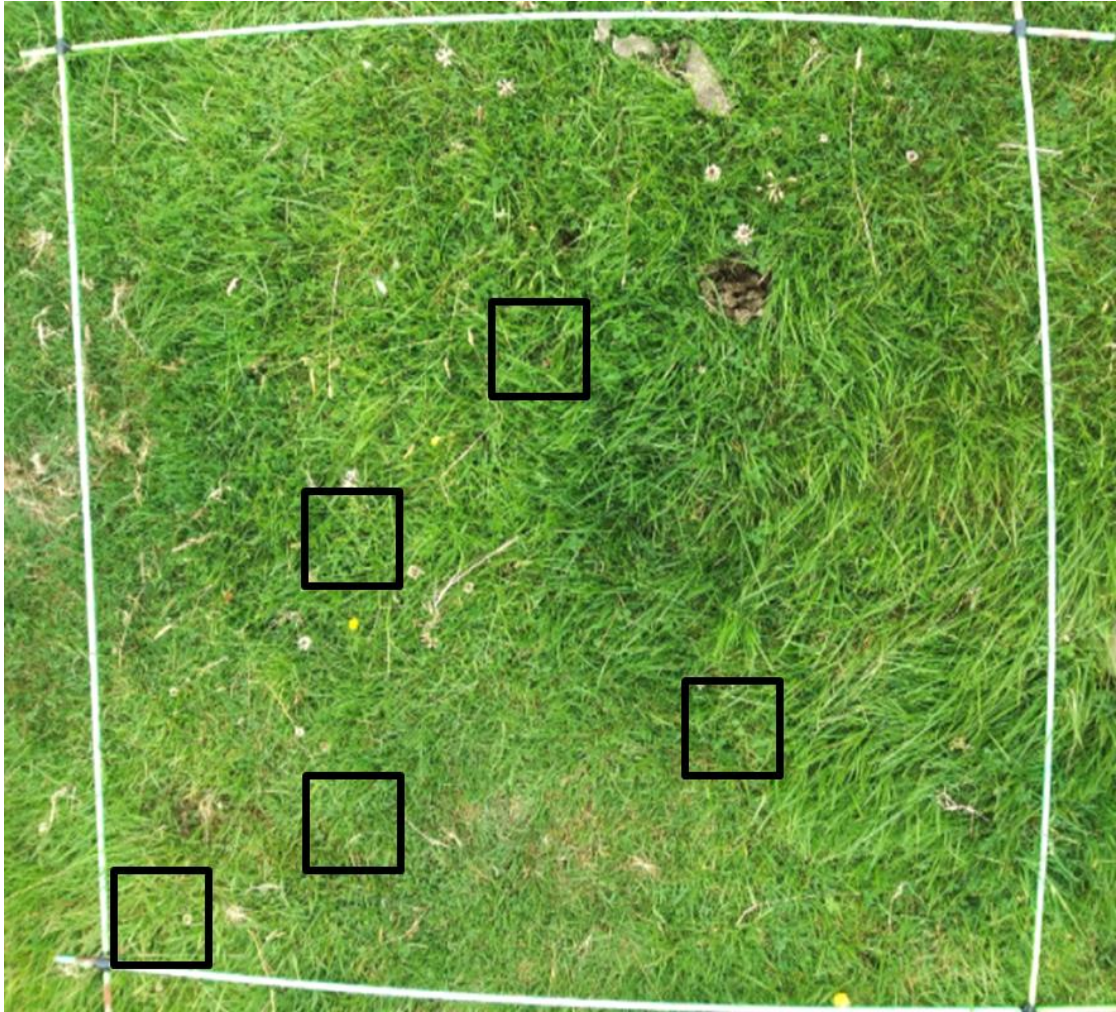
1567 *Figure 3.3: Schematic showing the sampling strategy for data collection (using Castle*
 1568 *Down as an example). The yellow line represents the 200m transect and the dark*
 1569 *blue squares represent the quadrats. The white squares represent the spatial*
 1570 *reference panels and the other grey and black squares represent calibration panels.*
 1571 *The green lines are the UAV flight path and the blue rectangle in the background*
 1572 *represents the area covered by the UAV-mounted Rikola camera.*

1573

1574 **3.3.2. Quadrat sampling**

1575 On each quadrat, the data was collected using the following sequence: grassland
 1576 variable % cover estimates, photographs, soil moisture, grass height, species
 1577 abundance (from which species richness was derived), spectral data and finally
 1578 destructive samples. For % cover, the grassland variables were: graminoids, forbs,
 1579 bryophytes, live material, bare ground, dead material and other (see Table 3.3).
 1580 Percentage cover was estimated by looking straight down onto the quadrat, to the
 1581 nearest 5%, using the dimensions of the quadrat and a ruler as a spatial reference.
 1582 Bryophytes were any species that belonged to the bryophyte group of non-vascular
 1583 plants. Live material cover is the sum total of the % cover of graminoids, forbs, and
 1584 bryophytes. Bare ground is the % cover of bare soil and rocks. Dead material was
 1585 considered to be any necromass visible above ground. “Other” refers to something
 1586 not considered in this study, which was usually dung but also included heather
 1587 patches on the M19 acid mire grassland. From these variables, two ratios were

1588 calculated: graminoid:forb ratio cover and live:dead ratio cover. Quadrat photos were
1589 taken with the camera looking straight down. Soil moisture data were collected at five
1590 random points on each quadrat using a HH2 Moisture Meter from Delta-T Devices
1591 which has a stated accuracy of $\pm 0.01 \text{ m}^3 \cdot \text{m}^{-3}$ or $\pm 1\%$ and has the functionality to take
1592 accurate readings in mineral rich and organic rich soils (Delta-T Devices, 2020).
1593 Grassland canopy height was established by taking five randomly located
1594 measurements on each quadrat with a ruler. This method was chosen as it is a
1595 relatively fast data collection approach and a drop disc compresses grass which
1596 would affect the spectral readings (Stewart et al., 2001). Species abundance was
1597 established for each quadrat by a botanical expert during spring for Ingleborough
1598 NNR and during summer for Parsonage NNR. This thesis defined species abundance
1599 as the % cover of each species within a 1m^2 quadrat, where a botanical expert
1600 estimated the cover of each species within each quadrat to the nearest 1% if the
1601 cover was 0-5%, or nearest 5% if the cover was >5%. Where % cover exceeded
1602 100%, this was due to more than one layer of vegetation being present. For example,
1603 on some grassland types bryophytes were covered by a canopy of graminoids. After
1604 all other data were collected including spectral data (see Section 3.3.3), five randomly
1605 located 10cm^2 grass cuttings were taken from each quadrat (see example in Figure
1606 3.4).



1607
 1608 *Figure 3.4: An overhead view showing how each quadrat was sampled by destructive*
 1609 *sampling.*

1610

1611 The grass cuttings were sorted into the following grass constituents: graminoids,
 1612 forbs, bryophytes, dead material and other (see Figure 3.5). Long and thin bladed
 1613 species were considered to be graminoids while broadleaved species were
 1614 considered to be forbs. Bryophytes were defined as any species that belonged to the
 1615 bryophyte group of non-vascular plants. Dead material was considered to be any
 1616 necromass found within a sample. In this thesis, “other” refers to the minute cuts of
 1617 grass which were too difficult to sort or bits of soil that were accidentally collected.
 1618 After sorting, grass cuttings were weighed, then oven-dried at 60°C for 72 hours, and
 1619 weighed again to determine moisture content (e.g. Bai et al., 2001). As the weighing
 1620 of grass samples collected in one season took approximately three weeks, the sorted
 1621 samples would be oven-dried at 60°C as close to the time of weighing of dry mass as
 1622 possible to ensure that no moisture was present in the samples. Moisture content

1623 was defined as wet mass subtracted from dry mass. Biomass is the sum total of the
1624 mass of graminoids, forbs, bryophytes and dead material. Live material mass is the
1625 sum total of the mass of graminoids, forbs and bryophytes. Three ratios were
1626 calculated: graminoid:forb ratio mass, graminoid:bryophyte ratio mass and live:dead
1627 ratio mass. Data on species abundance, grassland height and grassland constituent
1628 % cover were used to establish the CSM-condition of each quadrat using the NVC
1629 framework (see Section 3.4.1) (JNCC, 2004; 2006).

1630



1631

1632 *Figure 3.5: A grass sample separated into its constituent parts (clockwise from top-*
1633 *left): dead material, graminoids, other, forbs and bryophytes.*

1634

1635

1636 3.3.3. Grassland reflectance

1637 3.3.3.1. Spectral devices

1638 Before grass cuttings were taken, spectral data were collected using three hand-held
 1639 radiometers (an Analytical Spectral Device (ASD) FieldSpec Pro, a Spectral Vista
 1640 Corporation (SVC) HR-1024i and a CROPSCAN MSR 16R) as well as an Uncrewed
 1641 Aerial Vehicle (UAV) (i.e. DJI Matrice) with a Rikola multispectral camera on board.
 1642 Table 3.4 lists the spectral characteristics of these devices.

1643 The MSR 16R model of CROPSCAN multispectral radiometer (referred to as
 1644 CROPSCAN from now on) (Rochester, MN, USA) can accommodate up to 16 bands
 1645 in the 450-1750 nm spectral range. Upward and downward facing sensors measure
 1646 both incoming and reflected radiation which is used to calculate % reflectance. To
 1647 ensure data integrity (George, C. and Gerard, F. pers. comm. 7th July 2016) spectral
 1648 data was only collected when there was a minimum of 400 watts per metre squared
 1649 (W/m^2) incident irradiance, which is above the recommended minimum of 300 W/m^2
 1650 (CROPSCAN Inc., 2018). To keep data sets and results comparable, the 16 bands
 1651 chosen were as closely matching as possible to the bands of the Rikola multi-spectral
 1652 camera.

1653 The Analytical Spectral Device (ASD) FieldSpec Pro (Analytical Spectral Devices,
 1654 Boulder, USA, ASD Inc., 2002) and the Spectral Vista Corporation (SVC) HR-1024i
 1655 field spectrometer (SVC from now on) (Poughkeepsie, NY, USA, SVC, 2012) are very
 1656 similar hyperspectral instruments which collect data from > 1800 bands that can be
 1657 interpolated to produce a spectral signature across the 350-2500nm spectrum. Both
 1658 were loaned by the Field Spectroscopy Facility. The ASD was used to collect data in
 1659 Ingleborough NNR and the SVC to collect data in Parsonage NNR. This spectro-
 1660 radiometer collects hyperspectral data in the range of 350-1000nm at 1.4nm intervals
 1661 plus 1000-2500nm at 2nm intervals (ASD Inc., 2002). Data on 1869 bands are
 1662 available after water absorption bands have been removed (1350-1460nm and 1790-
 1663 1960nm).

1664 A drone was deployed to collect multispectral data at the field scale: a custom-built
 1665 DJI Matrice 600 (DJI, 2018) equipped with a Rikola VNIR camera, referred to as the
 1666 Rikola camera from now on. This camera has a FOV of 37° and a spectral range of
 1667 400-900nm. Thirty bands, each with 10nm bandwidth, can be selected within this

1668 range. Like with the CROPSCAN, to keep data sets and results comparable, bands
1669 were chosen to be as closely matching as possible to the bands of the CROPSCAN.

1670 Relative to the ASD or SVC, the CROPSCAN collects more limited spectral data but
1671 is easier to use in field, making it possible to collect a greater quantity of data
1672 spatially. Furthermore, the CROPSCAN has the added convenience of collecting
1673 upwelling and downwelling radiation simultaneously. The advantage of using a drone
1674 to collect multi- or hyperspectral data over using a hand-held device is that data can
1675 be collected on an entire field at a relatively high spatial resolution (6cm using a
1676 Rikola VNIR camera). A disadvantage is that data are collected on far fewer bands
1677 than some hand-held spectral devices (often only in the VIS and NIR regions of the
1678 EM spectrum), such as the ASD FieldSpec Pro, and a smaller region of the EM
1679 spectrum relative to many hand-held, aircraft-mounted or satellite-mounted spectral
1680 devices due to broad limitations related to the size and weight of the instruments
1681 mounted on any <20kg UAV. A more extensive list of the advantages of using UAVs
1682 to collect data is given by Anderson and Gaston (2013).

1683

1684 *Table 3.4: Summary of multispectral and hyperspectral devices used in the field.*

	ASD FieldSpec Pro	CROPSCAN MSR 16R	Rikola VNIR camera	SVC HR-1024i
Spectral range	350nm– 2500nm	450nm–1750nm	400-900nm	350nm–2500nm
Channels	2149	16	30	1024
Bandwidth (FWHM*)	3nm @ 350– 1000nm 10nm @ 1000–2500nm	10nm @ ≤870nm 11nm – 1240nm 13nm – 1640nm	10nm	≤3.3 nm, 700nm ≤9.5 nm, 1500nm ≤6.5 nm, 2100nm

Bands chosen	1869 bands across 350nm–2500nm – 280 bands in 1350-1460nm and 1790-1960nm ranges removed	470, 530, 560, 570, 647, 690, 700, 720 740, 760, 780, 850, 850, 860, 870, 1240, 1640	515, 530, 531, 550, 560, 570, 647, 655, 665, 675, 687, 690, 700, 710, 720, 730, 740, 750, 760, 770, 780, 800, 810, 820, 830, 840, 850, 860, 870, 880	1249 within 350nm–2500nm range - 1024 bands interpolated, then bands in 1350-1460nm and 1790-1960nm ranges removed
* <i>Full Width Half Maximum</i>				

1685

1686 **3.3.3.2. Spectral data collection**

1687 Using CROPSCAN and either the SVC or ASD spectral data was collected for the
1688 randomly placed quadrats along the 200m transect (see 3.3.2). Figure 3.6 shows how
1689 each quadrat was sampled using the hand-held spectrometers. To minimise the
1690 impact of shading, data were collected two hours either side of solar noon and on
1691 hilly sites transects ran up/downhill (rather than across the hill) although this was
1692 done as a precaution as the slope of the grasslands in this study was minimal (<5°).
1693 Quadrats were also kept on the south, west or south-west side of the person
1694 collecting the spectral data to prevent the person casting a shadow on the quadrats.
1695 Finally, to prevent the tape reflectance contaminating the quadrat reflectance
1696 acquired from the drone-mounted Rikola camera, quadrats were placed 60cm away
1697 from the tape measure.

1698 The CROPSCAN device was held 2m above the quadrats to collect nadir reflectance
1699 from a 1m diameter patch, holding the instrument at 2m was made easy by the
1700 design of the device. CROPSCAN data were collected every 1m producing 200 data
1701 points. When possible, triplicate data were collected at each data point and then
1702 averaged. The raw data were converted into reflectance using CROPSCAN software
1703 (processing raw data is explained in Section 3.4.3.1).

1704

1705



1706

1707 *Figure 3.6: An overhead view showing how each quadrat was sampled using two*
 1708 *hand-held spectrometers (blue = CROPSCAN, red = SVC/ASD) and by destructive*
 1709 *sampling (black squares).*

1710

1711 Spectral data were collected during the summer season using a SVC at Parsonage
 1712 Down NNR and an ASD at Ingleborough NNR. The SVC/ASD, fitted with an 18° field
 1713 of view lens, was held 0.79 m high to take spectral measurements of four 0.25m
 1714 diameter patches within each quadrat. A tape measure was used to help hold the
 1715 SVC sensor at 0.79m high. The SVC/ASD collects 25 readings in quick succession,
 1716 providing the user with one averaged reading. To produce calibrated spectral
 1717 reflectance signatures (see Section 3.4.3.2) and account for rapid irradiance changes
 1718 in the field, measurement pairs alternating between the grassland and a white
 1719 reference panel (Spectralon, Labsphere, NH, USA) were collected. The four patch
 1720 spectral signatures were averaged into a single quadrat spectral signature. The

1721 Matrice UAV was flown over target fields to cover an area of ~200x200m. White
1722 reference sheets were placed along the tape measure near each quadrat so that the
1723 quadrats could be located easily in drone images. Grey and black reference images
1724 were placed on either end of the study site to help calibrate the Rikola camera.

1725

1726 ***UAV-mounted Rikola camera***

1727 A UAV with a mounted Rikola VNIR camera was flown across all three grasslands on
1728 the 25th June 2018 within two hours of solar noon at a height of ~100m. To ensure
1729 the quality of the spectral data being collected, the transects had to be set up to
1730 prevent contamination of the spectral signatures of the quadrats by adjacent objects
1731 (e.g. by the tape measure) and so that the Rikola VNIR camera could be calibrated.
1732 White reference panels were placed adjacent to the quadrats so that the quadrats
1733 could be identified in the drone imagery and for the purpose of calibration. Quadrats
1734 were placed 60cm away from the A3-sized white reference panels and the tape
1735 measure to prevent corruption of the spectral data collected on quadrats. Grey and
1736 black reference panels (1m²) were also placed on the outskirts of each field for the
1737 purpose of calibrating the Rikola camera. The Rikola camera was calibrated using a
1738 black reference panel before flight. Calibrated imagery collected by the UAV-mounted
1739 Rikola camera were processed (explained in detail in Section 3.4.3.4) to
1740 georeferenced the images, normalise their illumination, calculate the reflectance
1741 values for each pixel then finally extract averaged (mean) reflectance values for the
1742 1m² areas within each quadrat.

1743

1744

1745

1746

1747 **3.4. Data pre-processing**

1748 **3.4.1. Grassland condition: converting a qualitative measure** 1749 **into a quantitative gradient**

1750 The partial least square regression (PLSR) model requires a continuous response
 1751 variable, so using mass (in g) and % cover as grassland variable responses is valid.
 1752 However, condition, as defined in the UK by the Common Standards Monitoring
 1753 (CSM) guidance booklets (i.e. National Vegetation Classification, NVC) (JNCC, 2004;
 1754 2006) is a qualitative and discrete measure established using grassland type specific
 1755 criteria. Therefore, instead of pursuing an approach which caters for a range of
 1756 response variable types (categorical, nominal, etc.) and has options to address
 1757 multicollinearity such as a penalised generalised linear model (Nelder and
 1758 Wedderburn, 1972) or a penalised generalised additive model approach (Hastie and
 1759 Tibshirani, 1986) this condition measure was simply converted to a continuous form
 1760 for direct use as the response with PLSR.

1761 The seven chosen grasslands were classified using the NVC system, before their
 1762 condition was determined, as each grassland type has its own set of condition-related
 1763 criteria in the CSM guidelines. To classify each grassland, species abundance data
 1764 collected on the ten quadrats established on each grassland were analysed using
 1765 MAVIS software (Smart et al., 2016) which gave each grassland a NVC category.
 1766 CSM guidelines (JNCC, 2004; 2006) were then used to determine how closely
 1767 related each quadrat was to the guidelines for the NVC category of that particular
 1768 grassland, except for relatively improved grasslands which were compared to the
 1769 guidelines for MG5 grasslands. Species abundance, % cover of grassland variables
 1770 and grass height measurements were compared to the NVC-specific condition criteria
 1771 in the CSM guidelines for every quadrat (summary of criteria provided in Table 3.5). A
 1772 “good” rating was given for each criterion met or a “bad” rating was given otherwise.
 1773 For example, if forb cover of 40-90% was a criterion then a “good” rating would be
 1774 given if forb cover is 50% but a “bad” rating would be given if forb cover is 20%. The
 1775 good:bad ratio was determined for each quadrat by calculating the ratio of the
 1776 number of “good” and “bad” criteria. This ratio became resultant CSM-condition
 1777 variable and had a continuous range from 0 to 1. No weighting was given to particular
 1778 criteria, so each criterion contributed equally to the good:bad ratio. Each NVC
 1779 category had a different set of criteria meaning that a different number of criteria were

1780 referred to for each target grassland. Furthermore, some guidelines were not used as
 1781 data were not available for this purpose such as signs of grazing.

1782

1783 *Table 3.5: Provides information related to how the NVC of each quadrat (and*
 1784 *therefore each grassland) was determined. This includes the alphanumerical*
 1785 *identification code of the criteria that was applied, criteria within that classification that*
 1786 *were applied, and criteria that it was not possible to apply because of a lack of data.*

Grassland	Grassland criteria applied	Criteria used	Criteria not used
CG2b	CG2 10 criteria	>30% and <90% forb cover, <5% scrub cover, <25% dead material cover, <5% bare ground cover, average height >2cm and <50cm, two or more positive indicator species, <20% agricultural species cover and <10% cover by any one agricultural species, <20% cover by rank grasses and sedges plus <10% cover for <i>Arrhenatherum</i> and <i>Dactylis</i> species, <=5% agricultural weeds, no introduced species	Extent, scrub and trees plus bracken, local distinctiveness
CG10a	CG10 8 criteria	<33% forb cover, <10% scrub cover, <10% dead material cover, <10% bare ground cover, <10% <i>Juncus effuses</i> cover, <25% <i>Ranunculus repens</i> and <i>Bellis perennis</i> cover, at least two positive species indicators	Extent, <1% non-native species, grazing indicators

		present, <1% negative species cover	
M19a	M19 7 criteria	<10% scrub cover, disturbance: <10% bare ground cover plus <10% damaged <i>Sphagnum</i> species cover, at least six positive species indicators present, <i>Sphagnum fallax</i> is not the only <i>Sphagnum</i> species, >50% cover for at least three indicator species, <1% negative species cover, no signs of burning	Extent, indicators of browsing (e.g. shrub grazing), peat erosion, <75% Ericaceous species cover, <1% non- native species
MG5b MG6b MG6c	MG5 7 criteria	>40 and <90% forb cover, <5% scrub cover, <25% dead material cover, <5% bare ground cover, at least two positive species indicators present, agriculturally favoured species cover and rank grasses and sedges cover: <10% for one species or <20% collectively, <5% agricultural weeds cover	Extent, height

1788 **3.4.2. Processing response data before model training**

1789 **3.4.2.1. Test for normality**

1790 One assumption made when using a linear regression approach such as PLSR is
 1791 that there is a normal distribution of errors. Furthermore, the results of PLSR can be
 1792 considered unreliable if affected by error heteroscedasticity. These issues can be
 1793 addressed by transforming non-normal response data (Meyer et al., 2019; Ripley et
 1794 al., 2019). As many of the grassland variable data sets appeared to be skewed based
 1795 on a subjective assessment of distribution graphs, a Shapiro-Wilk test for normality
 1796 was applied to quantitatively assess whether the distribution of each data set was
 1797 normal.

1798 The W value is calculated as:

1799

$$1800 \quad W = b^2 \div SS \quad (\text{eq. 3.1})$$

1801 Where:

1802

$$1803 \quad b = \sum_{i=1}^m a_i (x_{n+1-i} - x_i) \quad (\text{eq. 3.2})$$

1804

1805 With m being $n \div 2$ if n is even, or $(n-1) \div 2$ if n is odd, and:

1806

$$1807 \quad SS = \sum_{i=1}^n (x_i - \bar{x})^2 \quad (\text{eq. 3.3})$$

1808

1809 The closer the W value is to 1, the more normal the distribution is considered to be
 1810 although it is possible for values >0.95 to be applied to distributions that are clearly
 1811 non-normal subject to the sample size (Shapiro and Wilk, 1965). A p-value
 1812 (probability associated with W value) is also calculated, where the null hypothesis of
 1813 normal data distribution is rejected if $p < 0.05$. In the context of this thesis, response

1814 data were considered to be significantly skewed if the results of a Shapiro-Wilk test
1815 (Shapiro and Wilk, 1965) produced a p-value of <0.05 (i.e. at the 95% level).

1816 A one sample Kolmogorov-Smirnov test, Lilliefors test or an Anderson-Darling test
1817 could have been used for the same purpose (Razali and Wah, 2011). The one
1818 sample Kolmogorov-Smirnov test and related Lilliefors test compares the distribution
1819 of a given data set against an ideal normal distribution with the null hypothesis that
1820 the data set being analysed is from a normally distributed population. This is
1821 achieved by calculating the observed values against the expected cumulative relative
1822 frequencies that would exist if the data set followed an ideal normal distribution. The
1823 Kolmogorov-Smirnov test and Lilliefors test differ in the calculations made in
1824 determining whether the null hypothesis is rejected. The Anderson–Darling test
1825 evaluates whether a sample comes from a defined distribution, which in this context
1826 is a normal distribution (Razali and Wah, 2011). Although all tests achieve the same
1827 purpose and had no clear advantage in the context of this study, the Shapiro–Wilk
1828 test was chosen as it is considered to be the most powerful (Razali and Wah, 2011).

1829 One disadvantage of all aforementioned tests is that they are less powerful on small
1830 sample sizes, where the term “small sample sizes” has not been quantified.
1831 Therefore, it is not clearly defined whether the sample sizes used in this study
1832 constitute “small sample sizes”. It has been stated that the Shapiro–Wilk test requires
1833 relatively few samples to give reliable results but the recommendation is to use at
1834 least 50 samples (Razali and Wah, 2011) while Royston (1995) explains that any
1835 sample size between 3 and 5000 is viable for analysis using the Shapiro–Wilk test.
1836 This study used less than 50 samples for most analyses (10, 30, 40 or 90) where the
1837 Shapiro-Wilk test was still the more powerful than comparable tests (Razali and Wah,
1838 2011) but it was not made unambiguously clear if this sample size is sufficient for
1839 reliable results in this particular study. Also, the Shapiro–Wilk test is known not to
1840 work well in samples with many identical values (Shapiro and Wilk, 1965). This was
1841 the case when using bare ground for all grasslands and CSM-condition for
1842 Grasslands 1 and 6 as response variables in this thesis for example.

1843

1844 **3.4.2.2. Transformation of response variables**

1845 Response data that were not considered to have a Gaussian distribution after a
1846 Shapiro-Wilk test were transformed before PLSR analysis to help address the

1847 assumption of a normally distributed error term made by the PLSR analyses and to
 1848 address the issue of error heteroscedasticity. A log transformation was applied to the
 1849 response data if the response distribution was right- or left-skewed respectively,
 1850 where left-skewed response data were “reflected” before transformation (Meyer et al.,
 1851 2019; Ripley et al., 2019). Compositional data were also log transformed to remove
 1852 the constraints on data (i.e. 0-100% for cover data) and to account for the non-linear
 1853 relationship between spectral data and the condition-related variables chosen for this
 1854 thesis. An optimising constant (c) was included to optimise the transformation by
 1855 taking the extent of the skew into consideration (Meyer et al., 2019; Ripley et al.,
 1856 2019). The equation is:

1857

$$1858 \qquad \qquad \qquad \log(x + c) \qquad \qquad \qquad (\text{eq. 3.4})$$

1859

1860 Although log transforming compositional data helps deal with issues related to using
 1861 compositional data in regression analyses, using a log ratio transform before
 1862 regression (Aitchison, 1982) or using beta regression (Douma and Weedon, 2018)
 1863 would be a more effective but less generic approach to transforming response data.

1864

1865 **3.4.3. Grassland reflectance**

1866 **3.4.3.1. CROPSCAN data processing**

1867 Incoming and reflected irradiance data were collected by the CROPSCAN, then
 1868 converted to millivolt quantities which were stored in the data logger. To calculate
 1869 percent reflectance, the software makes sensor sun angle cosine corrections and
 1870 temperature corrections to the millivolt readings. Corrections for temperature are
 1871 necessary as dark readings (millivolts with no irradiance) and responsivity (millivolts
 1872 per watts/m² of irradiance) are affected by differences in temperature. Cosine
 1873 corrections are made to account for the sun angle using information on date, time,
 1874 latitude and longitude. The end product of converting and correcting raw millivolt data
 1875 is a CSV file with reflectance values for each of the sixteen bands collected at each
 1876 data with associated dates and times of data collection (CROPSCAN Inc., 2018).

1877 Some of the spectral data collected with the CROPSCAN during the spring fieldwork
1878 campaign used an incorrect hardware setup meaning that the spectral data were
1879 incorrectly calibrated. To account for this, data were collected using a CROPSCAN
1880 with the correct and the same incorrect setup used in Parsonage Down along the
1881 same 50m transect on a grassland in Oxfordshire (UK). The two spectral data sets
1882 were then compared to see if there was a consistent difference between comparable
1883 bands along the transect. As the spectral data collected on the same transect was
1884 consistently different between the correct and incorrect setup, a coefficient was
1885 calculated on each wavelength by calculating the difference in reflectance between
1886 the correct and incorrect setup. This coefficient was then applied to the incorrectly
1887 calibrated CROPSCAN data collected during spring at Parsonage Down NNR.

1888

1889 **3.4.3.2. ASD data processing**

1890 Binary files were converted to ASCII files, then absolute reflectance calculated for
1891 each band on each data point using white reference data for calibration using Excel
1892 with prepared macros provided by the Field Spectroscopy Facility. The water
1893 absorption bands (1350-1460nm and 1790-1960nm) were then removed as these
1894 bands have a signal to noise ratio too low for these data to be viable. After this, it was
1895 found that the integrity of these data had been compromised by the difficult weather
1896 conditions experienced at Ingleborough NNR so it was decided not to use these
1897 spectral data in analysis.

1898

1899 **3.4.3.3. SVC data processing**

1900 Raw data collected using the SVC were saved in the device as .sig files. An Excel
1901 spreadsheet with prepared macros was provided by the Field Spectroscopy Facility to
1902 calculate absolute reflectance for each measurement using paired white reference
1903 and target data. These calibrated reflectance values for 1024 bands are then
1904 interpolated across the spectral range of 350-2500nm to produce a reflectance
1905 spectral signature for every nanometre in the 350-980nm range and every two
1906 nanometres in the 980-2500nm range. Then the atmospheric water absorption bands
1907 were removed (1350-1520nm & 1790-1960nm) due to their low signal to noise ratio,
1908 leaving 1249 bands.

1909

1910 3.4.3.4. Rikola VNIR imagery processing

1911 To prepare the Rikola VNIR imagery for analysis, several processing steps were
1912 necessary; which included pre-processing (calibration), georeferencing the images,
1913 normalising the images for illuminance, calculating reflectance, autoscaling the
1914 reflectance values then extracting the reflectance values for analysis.

1915

1916 *Pre-processing (calibration)*

1917 Multispectral images collected using the Rikola camera were calibrated using Rikola
1918 Hyperspectral Imager v2.1 software. Readings were taken from a black reference
1919 panel prior to each flight, which was used as a dark reference that the drone images
1920 were calibrated against. The results of pre-processing were stacks of multispectral
1921 images of reflected irradiance values, each image representing data collected on a
1922 wavelength.

1923

1924 *Georeferencing*

1925 As a drone collects images on a target grassland, data on each band are not
1926 collected simultaneously for each image meaning that these bands are not
1927 georeferenced against each other. The georeferencing of images is necessary to
1928 ensure that spectral data truly represent a particular space such as a quadrat. Firstly,
1929 Environmental for Visualising Images (ENVI) software was used to separate each
1930 multispectral image into 30 mono-band images. ArcGIS v10.6 was then used to align
1931 the 30 images to each other. These images were then “stacked” to produce a
1932 georeferenced multispectral image.

1933

1934 *Normalising illumination*

1935 Despite drone imagery being collected at Parsonage NNR in clear sky conditions
1936 within two hours of solar noon, some parts of the drone imagery had far higher
1937 illuminance relative to other parts of the imagery. This within-image variance in

1938 illuminance is related to the solar zenith angle and the view angle of the camera (Roy
 1939 et al., 2016) and can make the results of regression analysis erroneous as the
 1940 predicted response values can simply be a reflection of illuminance values. To ensure
 1941 the integrity of the results of PLSR statistical modelling, images were normalised
 1942 against a column of pixels that represented the average illuminance for the image
 1943 using R software (v. 3.5.1).

1944

1945 ***Calculating reflectance values***

1946 R software (v. 3.5.1) was used to calculate the reflectance of each pixel value
 1947 (radiance) for all images. As reflectance is the proportion of radiation not absorbed or
 1948 transmitted, the following equation was applied to each pixel value:

1949

$$1950 \quad P_{ref} = P_{rad} \div R_{rad} \times R_{ref} \quad (\text{eq. 3.5})$$

1951

1952 Where P_{ref} refers to pixel reflectance, P_{rad} refers to pixel radiance, R_{rad} refers to
 1953 radiance from a reference panel and R_{ref} refers to reflectance from a reference panel.
 1954 Reference panel readings were taken using a SVC on a grey panel.

1955

1956 ***Extracting quadrat reflectance data from the images***

1957 To train PLSR statistical models using spectral reflectance as predictors, reflectance
 1958 values calculated from Rikola imagery had to be extracted from each quadrat. Once
 1959 the processing of Rikola images had been completed to produce georeferenced
 1960 pixels of reflectance values, reflectance values were extracted from all 30 quadrats
 1961 set up in Parsonage Down NNR during the summer fieldwork campaign. Using ENVI
 1962 software, a “region of interest” was established on top of each 1m^2 quadrat which
 1963 calculated the average reflectance values for each band using all of the 6cm^2 pixel
 1964 values within. These average values were extracted for use as training data for PLSR
 1965 statistical models. Taking the average value was considered to be the simplest viable
 1966 approach and the most comparable with other literature, but other calculations can be
 1967 utilised instead such as the variation, maximum value and minimum value.

1968

1969 **3.4.3.5 Scaling of reflectance data**

1970 Prior to applying PLSR, autoscaling was used to scale spectral reflectance data to a
 1971 mean of zero and a standard deviation of one at each spectral band (Farrés et al.,
 1972 2015; Wold et al., 2001) for data collected with all spectral devices used in this thesis.
 1973 Autoscaling is defined as:

1974

$$1975 \quad \tilde{x}_{ij} = \frac{x_{ij} - \bar{x}_i}{s_i} \quad (\text{eq. 3.6})$$

1976

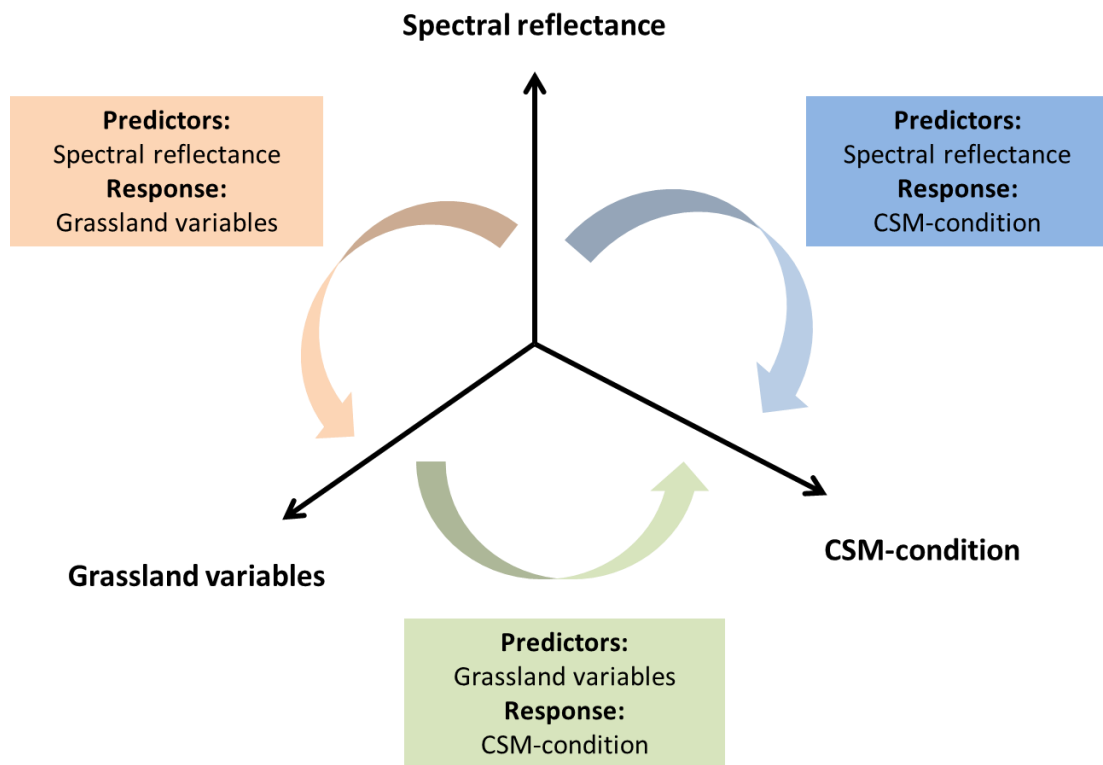
1977 Where the average of all spectral values for a quadrat is taken away from the spectral
 1978 value, then this value is divided by the standard deviation of all spectral values for a
 1979 quadrat to get the autoscaled value. Autoscaling addresses assumptions made when
 1980 using PLSR (Farrés et al., 2015; Wold et al., 2001) by de-emphasizing the relatively
 1981 higher and highly variable values in the near and short wave-infrared regions of the
 1982 EM spectrum (van den Berg et al., 2006; Haaland and Thomas, 1988) and also
 1983 prevents the results of the VIP analyses (explained in Section 3.5.2.1) from being
 1984 biased. One alternative is to use range scaling which is sensitive to outliers. Another
 1985 option is Pareto scaling which is sensitive to large fold changes, i.e. differences
 1986 between the values of the predictors.

1987

1988 **3.5. Analytical methods**

1989 The overarching approach (summarised in Figure 3.7) was to apply partial least
 1990 squares linear regressions between grassland reflectance, grassland variables and
 1991 condition data to explore the strength of the relationships between (1) grassland
 1992 reflectance and grassland CSM-condition, (2) grassland reflectance and grassland
 1993 variables and (3) grassland variables and grassland CSM-condition. This approach
 1994 was designed to establish if there is a consistent relationship between grassland
 1995 reflectance and grassland CSM-condition and which of the chosen grassland
 1996 variables are more likely to contribute to this relationship. In other words, can

1997 grassland variables form the basis for remotely sensed based approaches to
 1998 monitoring grassland condition? And which grassland variables are the most
 1999 suitable?



2000

2001 *Figure 3.7: Schematic of overarching approach used to establish if remote sensing*
 2002 *can be used to determine grassland condition and to identify which spectral bands*
 2003 *and which grassland variables are particularly suited for condition monitoring using*
 2004 *remote sensing.*

2005

2006 **3.5.1. Testing for significant difference of grassland variables** 2007 **between grassland sites**

2008 Botanical experts provided support in selecting the target grasslands, one reason for
 2009 selecting them is that the grasslands should be as different in their characteristics as
 2010 possible to represent a range of different grassland types. It was hypothesised that
 2011 these different characteristics would be reflected in significantly different quantities of
 2012 grassland variables. For example, an undergrazed acid mire grassland will have

2013 significantly different quantities of graminoids compared to an overgrazed alkaline
 2014 grassland. A Wilcoxon rank sum test (a.k.a. Mann-Whitney U test) (Bauer, 1972) is a
 2015 non-parametric test for significant difference between the medians of two
 2016 independent data sets. This method was used to establish whether there were
 2017 significant differences between grassland sites in terms of the grassland variable
 2018 distributions. Differences were considered significant if $p \leq 0.05$ (i.e. at the 95%
 2019 level). A non-parametric method was chosen as almost all of the mass and % cover
 2020 data sets were found to have a non-normal distribution by the Shapiro-Wilk test
 2021 (Whitley and Ball, 2002). The two-sided version of the test does not suggest the
 2022 directionality if two data sets are deemed to be different, which was considered
 2023 advantageous when dealing with a combination of left-skewed and right-skewed data.
 2024 This approach was chosen as the data sets being compared were not matching (as
 2025 the data being compared was collected on different grasslands), ruling out the use of
 2026 analyses such as the Sign test or Wilcoxon Signed Rank Test (Whitley and Ball,
 2027 2002). Also, data sets were compared against each other (i.e. between two
 2028 grasslands) meaning that analyses that compare groups of data sets and produce
 2029 one result such as a Kruskal-Wallis test were not considered appropriate.

2030 Boxplots showing the mass or % cover of grassland constituents for each grassland
 2031 were produced to visualise the differences in distribution. To test for significant
 2032 differences in the values of each grassland variable between different grasslands, an
 2033 unpaired two-sample Wilcoxon test was applied using R software (version 3.4.2 or
 2034 3.5.1). This non-parametric method, which compares the medians of each data set,
 2035 can be applied to skewed data to compare two independent groups of samples. The
 2036 equation is as follows:

2037

$$2038 \quad U_1 = n_1 n_2 + n_1 (n_1 + 1) / 2 - R_1 \quad (\text{eq. 3.7})$$

2039

2040 And:

2041

$$2042 \quad U_2 = n_1 n_2 + n_2 (n_2 + 1) / 2 - R_2 \quad (\text{eq. 3.8})$$

2043

2044 Where n is the sample size and R is the sum of ranked values. The smaller of the U
 2045 values from the two sets of samples is chosen. A U value closer to zero suggests that
 2046 the null hypothesis can be rejected, but this can only be done after comparing the U
 2047 value against a table of significant U values. The significant U value depends on the
 2048 sample size and the alpha value chosen (default is 0.5 which is the equivalent of the
 2049 95% level). If U is equal to or less than the significant U value then the null
 2050 hypothesis, which in this case is that the mass or % cover of grassland variables
 2051 between two grasslands is not significantly different, can be rejected.

2052

2053 **3.5.2. Partial least squares regression**

2054 In the context of this thesis, multicollinearity can occur when spectral bands or
 2055 grassland variable values (i.e. predictors) can be predicted to a high degree of
 2056 accuracy by other spectral bands or grassland variables. The use of redundant
 2057 variables (i.e. multicollinear variables) increases the likelihood of model overfitting
 2058 (Wold et al., 2001). Therefore, it was deemed important to consider a statistical
 2059 modelling approach that helps deal with the issues of multicollinearity and model
 2060 overfitting.

2061 Firstly, to test whether a predictor decomposition approach such as PLSR was
 2062 necessary, correlation matrices were produced to test the strength of multicollinearity
 2063 between predictors. It was deemed that an approach such as PLSR would be
 2064 necessary to deal with multicollinearity if there were any significant correlations. This
 2065 is important as weak correlations would suggest a PLSR methods would not be worth
 2066 following and a less complex modelling approach such as an ordinary least squares
 2067 (OLS) regression would suffice (i.e. standard regression). Results were considered
 2068 significant if the correlation coefficient value (r) came within the ranges of $r > +0.8$ or r
 2069 < -0.8 and was accompanied with by a P value ≤ 0.05 .

2070 As it was deemed necessary to choose a method that helped overcome the issues of
 2071 multicollinearity and overfitting (See Figure 4.1, Section 4.4.1); partial least squares
 2072 regression (PLSR), also called projection of latent structures regression, was chosen
 2073 for analysis. PLSR (Wold et al., 2001) decomposes the predictor and response data
 2074 sets simultaneously into relatively few orthogonal components (latent variables) that
 2075 explain as much of the covariance between predictors and responses as possible. A
 2076 linear regression step then uses these components to predict the responses.

2077 The latent variables can also be referred to as X-scores which predict Y and model X.
 2078 X-scores can be denoted as t_a where $a = (1, 2...A)$ and A is the number of X-scores.
 2079 They are estimated as linear combinations of the original variables x_k with the
 2080 weighting coefficients w_{ka} where $k = (1...K)$ and K is the number of X variables. The
 2081 equation for t_a (or t_{ia} for one indexed object) is:

2082

$$2083 \quad t_{ia} = \sum_k W_{ka} X_{ik} \quad (\text{eq. 3.9})$$

2084

2085 The X-scores are multiplied by the loadings p_{ak} , which should represent good
 2086 summaries of X:

2087

$$2088 \quad X_{ik} = \sum_a t_{ia} p_{ak} + e_{ik} \quad (\text{eq. 3.10})$$

2089

2090 Where e_{ik} represents the X-residuals, which should be relatively small if the loadings
 2091 (p_{ak}) genuinely represents a good summary. To calculate the multivariate Y (y_{im}), Y-
 2092 scores (u_a) are multiplied by the weights c_{am} , g_{im} represents the Y-residuals:

2093

$$2094 \quad y_{im} = \sum_a u_{ia} c_{am} + g_{im} \quad (\text{eq. 3.11})$$

2095

2096 The X-scores are used as predictors of Y as follows:

2097

$$2098 \quad y_{im} = \sum_a c_{ma} t_{ia} + f_{im} \quad (\text{eq. 3.12})$$

2099

2100 The Y-residuals (f_{im}) express the deviations between the observed and modelled
 2101 responses. Because of Eq. 3.9, Eq. 3.12 can be rewritten to look like a multiple
 2102 regression model:

2103

$$2104 \quad y_{im} = \sum_a c_{ma} \sum_k w_{ka} x_{ik} + f_{im} = \sum_k b_{mk} x_{ik} + f_{im} \quad (\text{eq. 3.13})$$

2105

2106 The PLS-regression coefficients (b_{mk}) can be written as:

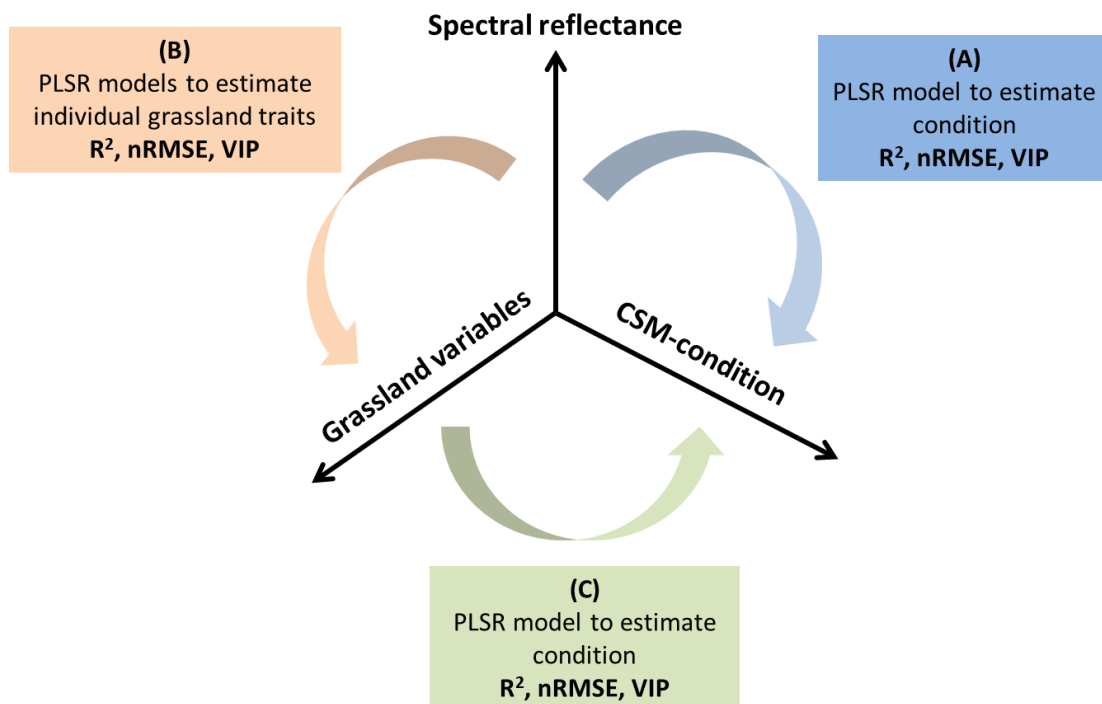
2107

$$2108 \quad b_{mk} = \sum_a c_{ma} w_{ka} \quad (\text{eq. 3.14})$$

2109

2110 These coefficients are used to calculate the fitted value(s) of the response variable.

2111 One advantage that PLSR has over regression methods that use PCA regression, or
 2112 a similar approach, is that PCA regression produces components from predictors that
 2113 explain as much of the variance of the predictors as possible before regression
 2114 analysis but does not utilise response data to establish the best way to predict as
 2115 much of the variance of the response data as possible. Another advantage to using
 2116 PLSR is that this analysis can be followed by a variable importance in projection
 2117 (VIP) analysis to determine which variables are most important in predicting the
 2118 response values. Spectral data were autoscaled (explained in Section 3.4.3.5) before
 2119 analysis. Although there are few studies that compare VIP to similar analyses, Farrés
 2120 et al. (2015) found that VIP projections were easier to interpret than selectivity ratio
 2121 projections (another test to ascertain which variables are most important in predicting
 2122 the response values, which is calculated as the ratio between the explained and the
 2123 residual (unexplained) variance for each variable) when dealing with mass
 2124 spectrometry data.



2125

2126 *Figure 3.8: Schematic showing the partial least squares regression (PLSR) approach*
 2127 *developed to establish if spectral data can be used to determine grassland condition*
 2128 *(A) and to identify which spectral bands (B) and which grassland variables (C) are*
 2129 *particularly suited for condition monitoring using spectral remote sensing. R^2 ,*
 2130 *normalised root mean square error (nRMSE) and variable importance in projection*
 2131 *(VIP) are used to evaluate and compare model performance.*

2132

2133 PLSR (Mevik et al., 2019; Wold et al., 2001) was used to assess the ability of spectral
 2134 data to predict grassland variables and CSM-condition (A and B in Figure 3.8), plus
 2135 the ability of grassland variables to predict CSM-condition (C in Figure 3.8). The
 2136 coefficient of determination (R^2) is an ‘in-sample’ measure that represents the % of
 2137 variance of the response variable explained by the regression model, and a leave-
 2138 one-out cross validation root mean square error (RMSE) is an alternative ‘out-of-
 2139 sample’ measure of the accuracy of the model (Wold et al., 2001). This thesis used
 2140 adjusted R^2 , which compensates for the addition of predictors by only increasing if the
 2141 new latent variable enhances the model more than what would be expected by
 2142 chance, which is defined as:

2143

$$R_{adj}^2 = 1 - \left(1 - \frac{\sum_i (y_i - \hat{y}_i)^2}{\sum_i (y_i - \bar{y})^2} \right) \frac{n-1}{n-p-1} \quad (\text{eq. 3.15})$$

2145

2146 Where y represents the measured values, \hat{y} represents the predicted values, \bar{y}
 2147 represents the average measured value, p represents the total number of explanatory
 2148 variables in the model and n represents the number of samples. To make the
 2149 performance of different PLSR models comparable, RMSE was normalised (nRMSE):

2150

$$nRMSE = 100 \frac{\frac{1}{N} \sum_{i=1}^N (S_i - O_i)^2}{sd(O_i)} \quad (\text{eq. 3.16})$$

2152

2153 Where S refers to the predicted values and O refers to the observed values. This
 2154 made different model runs comparable (Bigiarini, 2019). R^2 and nRMSE were used to
 2155 compare model performance between grassland sites. R^2 results were considered
 2156 strong ($R^2 > 0.7$), moderate (R^2 of 0.5-0.7) or weak ($R^2 < 0.5$) based on previous
 2157 literature (Capolupo et al., 2015; Doughty et al., 2011; Roelofsen et al., 2014) whilst
 2158 models with nRMSE > 100 were considered weak as models with this level of
 2159 prediction accuracy using true data are no more accurate than a model using
 2160 randomised data. Higher R^2 values and lower nRMSE values were considered to be
 2161 indicative of a better performing PLSR model. A linear regression approach to
 2162 predicting grassland variable values may underestimate the largest (Psomas et al.,
 2163 2011) or smallest values (Chen et al., 2009) as the relationship between spectral data
 2164 and grassland variables may not be linear.

2165 There are other analytical methods that help deal with overfitting and multicollinearity.
 2166 A few predictors can be manually selected (e.g. vegetation indices) or selected
 2167 through other analyses to reduce multicollinearity and make overfitting less likely.
 2168 This can be achieved by decomposing predictors into relatively few components prior
 2169 to regression (e.g. PCA) or by applying methods that incorporate the use of latent
 2170 variables other than PLSR such a penalised generalised additive modelling approach
 2171 (Dormann et al. 2013).

2172

2173 **3.5.2.1. Variable Importance in Projection**

2174 Variable Importance in Projection (VIP) coefficients can be used to calculate the
 2175 relative contribution of each predictor when predicting the responses (Farrés et al.,
 2176 2015; Wold et al., 2001). Farrés et al. (2015) defined the VIP score for j^{th} variable as:

2177

$$2178 \quad VIP_j = \sqrt{\frac{\sum_{f=1}^F w_{jf}^2 \cdot SSY_{f \cdot J}}{SSY_{total} \cdot F}} \quad (\text{eq. 3.17})$$

2179

2180 Where VIP_j is a measure of the global contribution of j variable in the complete PLSR
 2181 model, SSY_{total} is the total sum of squares explained of the responses, F is the total
 2182 number of components, w_{jf} is the weight value for j variable and f component and
 2183 squaring this is considered to give the importance of the j_{th} variable in each f_{th}
 2184 component, SSY_f is the sum of squares of explained variance for the f_{th} component
 2185 and J number of X variables. A more detailed explanation of the methods of VIP has
 2186 been provided by Wold et al. (2001) and Farrés et al. (2015).

2187 In the context of this study, VIP was used to identify key spectral bands for predicting
 2188 grassland variables plus condition (A and B in Figure 3.8) and key grassland
 2189 variables for predicting grassland condition (C in Figure 3.8). Spectral bands or
 2190 grassland variables with VIP coefficients $\Rightarrow 1$ were considered to be important
 2191 (Farrés et al., 2015).

2192

2193 **3.5.2.2. Model fit and validation**

2194 Leave-one-out cross validation (LOO-CV) was used to test the predictive ability of
 2195 each model (Mevik et al., 2019; Wold et al., 2001) where the RMSE values were
 2196 derived from LOO-CV then normalised (nRMSE) so that PLSR models were directly
 2197 comparable. To avoid overfitting, the number of latent variables (referring to the
 2198 PLSR components derived from the spectral bands) for each model run was
 2199 determined by the lowest prediction error sum of squares (PRESS) value.

2200 For each predictor to response combination, model validation was established by
 2201 calibrating a PLSR model m times where 80% of the quadrat data used for training
 2202 was chosen randomly for each model run. To establish m , first the binomial
 2203 coefficient was used to establish the maximum number of iterations of 80% of the
 2204 quadrat data without repetition or replacement for each combination of grasslands:

2205

$$2206 \quad m = \frac{n!}{r!(n-r!)} \quad (\text{eq. 3.17})$$

2207

2208 Where in this context n is the number of quadrats and r represents the sample size
 2209 which is set to 80%. Where analyses were conducted on individual grasslands (i.e. n
 2210 = 10 and $r = 8$), $m = 45$ but where grasslands were analysed collectively (such as
 2211 where all three Parsonage grasslands were analysed collectively), m was considered
 2212 to be too large to make computing the results realistic so m was limited to 1000 for
 2213 these analyses.

2214 As the variance in the training data means that there will also be variance in the fitted
 2215 models, the median of the resulting 45 or 1000 R^2 and 45 or 1000 nRMSE values
 2216 from the iterated PLSR model runs were used as the final results (i.e. a form of
 2217 bagging (Breiman, 1994), these will be called the iterated model runs or iterated
 2218 results from now on) to account for this variance and reduce the chance of overfitting.
 2219 A non-parametric method was used to calculate 99% confidence intervals of the R^2
 2220 and nRMSE results to capture the variability of the iterated model runs (see Section
 2221 3.5.2.3) (Campbell and Gardner, 1988).

2222 To establish if the resulting PLSR models (referred to as actual models) provided
 2223 predictions that are more accurate to that found by chance in a random case
 2224 (referred to as random models), PLSRs were run 44 or 999 more times for each
 2225 predictor to response combination, but with the response variable values randomly
 2226 assigned to a different set of predictors (referred to as random models). Then, the
 2227 median result of the actual models were ranked against the results of the 44 or 999
 2228 random models to establish its place in this ranking. If the actual model results were
 2229 placed in the top 5% most accurate fits, in this case where the results placed in
 2230 position 950 or above where $m = 1000$, then the actual model R^2 or nRMSE values
 2231 can be said to be significant at the 95% level.

2232

2233 **3.5.2.3. Confidence intervals (CIs)**

2234 Confidence intervals can be used to determine a range of values that have a set
 2235 probability (usually 95% chance) of including the population median. The following
 2236 equation was used to calculate the lower and upper confidence intervals:

2237

$$2238 \quad (n \div 2) - 2.58 \times (\sqrt{n} \div 2) \quad (\text{eq. 3.18})$$

$$2239 \quad 1 + (n \div 2) + 2.58 \times (\sqrt{n} \div 2) \quad (\text{eq. 3.19})$$

2240

2241 In this study, confidence intervals were calculated with 99% confidence to capture the
 2242 variability of the iterated PLSR runs meaning that there is a 1% chance that the
 2243 population median would be outside of the calculated range of values. A relatively
 2244 narrow CI range suggests greater precision of the sample statistic as an estimate of
 2245 the overall population value (Campbell and Gardner, 1988). In the context of this
 2246 study, a narrower CI range suggests that the median value of the iterated PLSR runs
 2247 is more representative of all 45 or 1000 results. In other words, the distribution of the
 2248 iterated R^2 and nRMSE results is relatively narrow.

2249

2250 **3.5.2.4. Coefficient of variation**

2251 To test the stability and consistency of the PLSR model runs, the coefficient of
 2252 variation (CV) was calculated for all of the model runs for each grassland variable
 2253 and for CSM-condition to highlight which of these responses produced the most
 2254 consistent (strong or weak) R^2 and nRMSE results. The equation for calculating CV
 2255 is:

2256

$$2257 \quad CV = \frac{\sigma}{\mu} \times 100 \quad (\text{eq. 3.20})$$

2258

2259 In practical terms, this approach would highlight any grassland variables including
 2260 CSM-condition that could be consistently predicted (or not predicted) across
 2261 grasslands, seasons and when using different spectral devices.

2262

2263 3.6. Summary of the main chapters

2264 Where and when spectral data were successfully collected, and with which devices,
 2265 influenced which data sets were utilised for each of the main chapters in this thesis.
 2266 While the main analytical approach remained the same, reflectance data were
 2267 combined in different ways with the other data sets in the next three chapters. Table
 2268 3.6 summarises the main characteristics of each study.

2269

2270 *Table 3.6: Summarises some of the characteristics of the data sets used in the main*
 2271 *chapters of this thesis. This includes where data were collected, which season, which*
 2272 *spectral devices were used and the scale of the data collection.*

Chapter	Locations	Seasons	Spectral devices	Sample sizes (n)	Scale
Chapter 4	Ingleborough NNR Parsonage NNR	Summer-Jun'17 Summer-Jun'18	CROPSCAN*	10, 30, 40 or 70	1m ²
Chapter 5	Parsonage NNR	Spring-Apr'18 Summer-Jun'18 Autumn-Sep'18	CROPSCAN*	10, 30, or 90	1m ²
Chapter 6	Parsonage NNR	Summer-Jun'18	CROPSCAN*, Rikola camera & and SVC +	10 or 30	1m ² and 200x1m

*CROPSCAN data were successfully collected during the summer 2017 at Ingleborough NNR and during 2018 for all three seasons at Parsonage NNR.
 + During summer 2018, good quality SVC spectral data were collected at Parsonage NNR, on 28 of 30 quadrats.
 & Good quality Rikola camera imagery was also collected during summer 2018 at Parsonage NNR.

2273

2274 All three studies utilised traditional (mass, % cover) data and CROPSCAN spectral
2275 data collected on three grasslands at Parsonage Down NNR during the summer
2276 season. All studies also used PLSR, VIP and CV to understand which grassland
2277 variables (including CSM-condition) can be predicted with a reasonable level of
2278 accuracy and precision using scaled spectral data as predictors plus whether
2279 unscaled grassland variables can predict CSM-condition with acceptable accuracy
2280 and precision (Question 4, see Section 1.2 for list of questions). The impact of using
2281 mass or % cover variables on the results was also investigated across all three
2282 studies (Question 5). In addition, all models trained in each study were compared
2283 with models trained with randomised data to test if the models have stronger
2284 predicting power than models trained with randomised data.

2285 VIP was used to understand which spectral bands, when used as predictors, had
2286 predictive power considered significant ($VIP \Rightarrow 1$) when predicting grassland
2287 variables and CSM-condition, plus which grassland variables had significant
2288 predictive power when predicting CSM-condition (Questions 6 and 8). One reason for
2289 this analysis was to help establish whether access to reflectance recorded across a
2290 broader range of the spectrum, where SWIR spectral values are included, instead of
2291 only utilising the visible and near-infrared (NIR) spectrum to successfully predict
2292 grassland variables and CSM-condition.

2293 The first study (Chapter 4) also uses data collected on four grasslands at
2294 Ingleborough NNR during the summer, meaning that data from seven grasslands
2295 within the summer season were analysed. This study was conducted to investigate
2296 (Question 1) whether the chosen grassland variables form the basis for RS- based
2297 grassland condition monitoring and, related to this, whether these grassland variables
2298 are the most suitable for estimating grassland condition on a range of different
2299 grassland types? The second study (Chapter 5) uses data collected during spring,
2300 summer and autumn on three grasslands at Parsonage Down NNR, to investigate
2301 (Question 2) the relationship between reflectance and grassland variables plus CSM-
2302 condition across the growing seasons. This study also explores which time of the
2303 year is most effective for RS based CSM-condition monitoring or if using reflectance
2304 data from three seasons would be more effective. The third study (Chapter 6)
2305 consists of two parts. The first part compliments the VIP analysis by comparing the
2306 predictive power of models trained with spectral data from three different spectral
2307 devices (Questions 3 and 7). The second part tests whether models trained with data

2308 from all three grasslands and using CROPSCAN data as predictors can be
2309 extrapolated from patch level (1m²) to field level (200x1m).

2310

2311 **3.6.1. Varying sample information within and across sites**

2312 In order to assess the effects of combining datasets and how sample size may
2313 change results, while at the same time potentially contaminating the PLSR fit with
2314 data representing different processes as a consequence of using data from different
2315 grassland types, the PLSR models were fitted using combined data. For the first
2316 study (Chapter 4), these data consisted of: (1) both locations (where all seven
2317 grassland sites are analysed together: 70 quadrats), (2) one NNR location at a time
2318 (analysing data from four Ingleborough NNR sites: 40 quadrats or three Parsonage
2319 NNR sites: 30 quadrats), and (3) each individual grassland site (analysis of 10
2320 quadrats in each of the seven sites). Thus sample size is one of $n = 10, 30, 40$ or 70 .
2321 For the second study (Chapter 5), the PLSR models were fitted using combined data
2322 consisting of all three grasslands collectively (30 quadrats per season) and each
2323 individual grassland site (10 quadrats per season). Also, PLSR models were fitted
2324 with data from all three seasons (30 quadrats per grassland, 90 quadrats for all
2325 grasslands) or from one season (10 quadrats per grassland where data were
2326 collected during spring, summer or autumn). Therefore, the sample size is one of $n =$
2327 $10, 30,$ or 90 . For the third study (Chapter 6), PLSR models were fitted with data from
2328 all three Parsonage sites or each individual grassland site ($n = 10$ or 30).

2329

2330 **3.7. Summary of the methods**

2331 This chapter has provided details of the approach taken in this thesis to assess the
2332 condition of grasslands using RS techniques, addressing each of the questions
2333 specified at the beginning of this chapter. Grasslands were defined in the context of
2334 this thesis and a description of the study sites provided. Details were also provided
2335 on which data sets were collected, how those data were collected and how those
2336 data were analysed.

2337 To address Questions 1, 2 and 5 posed in Section 1.2, data were collected from
2338 seven grassland sites across two locations that represent a range of grassland types,

2339 grazing regimes and improvement levels; data were successfully collected over three
2340 seasons on three grasslands at Parsonage NNR and during the summer on four
2341 grasslands at Ingleborough NNR. On each of these seven grasslands, a 200m
2342 transect was set up and ten quadrats (1m²) placed along it at random. On each
2343 quadrat, the following data sets were collected then utilised in analysis: species
2344 abundance, the mass and % cover of grassland variables, grass height and spectral
2345 data. Species abundance, the % cover of grassland variables and grass height were
2346 used to define a quantitative metric considered representative of grassland condition
2347 which was labelled “condition”. To address Question 3, a CROPSCAN was used to
2348 collect spectral data along the entirety of each transect (200 x 1m² grass patches)
2349 and a UAV-mounted Rikola VNIR camera collected multi-band imagery on all seven
2350 grasslands

2351 To address Questions 4 and 5, PLSR was used to assess the link between spectral
2352 data (predictors) and grassland variables including CSM-condition (responses) plus
2353 the link between grassland variables (predictors) and CSM-condition (response).
2354 When spectral data were used as predictors; different spectral devices were used, or
2355 the SWIR part of the spectrum was removed before analysis, to test whether using
2356 the full spectral range made available by some spectral devices is required to
2357 successfully monitor grassland condition (addressing Questions 6 and 7). VIP was
2358 used to highlight which spectral wavelengths were significantly important in predicting
2359 grassland variables including CSM-condition plus which grassland variables were
2360 significantly important in predicting CSM-condition (addressing Question 8). The CV
2361 for the iterated model runs identified which grassland variables including CSM-
2362 condition could be consistently predicted (or not predicted) across grasslands,
2363 seasons and when using different spectral devices.

2364 **Chapter 4 - Assessing the condition**
2365 **of semi-natural grasslands using**
2366 **CROPSCAN field radiometry at**
2367 **patch level (1m²)**

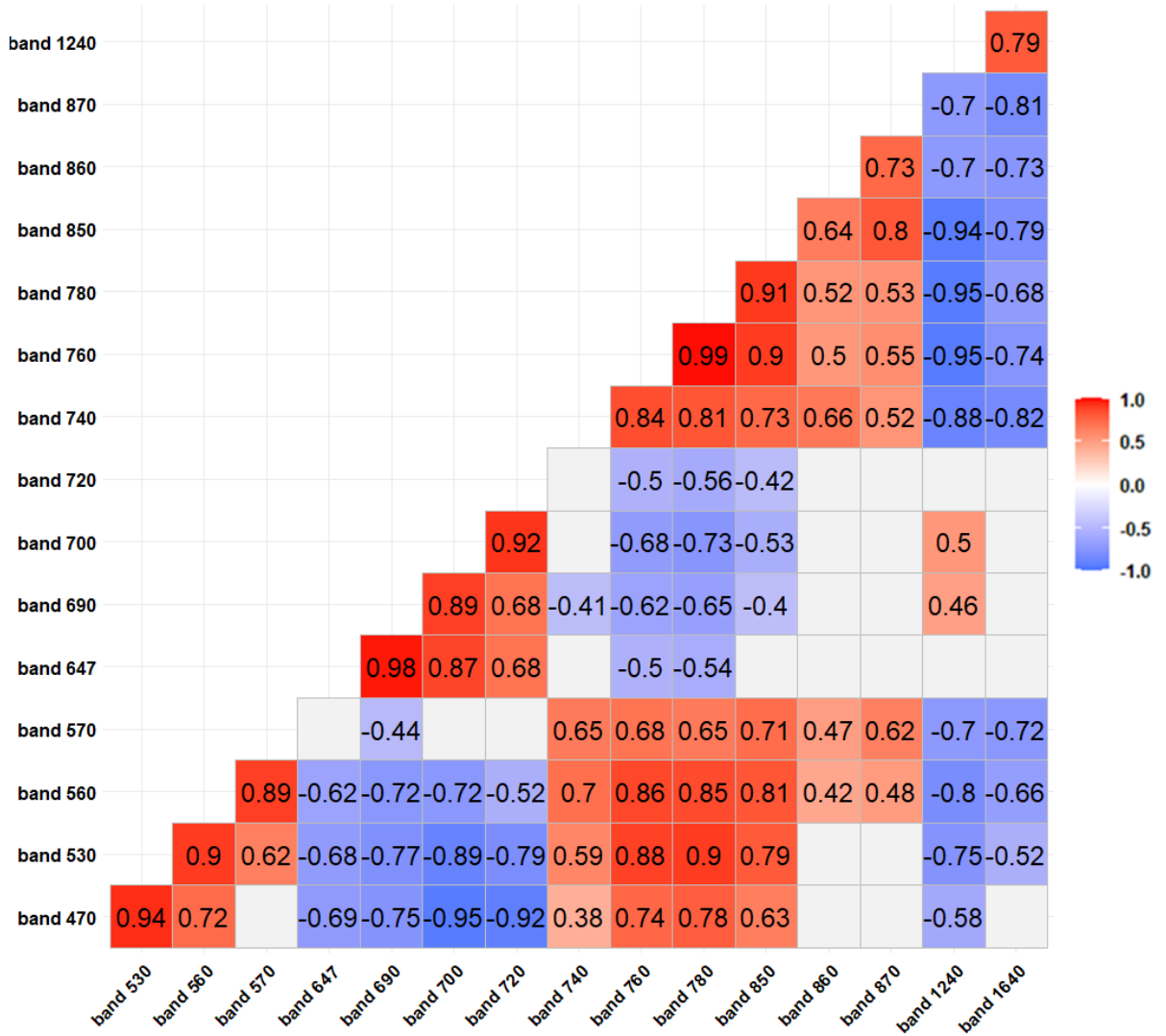
2368 **4.1. Predictor correlation matrices**

2369 Correlation matrices (Figure 4.1 and Appendix Figures 1 and 2) were produced to
2370 investigate whether there were strong correlations between the spectral bands used
2371 as predictors in some PLSR models and also between the grassland variables used
2372 as predictors in other PLSR models using the data sets used for each of the main
2373 chapters in this thesis. Figure 4.1 presents correlation matrices which used the
2374 smallest sample size as an example, where the correlations were found using data
2375 from Parsonage grasslands collected during the summer only (30 quadrats, data set
2376 used in Chapter 6). The correlation plots presented in Appendix Figures 1 and 2 used
2377 data collected during summer from seven grasslands across two locations (70
2378 quadrats, data set used in Chapter 4) and from Parsonage grasslands collected
2379 across three seasons (90 quadrats, data set used in Chapter 5).

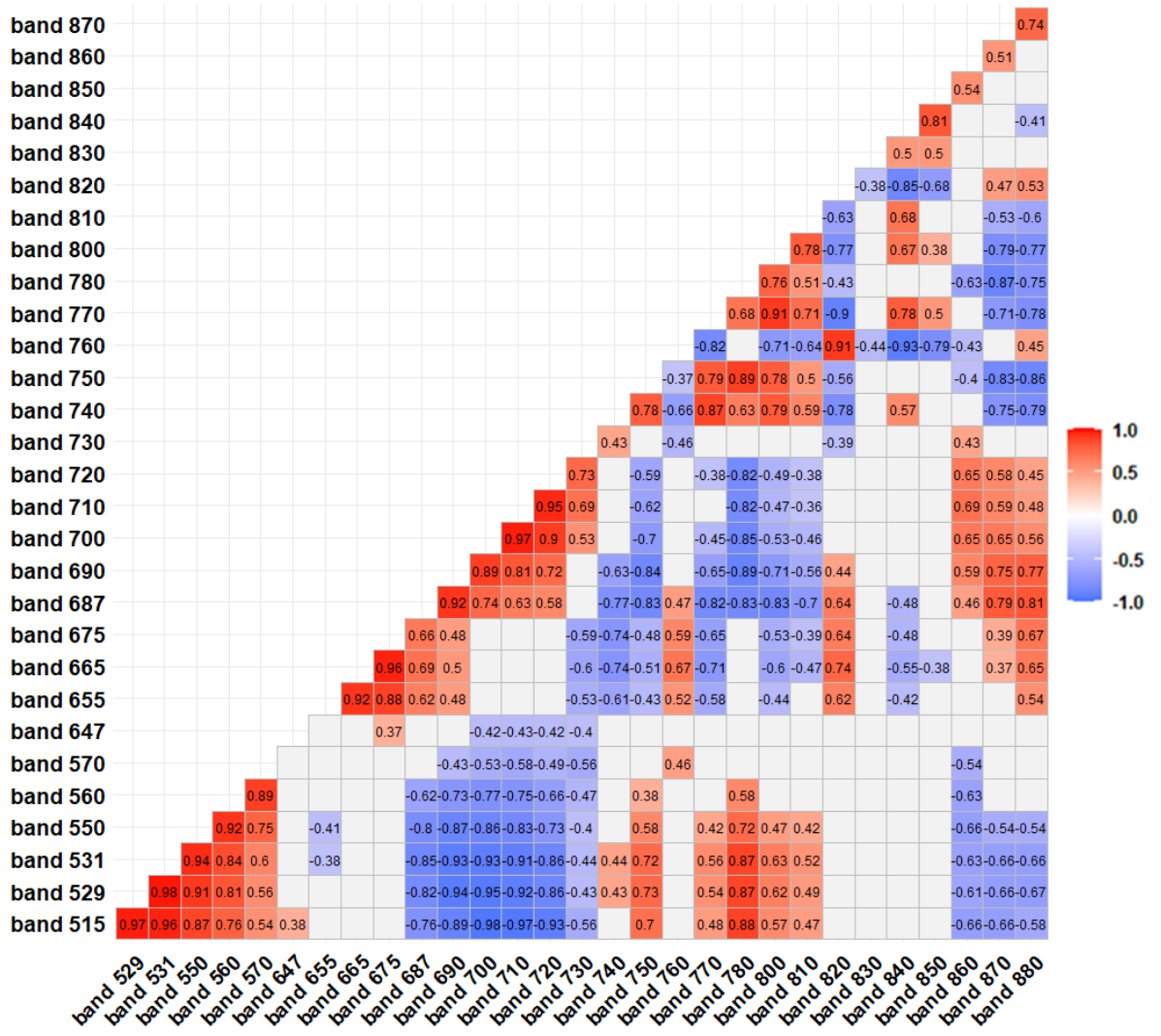
2380 Figure 4.1a shows results from using CROPSCAN data while Figure 4.1b shows
2381 results from using Rikola camera (UAV) data. Correlation matrices were not produced
2382 for the ASD/SVC spectral devices as these devices have bands that match the
2383 CROPSCAN and Rikola camera. Figure 4.1c shows results from using mass data
2384 while Figure 4.1d shows results from using % cover data. The correlation matrix for
2385 the spectral bands indicated statistically significant correlations of $r < -0.8$ and $r >$
2386 $+0.8$ between bands in the visible part of the spectrum and also between some bands
2387 in the NIR region of the spectrum (Figure 4.1a and b). The correlation matrices for the
2388 mass and % cover-based grassland variables similarly resulted in a few significant r
2389 values $r < -0.8$ and $r > +0.8$ (Figure 4.1c and d). Furthermore, the p-value was
2390 calculated for each correlation and any correlation that was not considered to be
2391 significantly different from $r = 0$ (95% value) was greyed out. Similar results were
2392 produced from using CROPSCAN, mass and % cover data collected on all seven

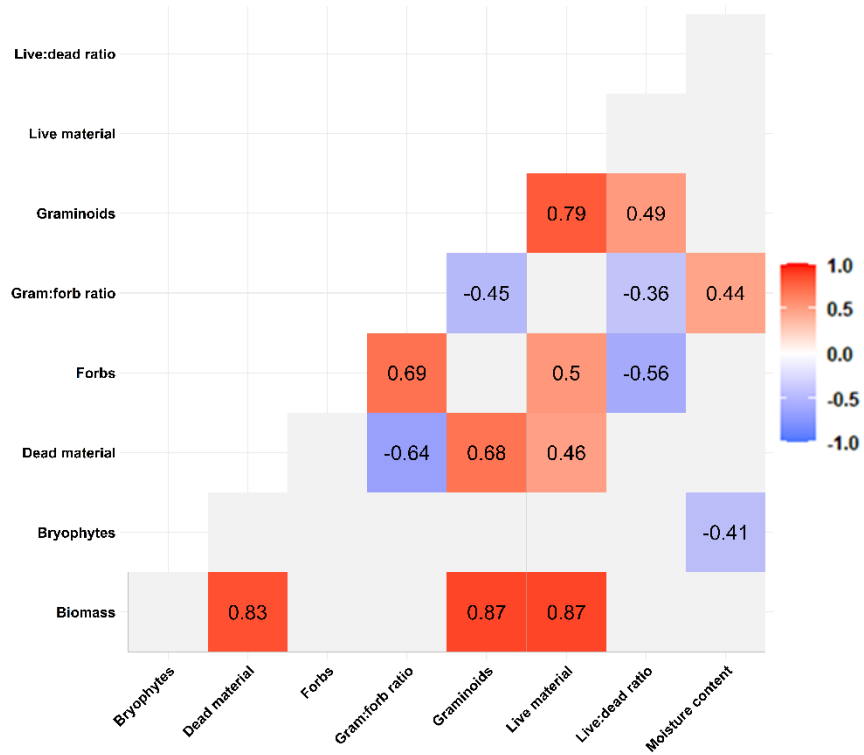
2393 grasslands during summer (Appendix Figure 1) and on Parsonage grasslands
 2394 collected over three seasons (Appendix Figure 2).

2395

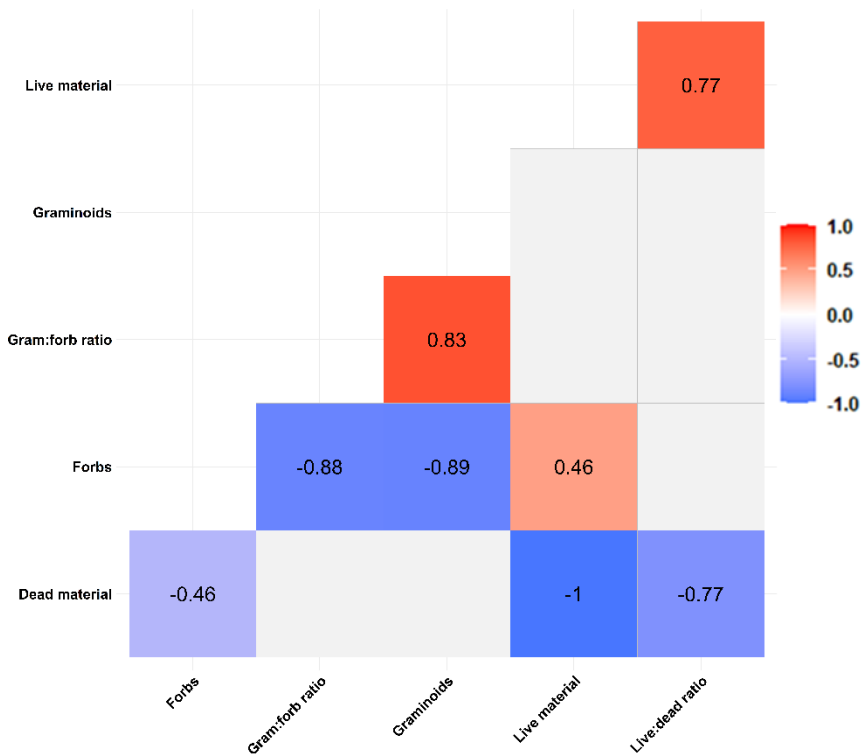


2396





2398



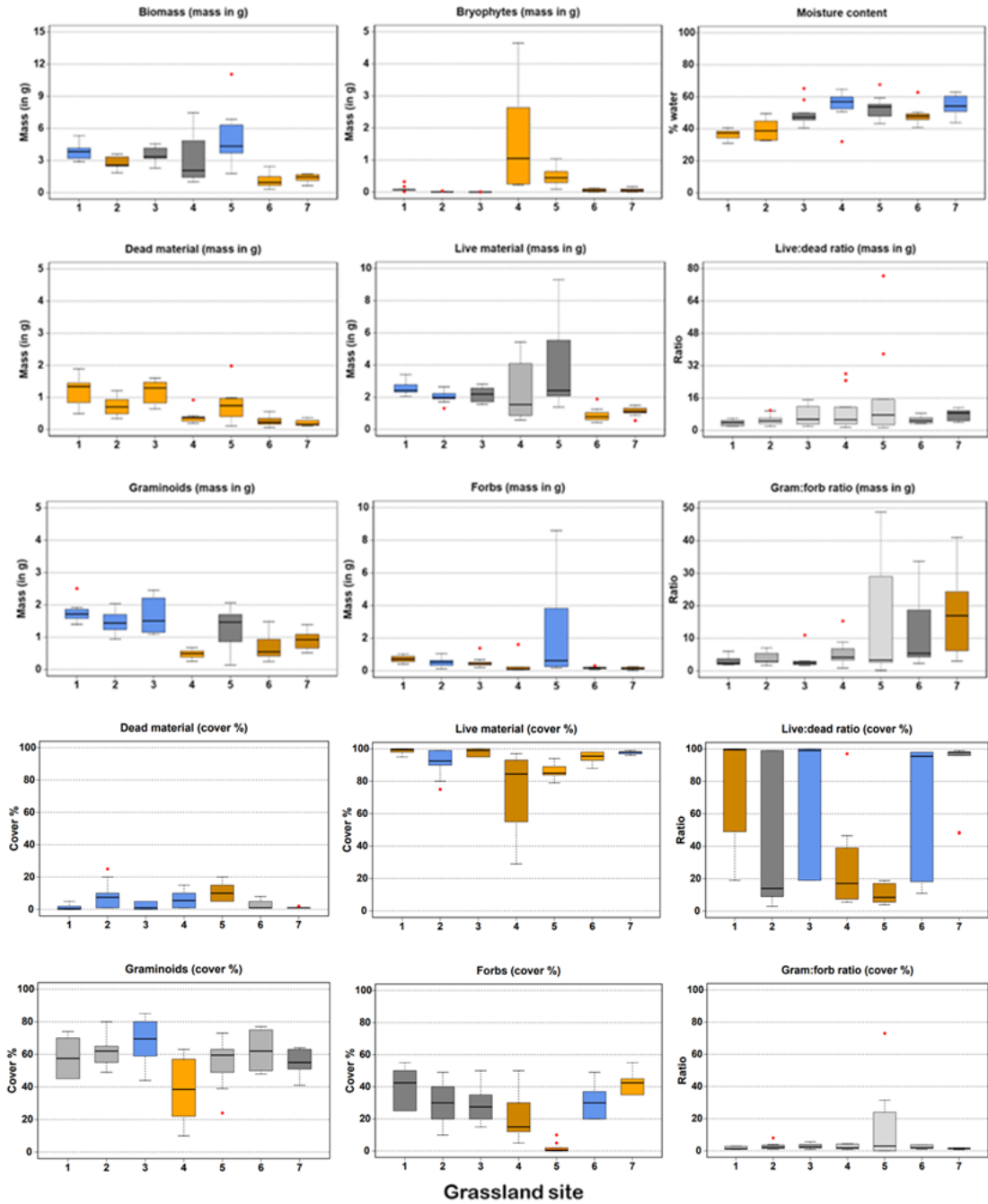
2399

2400 *Figure 4.1: Correlation matrices between predictors used in PLSR modelling a)*
 2401 *spectral bands from CROPSCAN, b) spectral bands from Rikola VNIR camera, c)*
 2402 *mass data, d) % cover data where n = 30 (data from Parsonage grasslands).*
 2403 *Correlation coefficients that are not statistically significant (alpha >= 0.05) are*
 2404 *blanked out.*

2405

2406 **4.2. Grassland site characteristics**

2407



2408

No. significantly different grasslands



2409

2410 *Figure 4.2: Boxplots of grassland variables (mass in g and cover in %) for the seven*
2411 *grassland sites. The boxplot colours summarise the unpaired two-sample Wilcoxon*
2412 *test results between grassland types: A grassland variable was considered*
2413 *significantly different between two grasslands if $p < 0.05$; the boxplot of each grassland*
2414 *site is coloured according to the number of sites from which it is significantly different.*

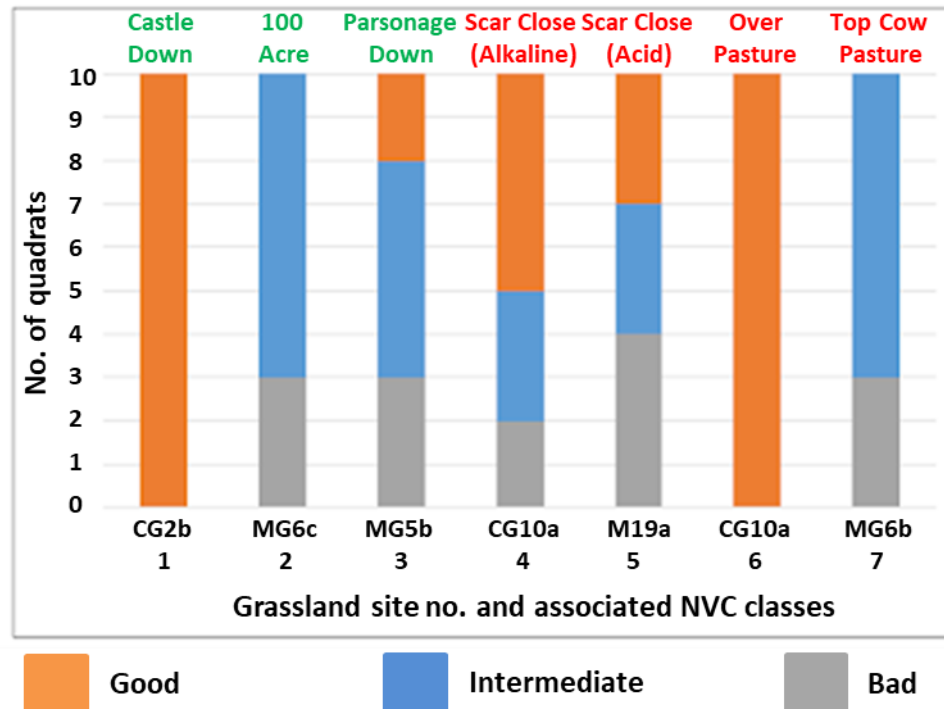
2415

2416 The Wilcoxon tests for the mass-based grassland variables show that for bryophytes
2417 mass, dead material mass and forbs mass; at least five of the seven grassland sites
2418 were significantly different in their distribution from at least four other sites. Three
2419 grassland sites were significantly different from at least four other sites for the
2420 grassland variables biomass, graminoids mass and moisture content. Live material
2421 mass, gram:forb ratio mass and live:dead ratio mass have less than three grasslands
2422 that were significantly different from at least four of the other grasslands.

2423 The Wilcoxon tests for the % cover-based grassland variables show that all grassland
2424 sites were significantly different in their distribution from at least four other sites for
2425 dead material cover and live:dead ratio cover. Three grassland sites were
2426 significantly different from at least four other sites for forbs cover and live material
2427 cover. Gram:forb ratio cover and graminoids cover had no grasslands that were
2428 significantly different to at least four other grasslands.

2429 Figure 4.3 shows the condition scores according to the CSM guidance at quadrat
2430 level for each grassland site, indicating the level of variation in condition within each
2431 site. Three sites (Sites 3, 4 and 5) show quadrat level conditions that range from bad
2432 to good; two other sites (Sites 2 and 7) have quadrat conditions that vary between
2433 bad and intermediate, and the two remaining sites (Sites 1 and 6) show all quadrats
2434 in good condition.

2435



2436

2437 *Figure 4.3: Absolute numbers of quadrats of each level of condition per grassland*
 2438 *according to the UKCSM criteria and grassland NVC classifications for each of the*
 2439 *seven grassland sites. Sites 1 to 3 are for Parsonage Down NNR (names in green)*
 2440 *and Sites 4 to 7 are for Ingleborough NNR (names in red). Good condition means*
 2441 *that >80% UKCSM criteria are met, intermediate is 60-80% of criteria met and bad is*
 2442 *<60% criteria met.*

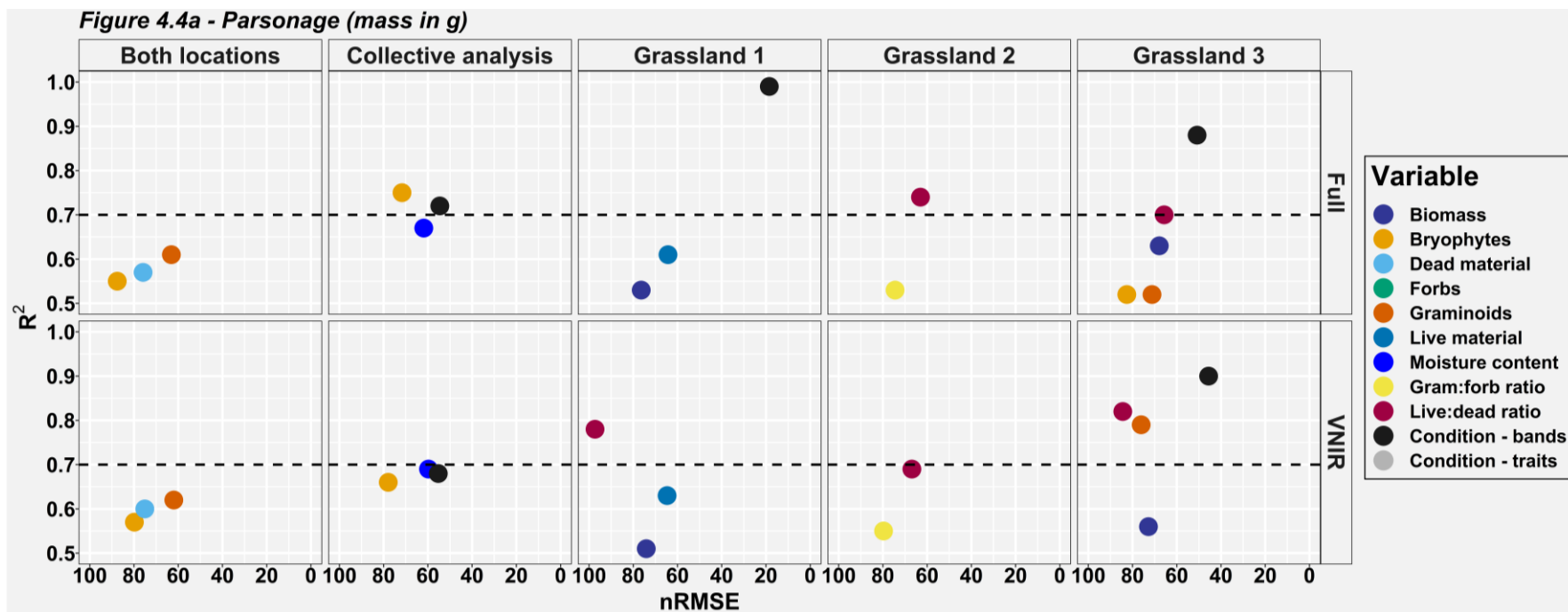
2443

2444 **4.3. Predicting grassland variables and condition using PLSR**

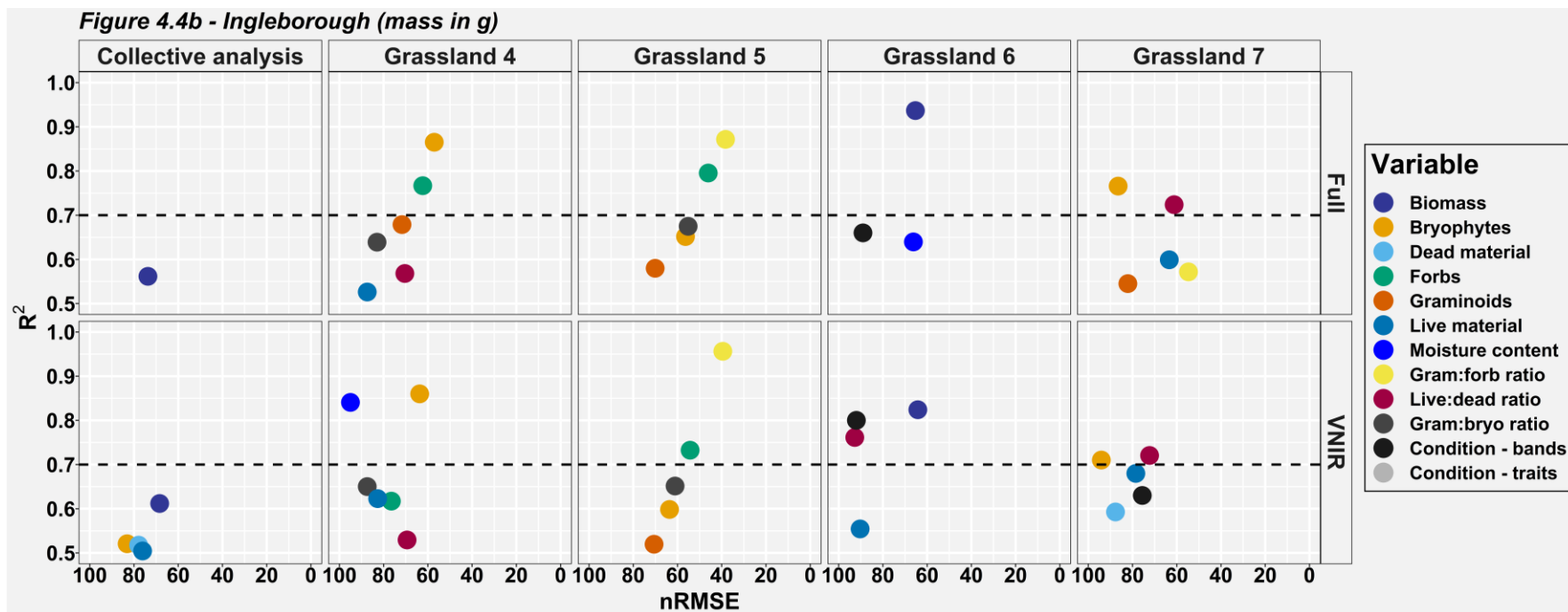
2445 The median R^2 and nRMSE results of using PLSR modelling where $R^2 \Rightarrow 0.5$ and
 2446 nRMSE ≤ 100 , from 45 runs for individual grasslands or 1000 runs for collective
 2447 grasslands, to predict mass and % cover grassland variables plus CSM-condition
 2448 using spectral data can be seen in Figure 4.4 while the full results are presented in
 2449 Appendix Figure 3. The success in predicting these variables from spectral data is
 2450 partly dependent on whether the models are using data from both locations (total of
 2451 70 quadrats), a single location (total of 30 or 40 quadrats which has been termed
 2452 “collective analysis” for the three or four sites, respectively) or a single site (10
 2453 quadrats) with a broad trend of model performances improving (higher R^2 and lower
 2454 nRMSE) when the data used is limited to a specific location and then site. Using the

2455 full band set (16 bands) including SWIR (i.e. FULL) or the VNIR only bands (14
2456 bands), impacts only when the data used is limited to a specific grassland site.

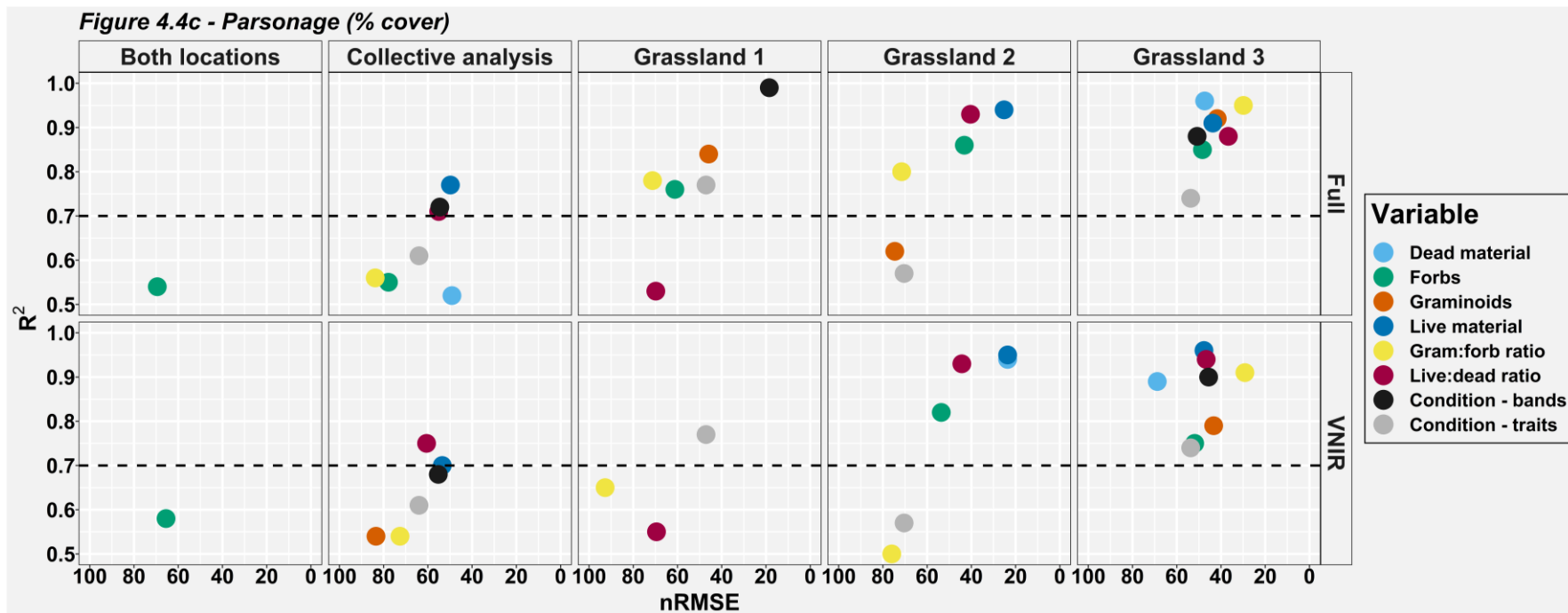
2457 When mass grassland variable data from all seven grasslands are analysed as one
2458 using data for both locations combined (given as top left plot in Figure 4.4a) the
2459 PLSR models for bryophytes mass, dead material mass and graminoids mass stand
2460 out with R² values of >0.5 and nRMSE <100. When % cover grassland variable data
2461 is used (given as top left plot in Figure 4.4c), only forbs cover has a R² value of >0.5
2462 value and nRMSE value <100.



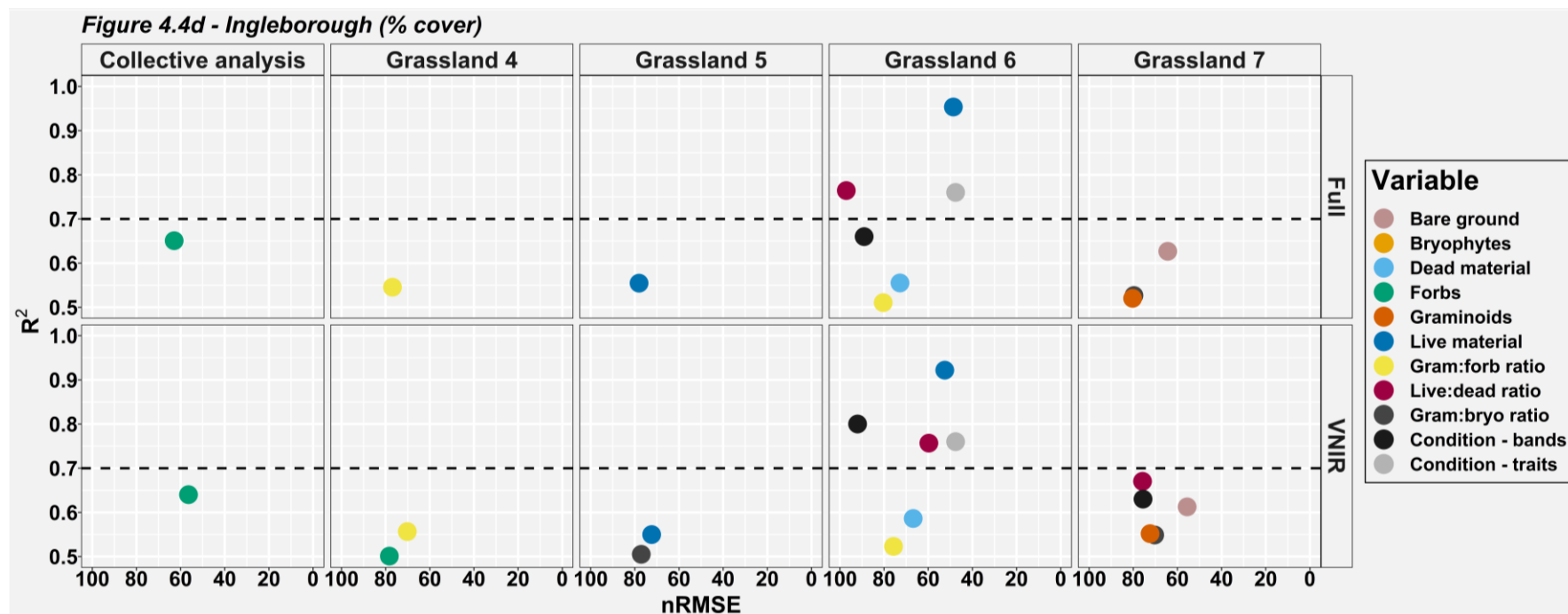
2463



2464



2465



2466

2467 *Figure 4.4: Plots for results of 426 PLSR regressions where $R^2 \Rightarrow 0.5$ and $nRMSE \leq 100$, each of which represent the median R^2 and*
 2468 *$nRMSE$ values of the iterated model runs, where (i) spectral data (either FULL or VNIR) were used to predict grassland variables*
 2469 *(coloured dots) and CSM based condition (black dot) and (ii) grassland variables were used to predict CSM based condition (white dot).*
 2470 *Panels a and b show results for mass based analysis; c and d for % cover based analysis.*

2471 When grassland sites from both locations are analysed collectively (all seven grasslands);
2472 bryophytes mass, dead material mass, graminoids mass and forbs cover were predicted with
2473 $R^2 > 0.5$ and $nRMSE < 100$ whilst other PLSR model runs produced R^2 values < 0.5 . When
2474 grassland sites from each location are analysed collectively (referring to three and four sites
2475 combined for Parsonage and Ingleborough, respectively), most grassland variables were
2476 predicted with $R^2 > 0.5$ and $nRMSE < 100$ for Parsonage when predicting % cover data,
2477 whereas only a few variables achieved this level of accuracy when predicting mass data;
2478 bryophytes mass and moisture content plus CSM-condition (black dots in Figure 4.4) when
2479 predicting with spectra. Relatively few variables were predicted with $R^2 > 0.5$ and $nRMSE$
2480 < 100 for Ingleborough; only forbs cover, biomass and dead material mass.

2481 When grassland sites at Parsonage or Ingleborough are analysed individually for predicting
2482 mass or % cover grassland variable data, many PLSR model fits produced R^2 values > 0.5
2483 and $nRMSE < 100$ except for Grasslands 2 and 3 when using mass grassland variable data
2484 or Grassland 5 when using % cover grassland variable data where only 2-3 model fits
2485 produced R^2 values > 0.5 and $nRMSE < 100$.

2486 Of 426 model runs in total (using mass and % cover data); 188 produced results of $R^2 > 0.5$
2487 and $nRMSE < 100$; with live:dead ratio (27 model runs) producing the most followed by forbs,
2488 graminoids, dead material, gram:forb ratio (19-21 model runs for each grassland variable).
2489 More accurate performances in order of number of $R^2 > 0.7$ results are for live:dead ratio (17
2490 model runs), forbs (12 model runs), live material (11 model runs) and gram:forb ratio (10
2491 model runs).

2492 The success in predicting grassland variables from spectral data was dependent on whether
2493 the variables were expressed in terms of mass or % cover and the difference in performance
2494 varied from small to substantial depending on the grassland variable. When 144 comparable
2495 mass and % cover based models are compared against each other; % cover achieved higher
2496 R^2 results than mass for Parsonage and Ingleborough locations in 9 of 14 comparable
2497 models and lower $nRMSE$ results in 10 of 14 comparable models. Also, % cover achieved
2498 higher R^2 results than mass for Parsonage in 44 of 54 comparable models and lower $nRMSE$
2499 results in 42 of 54 comparable models. For Ingleborough grasslands, mass had higher R^2
2500 results than % cover for 43 of 76 comparable models and lower $nRMSE$ results in 49 of 76
2501 comparable models.

2502 The impact of utilising FULL spectral bands (16 bands across 470-1640nm range) as
2503 predictors relative to just the VNIR bands (14 bands across 470-870nm range) appears to be
2504 site specific, but generally, the difference in model performance is small ($R^2 < 0.05$ and
2505 $nRMSE < 10$). Of 188 model runs that produced results of $R^2 > 0.5$ and $nRMSE < 100$, 94 of
2506 them used FULL spectrum data whilst 86 of them used VNIR spectral data, where the other
2507 8 models predicted CSM-condition with grassland variables and therefore did not utilise
2508 spectral data.

2509 When the R^2 and $nRMSE$ results of 140 comparable models were compared between models
2510 that used FULL spectral data as predictors and models that used VNIR spectral data as
2511 predictors, VNIR produced stronger R^2 results in 10 of 14 model runs and lower $nRMSE$
2512 results for 12 of 14 model runs when comparing results from analysing both locations. FULL
2513 produced stronger R^2 results and lower $nRMSE$ results in 40 of 48 model runs when
2514 comparing results from analysing Parsonage grasslands. VNIR produced stronger R^2 results
2515 in 44 of 78 model runs and lower $nRMSE$ results for 37 of 78 model runs when comparing
2516 results from analysing Ingleborough grasslands.

2517 The PLSR models that used spectral data to predict CSM-condition delivered results of R^2
2518 > 0.5 (mostly $R^2 \Rightarrow 0.65$) and $nRMSE < 100$ when grasslands were analysed collectively and
2519 for Grassland 3 (Figure 4.4). When grassland variables were used to predict CSM-condition,
2520 models based on % cover data from individual sites or from Parsonage grasslands
2521 collectively performed best, most achieving $R^2 > 0.5$ and $nRMSE < 100$.

2522

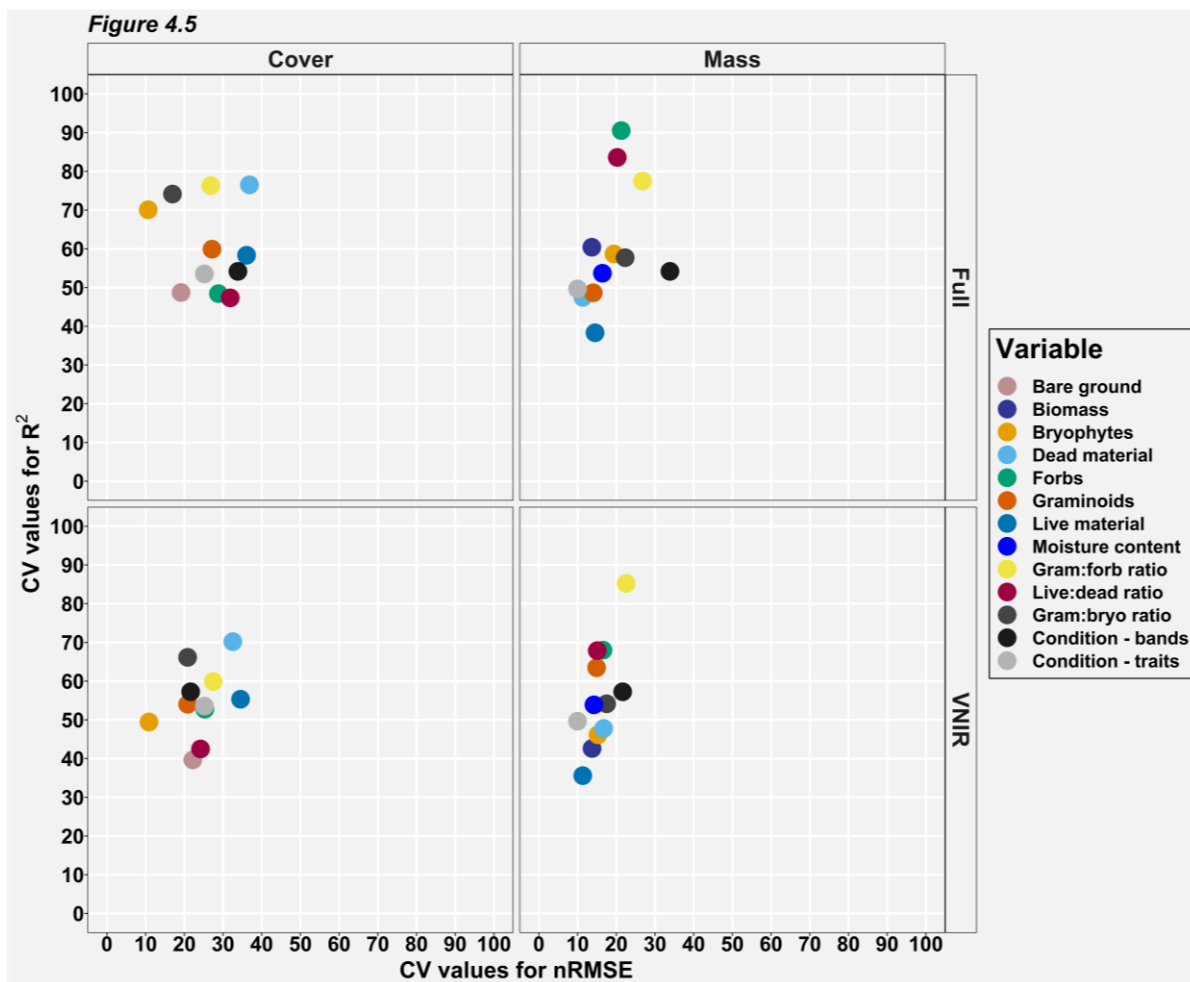
2523 **4.4. Stability and consistency between model runs using the same** 2524 **response variable**

2525 Figure 4.5 shows the % coefficient of variation (CV) found from the iterated model runs for
2526 the resulting R^2 and $nRMSE$ values of the site specific PLSR models that were calculated to
2527 evaluate the stability of model performances across sites for specific grassland variables.

2528 These results suggest that the performance of the models for bryophytes cover, forbs cover
2529 and live:dead ratio cover are relatively stable. Most grassland variables have a similar level
2530 of consistency when mass data are used. Overall, mass based models produce more
2531 consistent $nRMSE$ results across sites compared to % cover based models and VNIR-based
2532 models have slightly more consistent $nRMSE$ results between sites than FULL-based

2533 models. There is no overall trend showing which sets of results have more consistent R^2
 2534 results and whether using mass/cover or FULL/VNIR for more consistent results is grassland
 2535 variable specific.

2536

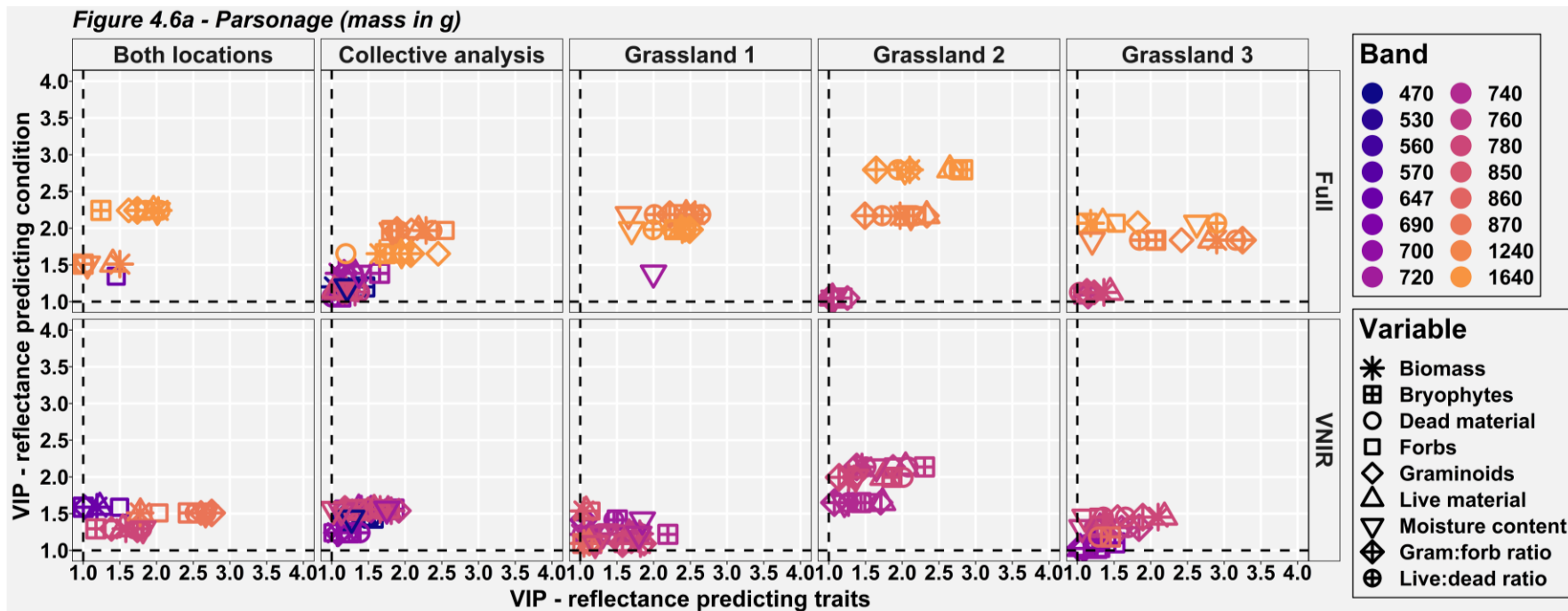


2537
 2538 *Figure 4.5: % coefficient of variation (CV) plots for the R^2 and nRMSE results of the site*
 2539 *specific PLSR models grouped per treatment (% cover - left; mass - right) and spectral input*
 2540 *data (full spectrum - top; VNIR - bottom).*

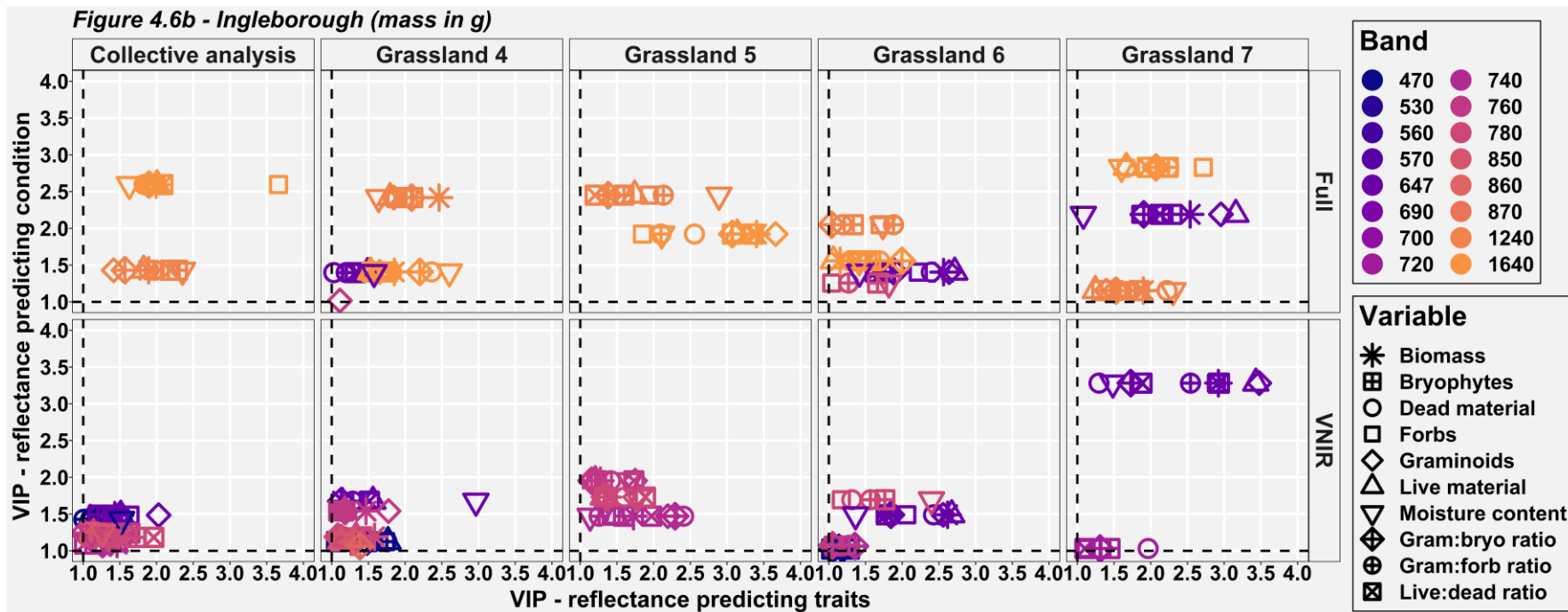
2541
 2542 **4.5. VIP analysis for spectral band and grassland variable selection**

2543 Figure 4.6 shows the results of using a VIP analysis to understand which spectral bands
 2544 were the most important predictors for predicting grassland variables, where only results =>

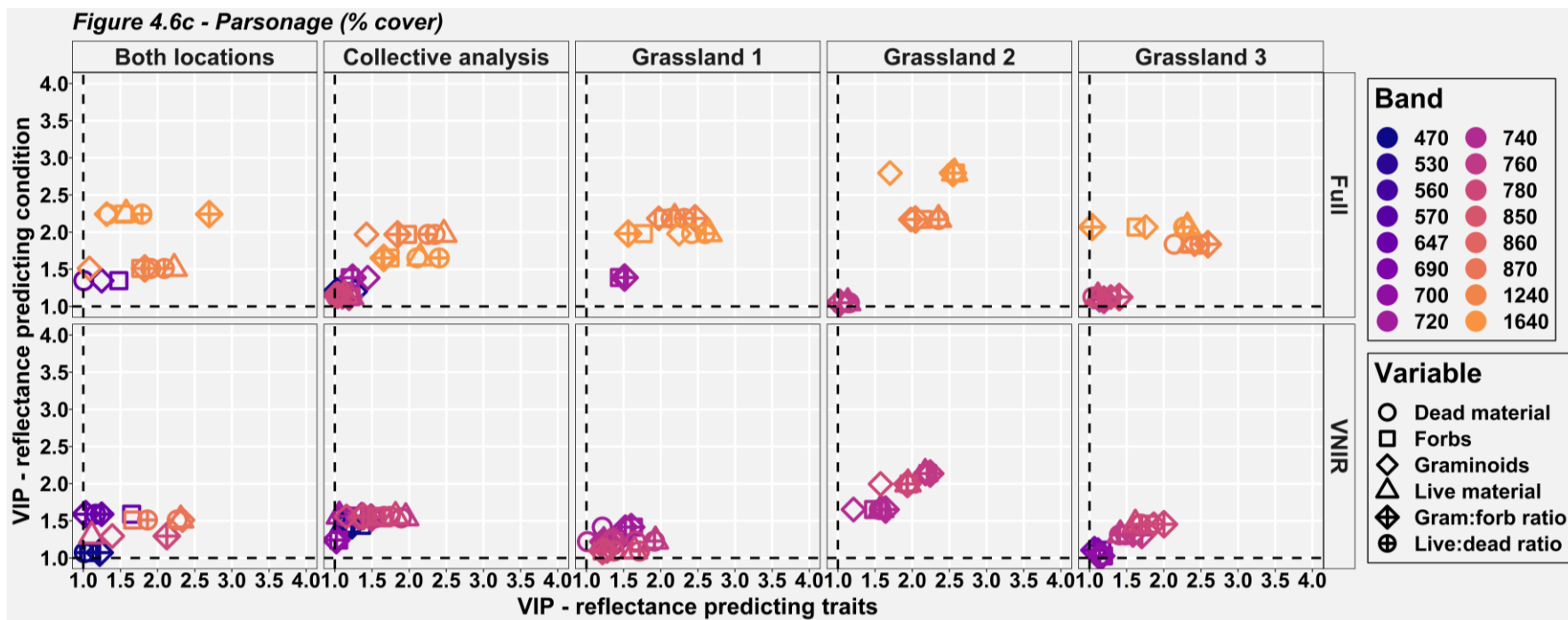
2545 1 have been included and therefore most of the results are not shown here. The results
2546 suggest that the two SWIR bands (1240 and 1640nm) are the most important for predicting
2547 grassland variables and condition across all grasslands, along with the red edge (647nm)
2548 and upper NIR bands for some grasslands. When VNIR data are used; the upper NIR bands
2549 plus the red edge are most important for predicting grassland variables and CSM-condition.
2550 When grassland variables are used to predict condition (Figure 4.7); gram:bryo ratio cover
2551 (where applicable), gram:forb ratio cover and live:dead ratio cover plus forbs cover and
2552 graminoids cover are important for a range of grasslands. Other grassland variables were
2553 only important in predicting CSM-condition on some grasslands, with these grasslands being
2554 different depending on the grassland variable.



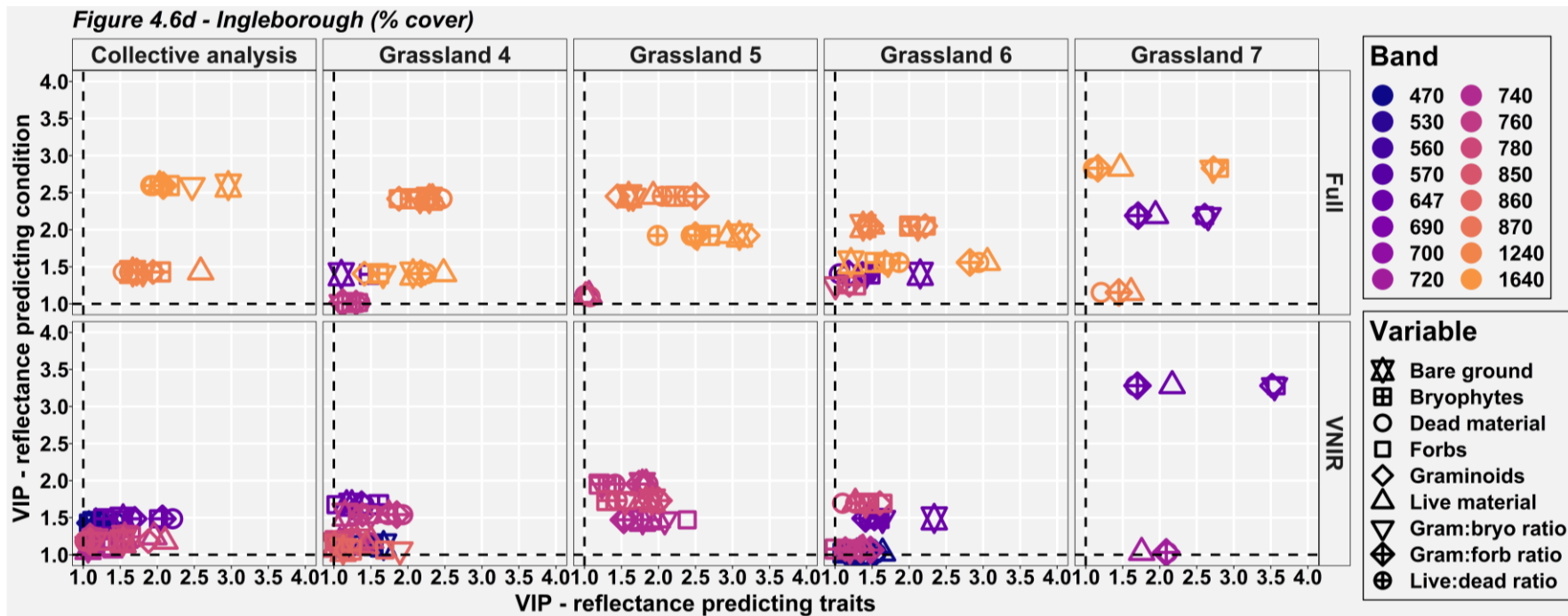
2555



2556



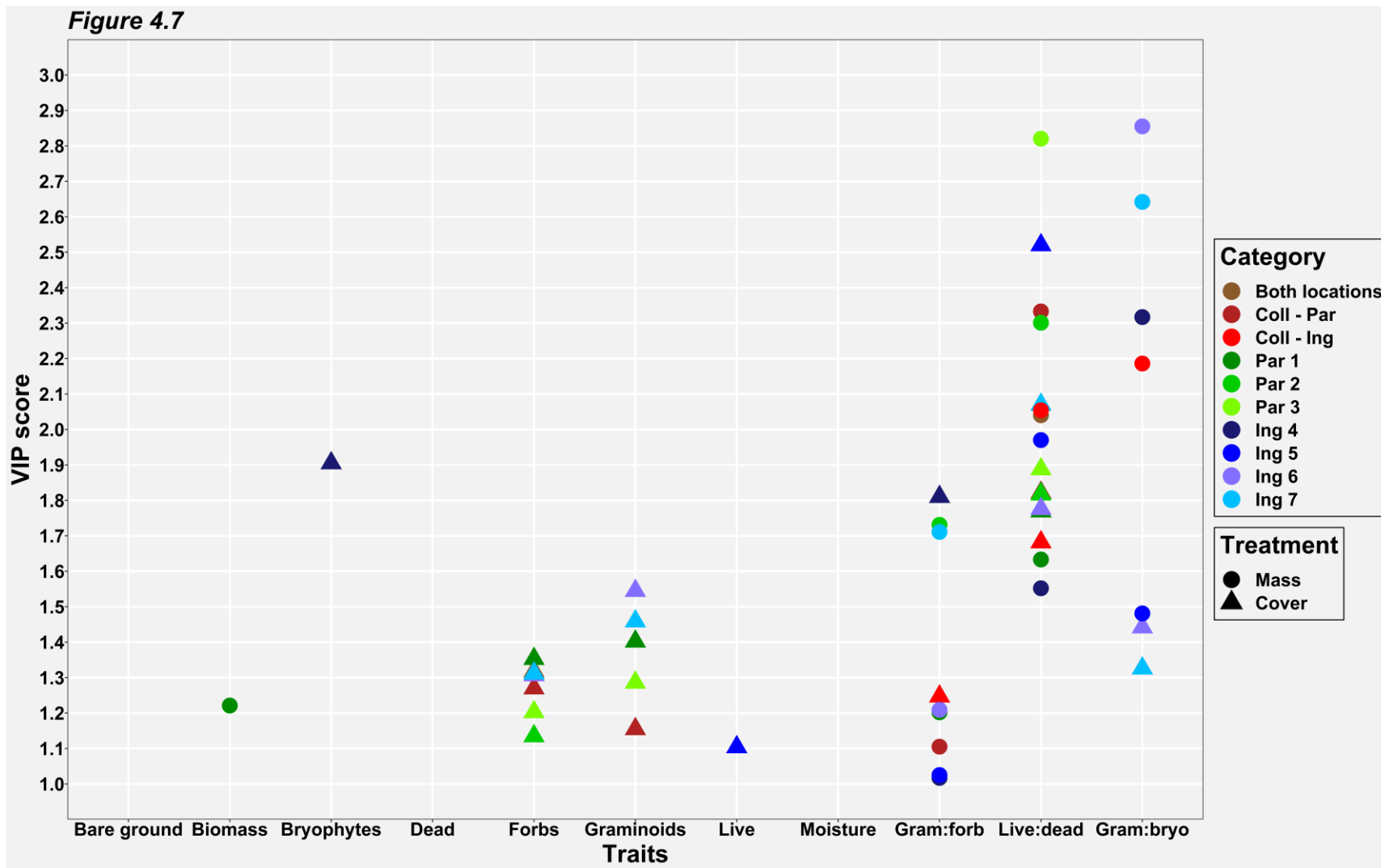
2557



2558

2559 *Figure 4.6: VIP plots showing which combinations of spectral bands (predictors) and which responses (grassland variables on x axis*
 2560 *and CSM-condition on y axis) are most important in the PLSR models used in this study.*

2561



2562

2563 *Figure 4.7: VIP plot showing which grassland variables are most important in predicting CSM-condition using either mass or % cover*

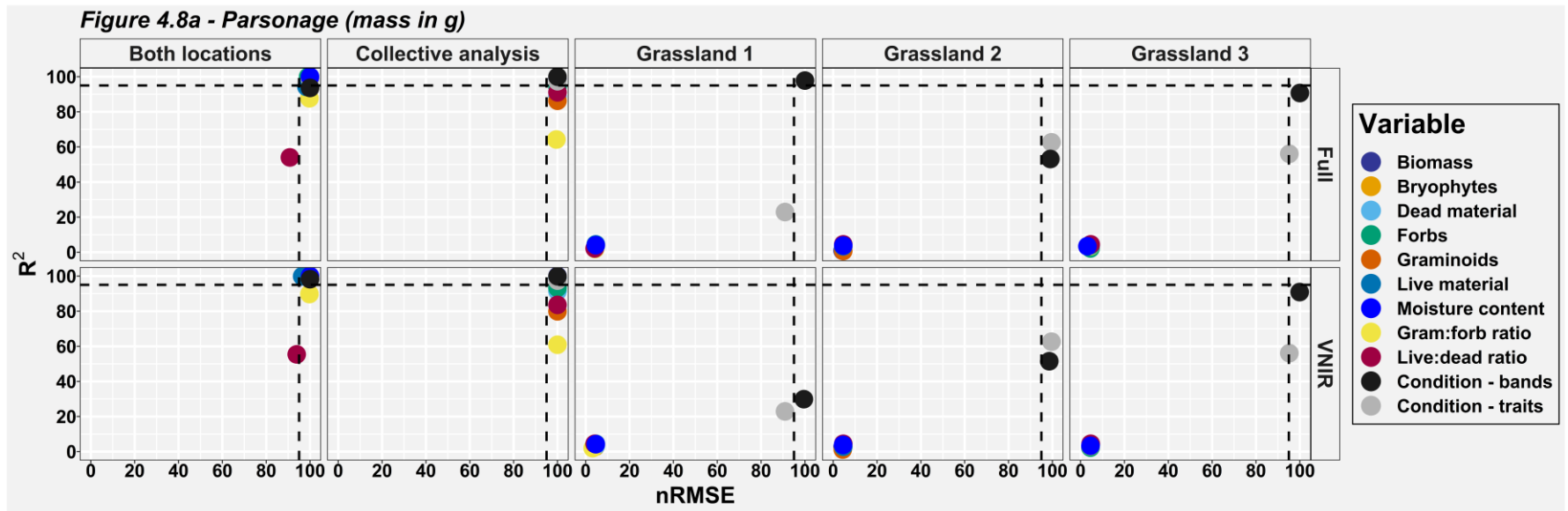
2564 *data from analysing grasslands individually or collectively for one or both locations.*

2565 **4.6. Comparison of PLSR models trained with actual data and PLSR**
2566 **models trained with random data**

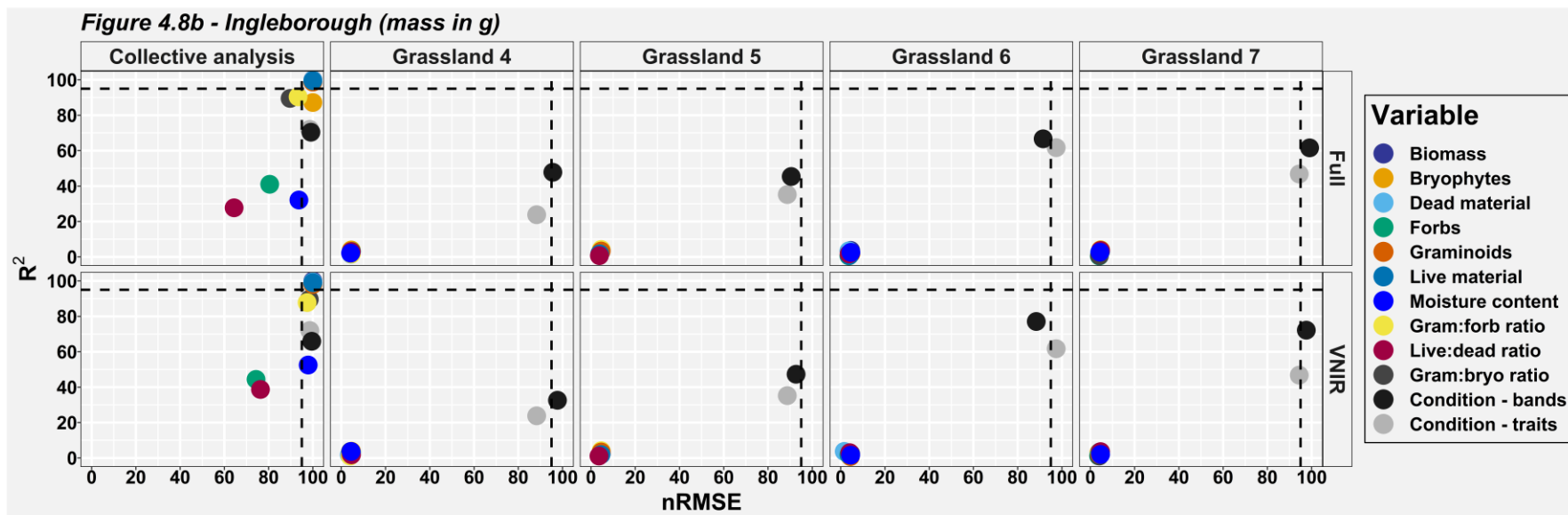
2567 The actual data results, as seen in Figure 4.4, were compared against the results of iterative
2568 model runs (either 44 for individual grassland analysis or 999 for collective grassland
2569 analysis) with randomised response variable values to test if the results run with the actual
2570 data genuinely produce reasonable results in comparison to models with randomised data.
2571 The results are plotted in Figure 4.8, where points close to the top right corner of the graph
2572 are of interest.

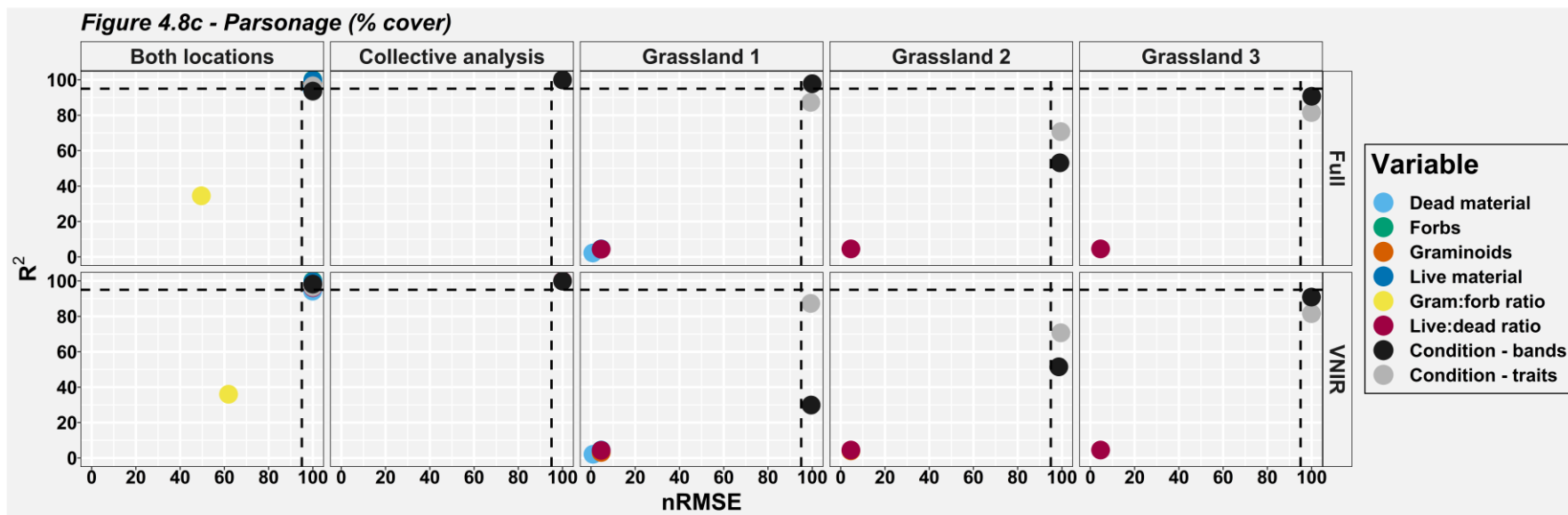
2573 The results suggest that models using the true data (actual models) are only superior to
2574 models using randomised data (random models) depending on the size and combination of
2575 the data being used. At the 95% level, actual models consistently perform more accurately
2576 than random models when data from both locations are used. When using data from
2577 collective analysis (30 quadrats for Parsonage and 40 for Ingleborough) the actual models
2578 almost always produce stronger nRMSE results but not stronger R² results. Using data from
2579 individual grasslands (10 quadrats) to train PLSR models results in models that are not
2580 considered to be more reliable than a random model.

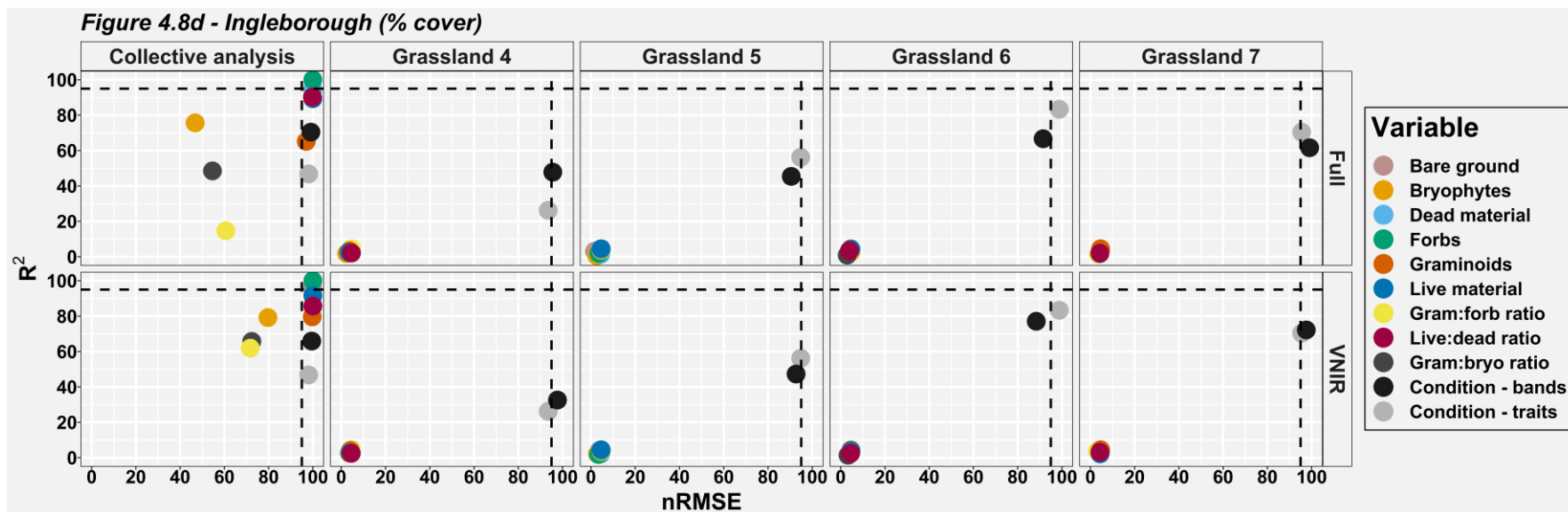
2581



2582







2585

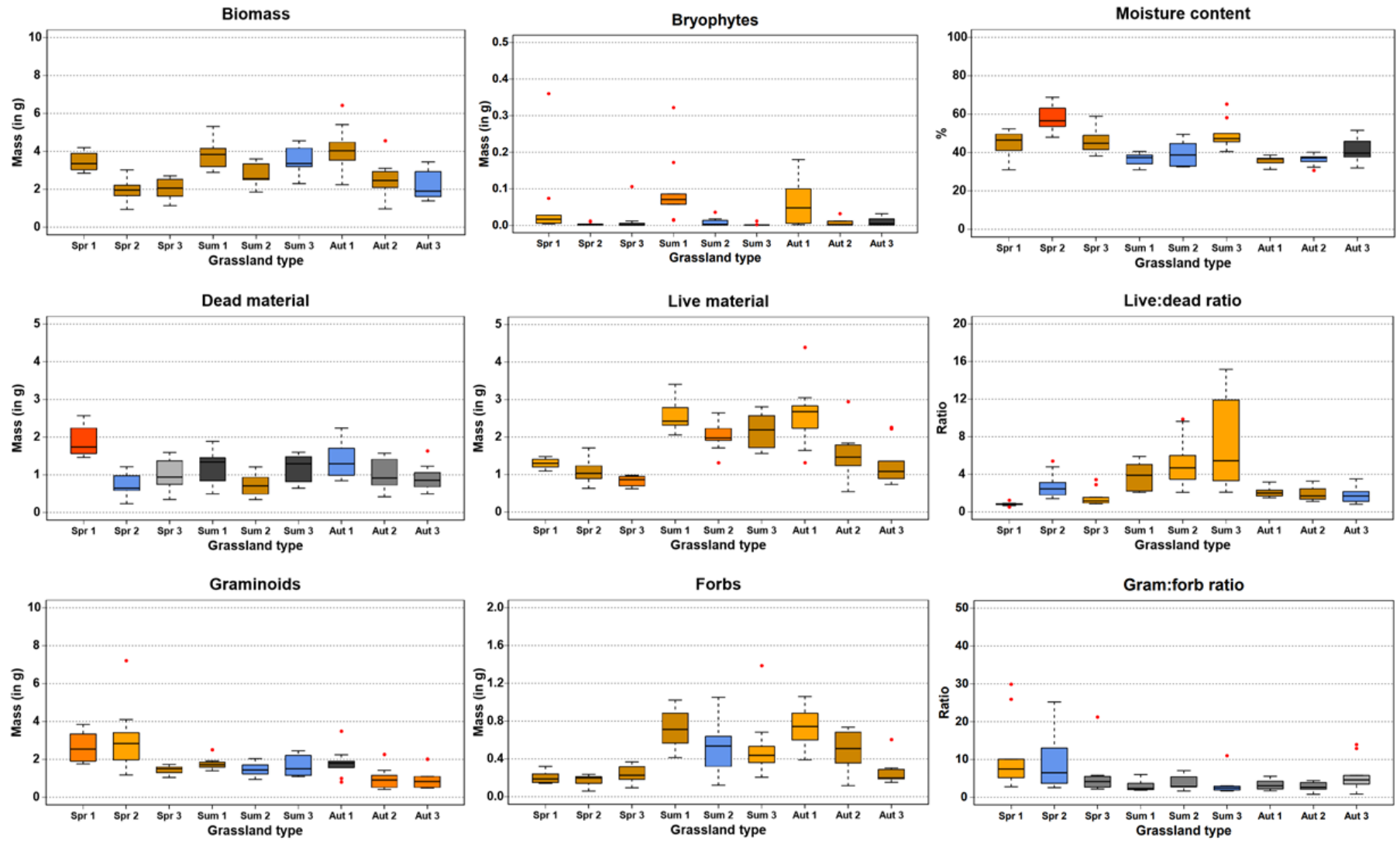
2586 *Figure 4.8: Comparison of the median values of iterated model runs using actual response data and 44 or 999 model runs (dependent*
 2587 *on whether grasslands were analysed individually or collectively) using randomised response data. The plot shows the ranking of the*
 2588 *actual model out of the maximum iterated runs (either 45 for individual grasslands or 1000 for collective grasslands), where high*
 2589 *rankings (e.g. >950 for the 95% level) are sought*

2590 **Chapter 5 - Assessing seasonal**
2591 **effects on the condition of**
2592 **calcareous semi-natural grasslands**
2593 **using CROPSCAN field radiometry**
2594 **at patch level (1m²)**

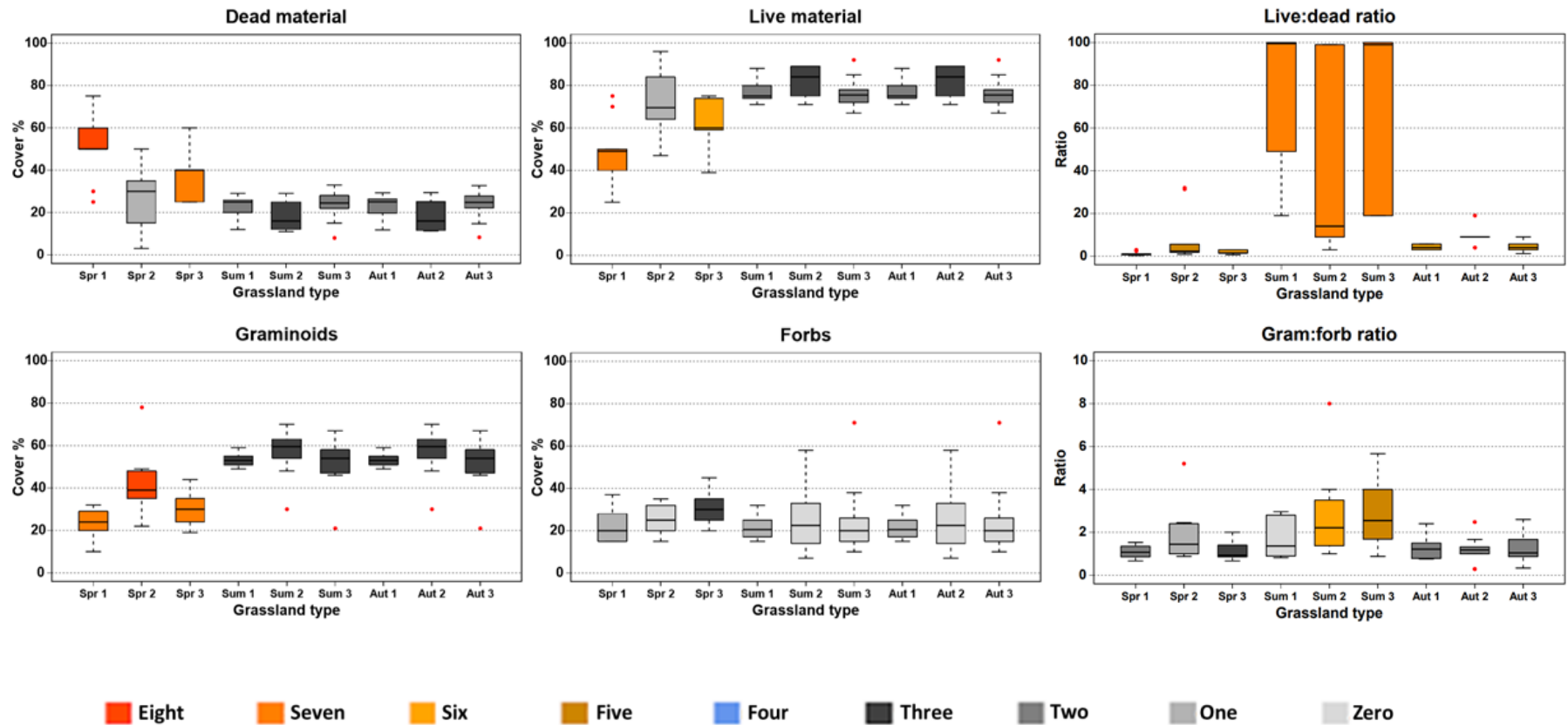
2595 **5.1. Grassland site characteristics**

2596 The boxplots seen in Figure 5.1 show the quantity of each variable for each
2597 grassland and season, including the results of significant difference tests between
2598 grassland types across seasons. Overall, the Wilcoxon tests for grassland variables
2599 show that some mass-based grassland variables are generally significantly different
2600 on the three different grasslands across three seasons whilst cover-based grassland
2601 variables were generally not significantly different to each other. The Wilcoxon tests
2602 for the mass-based variables show that for variables biomass, bryophytes mass, live
2603 material mass, live:dead ratio mass and forbs mass most of the nine grassland site
2604 and season combinations were significantly different in their distribution from at least
2605 five other site-season combinations. The Wilcoxon tests for the cover-based
2606 grassland variables shows that live:dead ratio cover was generally significantly
2607 different in distribution between grasslands and seasons. Also, at least two
2608 grasslands during spring had significantly different distributions for the variables dead
2609 material cover, live material cover and graminoids cover when compared to other
2610 site-season combinations but other grassland variables had no grasslands that were
2611 significantly different to at least four other site-season combinations.

2612



2613



2614

2615

2616 Figure 5.1: Boxplots of the mass or % cover values of grassland variables for the three grassland sites. The boxplot colours summarise
 2617 the unpaired two-sample Wilcoxon test results between grassland types and seasons: a grassland variable was considered significantly
 2618 different between two grasslands if $p < 0.05$; the boxplot of each grassland site is coloured according to the number of different site-
 2619 season combinations from which it is significantly different.

2620 **5.2. Predicting grassland variables and CSM-condition using** 2621 **PLSR**

2622 The median R² and nRMSE results of the PLSR modelling from the iterated model
2623 runs to predict mass and % cover grassland variables including CSM-condition
2624 variables can be seen in Figures 5.2 and 5.3 Overall, most variables were predicted
2625 with R² values >0.5 and nRMSE results <100 for at least some grasslands and
2626 seasons, but there are few patterns where a particular variable is predicted
2627 consistently across grasslands and seasons. Analysing data from all grasslands
2628 collectively ($n = 30$ or 90 for one or for all three seasons) produced PLSR models
2629 with R² >0.5 and nRMSE <100 for a similar number of grassland variables as
2630 analysing data from single sites ($n = 10$ or 30 for one or all three seasons) for most
2631 seasons, a clear exception being autumn for some grasslands when using % cover
2632 variable data. Removing the SWIR bands before analysis (14 bands, labelled VNIR)
2633 does not appear to have a big impact on the results relative to using the full spectral
2634 data set (16 bands, labelled FULL).

2635

2636 **5.2.1. Mass-based grassland variable data**

2637 The results of using grassland variables derived from mass data as response data in
2638 the model runs where R² => 0.5 and nRMSE <= 100 can be seen in Figure 5.2 and
2639 the full results are presented in Appendix Figure 4. When grasslands are analysed
2640 collectively for all seasons ($n = 90$); graminoids mass (when using FULL), live
2641 material mass and live:dead ratio mass have R² values 0.5-0.7 but all other results
2642 are <0.5. For spring ($n = 30$); biomass, dead material mass, graminoids mass, live
2643 material mass and live:dead ratio mass all produced results of R² >0.5 and nRMSE
2644 results <100. For summer ($n = 30$); bryophytes, moisture content and CSM-condition
2645 predicted with spectral data produced results of R² =>0.5 and nRMSE results <100.
2646 For autumn ($n = 30$); biomass, forbs mass, graminoids mass, and live material mass
2647 had results of R² =>0.5 and nRMSE results <100.

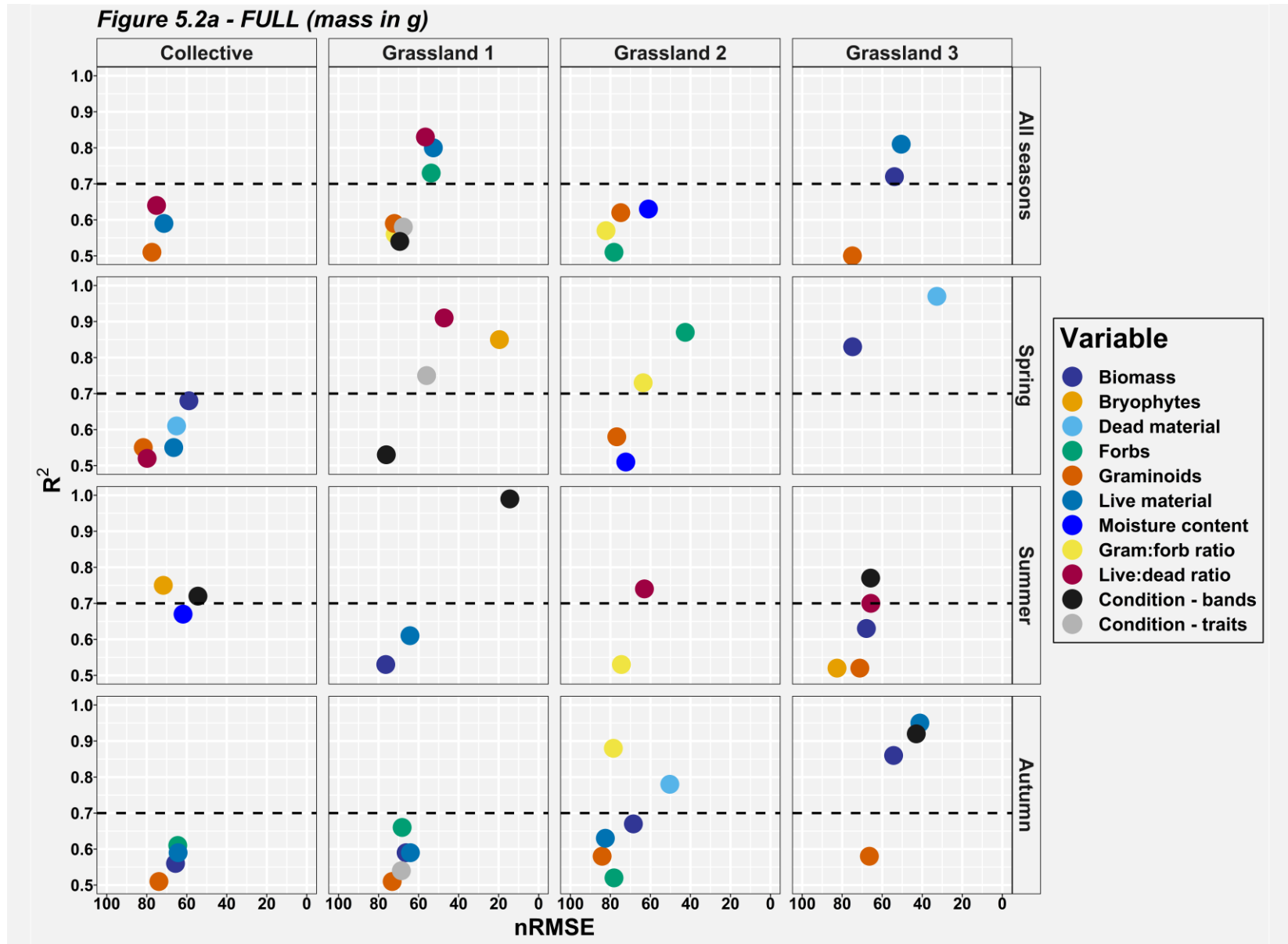
2648 When grasslands are analysed individually ($n = 30$ for all seasons or $n = 10$ for one
2649 season), there were some significant results but there is no obvious pattern in the
2650 results for any grassland variable except that gram:forb ratio mass is predicted
2651 consistently with R² values =>0.5 for Grassland 2. The grassland variables that

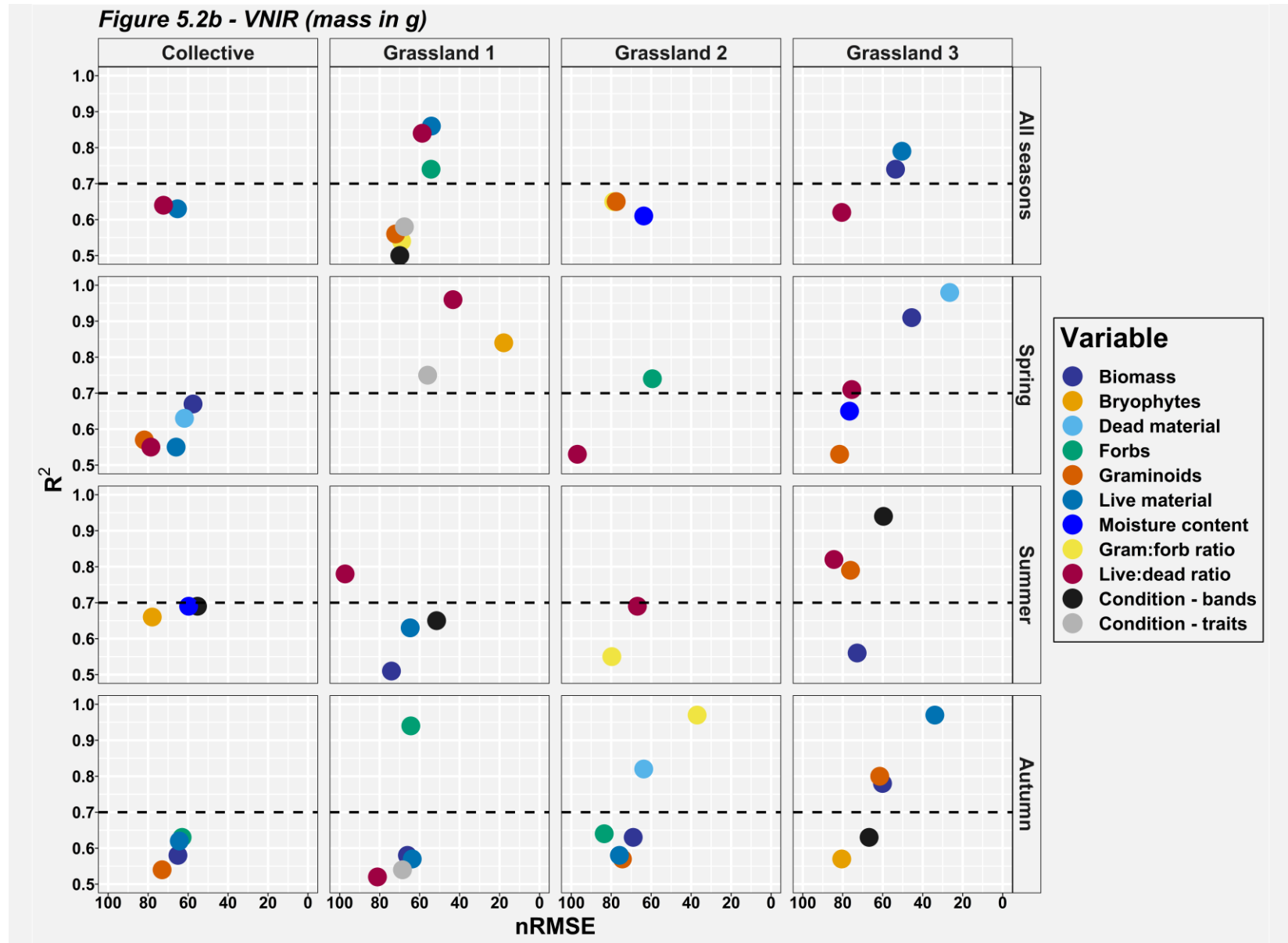
2652 produce the greatest number of significant results are biomass, graminoids mass and
2653 live material mass plus live:dead ratio mass when using VNIR.

2654 Of 512 model runs (Figures 5.2 and 5.3); 243 produced R² results => 0.5 and nRMSE
2655 <100, 128 of which have R² results => 0.7. All grassland variables except bryophytes
2656 mass had >10 results of R² =>0.5 and nRMSE <100. Live material mass, graminoids
2657 mass and live:dead ratio mass have the most PLSR models with R² results => 0.5
2658 and nRMSE <100 with 38, 39 and 40 respectively. Using % cover grassland variable
2659 data produced 119 PLSR models with R² results => 0.5 and nRMSE <100 whilst
2660 using mass grassland variable data produced 124 such results, suggesting that using
2661 mass grassland variables a similar number of moderate to strong PLSR models than
2662 using % cover data.

2663 Analysing data from all grasslands collectively produced fewer PLSR models with R²
2664 results => 0.5 and nRMSE <100 (50) than analysing data from individual grasslands;
2665 62 for Grasslands 1 and 2, and 70 for Grassland 3. A similar number of PLSR models
2666 with R² results => 0.5 and nRMSE <100 results were produced for FULL and VNIR;
2667 Using FULL spectral data produced 125 such results whilst using VNIR spectral data
2668 produced 118 such results. Using data from all seasons produced more PLSR
2669 models with R² results => 0.5 and nRMSE <100 (69) than using data from one
2670 season; 53, 57 and 63 for spring, autumn and summer respectively. The results for
2671 one season, particularly for spring, could have been affected by a relatively high
2672 quantity of dead material on the grasslands (Yang and Guo, 2014).

2673





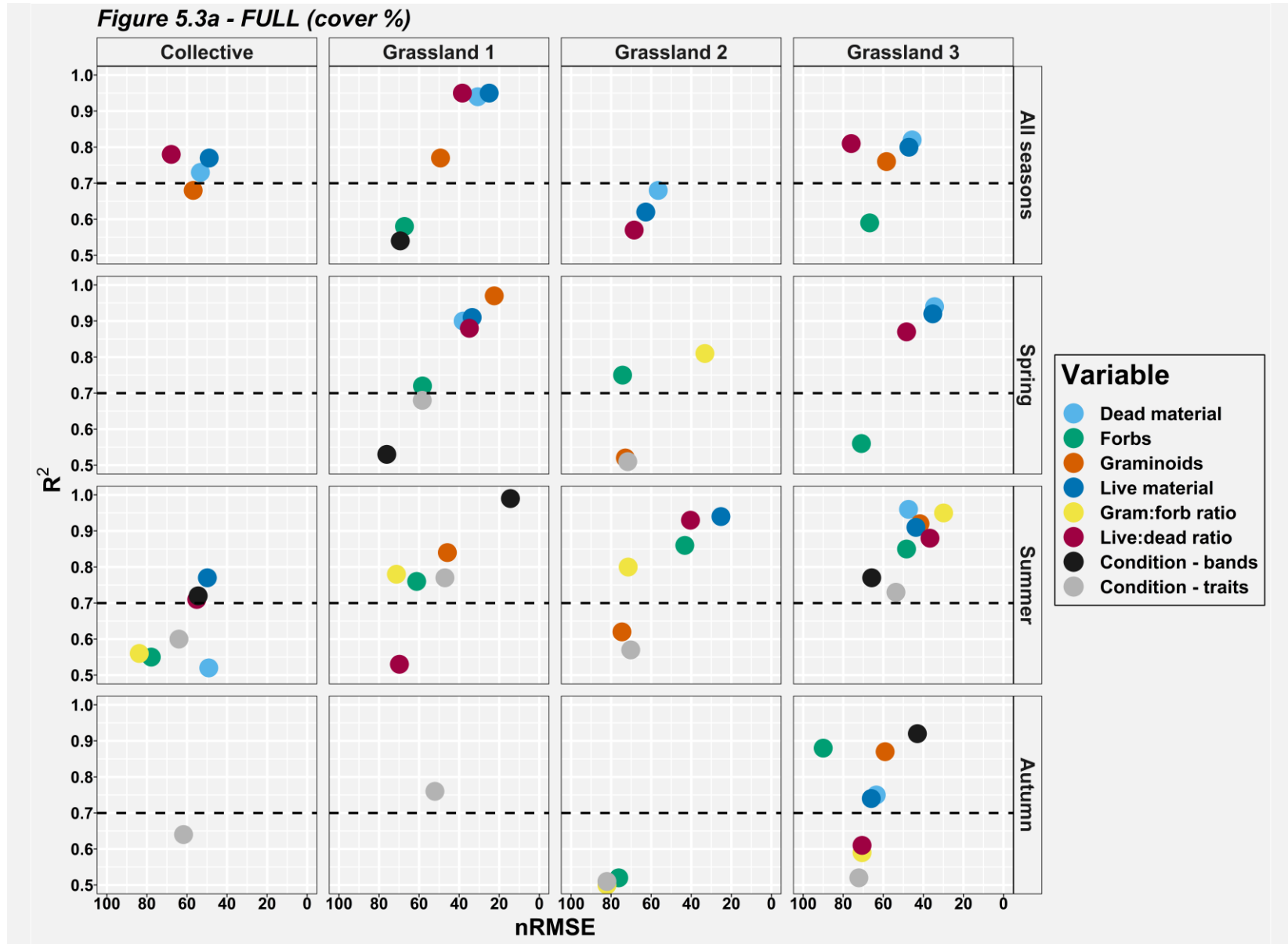
2676 *Figure 5.2: Median results of iterated model runs where spectral data were used to predict CSM-condition and mass-based grassland*
2677 *variables for each of the three seasons (n = 10 or 30) and for all seasons (n = 30 or 90). Also included are the results of predicting CSM-*
2678 *condition using grassland variables as predictors.*

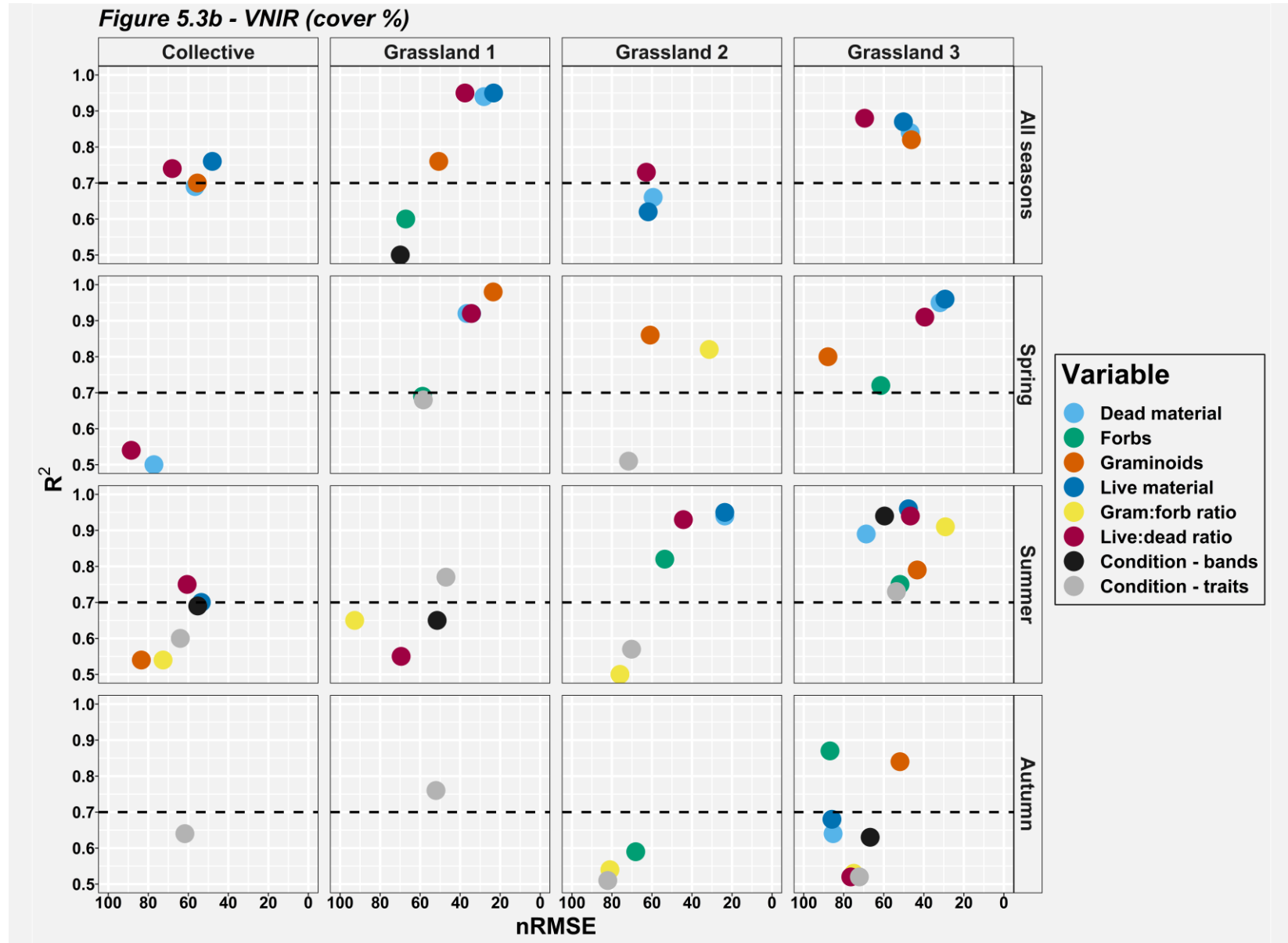
2679 **5.2.2. Cover-based grassland variable data**

2680 The results of using % cover grassland variable data as response data can be seen
2681 in Figure 5.3. When grasslands are analysed using data from all seasons; most
2682 grassland variables produced significant results for at least one grassland but dead
2683 material cover, graminoids cover, live material cover and live:dead ratio cover
2684 consistently produced R² values => 0.5 and nRMSE <100. When grasslands are
2685 analysed collectively for one season, most grassland variables were predicted with R²
2686 values => 0.5 for summer but almost all had R² values <0.5 except dead material
2687 cover and live:dead ratio cover when using VNIR data. When grasslands are
2688 analysed individually for one season, the grassland variables that produced
2689 significant results for all or nearly all of these grasslands and seasons (except
2690 Grasslands 1 and 2 for autumn) include forbs cover, graminoids cover, live material
2691 cover and live:dead ratio cover.

2692

2693





2696 *Figure 5.3: Median results of iterated model runs where spectral data were used to predict CSM-condition and cover-based grassland*
2697 *variables for each of the three seasons (n = 10 or 30) and for all seasons (n = 30 or 90). Also included are the results of predicting CSM-*
2698 *condition with grassland variables data.*

2699 **5.2.3. Predicting CSM-condition with spectral data or grassland variables**

2700 Of 32 model runs where spectral data were used as predictors of CSM-condition
2701 (Figures 5.4 and 5.5); 11 produced R² results => 0.5 and nRMSE <100, 5 of which
2702 have R² results => 0.7. Most of these PLSR models were for Grasslands 1 and 3 (5
2703 and 4 model runs respectively), the other two results being from analysing grasslands
2704 collectively. Using FULL spectral data produced 6 PLSR models with R²>0.5 whilst
2705 VNIR produced 5 PLSR models with R²>0.5. Using data collected in summer
2706 produced far more PLSR models with R²>0.5 (6) than using data from other seasons
2707 or analysing data from all seasons collectively (5 model runs in total, 1-2 from each
2708 season or from collective analysis).

2709 Of 32 model runs where grassland variables were used to predict CSM-condition
2710 (Figures 5.4 and 5.5); 13 of 32 model runs had R² results >0.5, 4 of which had R²
2711 results => 0.7. Of these 13 model runs, 10 were produced using % cover data but
2712 there were no other clear patterns in the results beyond this.

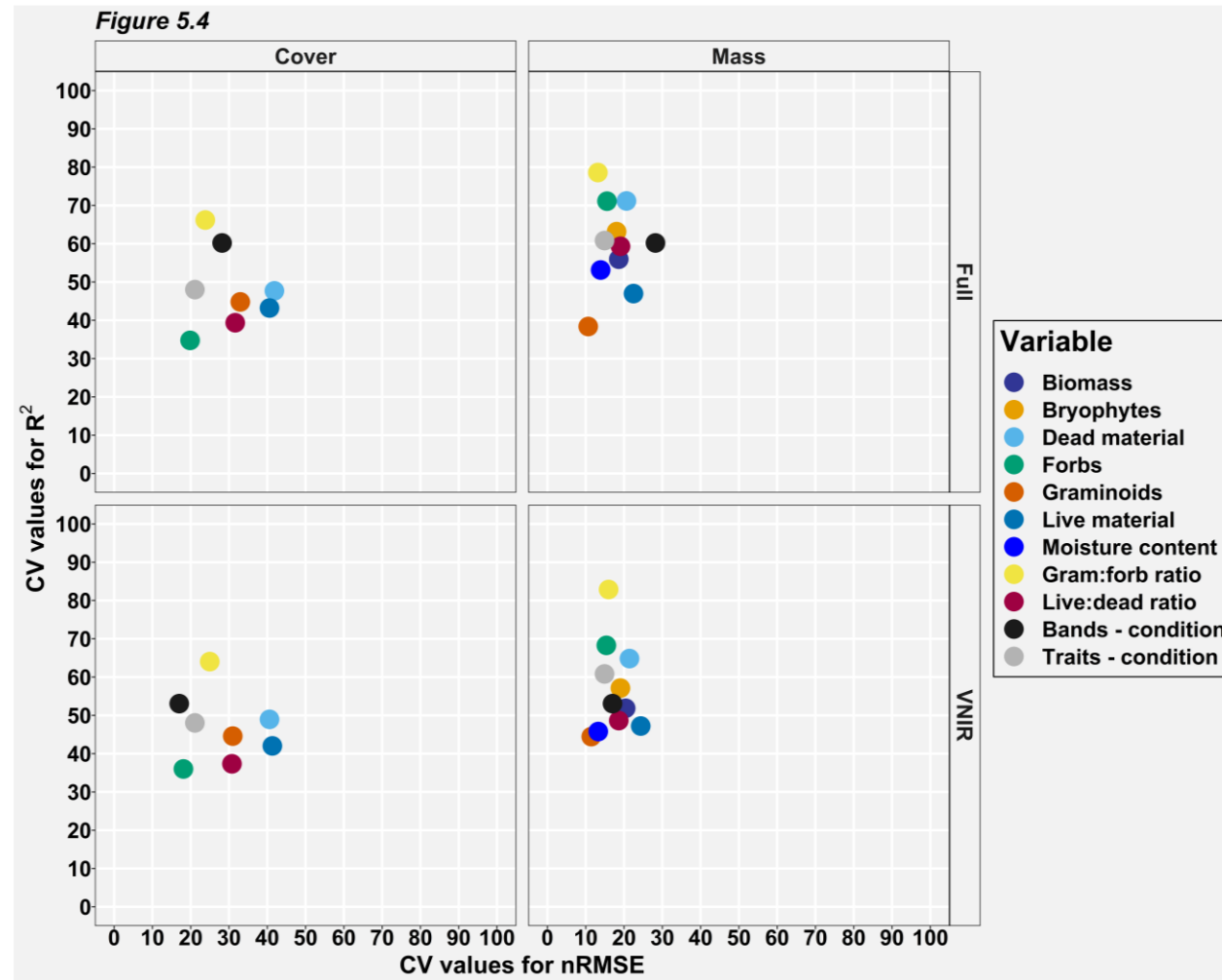
2713

2714 **5.3. Stability and consistency between model runs using the**
2715 **same response variable**

2716 Coefficient of variation (CV) was calculated to evaluate the stability of model
2717 performances across sites for specific variables. Figure 5.4 shows the % CV found
2718 from the iterated PLSR model runs for the resulting site specific R² and nRMSE
2719 values. Overall, models using cover-based grassland variables produce more
2720 consistent R² results but less consistent nRMSE results than models using mass-
2721 based grassland variables. For CSM-condition, this trend is reversed. Whether FULL-
2722 based models or VNIR-based models produce more stable results is grassland
2723 variable dependent although the results are generally similar.

2724 When using % cover data; model performances for forbs cover, graminoids cover and
2725 live:dead ratio cover are relatively stable. When using mass data; model
2726 performances for graminoids mass were the most stable with biomass, live material
2727 mass, moisture content and live:dead ratio mass also being relatively stable.

2728



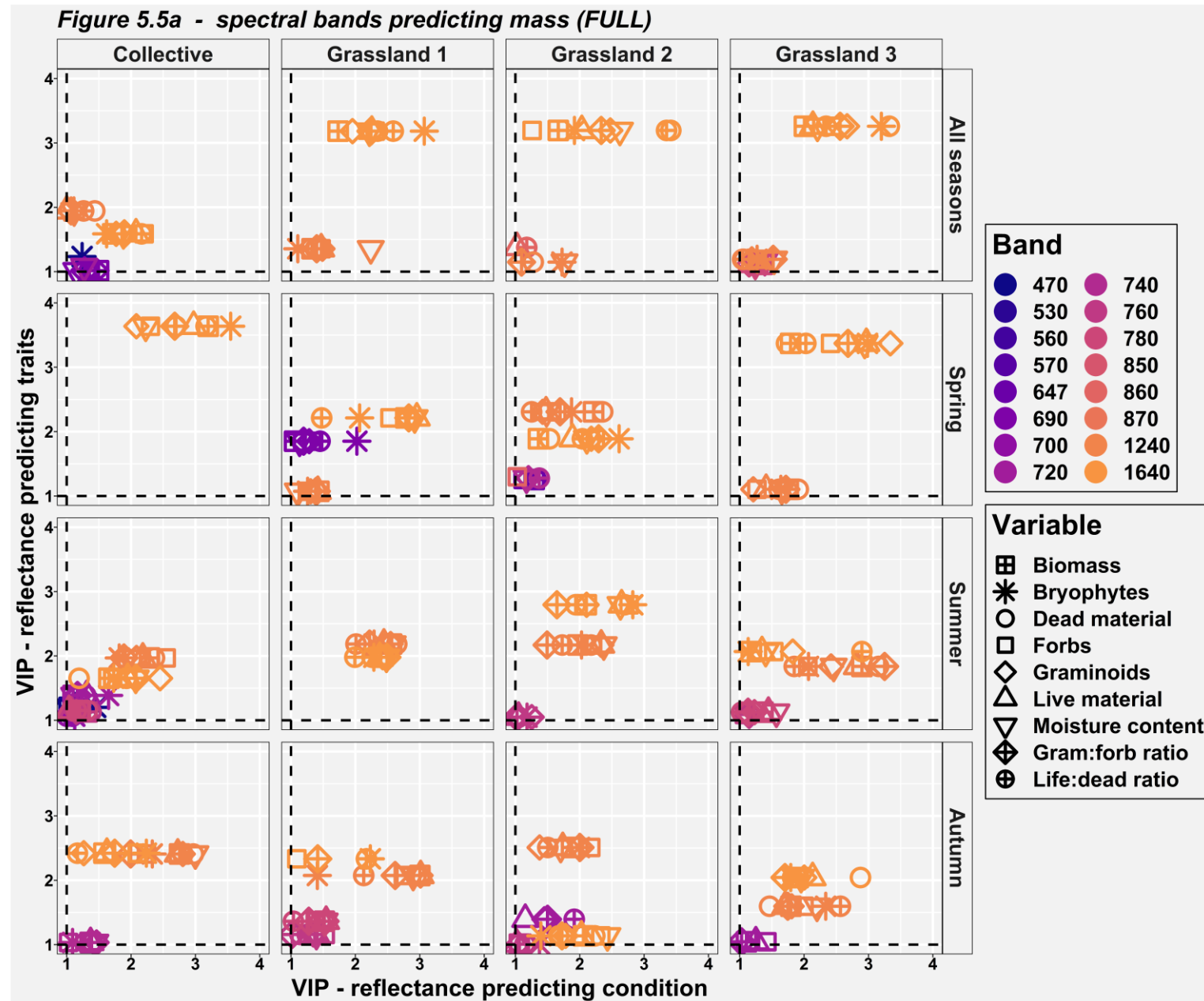
2729

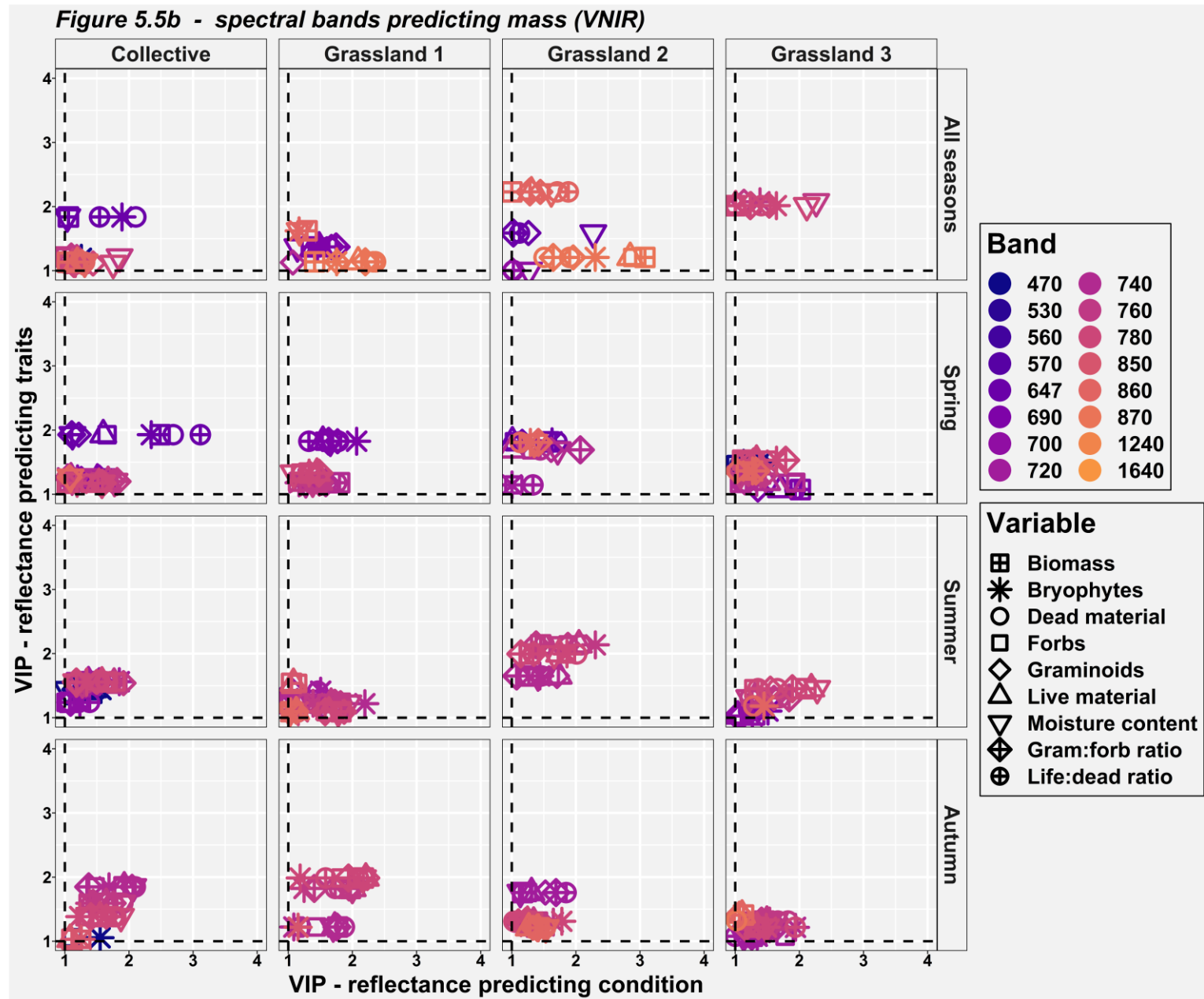
2730 Figure 5.4: % coefficient of variance (CV) for the R² and nRMSE results of the site specific PLSR models grouped per treatment and
 2731 spectral input data.

2732 **5.4. VIP analysis for spectral band and grassland variable**
2733 **selection**

2734 **5.4.1. Mass and cover data**

2735 Figures 5.5 and 5.6 show the results of using a VIP analysis to understand which
2736 spectral bands were the most important predictors for predicting grassland variables,
2737 where only important results ($\Rightarrow 1$) have been included. The results suggest that
2738 when using the FULL spectrum, the SWIR bands (1240 and 1640nm) are
2739 consistently important whether grasslands are analysed collectively or individually.
2740 For Grassland 3, some NIR bands plus 470nm and 647nm were also important.
2741 When VNIR spectral data were used; for Grasslands 1-2 plus collective analysis,
2742 bands within the 740-860nm were significant. Bands 470nm and 647nm were also
2743 important when grasslands were analysed collectively. The results for Grassland 3
2744 were similar to using the FULL spectrum minus the SWIR bands.

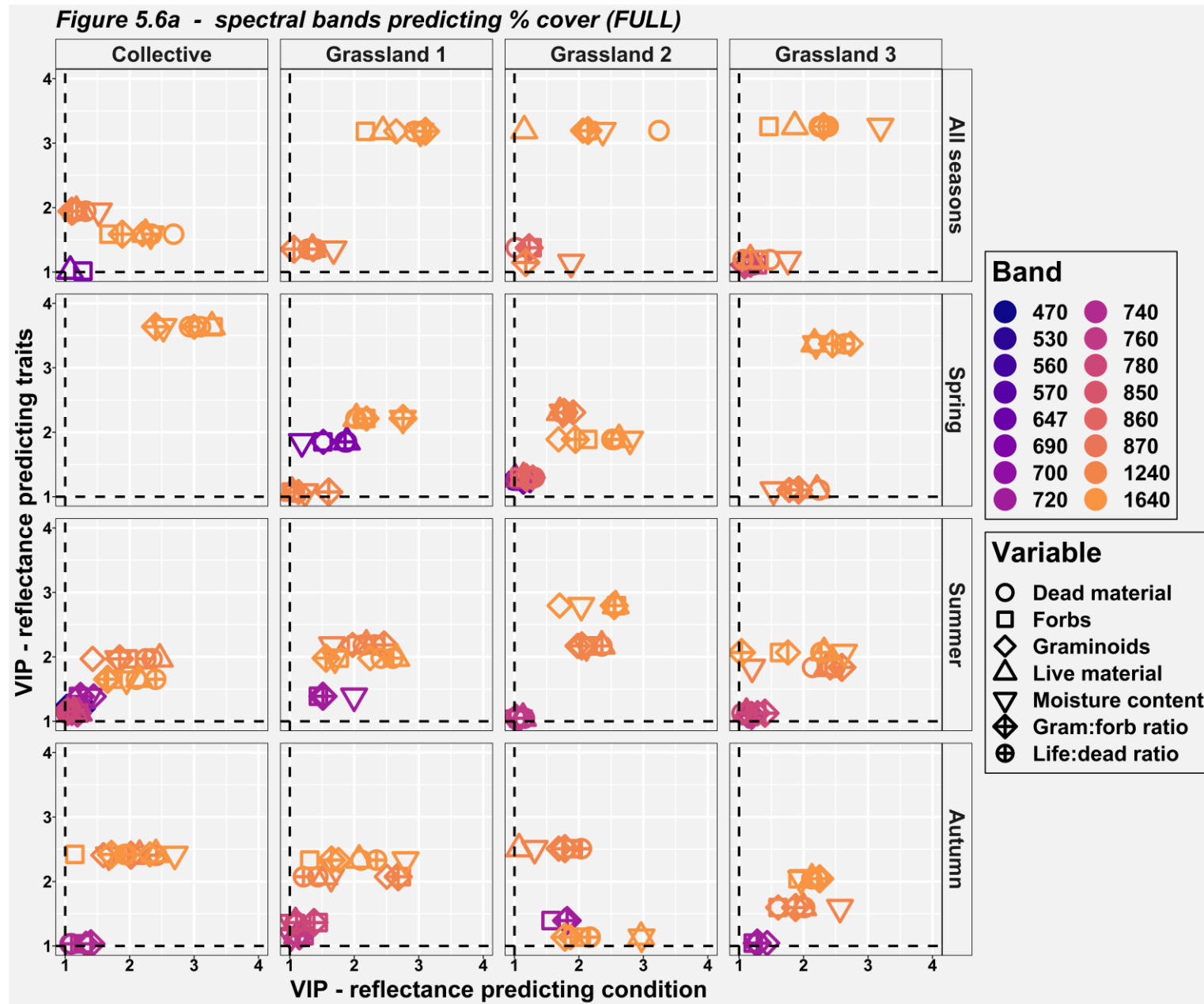


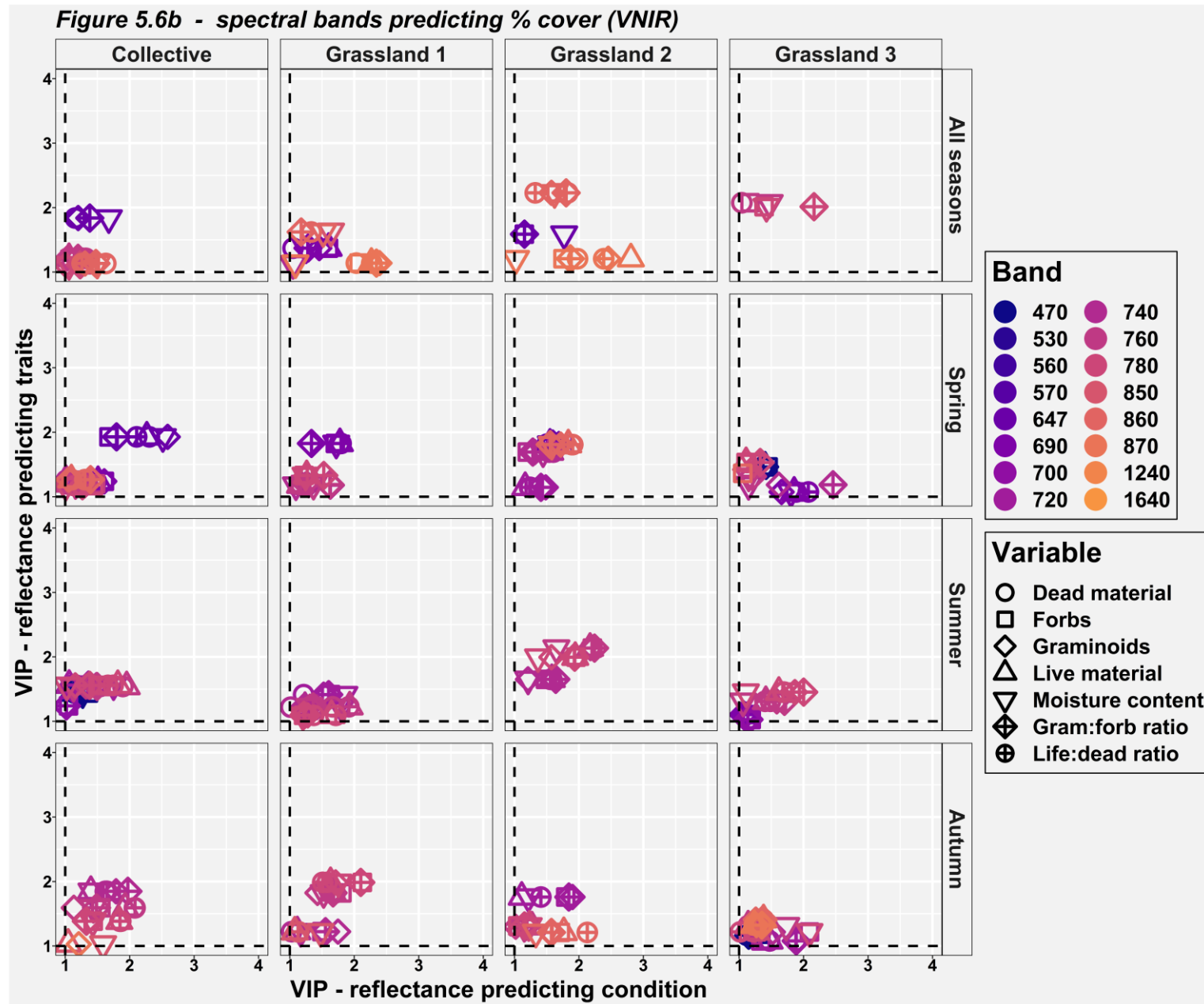


2747 *Figure 5.5: VIP plots showing which combinations of spectral bands (predictors) and which responses (grassland variables on x axis*
2748 *and CSM-condition on y axis) are most important in the study PLSR models where a) PLSR models trained with FULL spectral data and*
2749 *mass-based grassland variables and b) PLSR models trained with VNIR spectral data and mass-based grassland variables.*

2750

2751

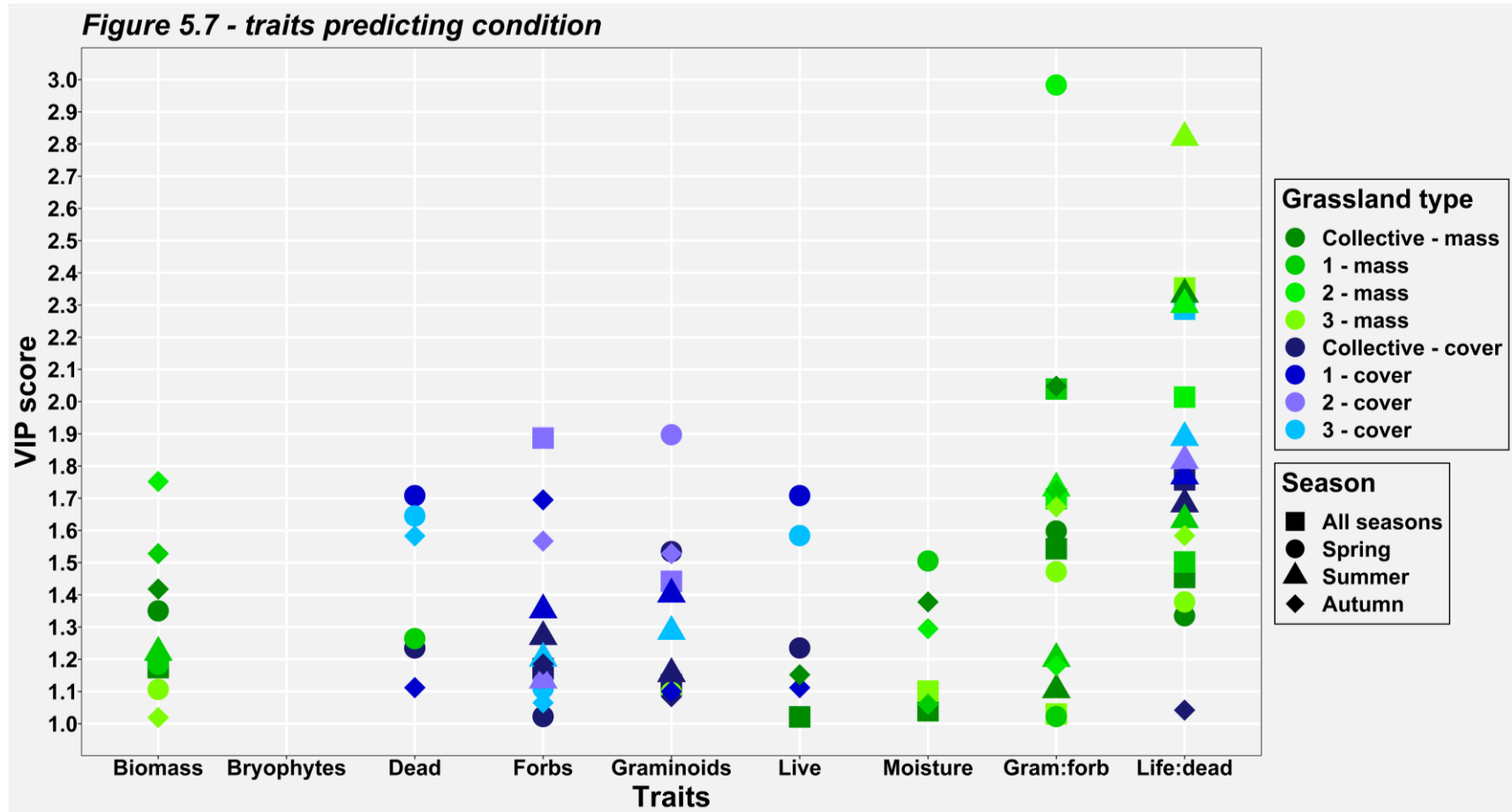




2754 *Figure 5.6: VIP plots showing which combinations of spectral bands (predictors) and which responses (grassland variables on x axis*
2755 *and CSM-condition on y axis) are most important in the study PLSR models where a) PLSR models trained with FULL spectral data and*
2756 *cover-based grassland variables and b) PLSR models trained with VNIR spectral data and cover-based grassland variables.*

2757 **5.4.2. Grassland variables predicting condition**

2758 Figure 5.7 shows the results of using grassland variable data to predict CSM-
2759 condition. Overall, multiple variables are significant for predicting condition but these
2760 grassland variables are different depending on whether mass or cover data are used.
2761 When mass data were used, the most important grassland variables were biomass,
2762 gram:forb ratio mass, live:dead ratio mass and moisture content. Primarily; forbs
2763 cover and graminoids cover were important when cover data were used although
2764 dead material cover, live material cover and live:dead ratio cover also had
2765 importance. These trends exist when analysing data from any one season or for all
2766 seasons.



2767

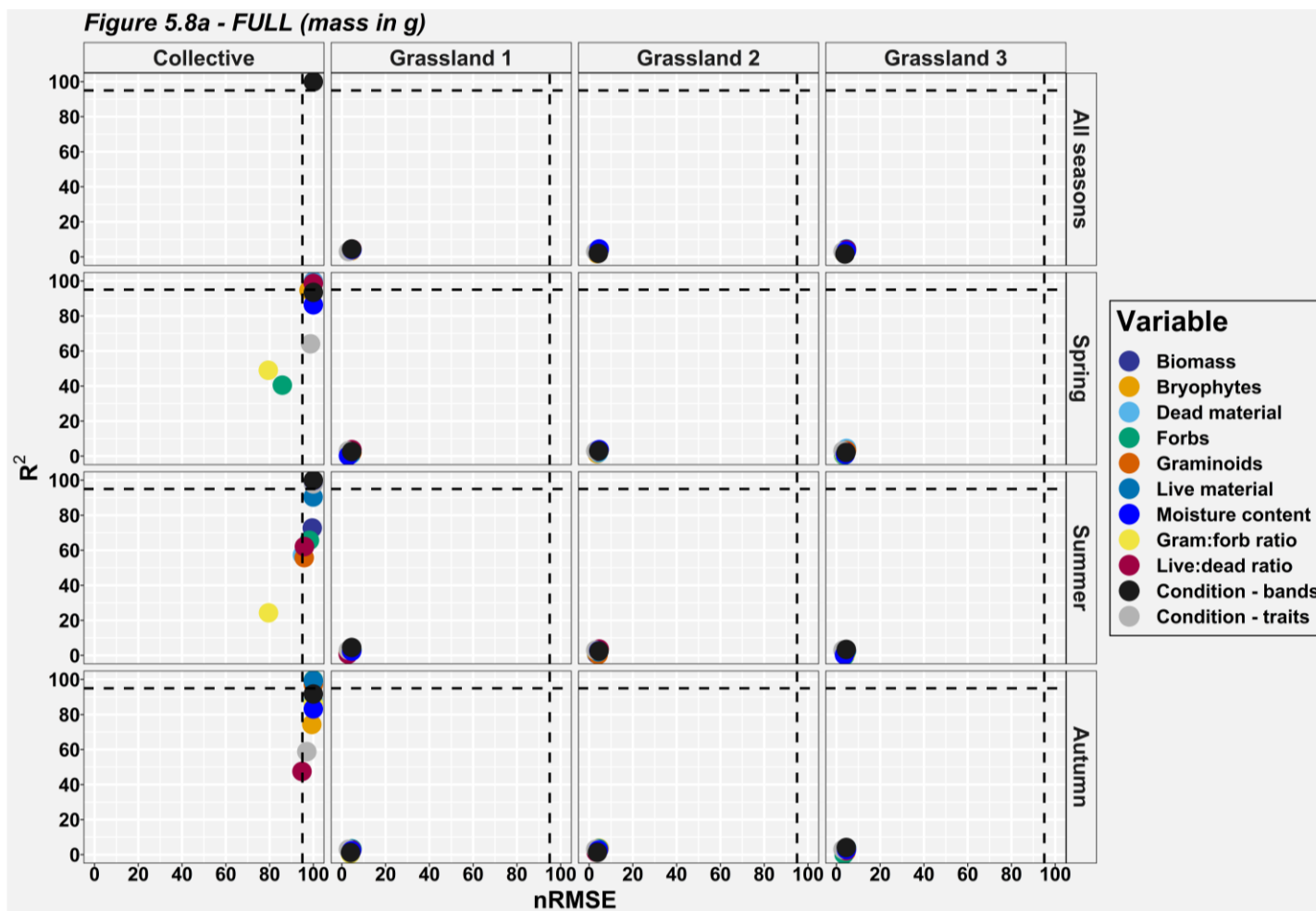
2768 *Figure 5.7: VIP plot showing which grassland variables are most important in predicting CSM-condition using either mass- or cover-*
 2769 *based grassland variables from analysing grasslands individually or collectively or for one or all seasons.*

2770 **5.5. Comparison of PLSR models trained with actual data and**
2771 **PLSR models trained with random data**

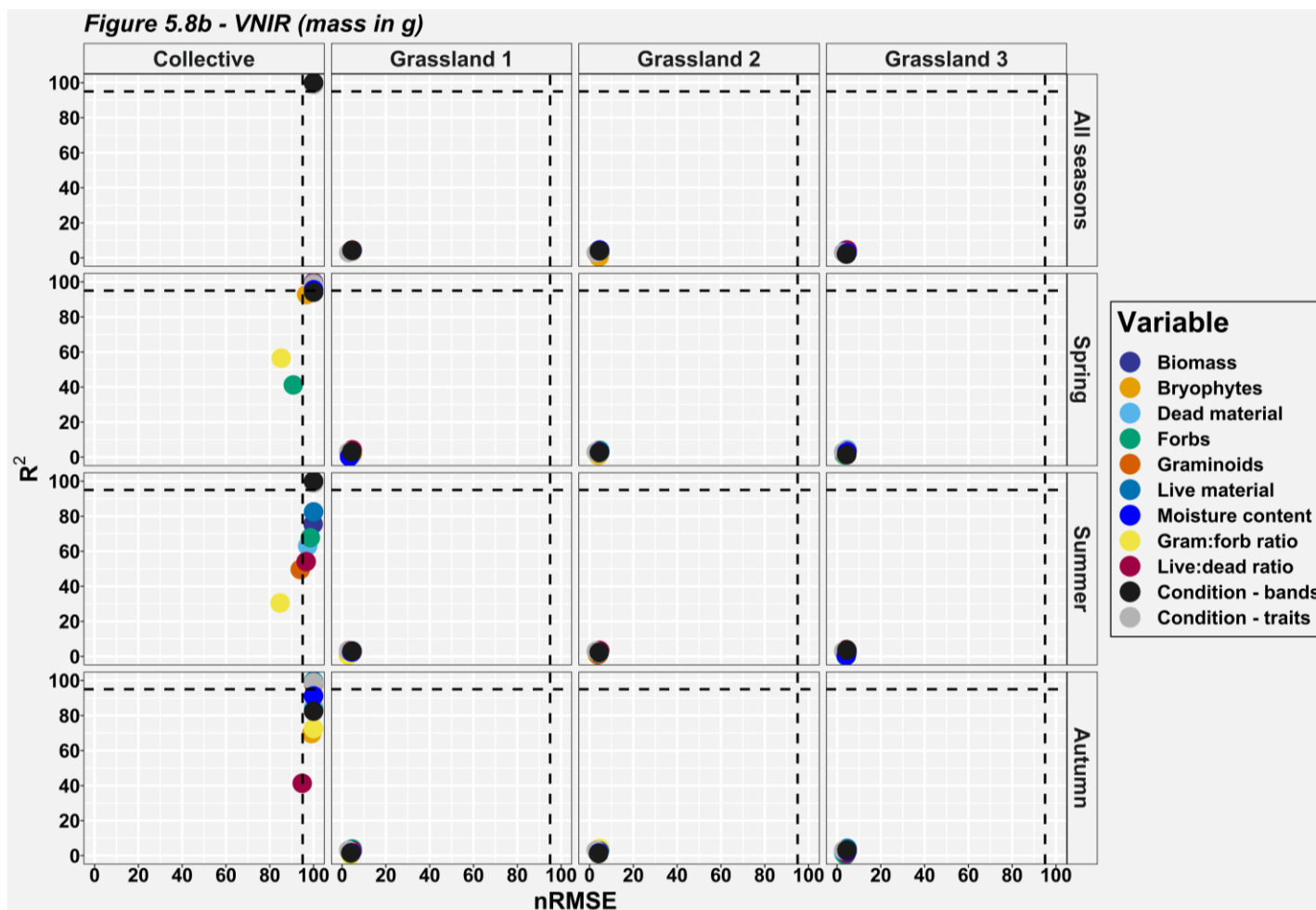
2772 The median values of R² and nRMSE results presented in Figures 5.2 and 5.3 (i.e.
2773 actual models) were compared against the results of 999 further model runs with
2774 randomised response variable values (randomised models) to test if the results run
2775 with the actual data genuinely produce reliable results. The results of comparing
2776 actual models to randomised models can be seen in Figures 5.8 and 5.9, where
2777 actual models that beat at least 950 randomised models (95% level) are considered
2778 consistently superior to randomised models.

2779 These results suggest that producing actual models that are superior to randomised
2780 models depends on the quantity of data being used but also whether data were
2781 collected over one season or multiple seasons. When data from all three grasslands
2782 and for all seasons (n = 90) are used, the median R² and nRMSE results are
2783 consistently superior to randomised models. When grassland data are analysed
2784 collectively for all grasslands and one season, almost all median nRMSE results, and
2785 median R² results for a few grassland variables, produces results that are
2786 consistently superior to results from randomised models at 95% level though some
2787 grassland variables are at least consistently superior to results from randomised
2788 models at an 80% level. When data from one grassland and one season are used (n
2789 = 10) or all seasons and one grassland (n = 30), the actual models are no more
2790 robust than randomised models.

2791



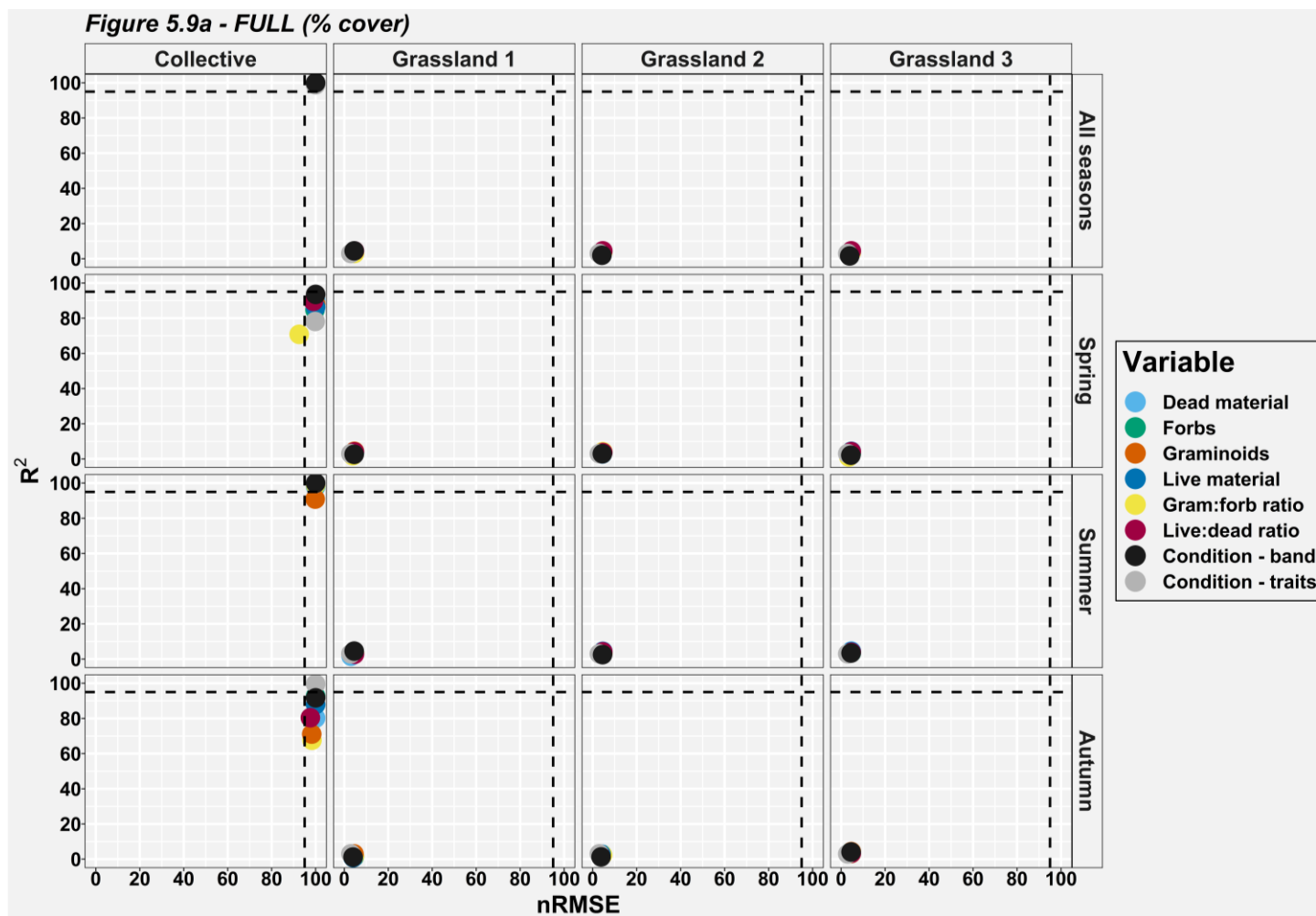
2792



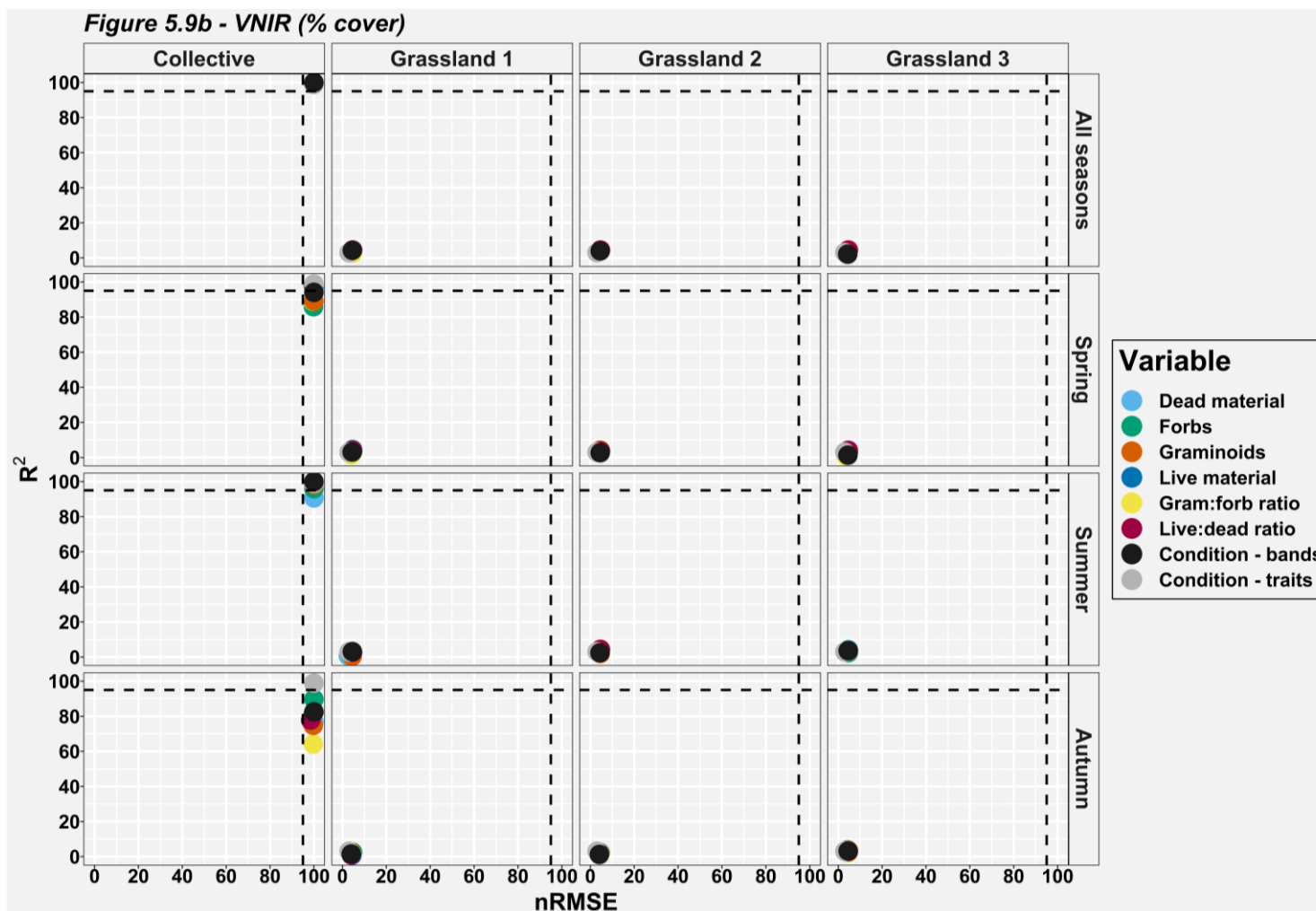
2793

2794 *Figure 5.8: Rankings of the median values of iterated model runs using actual mass response data and also iterated model runs using*
 2795 *randomised response data, where rankings >95% level are considered significant for the actual model fit.*

2796



2797



2798

2799 *Figure 5.9: Rankings of the median values of iterated model runs using actual % cover response data and iterated model runs using*
 2800 *randomised response data, where rankings >95% are considered consistently superior to randomised models*

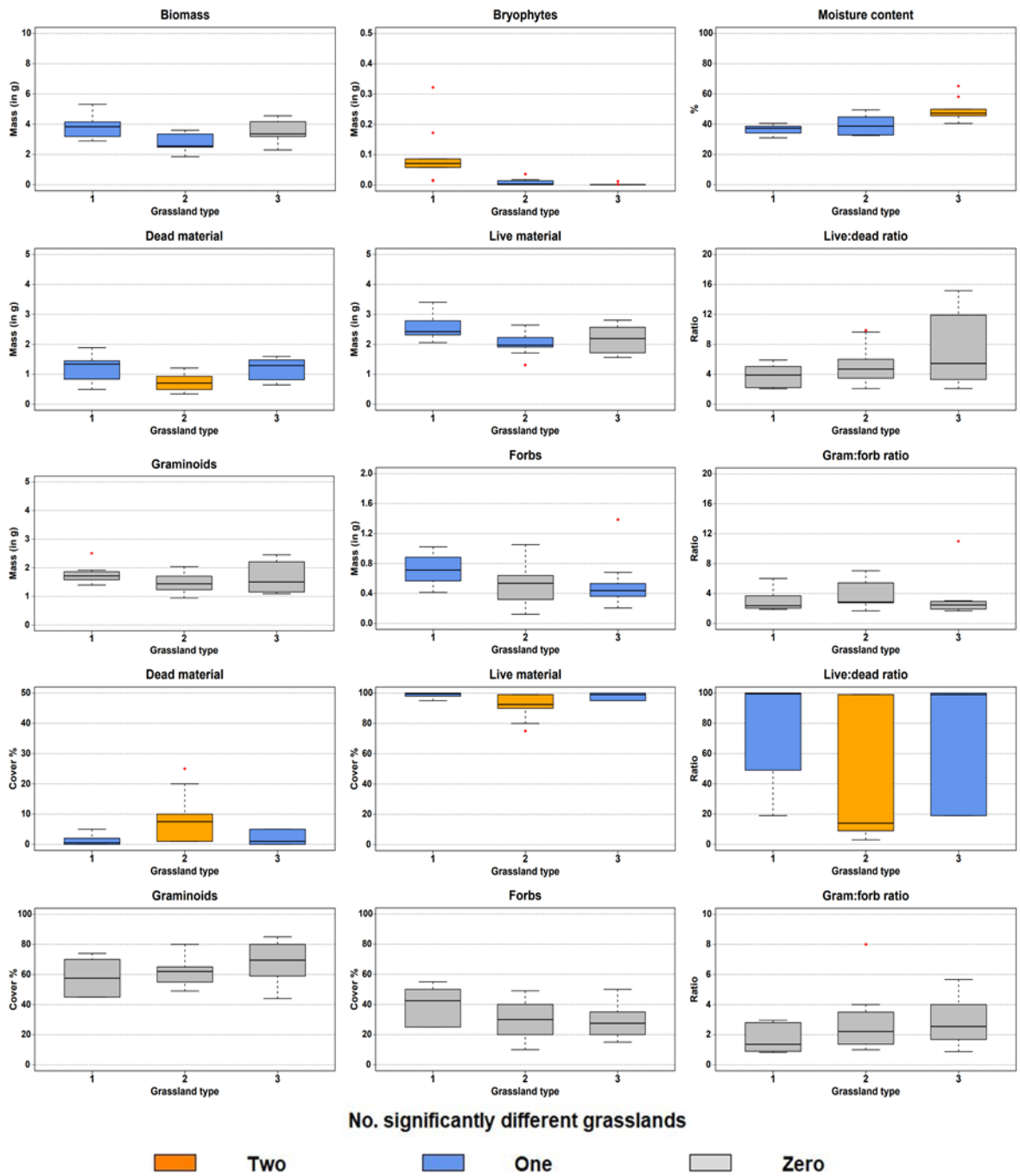
2801 **Chapter 6 - Comparison of patch**
2802 **level (1m²) spectral data from**
2803 **different devices and an**
2804 **assessment using field level**
2805 **(200x1m) CROPSCAN data when**
2806 **predicting condition-related**
2807 **grassland variables on calcareous**
2808 **semi-natural grasslands**

2809 **6.1. Grassland site characteristics**

2810 The boxplots of Figure 6.1 show the quantity of each grassland variable for each
2811 grassland together with the results of significant difference tests between grassland
2812 types, using an unpaired two-sample Wilcoxon test. This differs from a similar
2813 projection in Chapter 5 (Figure 5.1) in that only data collected during the summer are
2814 analysed. Overall, the Wilcoxon tests for grassland variables show that some
2815 grassland variables are significantly different at least between two grasslands. The
2816 Wilcoxon tests for the mass-based grassland variables show that for biomass, forbs
2817 mass and live material mass; two grasslands are significantly different from one other
2818 grassland. For dead material mass and moisture content; two grasslands are
2819 significantly different from one other grassland and one grassland from two others.
2820 For bryophytes mass, all grasslands are significantly different from each other. The
2821 Wilcoxon tests for the cover-based grassland variables show that for dead material
2822 cover, live material cover and live:dead ratio cover; two grasslands are significantly
2823 different from one other grassland and one grassland from two others.

2824

2825



2826

2827 *Figure 6.1: Boxplots of the grassland variable values for the three grassland sites.*

2828 *The boxplot colours summarise the unpaired two-sample Wilcoxon test results*

2829 *between grassland types where the colour represents the number of sites from which*

2830 *each grassland variable is significantly different ($p < 0.05$).*

2831

2832 **6.2. Predicting grassland variables and condition using PLSR**

2833 The median R² and nRMSE results of the PLSR modelling from the iterated model
2834 runs to predict mass, % cover grassland variables and CSM-condition using spectral
2835 data from the three different devices as predictors where R² => 0.5 and nRMSE <=
2836 100 can be seen in Figures 6.6 and 6.7, with the full results presented in Appendix
2837 Figure 5. Overall; when PLSR models were trained with data from all three
2838 grasslands (n = 30), using spectral data from different devices produced similar
2839 results. When PLSR models were trained with data from a single site (n = 10); there
2840 is no set pattern in the results as performance seems to be specific to the grassland
2841 and the spectral device used.

2842

2843 **6.2.1. Predicting mass-based grassland variable data**

2844 When grasslands are analysed collectively using spectral data from any device
2845 (Figure 6.2); bryophytes mass, moisture content and CSM-condition all produced R²
2846 results >0.5 (most are >0.7) and nRMSE <100 when using data from the Rikola
2847 camera. When grasslands are analysed individually; most of the significant results
2848 came from using spectral data from the Rikola camera, CROPSCAN and the SVC
2849 when using data from Grassland 1 plus from Grassland 3 when using a CROPSCAN.

2850

2851 **6.2.2. Predicting cover-based grassland variable data**

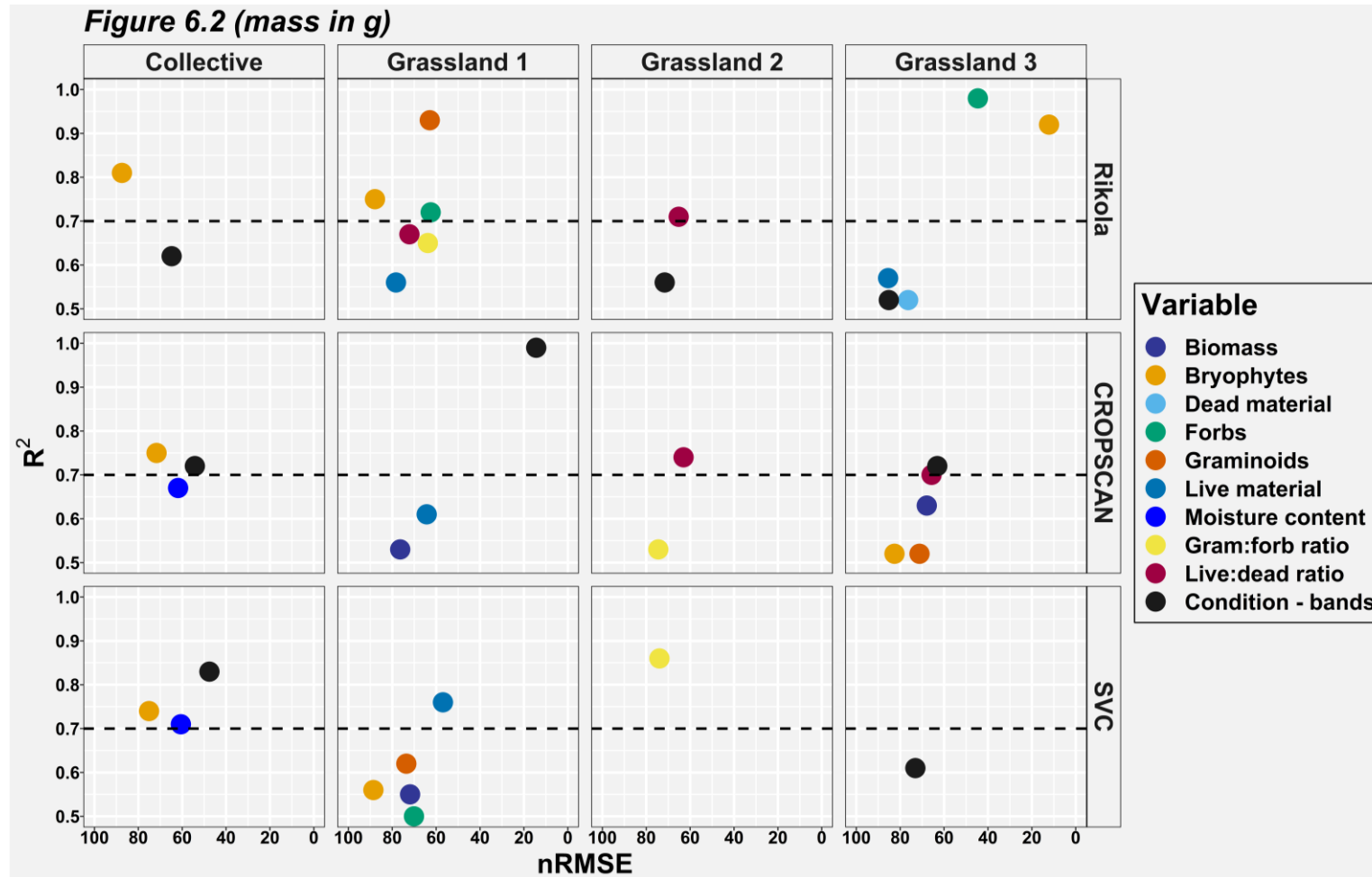
2852 When grassland were analysed collectively using spectral data from any device
2853 (Figure 6.3); most grassland variables produced R² values => 0.5 and nRMSE <100
2854 for at least one device but CSM-condition, live material cover, live:dead ratio
2855 cover produced significant results for all three devices with live material cover and
2856 CSM-condition producing R² results >0.7. When grasslands were analysed
2857 individually using spectral data from any device; most grassland variables produced
2858 significant results except for Grassland 1 when using spectral data from the SVC.

2859

2860 **6.2.3. Predicting CSM-condition using grassland variables**

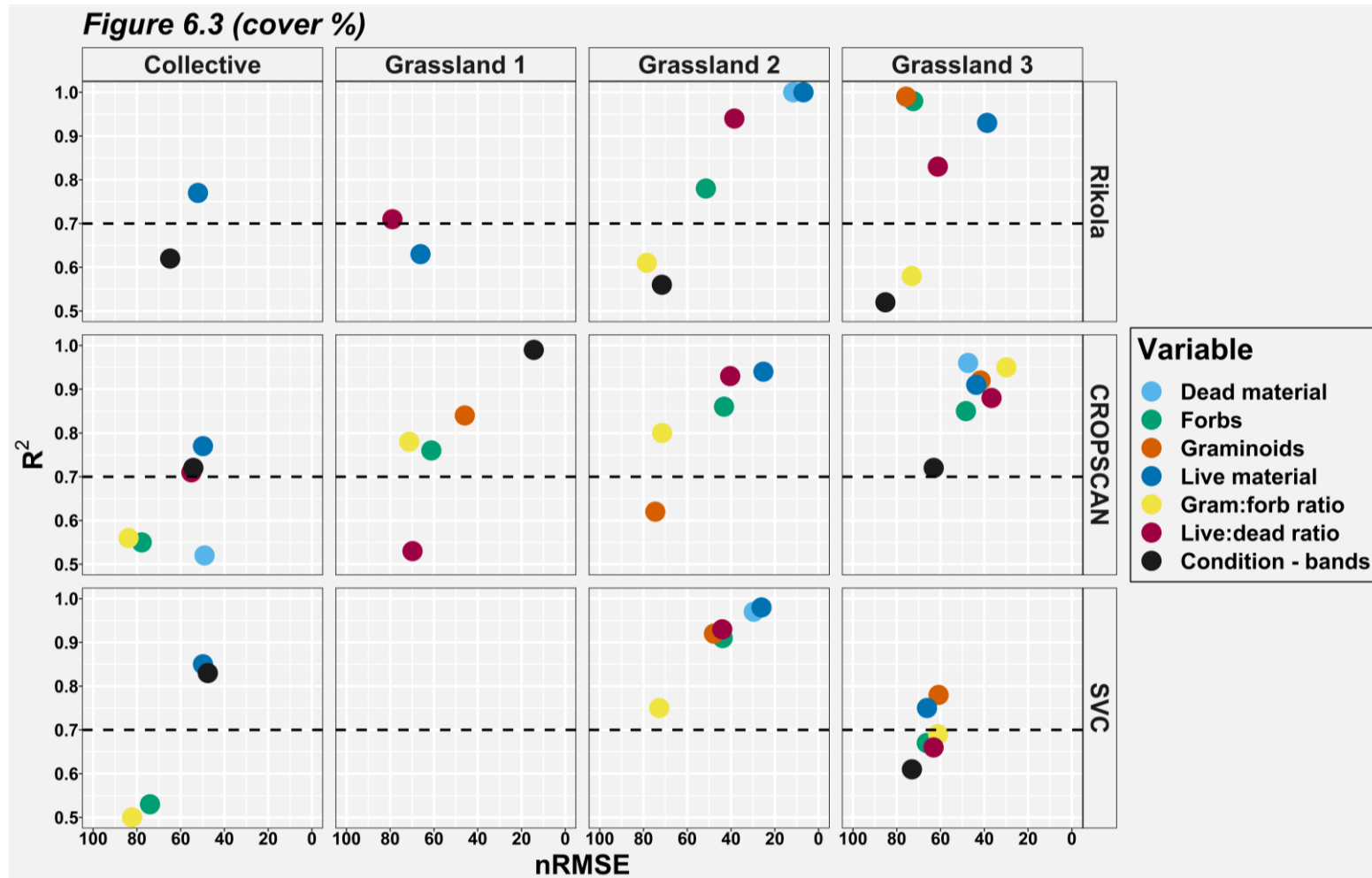
2861 Of 12 model runs when using spectral data to predict CSM-condition (Figures 6.6 and
2862 6.7); 8 produced R² results => 0.5 and nRMSE <100, 4 of which have R² results =>
2863 0.7. Most of the significant results were produced when analysing grasslands
2864 collectively (3) whilst analysing grasslands individually produced 1-2 significant
2865 results. Using different devices produced 2 results for the SVC and 3 significant
2866 results each for the CROPSCAN and Rikola camera. Of 8 model runs when using
2867 grassland variables to predict CSM-condition; 4 produced R² results => 0.5 and
2868 nRMSE <100, 2 of which have R² results => 0.7. All significant results using % cover
2869 data. Analysing grasslands collectively or individually produced 1 significant result
2870 each.

2871



2872

2873 Figure 6.2: Median results of iterated model runs where spectral data from three different devices were used to predict CSM-condition and
 2874 mass-based grassland variables for all grasslands collectively ($n = 30$) or single sites ($n = 10$).



2875

2876 Figure 6.3: Median results of iterated model runs where spectral data from three different devices were used to predict CSM-condition and
 2877 cover-based grassland variables for all grasslands collectively ($n = 30$) or single sites ($n = 10$).

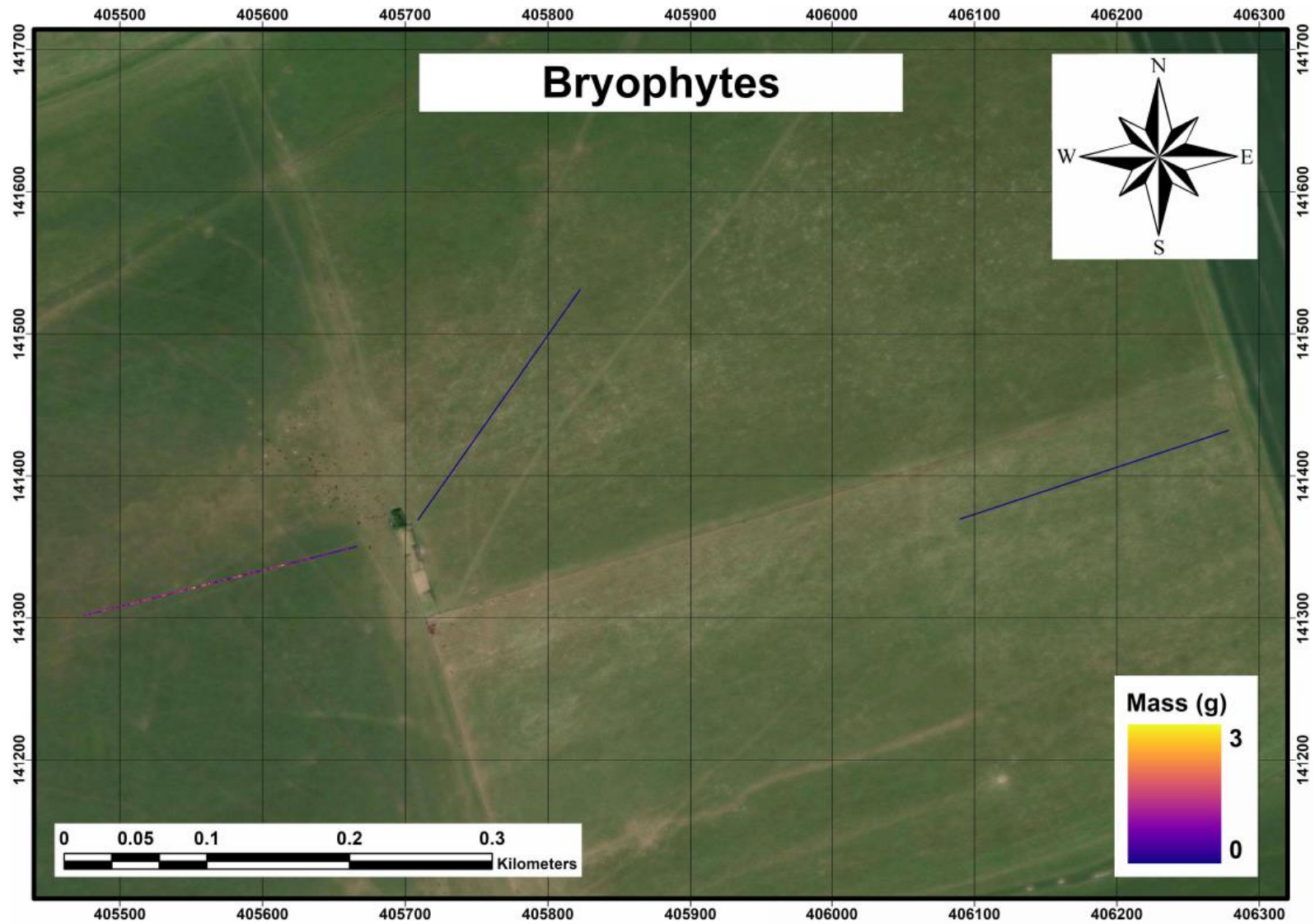
2878 **6.3. Comparing observed and predicted values**

2879 Each of the trained PLSR models produced predicted values for each grassland
2880 variable on each quadrat. These predicted values have been plotted against the
2881 observed values (1:1 lines have been included) for comparison in the appendix. The
2882 clusters of some grassland variables appear to be close to the 1:1 line. For other
2883 grassland variables, the 1:1 line appears to run closer to the main body of the cluster
2884 than to the lowest and/or highest observed values, suggesting that the PLSR models
2885 did not predict these values as accurately. For a few grassland variables, particularly
2886 live:dead ratio cover, the clusters appear to be scattered suggesting a low predictive
2887 power of the associated PLSR models.

2888

2889 **6.4. Extrapolating predicted grassland variables and condition**
2890 **using CROPSCAN data as predictors**

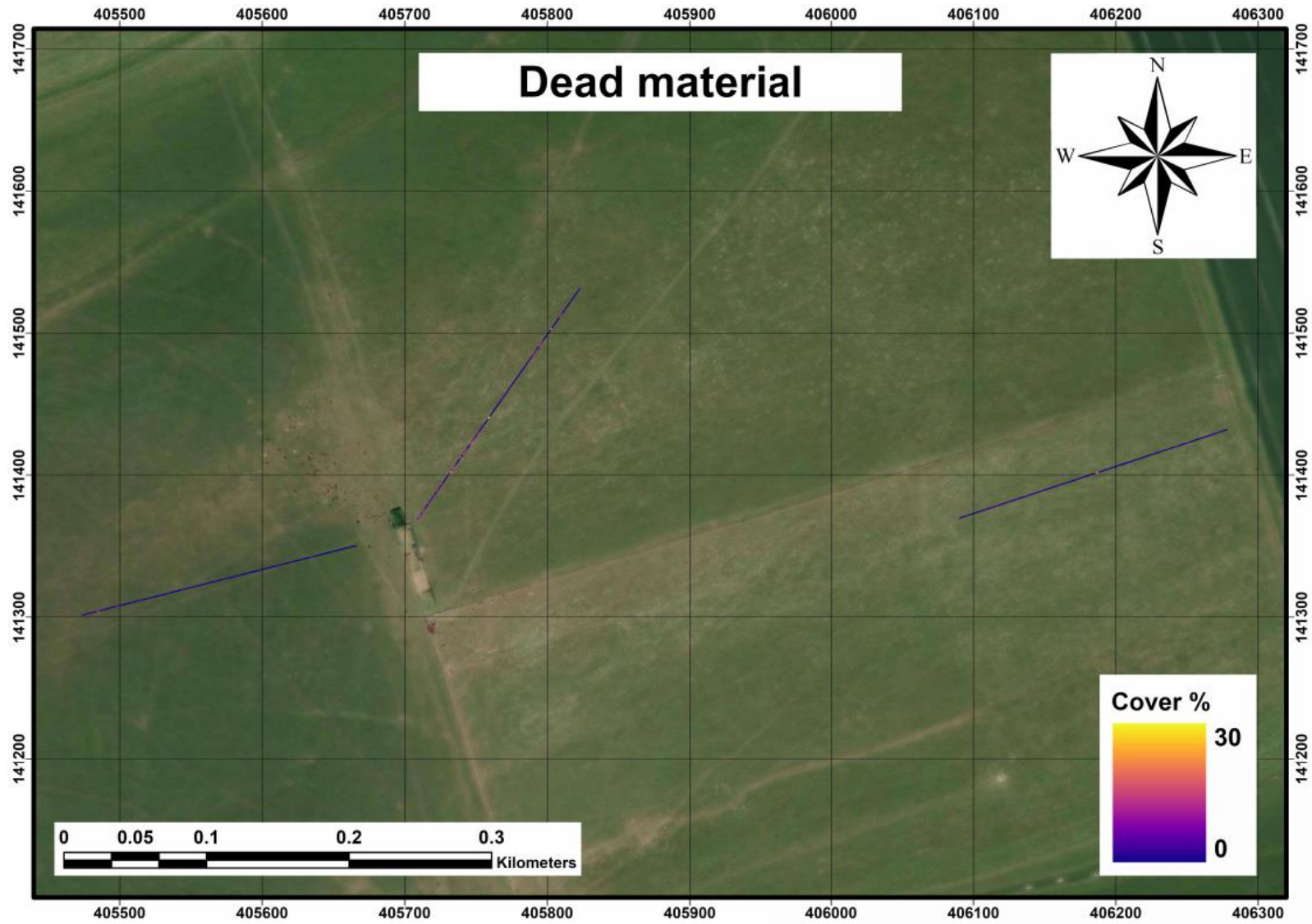
2891 Moderate to strong fitting PLSR models trained with data from all three grasslands
2892 collectively using CROPSCAN data as predictors were used to predict grassland
2893 variable values at field level (Figure 6.4).



2894

2895

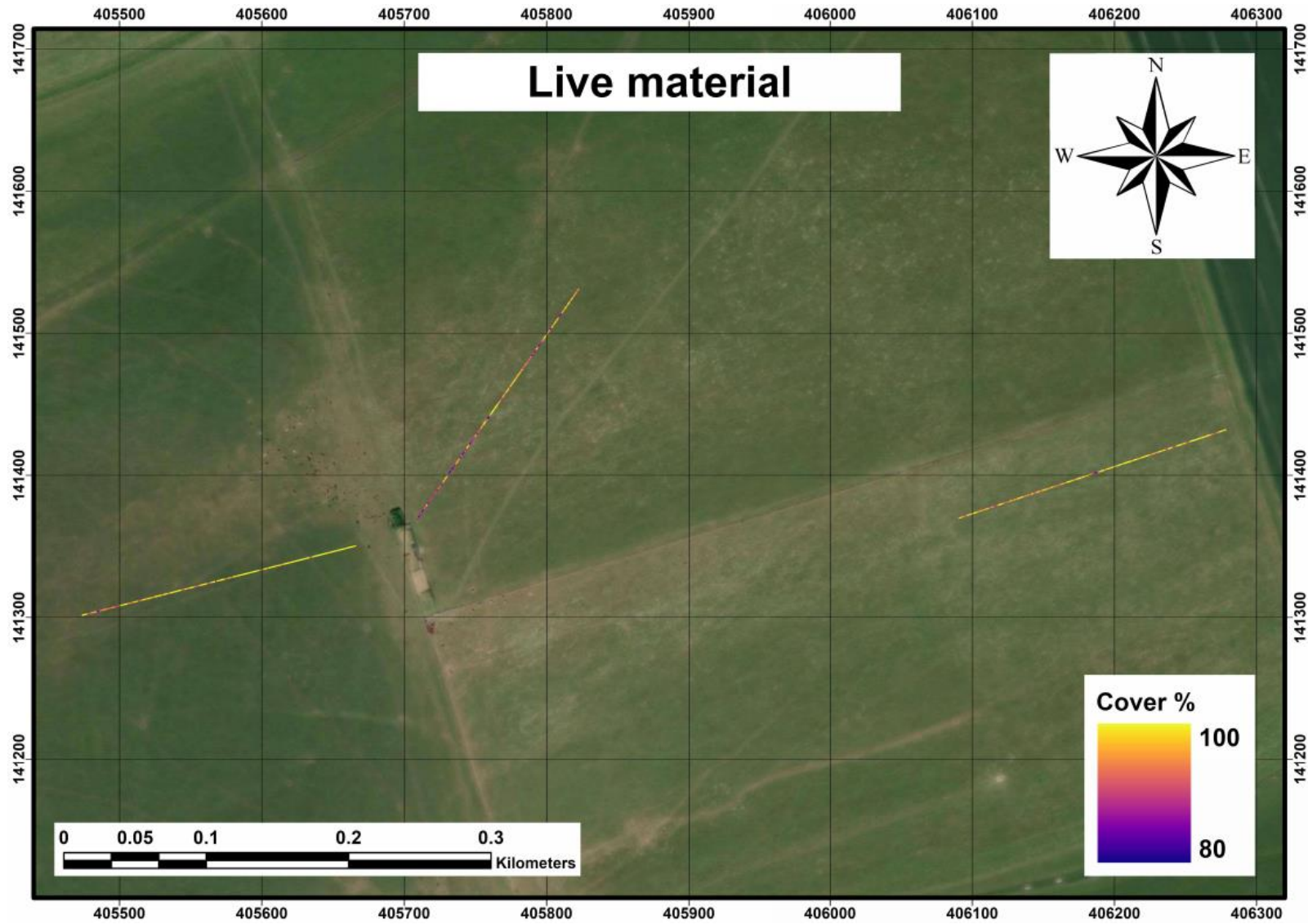
Figure 6.4a: Projection of bryophyte mass predicted values derived from a PLSR model trained with CROPSCAN spectral data.



2896

2897

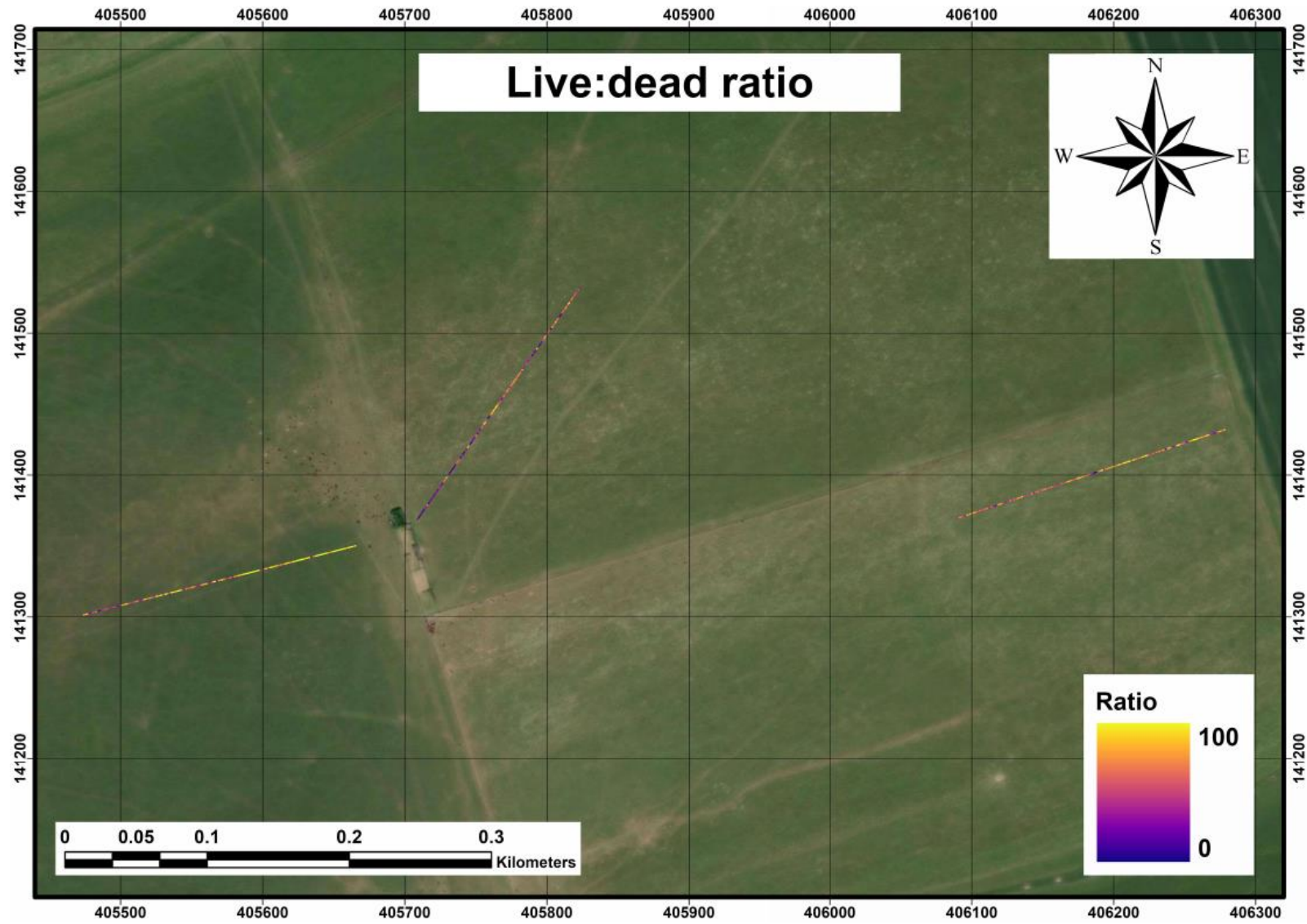
Figure 6.4b: Projection of dead material % cover predicted values derived from a PLSR model trained with CROPSCAN spectral data.



2898

2899

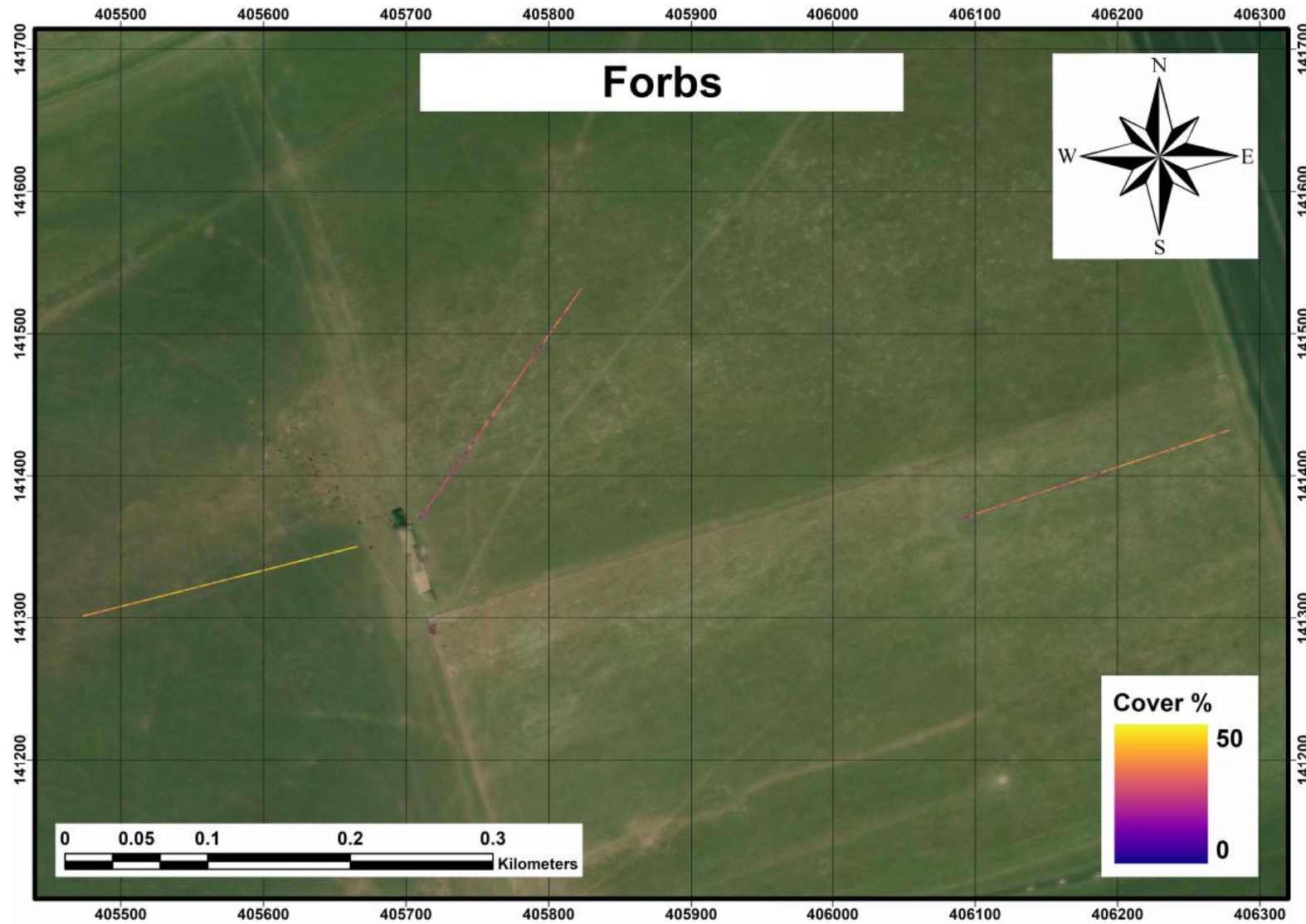
Figure 6.4c: Projection of live material % cover predicted values derived from a PLSR model trained with CROPSCAN spectral data.



2900

2901

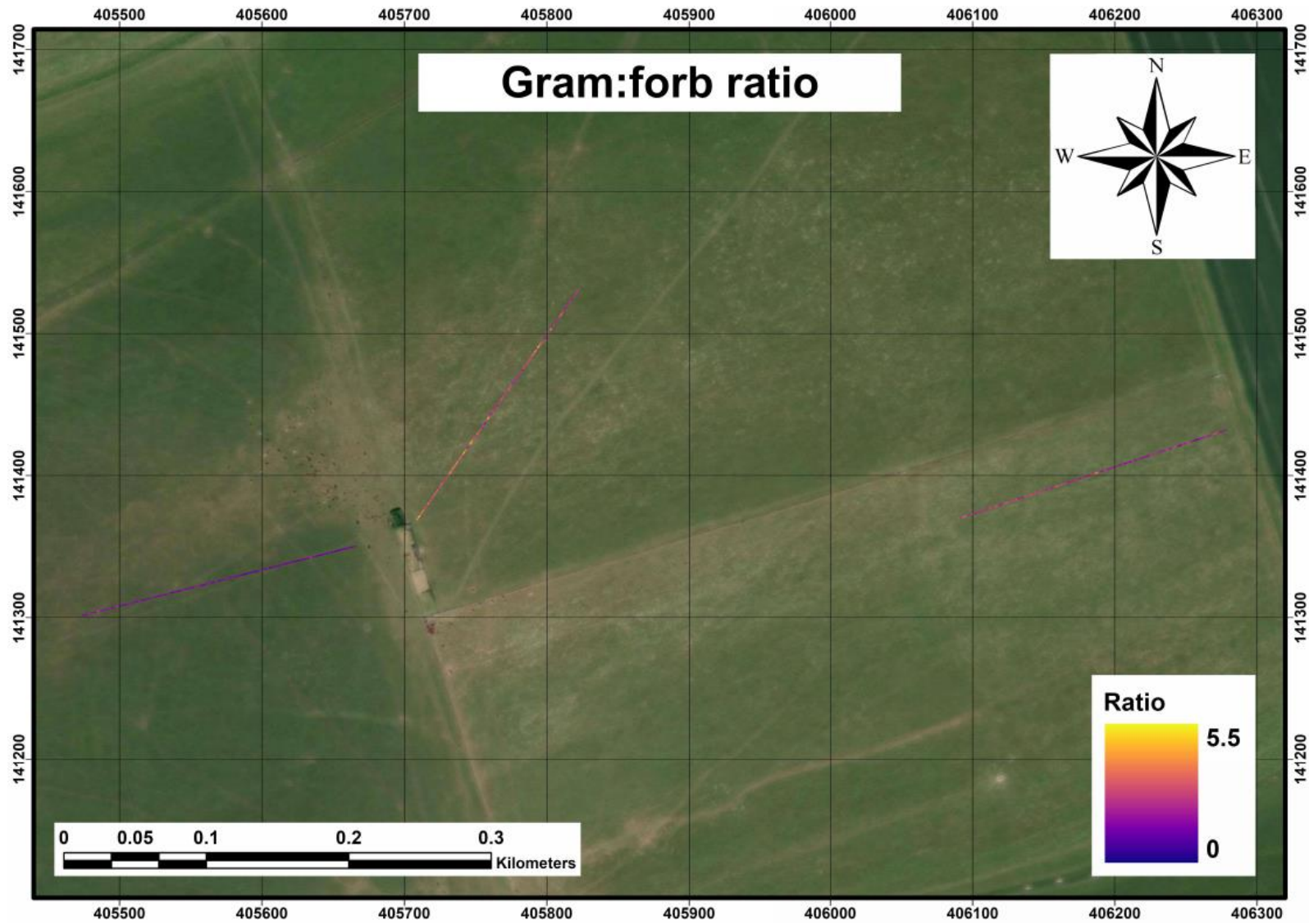
Figure 6.4d: Projection of live:dead ratio % cover predicted values derived from a PLSR model trained with CROPSCAN spectral data.



2902

2903

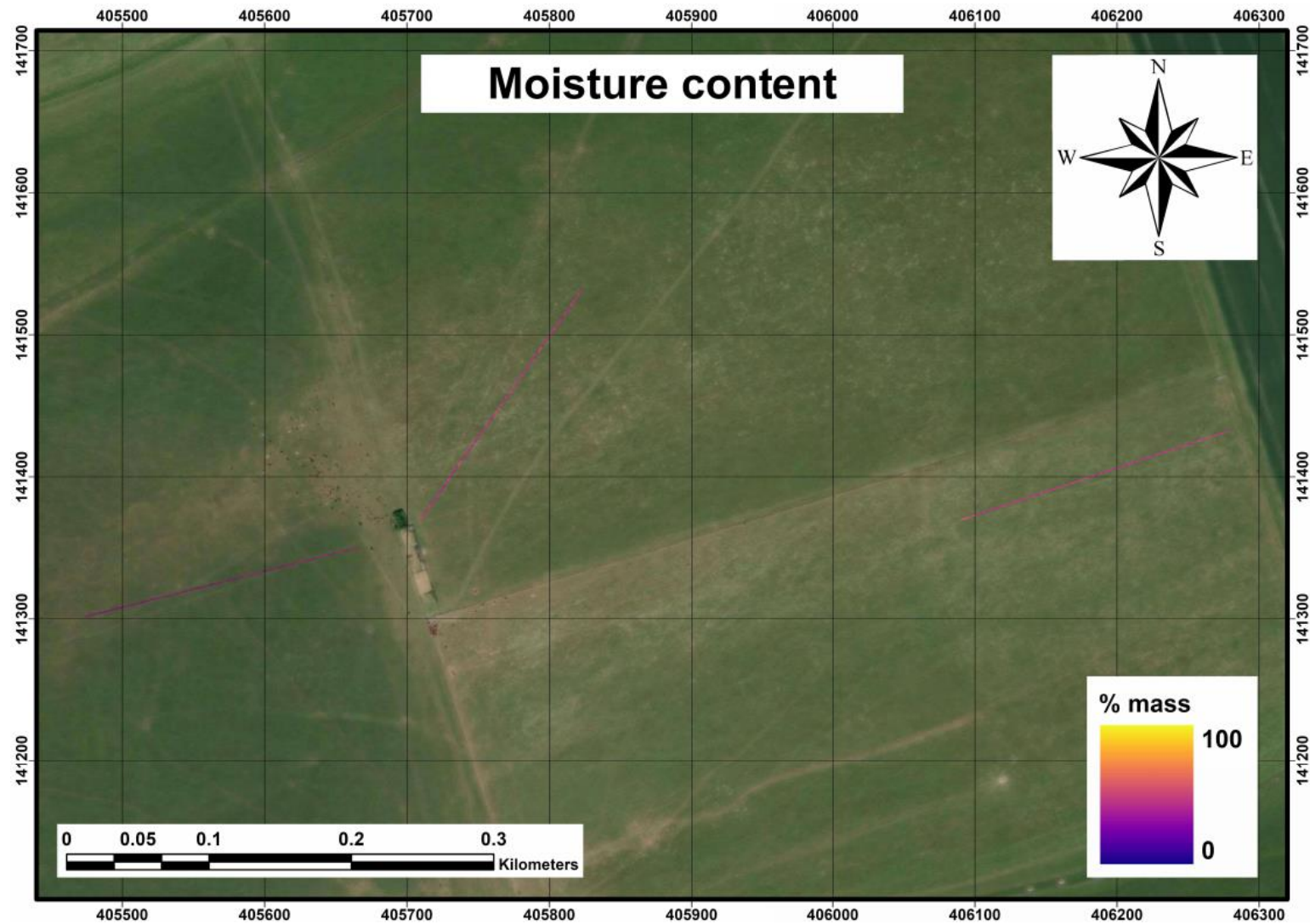
Figure 6.4e: Projection of forbs % cover predicted values derived from a PLSR model trained with CROPSCAN spectral data.



2904

2905

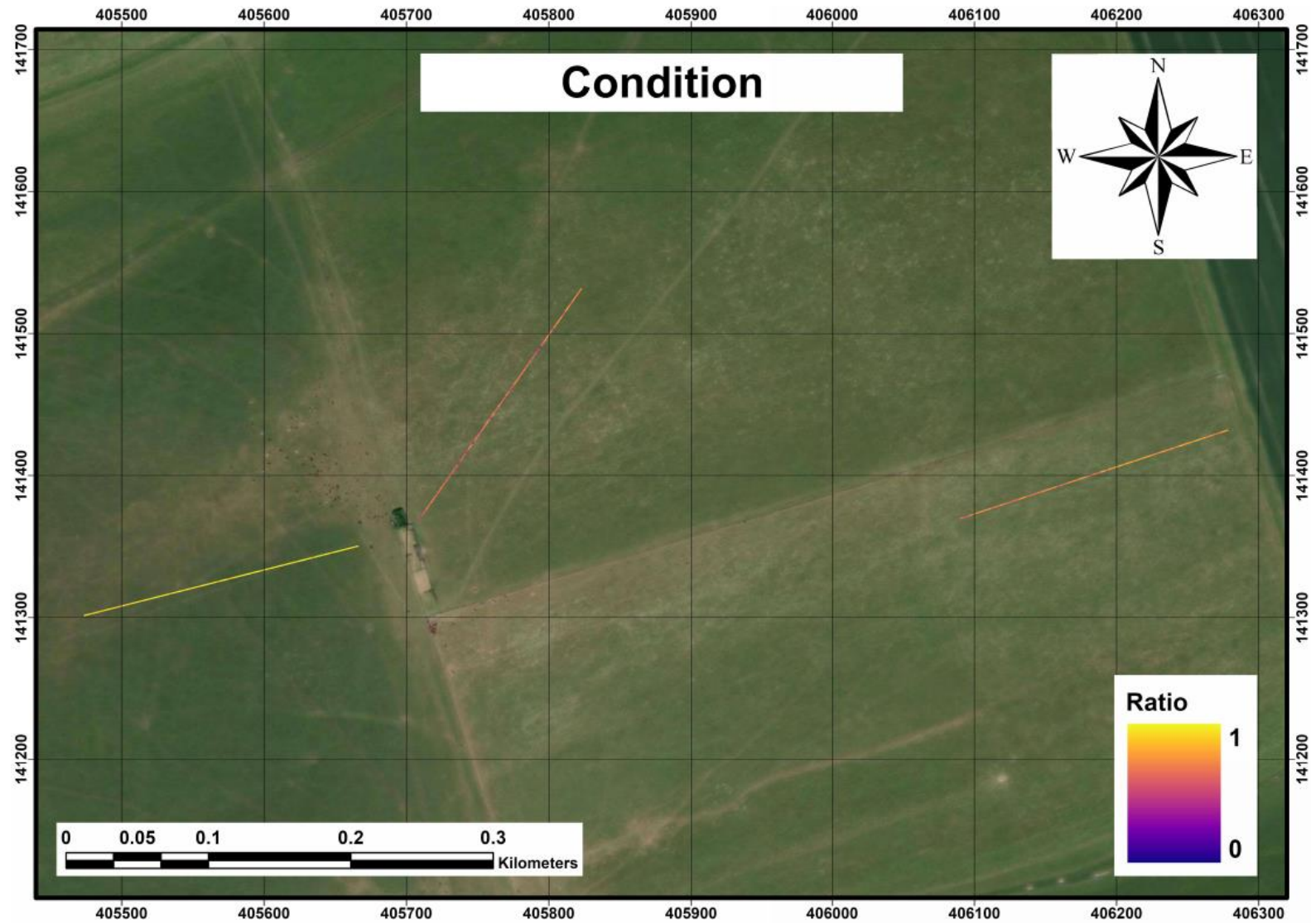
Figure 6.4f: Projection of gram:forb ratio % cover predicted values derived from a PLSR model trained with CROPSCAN spectral data.



2906

2907

Figure 6.4g: Projection of moisture content (% mass) predicted values derived from a PLSR model trained with CROPSCAN spectral data.



2908

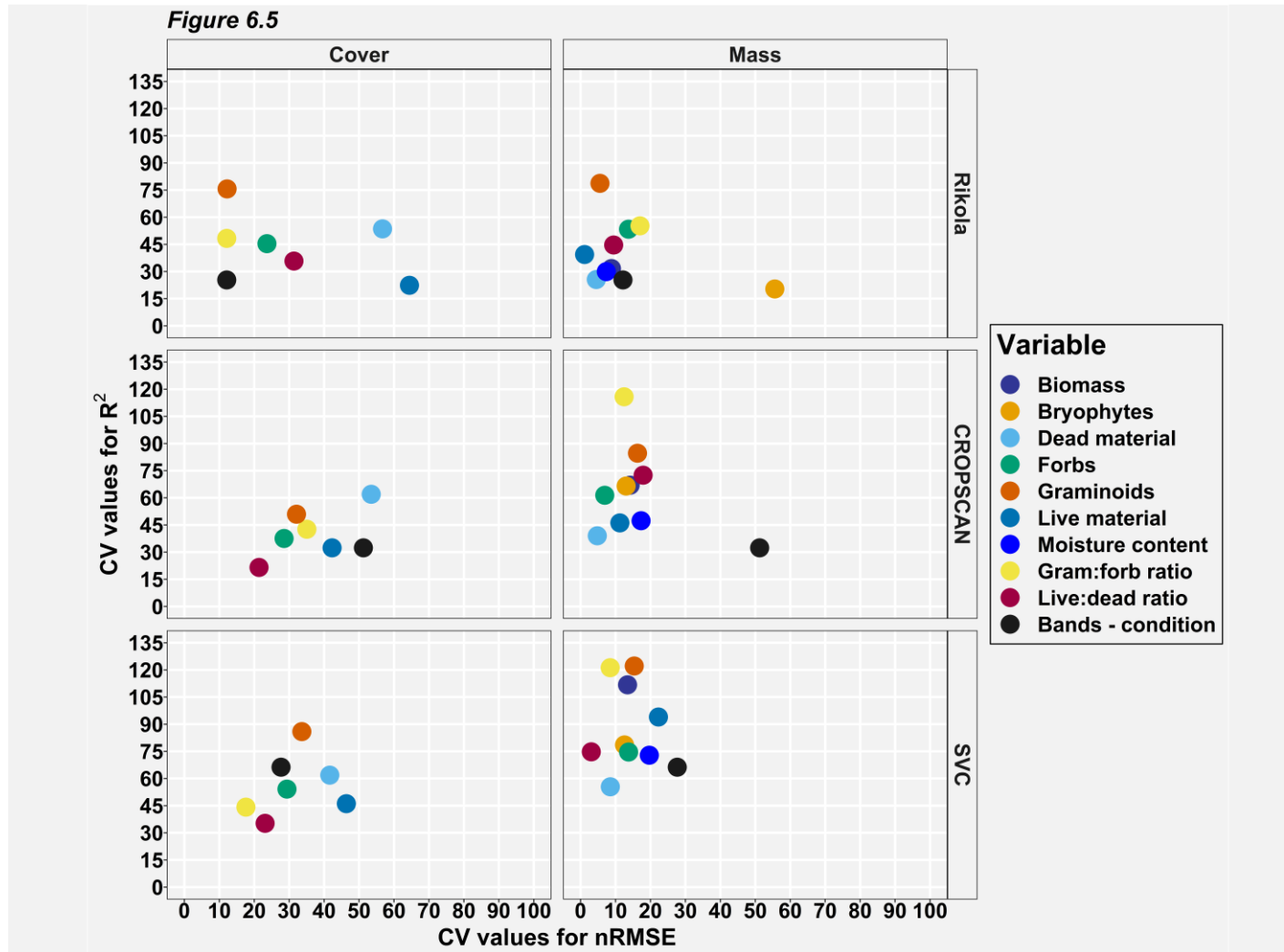
2909

Figure 6.4h: Projection of CSM-condition predicted values derived from a PLSR model trained with CROPSCAN spectral data.

2910 **6.5. Stability and consistency between model runs using the**
2911 **same response variable**

2912 Figure 6.5 shows the % CV of the median found from the iterated PLSR model runs
2913 and the resulting R² and nRMSE values of the site specific PLSR models that were
2914 calculated to evaluate the stability of model performances across sites for specific
2915 grassland variables. Lower CV values were considered to be more indicative of
2916 model stability. Overall, models predicting mass-based grassland variables produce
2917 more consistent R² results but less consistent nRMSE results than models predicting
2918 % cover-based grassland variables.

2919 The results between different spectral devices appear to be similar when predicting
2920 mass-based grassland variables and for most grassland variables when predicting
2921 cover-based grassland variables, with some of the grassland variables showing a
2922 different level of consistency when spectral data from the Rikola VNIR camera are
2923 used as predictors. When predicting % cover data, forbs cover, gram:forb ratio cover
2924 and live:dead ratio cover appear to be relatively consistent. When predicting mass
2925 data, dead material mass and moisture content are relatively consistent for all three
2926 devices. Other grassland variables are relatively consistent for the two devices; forbs
2927 mass, live material mass and live:dead ratio mass.



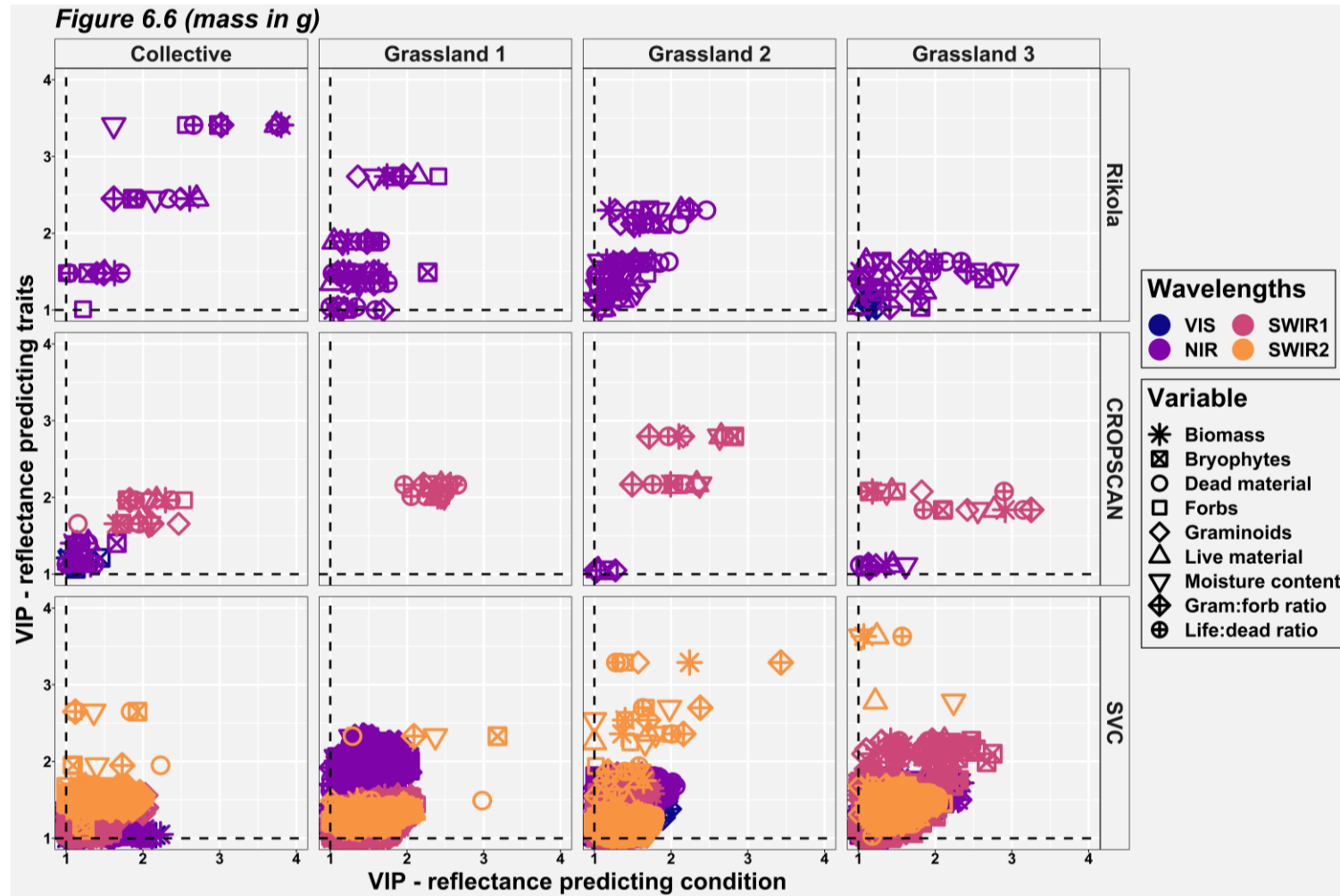
2928

2929 Figure 6.5: % coefficient of variation (CV) for the R^2 and nRMSE results of the site specific PLSR models grouped per treatment and spectral
 2930 input data from different spectral devices.

2931 **6.6. VIP analysis for spectral band selection**

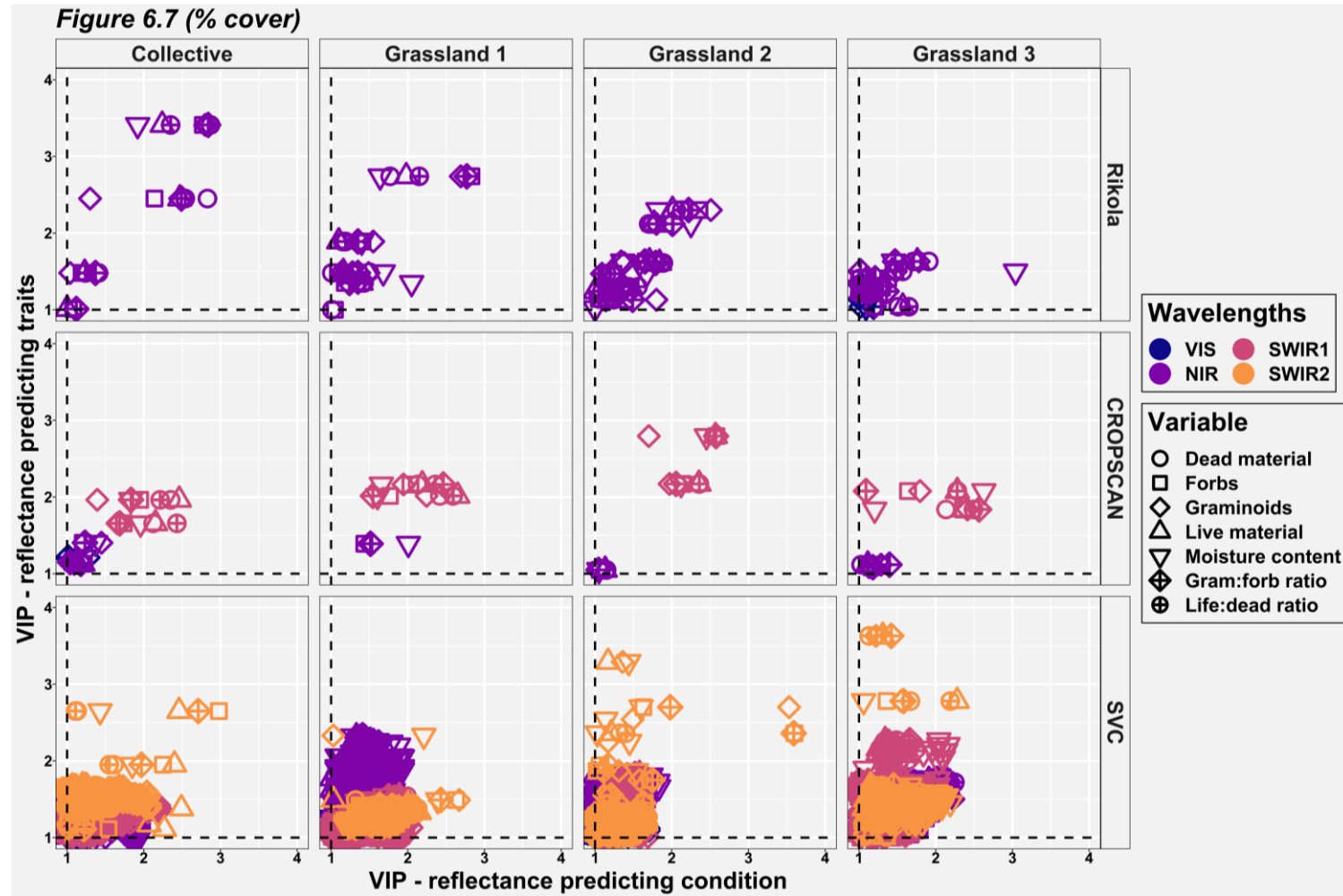
2932 Figures 6.6 and 6.7 show the results of VIP analysis, highlighting the spectral regions
2933 most important for predicting grassland variables (by mass or by % cover) and CSM-
2934 condition. For this analysis, the spectral bands were grouped into the following
2935 categories: VIS (300-700nm), NIR (701-900nm), SWIR1 (901-1640nm) and SWIR2
2936 (1640-2500nm). VIP values >1 were considered to be indicative of a strong predictor
2937 variable. The most significant region of the spectral signature for predicting any
2938 grassland variable depended on the spectral range of the device. In broad terms, for
2939 each device the outer part of the spectrum was most important. When using spectral
2940 data from the Rikola camera; the NIR part of the spectrum was most significant
2941 except for Grassland 2 where the VIS part of the spectrum was more significant for
2942 most grassland variables. When using spectral data from the CROPSCAN or SVC,
2943 the NIR and SWIR parts of the spectrum were generally more important.

2944



2945

2946 *Figure 6.6: VIP plots showing which regions of spectral data from three different devices and which responses (grassland variables on x axis*
 2947 *and CSM-condition on y axis) are most important in the study PLSR models where mass-based grassland variables are used as response*
 2948 *data.*



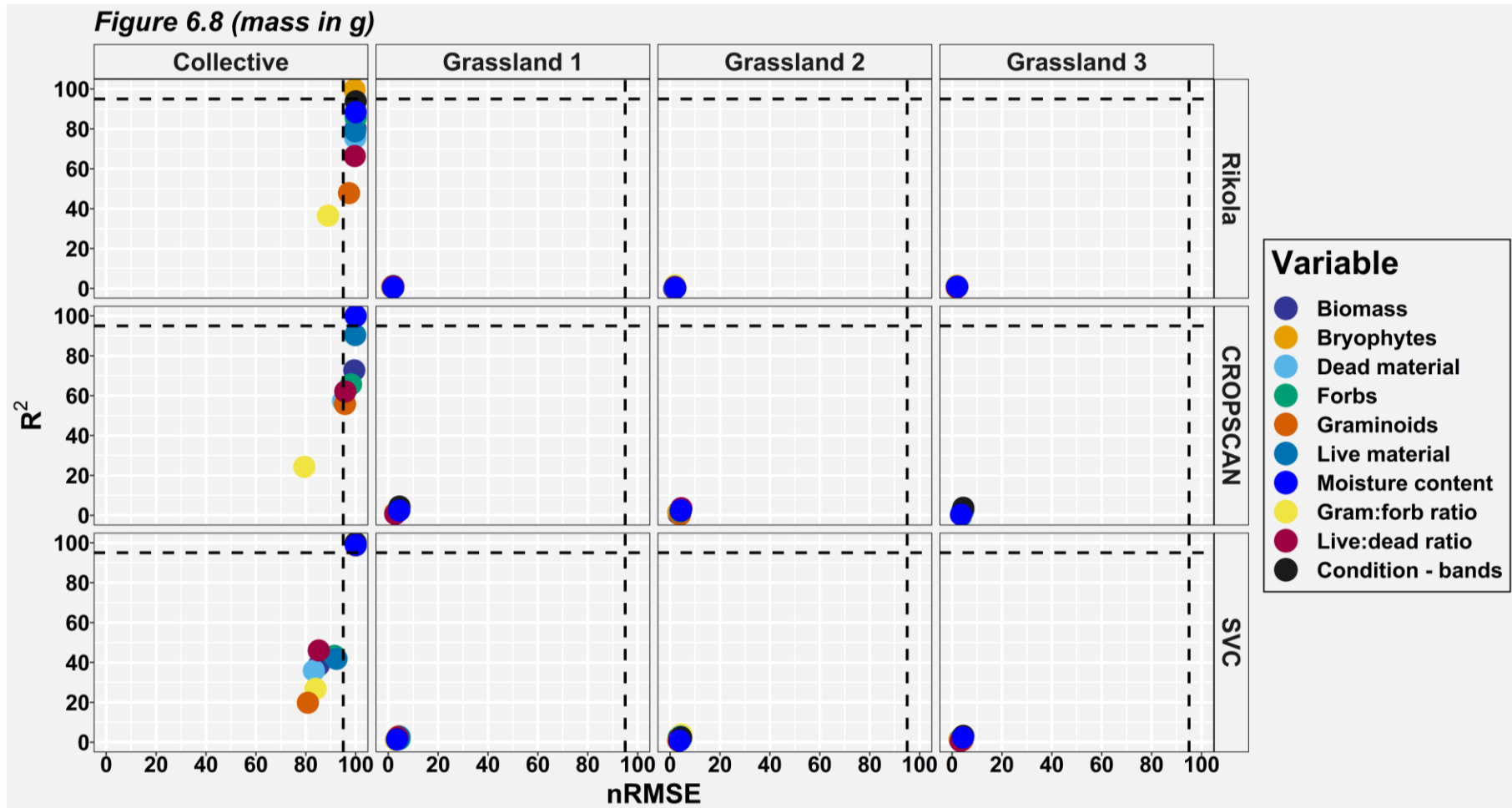
2949

2950 *Figure 6.7: VIP plots showing which regions of spectral data from three different devices and which responses (grassland variables on x axis*
 2951 *and CSM-condition on y axis) are most important in the study PLSRs where % cover-based grassland variables are used as response data.*

2952 **6.7. Comparison of PLSR models trained with actual data and**
2953 **PLSR models trained with random data**

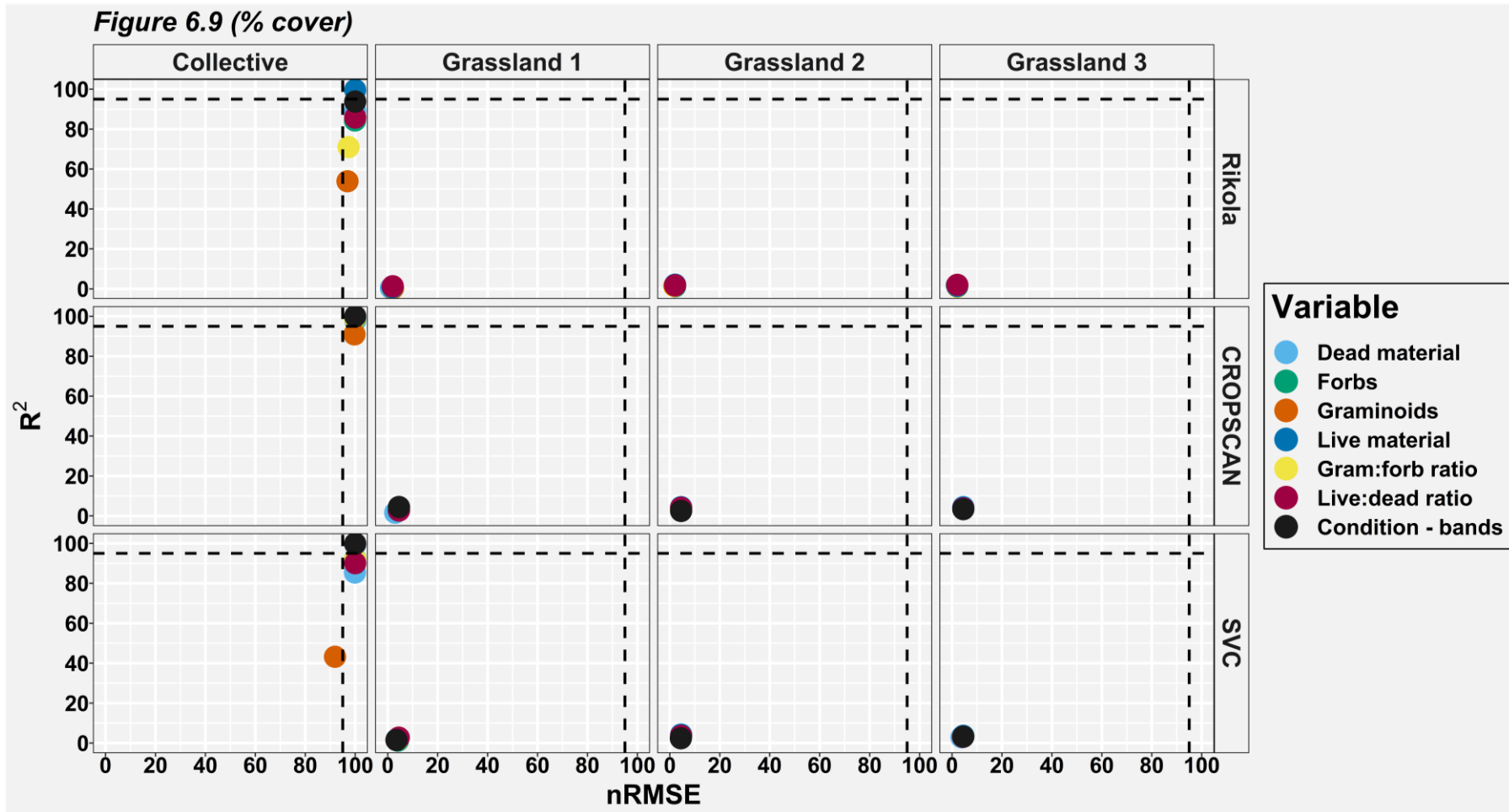
2954 The median values of R^2 and nRMSE results presented in Figures 6.2 and 6.3
2955 (referred to as actual models) were compared against the results of 999 further model
2956 runs with randomised response variable values (referred to as randomised models) to
2957 test the validity of the actual models. The results seen in Figures 6.8 and 6.9 suggest
2958 that producing actual or true models that are superior to a randomised model
2959 primarily depends on the quantity of data being used, not on the spectral device used
2960 to collect the spectral data being used as predictors. Almost all median nRMSE
2961 results, and median R^2 results for some grassland variables produces actual results
2962 that are consistently superior to results found by chance (i.e. from the randomised
2963 models), particularly when analyses are carried out on all grasslands collectively ($n =$
2964 30). Only some nRMSE results, and a few R^2 results, are consistently better in more
2965 than 95% of cases regardless of whether data from all grasslands or single sites are
2966 used to train the PLSR models ($n = 10$ or 30).

2967



2968

2969 *Figure 6.8: Rankings of the median values of the iterated model runs using actual mass response data and 999 model runs using randomised*
 2970 *mass response data, where rankings >95% are considered significant for the actual model fit.*



2971

2972 *Figure 6.9: Rankings of the median values of the iterated model runs using actual % cover response data and iterated model runs using*
 2973 *randomised % cover response data, where rankings >95% are considered significant for the actual model fit.*

2974 Chapter 7 – Discussion

2975 7.1. Effectiveness of using PLSR in a RS of 2976 grassland condition study

2977 PLSR has been utilised in grassland studies that used a range of RS devices,
2978 combinations of spectral data as predictors and grassland condition metrics as either
2979 responses or as predictors of other metrics. A PLSR modelling approach has been
2980 used in some studies to predict a wide range of biophysical and/or biochemical
2981 grassland variables at canopy scale (Capolupo et al. 2015; Schweiger et al. 2017;
2982 Wang et al. 2019) or leaf scale (Roelofsen et al. 2014). Other studies have targeted
2983 only a few related metrics or solitary metrics such as LAI (Darvishzadeh et al. 2008;
2984 Yuan et al. 2016), FAPAR (Sakowska et al. 2016), equivalent water thickness (Li et
2985 al. 2008), LDMC (e.g. Ali et al. 2019), nitrogen concentration (Polley et al. 2022; Yuan
2986 et al. 2016) plus soil pH and groundwater levels (Roelofsen et al. 2015).

2987 Many model comparison studies have been conducted to ascertain which modelling
2988 approach has superior predictive power for any given condition-related grassland
2989 variables and PLSR has been utilised in several of these model comparison studies.
2990 Linear regression models trained with vegetation indices (VIs) were also commonly
2991 included in model comparison studies. Capolupo et al. (2015) found that PLSR had
2992 superior performance to four VIs when predicting the quantities of a range of nine
2993 structural and biochemical grassland variables on experimental grasslands using
2994 drone-acquired hyperspectral imagery. The results of using VIs to predict three
2995 structural variables ranged from $R^2 = 0.3-0.599$ but ranged from $R^2 = 0.63-0.86$ when
2996 using PLSR. When predicting six biochemical variables, using VIs produced results of
2997 $R^2 = 0.001-0.51$ while PLSR results ranged from $R^2 = 0.21-0.8$. Wang et al. (2019)
2998 compared the ability of PLSR and Gaussian processes regression (GPR) to predict
2999 fifteen different grassland biochemical and structural variables on experimental
3000 grasslands using data from the NASA AVIRIS aircraft. Both modelling approaches
3001 produced models with moderate to strong predictive power for all variables except
3002 lignin and chlorophyll a + b with R^2 values > 0.55 (some with R^2 values > 0.8). Ali et
3003 al. (2019) found that PLSR had superior performance to using eleven different VIs

3004 when using Sentinel-2 spectral data to predict LDMC on wetlands ($R^2 = 0.71$)
3005 although four of the eleven VIs also produced relatively strong results ($R^2 = 0.67$).

3006 Some model comparison studies have also been conducted at patch level. Sakowska
3007 et al. (2016) assessed the performance of using data collected using an Analytical
3008 Spectral Device (ASD) set up to automatically collect spectral data across a swath of
3009 an experimental grassland, which was resampled to resemble Sentinel-2 data, to
3010 investigate the potential of the Sentinel-2 satellite to monitor three different
3011 biophysical parameters (CCC, FAPAR, and green FAPAR (GFAPAR)). One aspect of
3012 this study was a model comparison between the VIs, MLR and PLSR (where MLR
3013 and PLSR models were trained with full spectral data) to predict CCC and GFAPAR.
3014 Although PLSR models had superior predictive power for GFAPAR (adjusted $R^2 =$
3015 $0.77, 0.78,$ and 0.82 for VIs, MLR and PLSR respectively), the three modelling
3016 approaches had similar predictive power for CCC (adjusted $R^2 = 0.88, 0.9$ and 0.89
3017 for VIs, MLR and PLSR respectively). Darvishzadeh et al. (2008) compared the ability
3018 of PLSR and two VIs (NDVI and SAVI) to predict LAI and canopy chlorophyll content
3019 (CCC) at patch level on heterogeneous Mediterranean grasslands. Although PLSR
3020 produced higher R^2 results of 0.69 and 0.74 for LAI and CCC respectively, using VIs
3021 also had a moderate to strong predictive power with results of $R^2 = 0.49-0.64$ for LAI
3022 and $R^2 = 0.51-0.69$ for CCC. Yuan et al. (2016) used PLSR to predict the quantities of
3023 nitrogen concentration and leaf mass per area of two types of crops (sweet corn and
3024 snap beans) using different ranges of SVC spectral data as predictors. The results
3025 ranged from $R^2 = 0.8-0.96$ (model fit and validation results) depending on the spectral
3026 region utilised, with the strongest results either using the full spectral range available
3027 for the SVC (450-2400nm) or the 1500-2400nm range. Yuan et al. (2016) claimed
3028 that PLSR produced superior results based on a literature review, they did not carry
3029 out a comparison study themselves.

3030 Other studies have also used modelling approaches similar to PLSR that have
3031 produced models with moderate to strong predictive power, or found that other
3032 approaches produced models with stronger predictive power than PLSR. Homolová
3033 et al. (2014) compared the ability of VIs, stepwise MLR and PLSR to estimate five
3034 different condition-related grassland variables on grasslands that represented a
3035 range of grazing regimes. Hyperspectral imagery collected using the aircraft-mounted
3036 AISA Dual system were collected for use as model predictors. For four of the five
3037 variables (dead material, crude protein content, species diversity and soil carbon
3038 content) it was found that stepwise MLR had the strongest predictive power ($R^2 = 0.6-$

3039 0.97) but VIs were strongest for live material ($R^2 = 0.54$). Only the strongest results
3040 were presented, so it is not possible to say how much stronger the strongest models
3041 were relative to other trained models. Atzberger et al. (2015) compared two statistical
3042 modelling methods (predictive equations and VIs, both utilising *in situ* LAI and
3043 spectral data) and two radiative transfer models (RTM) inversion methods (one based
3044 on look-up-tables and one based on predictive equations) to estimate LAI using
3045 hyperspectral imagery collected by an aircraft-mounted HyMap sensor. All methods
3046 produced R^2 values of 0.75-0.91, but concerns were raised that the accuracy and
3047 robustness of the statistical modelling approaches decreases when fewer samples
3048 are used for calibration.

3049

3050 **7.2. The use of mass- or cover-based variables** 3051 **for condition assessment**

3052 The primary aim of this research is to assess the link between condition-related
3053 grassland variables, plus CSM-condition as defined in this thesis, with grassland
3054 spectral reflectance on semi-natural grasslands. As a precursor to achieving this aim,
3055 it was deemed necessary to select semi-natural grasslands that represented a
3056 spectrum of different grassland types for data collection which was done with an
3057 aspect of subjectivity. In other words, grasslands were chosen based on NVC type
3058 (based on several semi-quantitative measures) but also several other qualities that
3059 remained qualified rather than being converted to a quantity such as grazing
3060 intensity. To test whether the chosen grasslands represented a spectrum of
3061 significantly differing quantities of the condition-related variables chosen for this
3062 thesis, Wilcoxon rank sum tests were conducted on the mass and % cover of data
3063 collected on condition-related variables over space and time. The first test was
3064 conducted on all seven different grassland types chosen for this thesis. The second
3065 and third tests focussed on three chalk grasslands with differing levels of
3066 improvement, one of which focussed on the summer season and the other looked at
3067 data collected over three seasons.

3068 The exploratory boxplots in Figure 4.2, which used data from all seven grasslands
3069 collected during the summer, suggest that the mass of some grassland variables
3070 (bryophytes mass, dead material mass and forbs mass) can be used to differentiate
3071 between grassland types. The seven grasslands analysed are grasslands that

3072 strongly contrast in species, improvement level and grazing intensity. Also, biomass,
3073 graminoids mass and moisture content can be used to differentiate some of the
3074 seven different grassland types, particularly grasslands 6 and 7 which are a
3075 regenerated and a semi-improved grassland on limestone geology. Dead material
3076 cover and live:dead ratio cover can also be used to differentiate some grassland
3077 types, particularly grassland 5 which is an acid mire grassland. The results suggest
3078 that only some of the grassland variables considered in this study are significantly
3079 different between grasslands, though some of these results concur with the study of
3080 Fliervoet (1987) where biomass (and LAI) were found to be significantly different
3081 between different grassland types. When only the less strongly contrasting
3082 grasslands with differing levels of improvement located at Parsonage (Grasslands 1-
3083 3) are analysed (Figure 6.1), biomass, bryophytes mass, dead material mass, live
3084 material mass and moisture content showed significant differences in quantities
3085 between some grasslands with differing levels of improvement. The mass of other
3086 grassland variables plus all % cover grassland variables showed no significant
3087 difference in grassland variable quantities between grasslands. The results suggest
3088 that grasslands with differing levels of improvement may not necessarily have
3089 significantly different quantities of condition-related grassland variables. Biomass and
3090 dead material quantity depends on the species present and grazing/mowing regime
3091 (Bai et al., 2001); therefore if the same regime is applied to all grasslands (cow
3092 grazing using a similar number of cows confined to that particular grassland) then this
3093 could result in these grassland variables not being significantly different between
3094 grasslands. It is possible that some forb values plus graminoid and gram:forb ratio
3095 values are not significantly different between grasslands, despite Grassland 1 being
3096 more species rich. Grasslands 2 and 3 had forb species associated with more
3097 improved grasslands such as *Trifolium pratense* (Red Clover) and *Trifolium repens*
3098 (White Clover) (JNCC, 2004).

3099 When taking seasonality into consideration (Figure 5.1), no grassland variables for
3100 mass or % cover were significantly different between all grasslands and for all three
3101 seasons. Some grassland variables were significantly different on one or two
3102 grasslands for at least one season and spring is the season where grassland
3103 variables are more often significantly different. Mass data were significantly different
3104 between grasslands more frequently than % cover data, where many % cover
3105 grassland variables were not significantly different to any of the other grasslands. For
3106 % cover grassland variables, grasslands were significantly different between more

3107 grasslands over three seasons during spring for dead material, live material and
3108 graminoids.

3109 The results suggest that the different levels of improvement of the grasslands do not
3110 make them considerably different with respect to the grassland variables chosen for
3111 this study. One possibility is that it was not the quantities of forb and gram:forb ratio
3112 that were different but the forb species present. In other words, while the grasslands
3113 were structurally similar, more improved grasslands had forb species associated with
3114 these types of grasslands such as red clover and white clover while less improved or
3115 unimproved grasslands includes forb species associated with grasslands in better
3116 condition (JNCC, 2004; 2006). The structural complexity of grasslands, and how
3117 these changes in time, is discussed in Herben et al. (2000). In summary, Herben et
3118 al. (2000) explain how the spatial-temporal changes in patterns of species,
3119 particularly dominant species over a period of years, results in structural changes
3120 described as “fast” when looking at grasslands at a “small” scale but grasslands
3121 remain structurally similar over time at a “large” scale (small and large in this context
3122 was not defined by the authors, but small seems to refer to patches $\leq 0.25\text{m}^2$ based
3123 on referenced literature). This change is driven by a combination of internal and
3124 external factors and there are multiple theories behind the dynamics of the changes
3125 in species within a grassland over space and time. Species presence as well as
3126 abundance can change over time on a given patch, contributing to small-scale
3127 structural change

3128 The grasslands at Parsonage Down (Grasslands 1-3) were under-grazed in spring
3129 (Hope, S., 2018. pers. comm., 11 July), particularly Grassland 1, which may have
3130 contributed to the character of grassland variables being relatively different in spring
3131 relative to summer and autumn. In particular, it was observed that a relatively high
3132 quantity of dead material existed on the grasslands in spring. A build-up of dead
3133 material leading up to data collection in the autumn is also apparent when looking at
3134 how the quantities of dead material for each quadrat changes over time. Specific to
3135 this thesis, it could be that as the results of the Wilcoxon rank sum tests and the
3136 training of PLSR models for spring and autumn were impacted by this build-up of
3137 dead material. Although it is believed that dead material was the primary influence in
3138 seasonal differences, there are a list of other variables that could have contributed
3139 that cannot be tested in this thesis. These variables include seasonal changes in
3140 weather, changes in soil nutrients (and potentially pH through fertilisation),
3141 differences in grazing regime and differences in aspect and slope (Stevens et al.

3142 2016). The grasslands chosen for this study have the same grazing regime plus the
 3143 transects were placed where the slope was minimal ($0-4^{\circ}$) which would have
 3144 minimised the effect of aspect.

3145 It is possible that collecting data on grasslands that are not considerably different in
 3146 quantities of condition-related grassland variables had repercussions for PLSR model
 3147 training. The lack of variation in condition-related grassland variable quantities would
 3148 have limited the ability to detect changes in condition using trained PLSR models.
 3149 Alternatively, the lack of variation could be related to the small quantity of samples
 3150 collected where the full variation of condition-related grassland variables was not fully
 3151 captured.

3152

3153 **7.3. Predicting grassland variables and CSM-** 3154 **condition**

3155 **7.3.1. Predicting grassland variables and CSM-condition using** 3156 **spectral data as predictors**

3157 To directly address the primary aim of this research, PLSR was used to assess the
 3158 link between the mass or % cover of condition-related grassland variables plus CSM-
 3159 condition with grassland spectral reflectance. In general, the results of training PLSR
 3160 models using data ($n = 10$) from individual grasslands (Figures 4.4, 5.2, 5.3, 6.2, 6.3)
 3161 showed that most grassland variables can be predicted from reflectance data with R^2
 3162 values >0.5 and nRMSE values <100 . It is possible that overfitting has occurred for
 3163 results of $R^2 >0.9$, although aspects of the PLSR method should have prevented this
 3164 (Land et al., 2011). In contrast, when grassland sites are treated collectively (where
 3165 three, four or seven sites are combined or data collected over three seasons are
 3166 combined), most of the R^2 values of resulting PLSR models mostly drop below 0.5. In
 3167 other words, predictive models that are site specific appear to be more accurate than
 3168 those that aim to represent multiple sites. This outcome is entirely expected as
 3169 grouping data sets is mixing different populations and heightening structural
 3170 heterogeneity, even though this coincides with an increase in sample information
 3171 within the context of this thesis ($n = 30, 40, 70$ or 90). When the validity of PLSR
 3172 models is tested by comparing them with randomised models (Figures 4.8, 5.8, 5.9,
 3173 6.8 and 6.9), the results suggest that training PLSR models with 10 quadrats of data

3174 (where data collected on one grassland is utilised for model training so $n = 8$) was
3175 insufficient to produce a model fit that has significantly stronger R^2 and nRMSE
3176 values than a randomised model. Though nearly all actual models were superior to
3177 randomised models for nRMSE it has been shown that training PLSR models with
3178 <20 samples may lead to unreliable models (Goodhue et al., 2012).

3179 When PLSR models were trained with mass data from all three Parsonage
3180 grasslands collectively within or across seasons (Figures 5.2 and 5.3), more variables
3181 were moderately or strongly predicted in spring or autumn than summer. Conversely,
3182 when PLSR models were trained with % cover data, very few variables were
3183 predicted moderately or strongly during spring and autumn. When data from all three
3184 seasons were utilised to train PLSR models, models with moderate to strong
3185 predictive power were produced for particular variables regardless of whether mass
3186 or % cover data were used. This suggests that future studies should consider when
3187 data is collected as well as which data sets are collected and the quantity of data
3188 collected on each grassland. It is possible that the results of using % cover data to
3189 train PLSR models results in weaker predictions on grasslands with relatively high
3190 quantities of dead material when compared to training models with mass data.
3191 Although it has been demonstrated that a high dead material cover affects the
3192 spectral signature (Xu et al. 2014; Yang and Guo, 2014), potentially leading to
3193 weaker predictive models, this thesis used the same spectral data as predictors in
3194 PLSR models trained to predict mass and % cover of condition-related grassland
3195 variables. This suggests that changes in spectral signature due to high dead material
3196 cover was not the root cause of producing PLSR models with weak predictive power
3197 *per se* but could be related to the weak PLSR models trained with % cover from
3198 spring and autumn.

3199 A specific variable cannot be recommended for all grasslands and conditions
3200 achieving a higher R^2 or lower nRMSE depended on the grassland variable, how
3201 those data were collected (mass or % cover) and site with no obvious pattern.
3202 However, for some grassland variables (Figures 4.5, 5.4, 6.5) the model performance
3203 across sites was more consistent (i.e. low R^2 and nRMSE CVs). Variables used in
3204 model training that were relatively consistent across grasslands, seasons and
3205 spectral devices include biomass, bryophytes (mass and % cover), forb cover,
3206 moisture content, live:dead ratio cover and CSM-condition. Live material was
3207 relatively stable except when using % cover data with data from different spectral
3208 devices. Model results for other variables were relatively stable under a specific set of

3209 circumstances. For example, model performance for graminoids was relatively stable
3210 across seasons on Parsonage grasslands and for dead material mass when using
3211 different spectral devices. The inconsistencies in model performance highlighted by
3212 the CV results could be due to using an insufficient quantity of data to train some of
3213 the statistical models, in other words there is inconsistency because some PLSR
3214 models were trained with only 10 quadrats of data. Overall, there appears to be less
3215 consistency in results when using mass data relative to using % cover data for some
3216 grassland variables. This could be due to a lack of spatial coverage of sampling when
3217 collecting mass data, which meant that the complexity of the grasslands was not
3218 effectively captured.

3219 In broad terms, previous RS condition studies have used multispectral or
3220 hyperspectral RS data in combination with *in situ* data and models for the
3221 assessment of vegetation condition (e.g. Psomas et al., 2011). Few studies where
3222 grassland variables were predicted by RS methods included the use of grassland
3223 constituent mass and no studies have defined a comparable CSM-condition metric or
3224 used grassland variable data to predict a CSM-condition metric. Guo et al. (2005)
3225 used OLS regression and correlation analyses to link condition-related biophysical
3226 grassland variables with NDVI and LAI on a spatially heterogeneous prairie. Using
3227 regression and LAI values as predictors, patch level (1m^2) dry biomass was predicted
3228 with a R^2 value of 0.598 and moisture content with a R^2 value of 0.903. Furthermore,
3229 correlation coefficient values were between $r = 0.7-0.8$ when correlating LAI with
3230 biomass, graminoids and forbs and when correlating NDVI with moisture content.
3231 Correlation between LAI and moisture content was 0.903. Psomas et al. (2011)
3232 investigated the strength of the relationship between above ground biomass and
3233 spectral reflectance at patch level using multiple linear regression and VIs, where
3234 they found that feeding 2-4 specific spectral bands into an MLS regression produced
3235 the strongest predictions of biomass ($R^2 = 0.77-0.86$) and the R^2 results for all VIs
3236 were <0.6 . Chen et al. (2009) also tested the strength of the relationship between
3237 biomass and spectral data at patch level on spatially heterogeneous grasslands,
3238 using VIs as predictors in PLSR. This study collected data at different angles to better
3239 capture grassland structure and shadowing, but dead material was removed from
3240 destructive samples after spectral readings had been taken in spite of studies (Asner,
3241 1998; Asner et al., 2000; Xu et al., 2014) that show that dead material influences the
3242 spectral signature. If dead material % cover was low as suggested but not quantified,
3243 this may have not strongly influenced the spectral signature of quadrats (Yang and
3244 Guo, 2014). The highest R^2 values (0.52-0.54) were achieved by using PLSR and

3245 single narrow band reflectance or first-order derivative reflectance. Yang and Guo
3246 (2014) assessed the strength of the relationship between dead material % cover and
3247 a range of VIs using linear and non-linear regressions, where almost all of the results
3248 of using different VIs and different regressions were $R^2 = 0.53-0.56$, where data were
3249 collected on patches with dead material % cover of 45-56%. Davidson et al. (2006)
3250 compared OLS regression models trained to predict moisture content (absolute and
3251 relative) using different VIs and ranges of spectral data directly used as predictors.
3252 Using spectral data ranges and some VIs as predictors appeared to train models with
3253 relatively strong predictive power ($R^2 = 0.7-0.8$). However, the R^2 values of these two
3254 studies could be erroneous as multicollinearity effects were not addressed.

3255 When predicting biomass on a range of different grassland types (Chapter 4); of 16
3256 model runs that used data from Grasslands 1-3 (Parsonage), five model runs
3257 produced results of $R^2 > 0.5$ and $nRMSE < 100$ ($R^2 = 0.54-0.59$ and $nRMSE = 55.6-$
3258 76.8). Of 20 model runs for Grasslands 4-7 (Ingleborough), all had values of $R^2 > 0.5$
3259 and all but two had $nRMSE$ values of < 100 ($R^2 = 0.56-0.94$ and $nRMSE = 46.8-110.2$)
3260 with the results of the collective analyses having a range of $R^2 = 0.56-0.67$ and
3261 $nRMSE = 67.7-75.4$. It is not clear why biomass was predicted more effectively on
3262 some grasslands, or combination of grasslands, as there does not appear to be a link
3263 with grassland structure (taking structural complexity and grazing regime into
3264 consideration) or level of improvement and biomass prediction strength. Furthermore,
3265 there did not appear to be a clear link with a relative lack or abundance of a particular
3266 grassland variable and biomass prediction. Although weaker PLSR models generally
3267 seem to be trained with data collected on grasslands with a relatively high % cover of
3268 dead material and low % cover of forbs, this pattern is not strictly the case as
3269 Grassland 7 does not fit this pattern. Grassland 7 does not appear to be more heavily
3270 grazed than Grassland 6 or more improved than Grasslands 2 or 3.

3271 When dead material was predicted in this study; training PLSR models with mass
3272 data from both locations ($R^2 = 0.57-0.60$ and $nRMSE = 74.9-75.9$) or Ingleborough
3273 (Grasslands 4-7, $R^2 = 0.50-0.88$ and $nRMSE = 45.7-88.9$) almost always produced
3274 moderate to strong predictions. Relatively few PLSR models produced moderate to
3275 strong predictions when trained with % cover data from both locations or from
3276 Grasslands 4-7. When PLSR models were trained with data from Grasslands 1-3, the
3277 only moderate to strong prediction ($R^2 > 0.5$) that did not seem to be dubious (R^2
3278 > 0.9) was produced by a model trained with % cover data from all three grasslands
3279 collectively ($R^2 = 0.53$ and $nRMSE = 47.3$). It is not clear why destructive sampling

3280 captured dead material more effectively on Ingleborough grasslands compared to
3281 Parsonage grasslands. Grassland 2 (Parsonage) plus Grasslands 4 and 5
3282 (Ingleborough) have a dead material cover of 0-25% but the other grasslands have a
3283 lower dead material cover of 0-8%, suggesting that there is a relatively high variance
3284 in dead material within each location. This suggests that increased variance in %
3285 cover of dead material does not positively or negatively impact the predictive power
3286 of the PLSR models.

3287 When moisture content was predicted in this study; most of the predictions were
3288 weak ($R^2 < 0.5$) but stronger predictions ($R^2 > 0.5$) were produced by analysing
3289 Parsonage or Ingleborough grasslands collectively and for Grasslands 1, 4 and 6.
3290 There appears to be a pattern where the models with R^2 values > 0.5 were trained
3291 with data either from all grasslands within one location or from alkaline grasslands. It
3292 is not clear why this should be the case. Although all three Parsonage grasslands
3293 had a similar mean soil moisture ($0.104\text{-}0.111\text{m}^3$ water/ m^3 soil) and three of four
3294 Ingleborough grasslands also had a similar mean soil moisture ($0.358\text{-}0.409\text{m}^3$
3295 water/ m^3 soil), Grassland 5 is an acid mire grassland and had a relatively high mean
3296 soil moisture (0.787m^3 water/ m^3 soil). Other soil data were not collected to verify
3297 whether these soil moisture readings were affected by high organic content, which
3298 may be considered useful as increased organic content may make a soil more poorly
3299 draining. Also, Grasslands 3 (Parsonage), 4 and 5 (Ingleborough) had a relatively
3300 high variance in moisture content. Furthermore, training a PLSR model with
3301 Parsonage or Ingleborough grasslands collectively produces moderately strong
3302 models, but training a model with data from both locations produces a weak PLSR
3303 model.

3304 When predicting biomass within or across different seasons (Chapter 5), of the 32
3305 model runs using either FULL or VNIR spectral data, 19 model runs produced PLSR
3306 models with $R^2 \Rightarrow 0.5$ and $n\text{RMSE} < 100$, with a range of $R^2 = 0.5\text{-}0.91$ and $n\text{RMSE} =$
3307 $45.5\text{-}98.1$. The strongest six of these PLSR models, and the most PLSR models with
3308 $R^2 > 0.5$ of these 32 models, are for Grassland 3 with more of these PLSR models
3309 produced using autumn data. It is not clear why most of the strongest models were
3310 trained on data collected in autumn as the quantities of grassland variables for the
3311 summer season were generally similar (but with increased dead material cover in
3312 autumn relative to summer). Although canopy structure is considered to be primarily
3313 responsible for canopy level reflectance characteristics, biochemical variables were
3314 not considered in this study and this could have influenced the results to an

3315 unquantified extent (Cole et al. 2014). It seems clearer that a reduced amount of
3316 biomass and an increased amount of dead material would have affected the training
3317 of PLSR models to predict biomass in spring.

3318 Of 64 model runs for dead material (either mass or % cover responses and either
3319 FULL or VNIR predictors), 25 model runs produced PLSR models with $R^2 \Rightarrow 0.5$ and
3320 nRMSE <100 with a range of $R^2 = 0.5-0.97$ and nRMSE = 25.5-77.6. Of these model
3321 runs, 19 used % cover data. Also, analysing data from all seasons or spring produced
3322 most of the PLSR models with $R^2 \Rightarrow 0.5$. Asner et al. (2000) shows how seasonal
3323 changes in dead material influence the factors (i.e. grassland variables) that affect
3324 variability in spectral reflectance. A high dead material content had a relatively
3325 stronger influence on the visible part of the spectrum (40-60% of variance) but also
3326 on the NIR part of the spectrum (20-40% of variance). This may explain why most of
3327 the PLSR models with moderate or high predicting power were trained at least in part
3328 using spectral data from spring, when the dead material cover on the grasslands was
3329 particularly high (up to 70% cover). The influence of high dead material cover on the
3330 spectral signature may also have reduced the models' predictive power for other
3331 grassland variables (Asner et al. (2000); Xu et al. (2014); Yang and Guo (2014)).

3332 When PLSR models were run with moisture content as response data, most of the
3333 predictions were weak ($R^2 < 0.5$) but stronger predictions ($R^2 > 0.5$) were produced by
3334 analysing data from Parsonage grasslands collectively (Grasslands 1-3) for summer
3335 and for Grassland 2 for some seasons (spring, summer and when using data from all
3336 three seasons) plus Grassland 3 for spring. The results of comparing these models to
3337 models trained on randomised data (Figure 5.8) suggest that the models trained on
3338 data from individual grasslands are unreliable because of the low sample size. One
3339 possibility for stronger predictions of moisture content during the summer is that the
3340 sampling strategy better captured the variation in moisture content by chance.

3341 Variance for moisture content data is 2.05 for summer compared to 1.27 and 0.69 for
3342 spring and autumn respectively. Another reason could be the increased dead
3343 material cover during spring, and to a lesser extent, autumn having an impact on the
3344 spectral data which were then used as predictors in the models. Asner (1998)
3345 conducted an aircraft RS study on a range of semi-arid grasslands, shrublands and
3346 transition zones (succeeding from grasslands to shrublands) in the Brazilian Cerrado
3347 to link vegetation variables with the variation of wavelengths in the 400-2500nm
3348 spectral region. The results suggest that on grasslands; the dominant biophysical
3349 factors on the variation of reflectance in the 400-2500nm spectral region were soil

3350 reflectance, litter reflectance and transmittance (at the leaf level) and the fractional
3351 cover of grass canopies. Soil reflectance was the most dominant factor across the
3352 whole 400-2500nm spectral region, likely because of relatively sparse vegetation
3353 cover, but litter was the next dominant factor in the VNIR part of the spectrum.
3354 Although there was minimal soil cover on the grasslands chosen for this thesis, it
3355 could be that dead material and canopy structure had a relatively strong influence on
3356 the spectral signature which partly explains the results seen in Chapter 5.

3357 When comparing the prediction of grassland variables using data from different
3358 spectral devices (Chapter 6); models trained to predict bryophytes, moisture content
3359 and CSM-condition (but not for moisture content when using Rikola data) were the
3360 models with moderate to strong predictive power. When using % cover data; live
3361 material and CSM-condition were moderately to strongly predicted by models trained
3362 with spectral data from any three of the spectral devices used in this study. Models
3363 trained with CROPSCAN or SVC data also had moderate to strong predictive power
3364 for forb cover and gram:forb ratio cover. Models trained with CROPSCAN data also
3365 had moderate to strong predictive power for dead material cover and live:dead ratio
3366 cover.

3367 Yao et al. (2013) showed that models with stronger predicting power can be
3368 produced when trained using ASD spectral as predictors compared to using
3369 CROPSCAN spectral data as predictors (possibly due to an increased range or
3370 quantity of bands) although this study predicted nitrogen quantity on croplands. This
3371 thesis suggests that similarly good results can be produced from using CROPSCAN
3372 or SVC data, but it is possible that using the methods proposed in this thesis does not
3373 fully utilise the additional spectral data gained from using the SVC the way that some
3374 authors (e.g. Psomas et al., 2011) may have done.

3375 In general; different grasslands, spectral data or seasons did not produce a markedly
3376 different number of PLSR models with $R^2 \Rightarrow 0.5$ when spectral data were used to
3377 predict grassland variables and CSM-condition and when grassland variables were
3378 used to predict CSM-condition. An exception is that most of the superior PLSR
3379 models trained to predict CSM-condition with spectral data were trained using data
3380 collected in summer. When grassland variables were used to predict CSM-condition,
3381 most of the superior PLSR models were trained using % cover data.

3382 There are numerous potential reasons for the lack of consistency in predicting
3383 grassland condition-related variables across different grasslands and seasons. It is

3384 possible that a holistic study (Homolová et al., 2014; Lausch et al. 2018), or at least a
3385 wider-ranging study that captured data on more variables would have highlighted
3386 condition-related variables that could be more consistently predicted with a moderate
3387 to high level of accuracy and precision. It has also been suggested that time and
3388 resource restrictions prevent this (Lausch et al. 2018) and therefore the variables
3389 considered to be more promising based on the literature review were chosen.
3390 Alternatively, it could be that an approach that better accounted for at least some of
3391 the limitations pointed out in Section 7.7 would have led to more consistent results.
3392 For example, an approach where more data could be collected within time and cost
3393 constraints or a modelling approach that could better capture the variation in the
3394 condition-related variables chosen or could better predict the lowest and highest
3395 variable values (Chen et al. 2009; Psomas et al. 2011).

3396

3397 **7.3.2. Predicting CSM-condition using grassland variables**

3398 When using grassland variable data collected over a wider range of grasslands to
3399 predict condition (Chapter 4), the results suggest that some grassland variables are
3400 more important predictors of CSM-condition across different types of grasslands than
3401 others. For predicting CSM-condition across different types of grasslands, live:dead
3402 ratio using mass or % cover appears to be a particular important variable with other
3403 relatively important variables including forbs cover, graminoids cover, gram:forb ratio
3404 mass and gram:bryo ratio mass.

3405 When using grassland variable data collected over multiple seasons to predict
3406 condition (Chapter 5), the results suggest that which grassland variables are most
3407 important depend on whether mass or % cover data are used; biomass, gram:forb
3408 ratio mass, live:dead ratio mass and moisture content when using mass data but
3409 dead material cover, forbs cover, graminoids cover, live material cover and live:dead
3410 ratio cover when using % cover data. Focusing on data collected at Parsonage during
3411 the summer forbs cover, graminoids cover and live:dead ratio cover were important
3412 for predicting CSM-condition when using % cover data whilst gram:forb ratio mass
3413 and live:dead ratio mass were important when using mass data although there were
3414 slight differences between grasslands. When using mass data; biomass was
3415 important when using data from Grassland 1 and gram:forb ratio mass was not
3416 important for Grassland 3 whilst graminoids cover was not important to Grassland 2
3417 when using % cover data. As all of the grassland variables used in this thesis are

3418 considered to be related to condition, it is possible that these results are related to
3419 how well each grassland variable is captured by a particular method of data collection
3420 (i.e. % cover or mass) although it is possible that changes in vegetation across
3421 seasons and particularly the changes in dead material quantities had an impact on
3422 the results. Another possible reason for some of the aforementioned grassland
3423 variables being considered significant is that they were used, either directly or
3424 indirectly, as criteria to calculate CSM-condition. For example, dead material cover
3425 was a criterion for establishing CSM-condition for some grasslands which would
3426 relate to the grassland variable live:dead ratio cover.

3427

3428 **7.4. Extrapolating predicted grassland variables**

3429 The practical purpose of the research in this thesis is to provide land managers with a
3430 methods to monitor grassland condition on semi-natural grasslands with improved
3431 time-efficiency and spatial-temporal coverage. To achieve this, the results of PLSR
3432 models trained with CROPSCAN data were extrapolated from patch to field level
3433 (Figure 6.4). For extrapolation, an emphasis was placed on trained PLSR models that
3434 had been trained with grasslands from all grasslands collectively as other results in
3435 this thesis (Figures 4.8, 5.8, 5.9, 6.8 and 6.9) suggested that PLSR models trained
3436 using data from individual grasslands ($n = 10$) may not be able to consistently
3437 improve on models trained with random data. Most of the PLSR models trained with
3438 collective grassland data had weak predictive power ($R^2 < 0.5$ and/or $nRMSE > 100$)
3439 though most of the PLSR models trained using % cover and CROPSCAN data sets
3440 were at least of moderate predictive power ($R^2 > 0.5$ and/or $nRMSE < 100$). Although
3441 extrapolated predicted values have been presented in Figure 6.4, it is not clear how
3442 accurate these predictions are as it is not possible to externally validate the results
3443 aside from the leave-one-out cross-validation (LOO-CV) approach used to derive
3444 $nRMSE$ and the calculation of the PRESS statistic (used in this thesis to choose
3445 optimum number of components for model training) due to the small sample size of
3446 the data sets. External validation of the results using a data set completely separate
3447 from the one used to train the models would have been a more robust external
3448 validation approach (Ramspek et al. 2021). An example of a study which took this
3449 approach is Schweiger et al. (2017).

3450 Furthermore, it was observed from the drone data and the projections of the
3451 predicted values from the PLSR models that the pattern of grassland variable
3452 predicted values appears to follow the spatial pattern of the varying illumination levels
3453 of the imagery. In other words, a higher illumination value for that image pixel meant
3454 a higher grassland variable value predicted by the PLSR models. This suggests that
3455 issues caused by within *and* between image illumination have not been solved in this
3456 study and an effective solution does not currently exist to the knowledge of the
3457 author. This means that these results are not reliable as it would be necessary to
3458 equalise illumination variation both within and between images before analysis to
3459 prevent this issue for occurring. A potential solution to this issue is the use of VIs for
3460 model training, but multiple studies (e.g. Arroyo-Mora et al. 2021) have discussed the
3461 negative impact of variable illumination conditions on derived vegetation indices.
3462 Despite this, some authors have also discussed potential solutions for combining
3463 image processing with VIs selected specifically because of the reduced impact of
3464 variable illumination conditions on their calculation relative to some alternative
3465 methods such as those discussed in this thesis. For example, utilising reference
3466 panels as a means of correcting UAV imagery can improve the consistency of image
3467 illumination, but any approach that assumes relatively stable illumination during the
3468 flight, i.e. makes one calibration before or after the flight, can still lead to erroneous
3469 results. On the one hand, the use of spectral devices that collect repeated
3470 measurements of upwelling and downwelling radiation could provide solutions to
3471 variable illumination. Alternatively, authors may instead use an approach such as
3472 automated multiscale Retinex correction before calculating VIs to improve the validity
3473 of the results (Wang et al. 2023). Arroyo-Mora et al. (2021) found that an atmospheric
3474 correction approach should be chosen based on the conditions during the flight, i.e.
3475 using the MODTRAN-5 based radiative transfer model achieves better results in high
3476 direct irradiance conditions while an Empirical Line Model (ELM) approach is more
3477 applicable under more diffuse and variable irradiance conditions. They also found
3478 that the calculation of NDWI was less impacted by variable irradiance conditions than
3479 other VIs such as NDVI. Souza et al. (2021) found that calculations of NDVI, NDWI
3480 and the red edge inflection point were relatively stable compared to other VIs when
3481 comparing calculations derived from imagery collected in sunny conditions and
3482 imagery collected in cloudy conditions. Wang S et al. (2019) proposed using Tucker
3483 tensor decomposition to remove the effects of cloud shadowing as an added step to
3484 improving the reliability of images affected by cloudy conditions.

3485

3486 When the predicted values from the PLSR models trained with CROPSCAN spectral
3487 data were projected, the trend in the predicted values between grasslands appeared
3488 to be as expected. The regenerated calcareous grassland (Grassland 1, NVC = CG2)
3489 had an increased quantity of bryophyte mass, live material % cover, forbs % cover
3490 and CSM-condition plus decreased dead material % cover and gram:forb ratio
3491 (derived from % cover data) compared to the two semi-improved grasslands. These
3492 trends are associated with grasslands of a better condition although an increase in
3493 forbs % cover can be associated with more improved (lower condition) grasslands
3494 due to an increase % cover of species such as Red Clover (*Trifolium pratense*) and
3495 White Clover (*Trifolium repens*) (JNCC, 2004; 2006). As explained earlier, it was not
3496 possible to externally validate the results using a data set separate from model
3497 training therefore the only validation of the results was achieved using the leave-one-
3498 out cross-validation (LOO-CV) approach used to derive nRMSE.

3499 To the knowledge of the author, the only comparable literature currently available
3500 focused on prediction of biomass or grassland variables related to biomass such as
3501 grass height on experimental grasslands. Capolupo et al. (2015) used PLSR models
3502 trained using UAV-acquired spectral data as predictors of structural grassland
3503 variables. Their study was conducted on experimental grasslands over two seasons
3504 at field level. Using one season of data; wet biomass, height and dry biomass
3505 produced R^2 results of 0.72, 0.7 and 0.63 respectively. These results improved to
3506 >0.8 when two seasons of data were analysed collectively. Lussem et al. (2019) used
3507 OLS regression to estimate dry biomass on experimental grasslands that had a range
3508 of fertilisation (improvement) levels. Three VIs were calculated using spectral data
3509 collected with two UAV-mounted devices. The Plant Pigment Ratio Index was
3510 considered to produce more accurate predictions ($R^2 = 0.7$) than the NDVI ($R^2 = 0.63$)
3511 and Normalized Green Red Difference Index (NGRDI) with $R^2 = 0.57$ when these
3512 indices were used as predictors in the OLS regression. Although LOO-CV was
3513 applied, only absolute RMSE values were provided so the model error is not clear
3514 and it is not possible to compare model performance between models using R^2 and
3515 nRMSE results. As part of a wider study, Viljanen et al. (2018) used estimated grass
3516 height, VIs and spectral data collected with a UAV as separate or combined
3517 predictors of biomass on experimental fields; in this case to train OLS regression and
3518 random forest models using data collected on four different dates in June. The R^2
3519 and nRMSE results for each date ranged from 0.82-0.93. Again, it is not clear how
3520 model overfitting was prevented although it is unlikely to have happened if models
3521 were trained with only a few features. Michez et al. (2019) also estimated canopy

3522 height (this time using LiDAR data) then used either these estimated canopy height
3523 values, spectral data collected using a UAV, or a combination of the two to train four
3524 different types of models to predict biomass. Spectral data were either utilised in
3525 models as reflectance values or as VIs. The best performing model had a R^2 value of
3526 0.49 where the model was trained using a combination of estimated canopy height,
3527 reflectance values and VIs. Like the previous study, data sets were collected within
3528 one month (May) and therefore grassland variability over the growing season was not
3529 captured.

3530 Théau et al. (2021) estimated biomass and vegetation cover on experimental pasture
3531 plots using a range of methods; structure from motion (SfM) and non-linear
3532 regression to predict biomass plus a classification (cluster) analysis to estimate
3533 vegetation cover. A range of VIs, calculated by extracting spectral data collected with
3534 a drone, were used as predictors in the latter two analyses. Linear regression
3535 between estimated biomass using the SfM approach and observed biomass
3536 produced R^2 values of 0.93 and 0.94 for fresh and dry biomass respectively with
3537 nRMSE values <10%, although only 12 samples ($n = 12$) were used in this analysis
3538 plus it is not clear how the analysis was carried out and therefore how overfitting was
3539 prevented. For heavily-grazed grasslands where a structure from motion (SfM)
3540 approach is ineffective, the results of using green NDVI (GNDVI) as a predictor
3541 produced the most accurate predictions of estimating biomass with R^2 values of 0.80
3542 and 0.60 and nRMSE values of 24% and 29% for fresh and dry biomass respectively.
3543 Grüner et al. (2019) estimated canopy height using a SfM approach then estimated
3544 dry biomass with the aid of estimated canopy height using reduced major axis
3545 regression on experimental grasslands. The strength of the predictions of biomass
3546 ranged from $R^2 = 0.46-0.87$ subject to the treatment that a given experimental
3547 grassland had received, which was attributed to differences in the variability of the
3548 canopy structure of each grassland. It is not clear if confounding variables have some
3549 responsibility for the variation in results. Furthermore, this approach would possibly
3550 be flawed if used to estimate biomass on heavily grazed grasslands, but it is not clear
3551 if this is the case.

3552 This study did not use grass height as a grassland variable (although it played a
3553 minor role in determining CSM-condition) and the PLSR models trained using data
3554 from all Parsonage grasslands collectively presented in this study had weak
3555 predictive power for biomass. On the other hand, the PLSR models had strong
3556 predictive power ($R^2 \Rightarrow 0.7$) for live material % cover. All of the aforementioned

3557 papers used experimental grasslands as study sites and did not make available the
3558 data sets collected on these grasslands. It is possible that the standard linear
3559 regression approaches produced particularly strong results because the grassland
3560 data collected to train the models were uniform because the grasslands studied by
3561 the aforementioned authors (e.g. Viljanen et al. (2018)) were structurally
3562 homogeneous. In practical terms, the models would be overfitted as they would have
3563 no predicting power for more structurally heterogeneous grasslands. For this reason,
3564 it is thought that inferences made by authors such as Lussem et al. (2019) that
3565 biomass predictions on experimental grasslands can be transferred to other
3566 grasslands are likely to be false. Addressing this would require experimental
3567 grasslands to replicate the structural heterogeneity (both within and between
3568 grasslands) observed on semi-natural grasslands such as the grasslands selected for
3569 this thesis.

3570 A similar situation may have occurred with the mass-based observations in this study.
3571 Despite collecting data on more structurally heterogeneous grasslands, the models
3572 appeared to lack the ability to predict the highest mass values such as where
3573 tussocks were located. One reason could be that the data collection approach did not
3574 successfully capture the structural heterogeneity both within and between the
3575 grasslands in three dimensional space, a consequence of collecting a relatively small
3576 data set. Alternatively, a change in some grassland variable values did not result in a
3577 sufficient change in the spectral signature for the trained model to predict values that
3578 are much higher than most of the other grassland variable values. The inability of the
3579 models to predict much higher values could also be a result of using a linear
3580 regression approach.

3581

3582 **7.5. Choice of spectral bands**

3583 One goal of this thesis is to explore which spectral reflectance bands, and related to
3584 this which radiometry instruments and regions of the EM spectrum, would be most
3585 useful in training PLSR models with strong predictive power. This thesis used VIP to
3586 understand which model predictors were most important for the predictive power of
3587 the trained models. Spectral data from each device was autoscaled prior to analysis
3588 to remove the possibility of the VIP results being positively biased towards the NIR
3589 part of the spectrum. In general for all three devices used in this thesis, the VIP
3590 results (Figures 4.6, 5.5, 5.6, 6.6 and 6.7) suggest that the bands in the upper part of

3591 their spectral range (upper NIR and SWIR bands) were most important for predicting
3592 grassland variables. To use the CROPSCAN as an example; the most significant
3593 bands for predicting a wide range of grassland variables across different locations,
3594 seasons and when using different data types are the SWIR bands and upper NIR
3595 bands (760-1640nm) along with the red edge (647nm) and blue band (470nm) to a
3596 more limited extent. The importance of the upper NIR and SWIR bands, regardless of
3597 the device used, is highlighted by looking at how many wavelengths in these regions
3598 was considered an important predictor (Figures 6.6 and 6.7) for all of the PLSR
3599 models trained (Figures 6.2 and 6.3) for this particular study (Chapter 6).

3600 For the CROPSCAN (collects data on 16 wavelengths); the SWIR1 range produced
3601 nearly twice as many VIP values >1 (125) than the NIR range (77) and approximately
3602 six times more than using the VIS part of the spectrum (22) when predicting
3603 grassland variables, all of the VIP values >2 are in the SWIR1 range. For the Rikola
3604 camera (collects data on 30 wavelengths); the NIR range produced approximately six
3605 times more VIP values >1 (672) than using the VIS region of the spectrum (121)
3606 when predicting grassland variables. For the SVC (collects data on 1249
3607 wavelengths); the NIR and SWIR1 regions of the spectrum (8989 and 9753
3608 respectively) produced more VIP values >1 than the VIS or SWIR2 regions of the
3609 spectrum (4407 and 5183 respectively).

3610 These results suggest that the aforementioned bands better capture and/or are more
3611 sensitive to changes in CSM-condition and the condition-based grassland variables
3612 used in this study regardless of grassland, season or device. These results agree
3613 with some studies (e.g. Chen et al., 2009; Polley et al. 2020) and disagree with others
3614 (e.g. Capolupo et al., 2015) although the studies where the results disagree did not
3615 use instruments that collect data on the SWIR part of the spectrum. Despite this, it
3616 could be that the upper NIR bands being strong predictors of grassland variables and
3617 condition generally explains why the results of using FULL and VNIR data are similar.
3618 Furthermore, the CROPSCAN only collects data on two bands in the SWIR region of
3619 the EM spectrum.

3620 When considering the results of the VIP analysis (where specific bands in the VIS
3621 and red edge regions of the spectrum were also deemed important), one possibility is
3622 that these results are influenced by grassland canopy spectral reflectance being
3623 strongly influenced by chlorophyll and water absorption (Knipling, 1970). The VIP
3624 results could also be explained by previous studies which show the importance of
3625 NIR and SWIR bands in predicting grassland variables (Asner (1998); Chen et al.

3626 (2009); Roelofsen et al. (2015)). Chen et al. (2009) used spectral data ranging from
3627 400-1100nm in their analyses and used a band importance index (BII) to highlight
3628 which bands were most important in predicting biomass. The BII results suggested
3629 that parts of the NIR range and blue range of the spectrum were the most important
3630 ranges of bands for predicting biomass. These findings were reiterated when
3631 Pearson's correlation was used to test the strength of correlation between the
3632 reflectance at each wavelength and aboveground biomass. The results from this
3633 study match their results quite closely, except this study used two bands from the
3634 SWIR part of the spectrum which were also found to be important. Capolupo et al.
3635 (2015) found that VIS (450–545 nm) was most important in predicting some
3636 grassland variables including fresh biomass and grass height, but their study also
3637 used a more limited part of the spectrum (450-950nm). Using simulated spectral
3638 signatures, Xu et al. (2014) found that increased bare soil cover increased
3639 reflectance along the whole spectral signature whilst increased dead material cover
3640 decreased NIR reflectance and increased SWIR reflectance. Roelofsen et al. (2015)
3641 related changes in the NIR parts of the spectral signature to leaf orientation and LAI
3642 plus the SWIR part of the spectrum to water content in agreement with findings by
3643 Asner (1998).

3644 One aspect of this thesis is to try to understand how important it is to utilise SWIR
3645 data when training predictive models. In Chapters 4 and 5, models were trained with
3646 two different ranges of spectral data; VNIR (visible and NIR data) and FULL (VNIR
3647 plus two SWIR wavelengths). In Chapter 4, models trained with VNIR data produced
3648 higher R^2 and lower nRMSE results for most grassland variables when analysing
3649 grasslands from both locations or Ingleborough grasslands collectively. Full spectrum
3650 data (FULL) produced stronger predictions for most grassland variables and for
3651 condition when analysing Parsonage grasslands collectively. When the results of
3652 analysing individual grasslands are compared, whether using full spectrum or VNIR
3653 data produces higher R^2 values is dependent on the grassland type and grassland
3654 variable. For biomass, live material or dead material R^2 results (mass or % cover); full
3655 spectrum results are almost always weaker than using VNIR. Overall, the ratio
3656 between occasions when each produced stronger results was almost 1:1 in favour of
3657 using VNIR data. Both spectral data ranges produced a similar number of significant
3658 results ($R^2 > 0.5$ and nRMSE < 100).

3659 One of the aims of the thesis addressed in Chapter 6 was to assess whether spectral
3660 data from different devices can accurately predict CSM-condition or the mass or %

3661 cover of condition-related grassland variables and to compare the performance of the
 3662 PLSR models trained using data from these different spectral devices. Of 192 model
 3663 runs (Figures 6.6 and 6.7), 76 were considered moderate to strong on the basis that
 3664 the results had R^2 values \Rightarrow 0.5 and nRMSE $<$ 100; 35 model runs for CROPSCAN,
 3665 16 for the Rikola camera and 25 for the SVC. Some of these models (49) had R^2
 3666 values \Rightarrow 0.7; 20 for CROPSCAN, 14 for the Rikola camera and 15 for the
 3667 SVC. When comparing how many PLSR models made moderate to strong
 3668 predictions of grassland variables using spectral data from each device, no one
 3669 variable stands out as producing many more significant results than the others. All
 3670 grassland variables except biomass, bryophytes and dead material produced 10-13
 3671 significant results each (mass and % cover). Biomass and bryophytes were used in
 3672 half as many model runs (only mass data) and produced 3 and 5 significant results
 3673 respectively. All 5 of the significant results for dead material were the result of using
 3674 % cover data. Using % cover data produced 52 significant results whilst using mass
 3675 data produced 24 significant results. For the CROPSCAN, SVC and Rikola camera;
 3676 the ratio of significant results when using % cover data is 23:16:13 and when using
 3677 mass data it is 12:9:3. It is possible that relatively few models trained with Rikola
 3678 spectral data had moderate to strong predictive power because the SWIR region of
 3679 the spectrum is relatively sensitive to water content which correlates strongly with
 3680 chlorophyll content (and, in turn, biomass) in other studies (Sakowska et al., 2016).

3681

3682 **7.6. Practical implications of RS condition**

3683 **monitoring of grasslands**

3684 Unlike most comparable studies which are conducted on experimental or relatively
 3685 structurally homogeneous grasslands and in clear sky conditions, the RS studies of
 3686 grassland condition in this thesis were carried out on spatially heterogeneous
 3687 grasslands (within and between grasslands) and in changeable weather conditions
 3688 which can introduce error and uncertainty into RS studies. For example, Harzé et al.
 3689 (2016) found that specific leaf area (SLA), leaf dead matter content (LDMC), and
 3690 plant height are characterized by considerable intra-population variability (SLA: 72–
 3691 95%, LDMC: 78–100% and vegetative height: 70–94% of the variability of grassland
 3692 variables) as a result of within-site environmental heterogeneity including variables
 3693 such as soil depth and slope. It is thought that this variability plus variation in aspects

3694 of the grazing regime of each grassland, particularly grazing intensity (Bai et al.,
3695 2001) could have made it more difficult to link spectral data to grassland variables
3696 and condition on the semi-natural grasslands chosen for this study. Furthermore, on
3697 the mire grassland included in this study; tussocks, sinkholes and shrubs complicated
3698 the collection of good quality RS data because spectral data can be influenced by
3699 topography and canopy structure. Also, the calcareous grasslands of Ingleborough
3700 NNR included a limestone pavement where outcropping rocks affected the spectral
3701 signature. Although the aforementioned within-grassland variability of some
3702 grassland characteristics and geographic features may have increased model error in
3703 predicting the grassland variables included in this study, these features of semi-
3704 natural grasslands are not taken into consideration in studies conducted on
3705 experimental grasslands (e.g. Capolupo et al., 2015), meaning their methods may not
3706 be viable on semi-natural grasslands. In contrast to many other RS studies on
3707 grassland condition, the mass of grassland variables (graminoids, forbs, bryophytes
3708 and dead material in particular) were used as responses in regression analyses.
3709 These grassland variables can be linked to condition for the reasons explained in
3710 Chapter 2, in particular Sections 2.1 and 2.3.6.

3711 The results of this study have implications for future studies that try to predict
3712 condition-related grassland variables using a RS methods. If models need to be
3713 calibrated to individual grasslands (particularly grasslands that are as spatially
3714 heterogeneous as the ones studied) to produce stronger predictions, more *in situ*
3715 data is required to capture the within-grassland variability in grassland variables and
3716 related grassland canopy structure. Many of the models with values of $R^2 > 0.7$ were
3717 trained using data from individual grasslands ($n=10$ in this thesis), suggesting that
3718 site specific studies are more reliable. Comparing these results to the results of
3719 randomised models suggests that training statistical models with insufficient data lead
3720 to unreliable results even if the study is site specific (Goodhue et al., 2012).
3721 Therefore, the results of this study suggest that collecting sufficient data to train the
3722 models is critical and a sufficient quantity in this thesis was deemed to be 30
3723 quadrats. Receiving relatively high R^2 and low nRMSE results can be deceptive as
3724 these same models may not be able to consistently beat randomised models or
3725 deliver reproducible results, which also demonstrates the importance of model
3726 testing. In addition, it is also important to collect a sufficient quantity of data to allow
3727 for validation of the results using a data set separate from the data set used to train
3728 the models. The increased number of moderately strong PLSR models produced
3729 using data from all grasslands collectively, relative to Chapter 4 which included

3730 grasslands from Ingleborough NNR, suggests that using data from different
3731 grasslands may have a reduced impact on model strength if all of the grasslands are
3732 structurally similar. There are many variables other than canopy structure that
3733 influence the spectral signature and were not taken into consideration in this study
3734 such as biochemical variables. A study where a larger quantity of samples are
3735 collected on each grassland may confirm whether site specific studies produce
3736 superior results to studying multiple grasslands. Furthermore, using % cover or mass
3737 data seems to capture different condition-based grassland variables more effectively
3738 although % cover data can be collected more time-efficiently.

3739 It also seems necessary to use relatively high spatial resolution satellite or drone data
3740 that includes the capture of data on at least a couple of SWIR wavelengths to capture
3741 the spatial structural heterogeneity of target grasslands when comparing the
3742 predictive power of PLSR models trained with CROPSCAN data compared to models
3743 trained with Rikola data. The most advanced VNIR cameras mounted on <20kg
3744 drones currently available collect data on a 500-900nm range with a spatial resolution
3745 of <1m (6cm for the Rikola camera). The results of the PLSR and VIP analyses
3746 suggest that predicting grassland variables using this range of spectral data is viable
3747 but the strength of grassland variable prediction is dependent on grassland type,
3748 grassland variable and how the variable is captured (mass or % cover). Despite this,
3749 the results suggest that devices that collected spectral data on SWIR wavelengths
3750 (e.g. SVC), even if it is only two wavelengths (e.g. CROPSCAN) trained more models
3751 with a moderate to strong predictive power relative to using Rikola data.
3752 Considerations need to be made around collecting imagery with UAVs as within and
3753 between image illumination levels can have a detrimental impact on the viability of
3754 any results gained from using the spectral data from these images as predictors in
3755 models. The timing of the flight needs to be as close to the time of highest sun as
3756 possible to minimise within and between image illumination variability. The vignetting
3757 effect (reduction in illumination at the periphery of the image) also needs to be
3758 considered as it will contribute to within image illumination variability (Kordecki et al.,
3759 2016). A contributing factor to this issue may have been that this thesis chose the
3760 PLSR modelling approach, which can be sensitive to issues related to the viewing
3761 angle of the spectral device and the sun as well as surface property differences such
3762 as canopy structure (Li et al. 2016).

3763

3764 7.7. Study limitations

3765 This study directly attempted to address issues around monitoring the condition of
3766 semi-natural grasslands which had practical implications for the robustness of the
3767 results from this work. As so many hypotheses were tested at once, the results may
3768 have been affected by the multiple testing hypothesis and the “look-elsewhere” effect.
3769 Although steps were taken to ensure that the results of this study are reproducible
3770 (making it unlikely that the “look-elsewhere” effect is happening), training such a large
3771 number of PLSR models has complicated making inferences from the results.
3772 Furthermore, PLSR models cannot accommodate a fixed-effect which refers to
3773 instances where all the values of the response variable are the same. This prevented
3774 PLSR models being trained to predict “bare ground” and “graminoid:bryophyte ratio”
3775 for Parsonage grasslands (Grasslands 1-3). Using PLSR as a statistical modelling
3776 approach seemed to underestimate the largest grassland variable values and
3777 overestimate the smallest grassland variable values (as seen in Psomas et al. (2011)
3778 and Chen et al. (2009) respectively), but whether using a non-linear regression
3779 approach *per se* would have produced superior results is debatable (Yang and Guo,
3780 2014). One possibility for the above limitations is the variation in spectra that can
3781 occur even when many of the variables of a target remain the same (e.g. Price, 1994)
3782 which can occur because of spatial and temporal variability in illumination, the
3783 problems of which would be exacerbated when using an insufficient quantity of
3784 training data in the statistical models. Some of the spectral data collected in spring
3785 were incorrectly calibrated and were corrected using spectral data collected at a
3786 separate site (see Section 3.4.3.1). It is believed that these corrected data were of
3787 sufficient quality for analysis, but it is possible that there was a minor impact on the
3788 accuracy and precision of models trained with these data. Data collected with an
3789 Analytical Spectral Device (ASD) at Ingleborough NNR was not viable as a result of
3790 the highly changeable weather conditions and cloud patterns. Weather conditions
3791 also prevented triplicate data collection with the CROPSCAN on all Ingleborough
3792 grasslands except the acid mire grassland plus the collection of spectral data at
3793 Ingleborough NNR during spring and autumn. Although the results of this study
3794 suggest that forbs can be predicted by spectral data with significant accuracy and
3795 precision if grasslands are analysed individually, only the species count was able to
3796 determine which species of forb existed in a target area. This may be an issue as
3797 some forb species are positive indicators while others are negative indicators of
3798 condition (JNCC, 2004; 2006). This could be inferred from the species abundance

3799 data in this study, but these data were only collected on quadrats during the spring
3800 period at Ingleborough NNR and the summer period at Parsonage NNR and species
3801 abundance on a given patch can change over time (Herben et al., 2000) therefore
3802 this is another limitation. CSM-condition was derived from CSM criteria where
3803 multiple data sets including species abundance and % cover grassland variables
3804 were used as inputs for the criteria. When % cover grassland variables were used as
3805 predictors of CSM-condition, there may have been positive bias as % cover “dead
3806 material” and “forbs” were also used for a few of the CSM criteria that CSM-condition
3807 was derived from. Furthermore, CSM-condition was calculated using criteria that
3808 were weighted equally in the calculation. It is acknowledged that the criteria weights
3809 used to calculate CSM-condition could be relaxed or refined and this should be
3810 further investigated to establish the optimum weightings of each criterion.

3811 The results of using the mass or % cover of grassland variables to demonstrate that
3812 the grasslands in this study are significantly different in character due to differing
3813 levels of fertilisation mostly suggested that this was not the case, but it is unclear if
3814 the methods used in this study were ineffective as Hollberg and Schellberg (2017)
3815 suggested that different intensities of fertilisation can be distinguished using VIs.
3816 Collecting % cover data of bryophytes was limited as they grow beneath graminoid
3817 and forb species. Also, some quadrats in spring had dead material cover values that
3818 were considered high (50-75% for quadrats 1-8 and 35-60% for seven quadrats on
3819 Grassland 3) which may have led to increased within-site variability of grassland
3820 variables and spectral signatures (Yang and Guo, 2014). The amount of error that
3821 may have been introduced by these factors is unknown but the total error for each
3822 model run has been quantified using nRMSE. Changing quadrat locations each
3823 season introduced spatial-variation to a temporal study which may have complicated
3824 the interpretation of the results. This was unavoidable as spectral data had to be
3825 collected on quadrats unaffected by destructive sampling as this sampling would
3826 have altered the canopy structure and therefore affected spectral data collection
3827 (Gitelson et al. 2019). Furthermore, the CSM guidelines suggested that 4m² quadrats
3828 should be used for assessing M19 grasslands but this study used 1m² quadrats.
3829 Finally, this study was also affected by major limitations specific to the extrapolation
3830 of the results from PLSR models trained with Rikola spectral data. Although the
3831 vignetting effect was addressed to an extent by removing a portion of the image
3832 peripheries, this study did not effectively solve the detrimental effect that within and
3833 between illumination variation can have on the accuracy of predicted grassland
3834 variable values. Furthermore, the predicted grassland variable values extrapolated to

3835 field level have not been independently verified against a separate data set to assess
 3836 the accuracy of the extrapolated results for PLSR models trained with Rikola or
 3837 CROPSCAN spectral data.

3838 Studies using the same approach as this paper should be conducted on other
 3839 spatially heterogeneous grasslands and collect a greater quantity of data to confirm
 3840 that the results would be consistent regardless of the target grassland. Alternatively,
 3841 a study that is better suited to capturing then mining spatial-temporal data should also
 3842 be completed to determine if seasonal data would increase the predictive power of
 3843 regression analyses on grassland variables and CSM-condition.

3844

3845 **7.8. Potential research opportunities**

3846 There are several directions that future research could take in relation to this thesis.
 3847 There is already a trend towards the increased use of UAVs as remote sensing
 3848 platforms. If the use of RS data collected with a UAV is to truly become viable,
 3849 issues related to between and within variances in image illumination would need to
 3850 be solved. Solving this issue could lead to grassland condition studies on semi-
 3851 natural grasslands at field level becoming viable. This could coincide with
 3852 advancements in UAV-mounted instruments, for example they could collect
 3853 hyperspectral data on a wider range of the EM spectrum or become more
 3854 economically accessible. As more very-high spatial resolution satellites are launched
 3855 and their imagery becomes more commonplace, it is possible that grassland
 3856 condition monitoring at field level will become financially viable but whether this is
 3857 scientifically possible may depend on which wavelengths data are collected.
 3858 Hyperspectral satellite imagery with a higher spatial and spectral resolution, for
 3859 example from EnMap, could also become more available for grassland condition
 3860 studies in future. Whether hyperspectral satellite imagery can be utilised may depend
 3861 on the cost of the imagery and the cost of acquiring sufficient computing power.

3862 Regarding machine learning techniques, a model comparison study that includes
 3863 further exploration of Bayesian (e.g. Zhao et al. 2013), kriging and neural network
 3864 (NN) techniques could lead to more accurate models although a larger data set may
 3865 be required to train accurate models (Li et al. 2016). For example, Li et al. (2016)
 3866 found that regression kriging and random forests residuals kriging predicted LAI more

3867 accurately than PLSR, random forests or artificial neural networks. Furthermore,
3868 using neural networks may be an effective way to overcome issues related to
3869 differences in illumination between and within multi- or hyperspectral images
3870 collected with a UAV. The neural network may produce reliable results without the
3871 necessity of image (histogram) equalisation subject to a sufficient amount of spectral
3872 data being utilised as training data and taken from different images to capture the
3873 changes in illumination (Thomas, T. pers. comm. 1st December 2020).

3874

3875

3876

3877

3878

3879

3880

3881

3882

3883

3884

3885

3886

3887

3888

3889 Chapter 8 - Conclusion

3890 This thesis assessed whether remote sensing techniques could be used to ascertain
3891 the condition, in the context of ecosystem services, of different types of grasslands by
3892 predicting condition-related grassland variables with a sufficient level of accuracy.
3893 This research is considered important as it could provide more time- and cost-
3894 effective approach to grassland monitoring, enabling superior spatial-temporal
3895 coverage and more timely intervention of conserving degrading grasslands. Previous
3896 studies had been conducted to address issues within this line of research, but these
3897 studies were generally limited by not directly tackling the issues around the remote
3898 sensing of grassland condition on working semi-natural grasslands. Finding a working
3899 solution to establishing the condition of semi-natural grasslands was considered most
3900 beneficial to land managers who may adopt this approach as a more cost- and -time
3901 efficient approach to condition monitoring with the added benefit of better spatial
3902 coverage than traditional monitoring techniques.

3903 This assessment was conducted by training PLSR models using spectral data
3904 collected with hand-held devices or by UAV as predictors and using the mass or %
3905 cover of condition-related grassland variables plus CSM-condition as responses.
3906 Grassland variables were also used as predictors of CSM-condition. The results
3907 suggest that it is possible to use these methods to accurately estimate some of the
3908 grassland variables chosen by this study subject to some caveats. The results
3909 suggested that, despite PLSR being suggested as a correct approach for use with
3910 small data sets and to avoid model overfitting, it is still possible to train models that
3911 seem to have moderate to strong predictive power but are actually unreliable if an
3912 insufficient quantity of data are used. More specifically, the results suggest that most
3913 of the PLSR models with moderate to strong predictive power in this thesis are not
3914 reliable if they are trained with data from only one grassland ($n = 10$). A sufficient
3915 amount of data to train PLSR models so that the results were considered reliable was
3916 considered to be at least 30 quadrats ($n = 30$). It is possible that collecting larger data
3917 sets on each grassland would have solved this issue, but data collection was limited
3918 by time and resources and therefore this is not clearly demonstrated in this thesis.
3919 Despite these limitations; it was possible to train PLSR models to predict some
3920 grassland variables to a moderate to high level of accuracy for some grasslands and
3921 seasons.

3922 This has implications for other similar studies which may have assumed their results
3923 were robust without using an effective external validation technique. There are also

3924 implications for land managers who are interested in implementing RS techniques to
3925 monitor the condition of grasslands as it would be necessary to collect a sufficient
3926 amount of data to train models with reliable results and to externally validate the
3927 results of extrapolated models. This suggests that collecting and separating a
3928 sufficient number of grass samples to establish the mass of grassland variables may
3929 not be practical but could lead to models trained to accurately predict some condition-
3930 related variables that would not be possible when using % cover data. The
3931 grasslands and time of year could also be factors when trying to accurately predict
3932 condition-related variables as the results of this thesis suggest that none of the
3933 grassland variables chosen for this thesis could be consistently predicted with
3934 reasonable accuracy across grasslands and seasons. The results of this thesis also
3935 suggest that choosing a spectral device that collects data on the SWIR part of the
3936 spectrum could help train more accurate models, but this is not crucial.

3937 A number of recommendations are suggested based on the findings of this thesis.
3938 The methods used in Chapter 6 to predict grassland variables at field level should
3939 include a data set separate from model training to externally validate the predicted
3940 values from extrapolated models. These proposed methods, with an external
3941 validation approach included, should be tested with an increased amount of response
3942 data (i.e. the mass or % cover of grassland variables) and across seasons to test the
3943 optimal amount of data and best seasons to collect data for training the most
3944 accurate models. If the limitations to using imagery collected by a UAV cannot be
3945 overcome (for example, by removing illumination differences within and between
3946 images), using a UAV-mounted spectrometer that collects patch level spectral data
3947 (i.e. comparable to a CROPSCAN) on many patches over an entire field may be a
3948 more suitable device for the prediction of grassland variables at field level. This
3949 opens up possibilities for training PLSR models and other types of models making a
3950 model comparison study using drone data possible. For example, some studies have
3951 used Bayesian techniques or neural networks to determine grassland condition.

3952 The final recommendations and considerations are for land managers contemplating
3953 adopting these methods for monitoring grasslands. Land managers would need to
3954 decide whether it is practical to collect and separate a sufficient number of grass
3955 samples to ensure the robustness of the PLSR models when trying to predict the
3956 mass of a given variable. Collecting % cover data on grassland variables is
3957 considerably more time-efficient but has its own set of limitations as specified in
3958 Chapter 7. When collecting spectral data; considerations need to be made around the
3959 spatial and spectral range of any device used, plus the weather conditions though

3960 clear sky weather conditions does not guarantee stable illumination. In short, the
3961 methods in this thesis offer a more cost- and time-effective solution to monitoring
3962 grassland condition but any land manager who implements the methods in this thesis
3963 would have to take the aforementioned points into consideration to increase the
3964 likelihood of training models with an acceptable predictive power.

3965

3966

3967

3968

3969

3970

3971

3972

3973

3974

3975

3976

3977

3978

3979

3980

3981

3982

3983

3984

3985 **References and Bibliography**

3986

3987 Aitchison, J. (1982), "The Statistical Analysis of Compositional Data", *Journal of the*
3988 *Royal Statistical Society. Series B, Statistical Methods*, Vol. 44 No. 2.

3989 Ali, A.M., Darvishzadeh, R., Shahi, K.R. and Skidmore, A. (2019), "Validating the
3990 Predictive Power of Statistical Models in Retrieving Leaf Dry Matter Content of
3991 a Coastal Wetland from a Sentinel-2 Image", *Remote Sensing*,
3992 Multidisciplinary Digital Publishing Institute, Vol. 11 No. 1936, pp. 1-17.

3993 Ali, I., Cawkwell, F., Dwyer, E., Barrett, B. and Green, S. (2016), "Satellite remote
3994 sensing of grasslands: from observation to management—a review", *Journal of*
3995 *Plant Ecology*, available at: <https://doi.org/10.1093/jpe/rtw005>.

3996 Anderson, K. and Gaston, K.J. (2013), "Lightweight unmanned aerial vehicles will
3997 revolutionize spatial ecology", *Frontiers in Ecology and the Environment*, Vol.
3998 11 No. 3, pp. 138–146.

3999 Anderson, M.C., Neale, C.M.U., Li, F., Norman, J.M., Kustas, W.P., Jayanthi, H. and
4000 Chavez, J. (2004), "Upscaling ground observations of vegetation water
4001 content, canopy height, and leaf area index during SMEX02 using aircraft and
4002 Landsat imagery", *Remote Sensing of Environment*, Vol. 92 No. 4, pp. 447–
4003 464.

4004 Arroyo-Mora, J. P., Kalacska, M., Inamdhar, D., Soffer, R., Lucanus, O., Gorman, J.,
4005 Naprstek, T., Schaaf, E. S., Ifimov, G., Elmer, K. and Leblanc, G. (2019),
4006 "Implementation of a UAV–Hyperspectral Pushbroom Imager for Ecological
4007 Monitoring", *Drones*, Vol. 3, No. 1, available at:
4008 <https://doi.org/10.3390/drones3010012>

4009 Arroyo-Mora, J. P., Kalacska, M., Lørke, T., Schläpfer, D., Coops, N. C., Lucanus, O.
4010 and Leblanc, G. (2021), "Assessing the impact of illumination on UAV
4011 pushbroom hyperspectral imagery collected under various cloud cover
4012 conditions", *Remote Sensing of Environment*, Vol. 258, available at:
4013 <https://www.sciencedirect.com/science/article/pii/S0034425721001140#bb001>
4014 5

4015 ASD Inc. (2002), *FieldSpec Pro User's Guide*, Analytical Spectral Devices, Inc.

- 4016 Asner, G.P. (1998), "Biophysical and Biochemical Sources of Variability in Canopy
4017 Reflectance", *Remote Sensing of Environment*. Vol. 64, pp. 234–253.
- 4018 Asner, G.P., Wessman, C.A. and Archer, S. (1998), "Scale Dependence of
4019 Absorption of Photosynthetically Active Radiation in Terrestrial Ecosystems",
4020 *Ecological Applications: A Publication of the Ecological Society of America*,
4021 Ecological Society of America, Vol. 8 No. 4, pp. 1003–1021.
- 4022 Asner, G.P., Wessman, C.A., Bateson, C. A., and Privette, J.L. (2000), "Impact of
4023 Tissue, Canopy, and Landscape Factors on the Hyperspectral Reflectance
4024 Variability of Arid Ecosystems", *Remote Sensing of Environment*. Vol. 74, pp.
4025 69–84.
- 4026 Asner, G.P., Martin, R.E., Knapp, D.E., Tupayachi, R., Anderson, C., Carranza, L.,
4027 Martinez, P., *et al.* (2011), "Spectroscopy of canopy chemicals in humid
4028 tropical forests", *Remote Sensing of Environment*, Vol. 115 No. 12, pp. 3587–
4029 3598.
- 4030 Asner, G.P., Martin, R.E., Anderson, C.B. and Knapp, D.E. (2015), "Quantifying forest
4031 canopy traits: Imaging spectroscopy versus field survey", *Remote Sensing of
4032 Environment*, Vol. 158, pp. 15–27.
- 4033 Atzberger, C., Darvishzadeh, R., Immitzer, M., Schlerf, M., Skidmore, A. and le Maire,
4034 G. (2015), "Comparative analysis of different retrieval methods for mapping
4035 grassland leaf area index using airborne imaging spectroscopy", *International
4036 Journal of Applied Earth Observation and Geoinformation*, Vol. 43, pp. 19–31.
- 4037 Bacour, C., Jacquemoud, S., Leroy, M., Hauteœur, O., Weiss, M., Prévot, L.,
4038 Bruguier, N., *et al.* (2002), "Reliability of the estimation of vegetation
4039 characteristics by inversion of three canopy reflectance models on airborne
4040 POLDER data", *Agronomie*, EDP Sciences, Vol. 22 No. 6, pp. 555–565.
- 4041 Badgery, W.B., Kemp, D., Yingjun, Z., Zhongwu, W., Guodong, H., Fujiang, H., Nan,
4042 L., *et al.* (2020), "Optimising grazing for livestock production and
4043 environmental benefits in Chinese grasslands", *Rangeland Journal*, CSIRO
4044 Publishing, Vol. 42 No. 5, pp. 347–358.
- 4045 Bai, Y., Abouguendia, Z. and Redmann, R.E. (2001), "Relationship between plant
4046 species diversity and grassland condition", *Journal of Range Management*,
4047 Vol. 54 No. 2, pp. 177–183.

- 4048 Bauer, D.F. (1972), "Constructing Confidence Sets Using Rank Statistics", *Journal of*
4049 *the American Statistical Association*, [American Statistical Association, Taylor
4050 & Francis, Ltd.], Vol. 67 No. 339, pp. 687–690.
- 4051 Baulcombe, D., Crute, I., Davies, B., Dunwell, J., Gale, M., Jones, J., Pretty, J., *et al.*
4052 (2009), *Reaping the Benefits: Science and the Sustainable Intensification of*
4053 *Global Agriculture*, The Royal Society.
- 4054 van den Berg, R.A., Hoefsloot, H.C.J., Westerhuis, J.A., Smilde, A.K. and van der
4055 Werf, M.J. (2006), "Centering, scaling, and transformations: improving the
4056 biological information content of metabolomics data", *BMC Genomics*, Vol. 7
4057 No. 142, pp. 1-15.
- 4058 Bengtsson, J., Bullock, J.M., Egoh, B., Everson, C., Everson, T., O'Connor, T.,
4059 O'Farrell, P.J., *et al.* (2019), "Grasslands-more important for ecosystem
4060 services than you might think", *Ecosphere*. Vol. 10 No. 2, pp. 1-20.
- 4061 Bigiarini, M.Z. (2019), *Package "HydroGOF"*, available at:
4062 <https://www.rdocumentation.org/packages/hydroGOF/versions/0.3-10>.
- 4063 Blackburn, G.A. (2002), "Remote sensing of forest pigments using airborne imaging
4064 spectrometer and LIDAR imagery", *Remote Sensing of Environment*. Vol. 82,
4065 pp. 311 – 321.
- 4066 Boyle, S.A., Kennedy, C.M., Torres, J., Colman, K., Pérez-Estigarribia, P.E. and de la
4067 Sancha, N.U. (2014), "High-resolution satellite imagery is an important yet
4068 underutilized resource in conservation biology", *PloS One*, Vol. 9 No. 1, pp. 1-
4069 11.
- 4070 Breiman, L. (1994), *Bagging Predictors*, No. 421, University of California. pp. 1-19.
- 4071 British Geological Survey. (2017), "UK Soil Observatory", available at:
4072 <http://www.ukso.org/> (accessed 11 January 2017).
- 4073 von Bueren, S.K., Burkart, A., Hueni, A., Rascher, U., Tuohy, M.P. and Yule, I.J.
4074 (2015), "Deploying four optical UAV-based sensors over grassland:
4075 challenges and limitations", *Biogeosciences*, Copernicus GmbH, Vol. 12 No.
4076 1, pp. 163–175.
- 4077 Bullock, J.M., Jefferson, R.G., Blackstock, T.H., Pakeman, R.J., Emmett, B.A.,
4078 Pywell, R.J., Grime, J.P., *et al.* (2011), "Semi-natural Grasslands", UNEP-
4079 WCMC, available at: <http://nora.nerc.ac.uk/id/eprint/15322/1/N015322CR.pdf>.

- 4080 Calaciura, B. and Spinelli, O. (2008), Management of Natura 2000 habitats. "6210
4081 Semi-natural dry grasslands and scrubland facies on calcareous substrates
4082 (*Festuco-Brometalia*) (*important orchid sites)", *European Commission*.
- 4083 Calderón, R., Navas-Cortés, J.A., Lucena, C. and Zarco-Tejada, P.J. (2013), "High-
4084 resolution airborne hyperspectral and thermal imagery for early detection of
4085 *Verticillium* wilt of olive using fluorescence, temperature and narrow-band
4086 spectral indices", *Remote Sensing of Environment*, Vol. 139, pp. 231–245.
- 4087 Campbell, M.J. and Gardner, M.J. (1988), "Calculating confidence intervals for some
4088 non-parametric analyses", *British Medical Journal*, Vol. 296 No. 6634, pp.
4089 1454–1456.
- 4090 Capolupo, A., Kooistra, L., Berendonk, C., Boccia, L. and Suomalainen, J. (2015),
4091 "Estimating Plant Traits of Grasslands from UAV-Acquired Hyperspectral
4092 Images: A Comparison of Statistical Approaches", *ISPRS International
4093 Journal of Geo-Information*, Multidisciplinary Digital Publishing Institute, Vol. 4
4094 No. 4, pp. 2792–2820.
- 4095 Chapungu, L., Nhamo, L. and Gatti, R.C. (2020), "Estimating biomass of savanna
4096 grasslands as a proxy of carbon stock using multispectral remote sensing",
4097 *Remote Sensing Applications: Society and Environment*, Vol. 17, pp. 1-10.
- 4098 Chen, J., Gu, S., Shen, M., Tang, Y. and Matsushita, B. (2009), "Estimating
4099 aboveground biomass of grassland having a high canopy cover: an
4100 exploratory analysis of in situ hyperspectral data", *International Journal of
4101 Remote Sensing*, Taylor & Francis, Vol. 30 No. 24, pp. 6497–6517.
- 4102 Chen, J.M., Rich, P.M., Gower, S.T., Norman, J.M. and Plummer, S. (1997), "Leaf
4103 area index of boreal forests: Theory, techniques, and measurements", *Journal
4104 of Geophysical Research: Atmospheres*. Vol. 102 No. D24, pp. 29429-29441.
- 4105 Chopping, M., Su, L., Rango, A., Martonchik, J.V., Peters, D.P.C. and Laliberte, A.
4106 (2008), "Remote sensing of woody shrub cover in desert grasslands using
4107 MISR with a geometric-optical canopy reflectance model", *Remote Sensing of
4108 Environment*, Vol. 112 No. 1, pp. 19–34.
- 4109 Cole, B., McMorrow, J. and Evans, M. (2014), "Spectral monitoring of moorland plant
4110 phenology to identify a temporal window for hyperspectral remote sensing of
4111 peatland", *ISPRS Journal of Photogrammetry and Remote Sensing: Official
4112 Publication of the International Society for Photogrammetry and Remote
4113 Sensing*, Vol. 90, pp. 49–58.

- 4114 Corbane, C., Alleaume, S. and Deshayes, M. (2013), "Mapping natural habitats using
4115 remote sensing and sparse partial least square discriminant analysis",
4116 *International Journal of Remote Sensing*, Taylor & Francis, Vol. 34 No. 21, pp.
4117 7625–7647.
- 4118 Craven, D., Forest I., Manning, P., Connolly, J., Bruelheide, H., Ebeling, A., Roscher,
4119 C. et al. (2016), "Plant Diversity Effects on Grassland Productivity Are Robust
4120 to Both Nutrient Enrichment and Drought", *Philosophical Transactions of the*
4121 *Royal Society of London, Series B, Biological Sciences*, Vol. 371 No.
4122 20150277, available at: <http://dx.doi.org/10.1098/rstb.2015.0277>.
- 4123 CROPSCAN Inc. (2018), "Multispectral Radiometers", available at:
4124 <http://www.cropscan.com/msr.html> (last accessed 9 November 2020).
- 4125 Curran, P.J. and Williamson, H.D. (1987), "Estimating the Green Leaf Area Index of
4126 Grassland with Airborne Multispectral Scanner Data", *Oikos*, [Nordic Society
4127 Oikos, Wiley], Vol. 49 No. 2, pp. 141–148.
- 4128 Dabrowska – Zielinska, K., Goliński, P., Jorgensen, M., Mølmann, J., Taff, G.,
4129 Tomaszewska, M., Golińska, B., et al. (2015), "New methodologies for
4130 grasslands monitoring", *Proceedings of 23rd International Grassland*
4131 *Congress 2015 - Keynote Lecture (XXIII IGC 2015)*, Range Management
4132 Society of India, Jhansi, U.P.India, p. 30.
- 4133 Darvishzadeh, R., Skidmore, A., Schlerf, M., Atzberger, C., Corsi, F. and Cho, M.
4134 (2008), "Estimation of Leaf Area Index and Chlorophyll for a Mediterranean
4135 Grassland Using Hyperspectral Data", *The International Archives of the*
4136 *Photogrammetry, Remote Sensing and Spatial Information Sciences*, Vol. 37
4137 No. B7, pp. 471-478.
- 4138 Davidson, A., Wang, S. and Wilmshurst, J. (2006), "Remote sensing of grassland–
4139 shrubland vegetation water content in the shortwave domain", *International*
4140 *Journal of Applied Earth Observation and Geoinformation*, Vol. 8 No. 4, pp.
4141 225–236.
- 4142 Delta-T Devices. (2020), "HH2 Moisture Meter", available at: <https://www.deltat.co.uk/product/hh2/> (accessed 9 November 2020).
- 4144 Derner, J.D. and Schuman, G.E. (2007), "Carbon sequestration and rangelands: A
4145 synthesis of land management and precipitation effects", *NUMBER*, Vol. 62
4146 No 2, pp. 77-85.

- 4147 Dixon, A.P., Faber-Langendoen, D., Josse, C., Morrison, J. and Loucks, C.J. (2014),
4148 “Distribution mapping of world grassland types”, edited by Ebach, M. *Journal*
4149 *of Biogeography*, Vol. 41 No. 11, pp. 2003–2019.
- 4150 DJI. (2015), *Phantom 3 Professional User Manual*, Da-Jiang Innovations, available
4151 at: [http://download.dji-](http://download.dji-innovations.com/downloads/phantom_3/en/Phantom_3_Professional_User_Manual_v1.0_en.pdf)
4152 [innovations.com/downloads/phantom_3/en/Phantom_3_Professional_User_M](http://download.dji-innovations.com/downloads/phantom_3/en/Phantom_3_Professional_User_Manual_v1.0_en.pdf)
4153 [anual_v1.0_en.pdf](http://download.dji-innovations.com/downloads/phantom_3/en/Phantom_3_Professional_User_Manual_v1.0_en.pdf).
- 4154 DJI. (2018), *Matrice 600 Pro User Manual*, Da-Jiang Innovations, available at:
4155 [https://dl.djicdn.com/downloads/m600%20pro/20180417/Matrice_600_Pro_Us](https://dl.djicdn.com/downloads/m600%20pro/20180417/Matrice_600_Pro_User_Manual_v1.0_EN.pdf)
4156 [er_Manual_v1.0_EN.pdf](https://dl.djicdn.com/downloads/m600%20pro/20180417/Matrice_600_Pro_User_Manual_v1.0_EN.pdf).
- 4157 Dodd, M.E., Silvertown, J., McConway, K., Potts, J. and Crawley, M. (1994),
4158 “Application of the British National Vegetation Classification to the
4159 Communities of the Park Grass Experiment through Time”, *Folia Geobotanica*
4160 *et Phytotaxonomica*, Springer, Vol. 29 No. 3, pp. 321–334.
- 4161 Dormann, C.F., Elith, J., Bacher, S., Buchmann, C., Carl, G., Carré, G., Marquéz,
4162 J.R.G., *et al.* (2013), “Collinearity: a review of methods to deal with it and a
4163 simulation study evaluating their performance”, *Ecography*, Wiley, Vol. 36 No.
4164 1, pp. 27–46.
- 4165 Doughty, C.E., Asner, G.P. and Martin, R.E. (2011), “Predicting tropical plant
4166 physiology from leaf and canopy spectroscopy”, *Oecologia*, Vol. 165 No. 2,
4167 pp. 289–299.
- 4168 Douma, J.C. and Weedon, J.T. (2018), “Analysing continuous proportions in ecology
4169 and evolution: A practical introduction to beta and Dirichlet regression”,
4170 *Methods in Ecology and Evolution*, Vol. 10, pp. 1412–1430.
- 4171 Dusseux, P., Vertès, F., Corpetti, T., Corgne, S. and Hubert-Moy, L. (2014),
4172 “Agricultural practices in grasslands detected by spatial remote sensing”,
4173 *Environmental Monitoring and Assessment*, Vol. 186 No. 12, pp. 8249–8265.
- 4174 Edina. (2017), “Digimap”, available at: <https://digimap.edina.ac.uk/> (accessed 11
4175 January 2017).
- 4176 Farrés, M., Platikanov, S., Tsakovski, S. and Tauler, R. (2015), “Comparison of the
4177 variable importance in projection (VIP) and of the selectivity ratio (SR)
4178 methods for variable selection and interpretation: Comparison of variable
4179 selection methods”, *Journal of Chemometrics*, Vol. 29 No. 10, pp. 528–536.

- 4180 Ferreira, L.G., Asner, G.P., Knapp, D.E., Davidson, E.A., Coe, M., Bustamante,
4181 M.M.C. and de Oliveira, E.L. (2011), "Equivalent water thickness in savanna
4182 ecosystems: MODIS estimates based on ground and EO-1 Hyperion data",
4183 *International Journal of Remote Sensing*, Taylor & Francis, Vol. 32 No. 22, pp.
4184 7423–7440.
- 4185 Filella, I. and Penuelas, J. (1994), "The red edge position and shape as indicators of
4186 plant chlorophyll content, biomass and hydric status", *International Journal of*
4187 *Remote Sensing*, Vol. 15 No. 7, pp. 1459–1470.
- 4188 Firn, J., Nguyen, H., Schütz, M. and Risch, A.C. (2019), "Leaf trait variability between
4189 and within subalpine grassland species differs depending on site conditions
4190 and herbivory", *Proceedings. Biological Sciences / The Royal Society*, Vol.
4191 286 No. 1907, pp. 1-10.
- 4192 Fliervoet, L.M. (1987), "Characterization of the canopy structure of Dutch grasslands",
4193 *Vegetatio*, Vol. 70, pp. 105–117.
- 4194 Franke, J., Keuck, V. and Siegert, F. (2012), "Assessment of grassland use intensity
4195 by remote sensing to support conservation schemes", *Journal for Nature*
4196 *Conservation*, Vol. 20 No. 3, pp. 125–134.
- 4197 Gamon, J.A., Somers, B., Malenovský, Z., Middleton, E.M., Rascher, U. and
4198 Schaepman, M.E. (2019), "Assessing Vegetation Function with Imaging
4199 Spectroscopy", *Surveys in Geophysics*, Vol. 40 No. 3, pp. 489–513.
- 4200 Gao, Q., Li, Y., Wan, Y., Lin, E., Xiong, W., Jiangcun, W., Wang, B., *et al.* (2006),
4201 "Grassland degradation in Northern Tibet based on remote sensing data",
4202 *Journal of Geographical Sciences*, Vol. 16 No. 2, pp. 165–173.
- 4203 Garnett, T. and Godfray, H.C.J. (2012), *Sustainable Intensification in Agriculture.*
4204 *Navigating a Course through Competing Food System Priorities. Food*
4205 *Climate Research Network and the Oxford Martin Programme on the Future*
4206 *of Food*, University of Oxford.
- 4207 Garnier, E., Shipley, B., Roumet, C. and Laurent, G. (2001), "A standardized protocol
4208 for the determination of specific leaf area and leaf dry matter content",
4209 *Functional Ecology*. Vol 15, pp. 688-695.
- 4210 Geerken, R., Zaitchik, B. and Evans, J.P. (2005), "Classifying rangeland vegetation
4211 type and coverage from NDVI time series using Fourier Filtered Cycle
4212 Similarity", *International Journal of Remote Sensing*, Taylor & Francis, Vol. 26
4213 No. 24, pp. 5535–5554.

- 4214 Gerard, F., Acreman, M., Mountford, O., Norton, L., Pywell, R., Rowland, C.,
4215 Stratford, C., *et al.* (2015), *Earth Observation to Produce Indices of Habitat*
4216 *Condition and Change JNCC Ref. C14-0171-0901*, Centre of Ecology and
4217 Hydrology.
- 4218 Gholizadeh, H., Gamon, J.A., Townsend, P.A., Zygielbaum, A.I., Helzer, C.J.,
4219 Hmimina, G.Y., Yu, R., *et al.* (2019), “Detecting prairie biodiversity with
4220 airborne remote sensing”, *Remote Sensing of Environment*, Vol. 221, pp. 38–
4221 49.
- 4222 Gitelson, A., Viña, A., Solovchenko, A., Arkebauer, T. and Inoueij, Y. (2019),
4223 “Derivation of canopy light absorption coefficient from reflectance spectra”,
4224 *Remote Sensing of Environment*, Vol. 231, No. 111276, available at:
4225 <https://doi.org/10.1016/j.rse.2019.111276>.
- 4226 Godfray, H.C.J. and Garnett, T. (2014), “Food security and sustainable
4227 intensification”, *Philosophical Transactions of the Royal Society of London.*
4228 *Series B, Biological Sciences*, Vol. 369 No. 1639, pp. 1-10.
- 4229 Goodhue, D.L., Lewis, W. and Thompson, R. (2012), “Does PLS Have Advantages
4230 for Small Sample Size or Non-Normal Data?” *The Mississippi Quarterly*,
4231 Management Information Systems Research Center, University of Minnesota,
4232 Vol. 36 No. 3, pp. 981–1001.
- 4233 Grant, K., Siegmund, R., Wagner, M. and Hartmann, S. (2015), “Satellite-based
4234 assessment of grassland yields”, *ISPRS - International Archives of the*
4235 *Photogrammetry, Remote Sensing and Spatial Information Sciences*, Vol. XL-
4236 7/W3, pp. 15–18.
- 4237 Grüner, E., Astor, T. and Wachendorf, M. (2019), “Biomass Prediction of
4238 Heterogeneous Temperate Grasslands Using an SfM Approach Based on
4239 UAV Imaging”, *Agronomy*, Multidisciplinary Digital Publishing Institute, Vol. 9
4240 No. 54, pp. 1-16.
- 4241 Gu, Y. and Wylie, B.K. (2015), “Developing a 30-m grassland productivity estimation
4242 map for central Nebraska using 250-m MODIS and 30-m Landsat-8
4243 observations”, *Remote Sensing of Environment*, pp. 291–298.
- 4244 Guo, X., Zhang, C., Wilmshurst, J.F. and Sissons, R. (2005), “Monitoring grassland
4245 health with remote sensing approaches”, in Noble, B.F., Martz, D.J.F. and
4246 Aitken, A.E. (Eds.), *Prairie Perspectives: Geographical Essays*, Vol. 8,
4247 University of Winnipeg, pp. 11–22.

- 4248 Guo, X., Wilmshurst, J.F. and Li, Z. (2010), "Environmental Research and Public
4249 Health", *International Journal of Environmental Research and Public Health*,
4250 Vol. 7, pp. 3513–3530.
- 4251 Gupta, N., Mathiassen, S.E., Mateu-Figueras, G., Heiden, M., Hallman, D.M.,
4252 Jørgensen, M.B. and Holtermann, A. (2018), "A comparison of standard and
4253 compositional data analysis in studies addressing group differences in
4254 sedentary behavior and physical activity", *The International Journal of*
4255 *Behavioral Nutrition and Physical Activity*, Vol. 15 No. 53, pp. 1-12.
- 4256 Haaland, D.M. and Thomas, E.V. (1988), "Partial Least-Squares Methods for Relation
4257 to Other Quantitative Calibration Extraction of Qualitative Information",
4258 *Analytical Chemistry*, Vol. 60 No. 11, pp. 1193–1202.
- 4259 Haboudane, D., Miller, J.R., Pattey, E., Zarco-Tejada, P.J. and Strachan, I.B. (2004),
4260 "Hyperspectral vegetation indices and novel algorithms for predicting green
4261 LAI of crop canopies: Modeling and validation in the context of precision
4262 agriculture", *Remote Sensing of Environment*, Vol. 90 No. 3, pp. 337–352.
- 4263 Halabuk, A., Mojses, M., Halabuk, M. and David, S. (2015), "Towards Detection of
4264 Cutting in Hay Meadows by Using of NDVI and EVI Time Series", *Remote*
4265 *Sensing*, MDPI, Vol. 7 No. 5, pp. 6107–6132.
- 4266 Harzé, M., Mahy, G. and Monty, A. (2016), "Functional traits are more variable at the
4267 intra- than inter-population level: a study of four calcareous dry-grassland
4268 plant species", *Tuexenia*, Floristisch-soziologische Arbeitsgemeinschaft e. V.
4269 (FlorSoz), Vol. 36, pp. 321–336.
- 4270 Hastie, T. and Tibshirani, R. (1986), "Generalized Additive Models", *Statistical*
4271 *Science: A Review Journal of the Institute of Mathematical Statistics*, Vol. 1
4272 No. 3, pp. 297–318.
- 4273 He, Y. and Guo, X. (2006), "Leaf Area Index estimation using remotely sensed data
4274 for Grasslands National Park", *Prairie Perspectives*, Vol. 9, pp. 105–117.
- 4275 He, Y., Guo, X. and Wilmshurst, J.F. (2007), "Comparison of different methods for
4276 measuring leaf area index in a mixed grassland", *Canadian Journal of Plant*
4277 *Science*, Vol. 87, pp. 803-813.
- 4278 Herben T, During HJ & Law R (2000). Spatio-temporal Patterns in Grassland
4279 Communities. In: *The Geometry of Ecological Interactions: Simplifying Spatial*
4280 *Complexity*, eds. Dieckmann U, Law R & Metz JAJ, pp. 48–64. Cambridge
4281 University Press.

- 4282 Hollberg, J.L. and Schellberg, J. (2017), "Distinguishing Intensity Levels of Grassland
4283 Fertilization Using Vegetation Indices", *Remote Sensing*, Multidisciplinary
4284 Digital Publishing Institute, Vol. 9 No. 81, pp. 1-20.
- 4285 Homolová, L., Schaepman, M.E., Lamarque, P., Clevers, J.G.P.W., de Bello, F.,
4286 Thuiller, W. and Lavorel, S. (2014), "Comparison of remote sensing and plant
4287 trait-based modelling to predict ecosystem services in subalpine grasslands",
4288 *Ecosphere*, Vol. 5 No. 8(100), pp. 1-29
- 4289 Ingerpuu, N., Liira, J. and Pärtel, M. (2005), "Vascular Plants Facilitated Bryophytes
4290 in a Grassland Experiment", *Plant Ecology*, Vol. 180 No. 1, pp. 69–75.
- 4291 Ishihara, M., Inoue, Y., Ono, K., Shimizu, M. and Matsuura, S. (2015), "The Impact of
4292 Sunlight Conditions on the Consistency of Vegetation Indices in Croplands—
4293 Effective Usage of Vegetation Indices from Continuous Ground-Based
4294 Spectral Measurements", *Remote Sensing*, MDPI, Vol. 7 No. 10, pp. 14079–
4295 14098.
- 4296 JNCC. (2004), *Common Standards Monitoring Guidance for Lowland Grassland*
4297 *Habitats*, JNCC, available at: <https://doi.org/10.4324/9780203446652-2>.
- 4298 JNCC. (2006), *Common Standards Monitoring Guidance for Upland Habitats*, JNCC.
- 4299 JNCC and DEFRA (on behalf of the Four Countries' Biodiversity Group). (2012), *UK*
4300 *Post-2010 Biodiversity Framework*, JNCC and DEFRA, available at:
4301 <http://jncc.defra.gov.uk/page-6189>.
- 4302 Jordan, C.F. (1969), "Derivation of leaf area index from quality of light on the forest
4303 floor", *Ecology*, Vol. 50, pp. 663–666.
- 4304 Kahmen, S. and Poschlod, P. (2008), "Effects of grassland management on plant
4305 functional trait composition", *Agriculture, Ecosystems & Environment*, Vol. 128
4306 No. 3, pp. 137–145.
- 4307 Knipling, E.B. (1970), "Physical and Physiological Basis for the Reflectance of Visible
4308 and Near-Infrared Radiation from Vegetation", *Remote Sensing of*
4309 *Environment*, Vol. 1, pp. 155–159.
- 4310 Kordecki, A., Palus, H., and Bal, A. (2016). "Practical Vignetting Correction Method
4311 for Digital Camera with Measurement of Surface Luminance Distribution",
4312 *Journal of VLSI Signal Processing Systems for Signal, Image, and Video*
4313 *Technology*, Vol. 10 No. 8, pp. 1417–24.

- 4314 Lamarque, P., Quétier, F. and Lavorel, S. (2011). "The diversity of the ecosystem
4315 services concept and its implications for their assessment and management",
4316 *Comptes Rendus Biologies*, Vol. 334 No. 5-6, pp. 441-449.
- 4317 Lausch, A., Bannehr, L., Beckmann, M., Boehm, C., Feilhauer, H., Hacker, J.M.,
4318 Heurich, M., *et al.* (2016), "Linking Earth Observation and taxonomic,
4319 structural and functional biodiversity: Local to ecosystem perspectives",
4320 *Ecological Indicators*, Vol. 70, pp. 317–339.
- 4321 Lausch, A., Bastian, O., Klotz, S., Leitão, P.J., Jung, A., Rocchini, D., Schaepman,
4322 M.E., *et al.* (2018), "Understanding and assessing vegetation health by in situ
4323 species and remote-sensing approaches", edited by Vihervaara, P. *Methods in
4324 Ecology and Evolution / British Ecological Society*, Vol. 9 No. 8, pp. 1799–
4325 1809.
- 4326 Lawley, V., Lewis, M., Clarke, K. and Ostendorf, B. (2016), "Site-based and remote
4327 sensing methods for monitoring indicators of vegetation condition: An
4328 Australian review", *Ecological Indicators*, Vol. 60, pp. 1273–1283.
- 4329 Li, I., Cheng, Y. B., Ustin, S., Hu, X. T. and Riaño, D (2008), "Retrieval of vegetation
4330 equivalent water thickness from reflectance using genetic algorithm (GA)-
4331 partial least squares (PLS) regression", *Advances in Space Research*, Vol.
4332 41, pp. 1755–1763.
- 4333 Li, X., Zhang, Y., Bao, Y., Luo, J., Jin, X., Xu, X., Song, X., *et al.* (2014), "Exploring
4334 the Best Hyperspectral Features for LAI Estimation Using Partial Least
4335 Squares Regression", *Remote Sensing*, Multidisciplinary Digital Publishing
4336 Institute, Vol. 6 No. 7, pp. 6221–6241.
- 4337 Li, Z., Wang, J., Tang, H., Huang, C., Yang, F., Chen, B., Wang, X., Xin, X. and Ge,
4338 Y (2016), "Predicting Grassland Leaf Area Index in the Meadow Steppes of
4339 Northern China: A Comparative Study of Regression Approaches and Hybrid
4340 Geostatistical Methods", *Remote Sensing*, Multidisciplinary Digital Publishing
4341 Institute, Vol. 8 No. 632, available at: doi:10.3390/rs8080632.
- 4342 Lillesand, T., Kiefer, R. W., Chipman, J. (2015), *Remote Sensing and Image
4343 Interpretation*, John Wiley and Sons, Hoboken, New Jersey, pp. 285–294.
- 4344 Liu, M., Wang, Z., Li, S., Lü, X., Wang, X. and Han, X. (2017), "Changes in specific
4345 leaf area of dominant plants in temperate grasslands along a 2500-km
4346 transect in northern China", *Scientific Reports*, Nature Publishing Group, Vol.
4347 7 No. 1, pp. 1–9.

- 4348 Loew, A., Bell, W., Brocca, L., Bulgin, C.E., Burdanowitz, J., Calbet, X., Donner, R.V.,
4349 *et al.* (2017), "Validation practices for satellite-based Earth observation data
4350 across communities: EO Validation", *Reviews of Geophysics*, Vol. 55 No. 3,
4351 pp. 779–817.
- 4352 Lu, S., Shimizu, Y., Ishii, J., Funakoshi, S., Washitani, I. and Omasa, K. (2009),
4353 "Estimation of abundance and distribution of two moist tall grasses in the
4354 Watarase wetland, Japan, using hyperspectral imagery", *ISPRS Journal of*
4355 *Photogrammetry and Remote Sensing: Official Publication of the International*
4356 *Society for Photogrammetry and Remote Sensing*, Vol. 64 No. 6, pp. 674–
4357 682.
- 4358 Lucieer, A., Robinson, S.A. and Turner, D. (2011), "Unmanned aerial vehicle (UAV)
4359 remote sensing for hyperspatial terrain mapping of Antarctic moss beds based
4360 on structure from motion (SfM) point clouds", *34th International Symposium*
4361 *on Remote Sensing of Environment*.
- 4362 Lussem, U., Bolten, A., Menne, J., Gnyp, M.L. and Bareth, G. (2019), "Ultra-High
4363 Spatial Resolution Uav-Based Imagery To Predict Biomass In Temperate
4364 Grasslands", *ISPRS - International Archives of the Photogrammetry, Remote*
4365 *Sensing and Spatial Information Sciences*, Vol. XLII-2/W13, pp. 443–447.
- 4366 Lyu, X., Li, X., Gong, J., Wang, H., Dang, D., Dou, H., Li, S., *et al.* (2020),
4367 "Comprehensive Grassland Degradation Monitoring by Remote Sensing in
4368 Xilinhot, Inner Mongolia, China", *Sustainability: Science Practice and Policy*,
4369 Multidisciplinary Digital Publishing Institute, Vol. 12 No. 3682, pp. 1-18.
- 4370 Maccherone, B. (2021). MODIS (Moderate Resolution Imaging Spectrometer).
4371 Available: <https://modis.gsfc.nasa.gov/>. Last accessed 05/09/2021.
- 4372 Mansour, K., Mutanga, O., Adam, E. and Abdel-Rahman, E.M. (2016), "Multispectral
4373 remote sensing for mapping grassland degradation using the key indicators of
4374 grass species and edaphic factors", *Geocarto International*, Taylor & Francis,
4375 Vol. 31 No. 5, pp. 477–491.
- 4376 Marsett, R.C., Qi, J., Heilman, P., Biedenbender, S.H., Carolyn Watson, M., Amer, S.,
4377 Wertz, M., *et al.* (2006), "Remote Sensing for Grassland Management in the
4378 Arid Southwest", *Rangeland Ecology & Management*, Vol. 59 No. 5, pp. 530–
4379 540.
- 4380 Masek, J.G. (2021). The Thematic Mapper. Available:
4381 <https://landsat.gsfc.nasa.gov/landsat-4-5/tm>. Last accessed 05/09/2021.

- 4382 Mathews, A.J. and Jensen, J.L.R. (2013), “Visualizing and Quantifying Vineyard
4383 Canopy LAI Using an Unmanned Aerial Vehicle (UAV) Collected High Density
4384 Structure from Motion Point Cloud”, *Remote Sensing*, Multidisciplinary Digital
4385 Publishing Institute, Vol. 5 No. 5, pp. 2164–2183.
- 4386 Mevik, B.H., Wehrens, R., Liland, K.H. and Hiemstra, P. (2019), *Pls Package: Partial*
4387 *Least Squares and Principal Component Regression. R Package Version*
4388 *2.7.2*, available at: <http://mevik.net/work/software/pls.html>.
- 4389 Meyer D, Dimitriadou E, Hornik E, Weingessel A, Leisch F, Chang C, Lin C. (2019),
4390 *Package “e1071”*, available at: [https://cran.r-](https://cran.r-project.org/web/packages/e1071/e1071.pdf)
4391 [project.org/web/packages/e1071/e1071.pdf](https://cran.r-project.org/web/packages/e1071/e1071.pdf).
- 4392 Michez, A., Lejeune, P., Bauwens, S., Herinaina, A.A.L., Blaise, Y., Castro Muñoz,
4393 E., Lebeau, F., *et al.* (2019), “Mapping and Monitoring of Biomass and
4394 Grazing in Pasture with an Unmanned Aerial System”, *Remote Sensing*,
4395 Multidisciplinary Digital Publishing Institute, Vol. 11 No. 473, pp. 1-14.
- 4396 Mirik, M. and Ansley, R.J. (2012), “Utility of Satellite and Aerial Images for
4397 Quantification of Canopy Cover and Infilling Rates of the Invasive Woody
4398 Species Honey Mesquite (*Prosopis Glandulosa*) on Rangeland”, *Remote*
4399 *Sensing*, Molecular Diversity Preservation International, Vol. 4 No. 7, pp.
4400 1947–1962.
- 4401 Möckel, T., Dalmayne, J., Prentice, H.C., Eklundh, L., Purschke, O., Schmidlein, S.
4402 and Hall, K. (2014), “Classification of Grassland Successional Stages Using
4403 Airborne Hyperspectral Imagery”, *Remote Sensing*, Multidisciplinary Digital
4404 Publishing Institute, Vol. 6 No. 8, pp. 7732–7761.
- 4405 Molinari, N.A. and D’Antonio, C.M. (2014), “Structural, compositional and trait
4406 differences between native- and non-native-dominated grassland patches”,
4407 edited by Wilson, S. *Functional Ecology*, Vol. 28 No. 3, pp. 745–754.
- 4408 Neely, C., Bunning, S., Wilkes, A. (2009), *Review of Evidence on Drylands Pastoral*
4409 *Systems and Climate Change; Implications and Opportunities for Mitigation*
4410 *and Adaptation*, No. 8, Food and Agricultural Organisation.
- 4411 Nelder, J.A. and Wedderburn, R.W.M. (1972), “Generalized Linear Models”, *Journal*
4412 *of the Royal Statistical Society. Series A* , Vol. 135 No. 3, pp. 370–384.
- 4413 Netzer, M., Chalmers, J. and Harris, N. (2011), *The Role of Remote Sensing in*
4414 *Monitoring Biofuel Feedstock and Land Use Changes*, Winrock International.

- 4415 Ni, J. (2004), "Estimating net primary productivity of grasslands from field biomass
4416 measurements in temperate northern China", *Plant Ecology*. Vol. 174, pp.
4417 217–234.
- 4418 Noss, R.F. (1990), "Indicators for Monitoring Biodiversity: A Hierarchical Approach",
4419 *Conservation Biology*. Vol. 4 No 4, pp. 355-364.
- 4420 Olofsson, P. and Eklundh, L. (2007), "Estimation of absorbed PAR across
4421 Scandinavia from satellite measurements. Part II: Modelling and evaluating
4422 the fractional absorption", *Remote Sensing of Environment*, Elsevier, Vol. 110
4423 No. 2, pp. 240–251.
- 4424 Pakeman, R.J., Eastwood, A. and Scobie, A. (2011), "Leaf dry matter content as a
4425 predictor of grassland litter decomposition: a test of the 'mass ratio
4426 hypothesis'", *Plant and Soil*, Vol. 342 No. 1, pp. 49–57.
- 4427 Pasolli, L., Asam, S., Castelli, M., Bruzzone, L., Wohlfahrt, G., Zebisch, M. and
4428 Notarnicola, C. (2015), "Retrieval of Leaf Area Index in mountain grasslands
4429 in the Alps from MODIS satellite imagery", *Remote Sensing of Environment*,
4430 Vol. 165, pp. 159–174.
- 4431 Planet Labs (2021), "Planet Monitoring", available at:
4432 <https://www.planet.com/products/monitoring/> (last accessed 18 September
4433 2021).
- 4434 Poschlod, P. and WallisDeVries, M. (2002), "The historical and socioeconomic
4435 perspective of calcareous grasslands - Lessons from the distant and recent
4436 past", *Biological Conservation*, Vol. 104 No. 3, pp. 361–376.
- 4437 Price, J.C. (1994), "How unique are spectral signatures?" *Remote Sensing of*
4438 *Environment*. Vol 49, pp. 181-186.
- 4439 Polley, H. W., Yang, C., Wilsey, B. J. and Fay, P. A. (2020), "Spectrally derived
4440 values of community leaf dry matter content link shifts in grassland
4441 composition with change in biomass production", *Remote Sensing in Ecology*
4442 *and Conservation*, Vol 6 No 3, available at: <https://doi.org/10.1002/rse2.145>.
- 4443 Polley, H. W., Collins, H. P. and Fay, P. A. (2022), "Community leaf dry matter
4444 content predicts plant production in simple and diverse grassland."
4445 *Ecosphere*. Vol 13 No 5, available at:
4446 <https://esajournals.onlinelibrary.wiley.com/doi/epdf/10.1002/ecs2.4076>.
- 4447 Psomas, A., Kneubühler, M., Huber, S., Itten, K. and Zimmermann, N.E. (2011),
4448 "Hyperspectral remote sensing for estimating aboveground biomass and for

- 4449 exploring species richness patterns of grassland habitats”, *International*
4450 *Journal of Remote Sensing*, Taylor & Francis, Vol. 32 No. 24, pp. 9007–9031.
- 4451 Punalekar, S.M., Verhoef, A., Quaife, T.L., Humphries, D., Bermingham, L. and
4452 Reynolds, C.K. (2018), “Application of Sentinel-2A data for pasture biomass
4453 monitoring using a physically based radiative transfer model”, *Remote*
4454 *sensing of environment*, Vol. 218, pp. 207–220.
- 4455 Pywell, R.F., Heard, M.S., Woodcock, B.A., Hinsley, S., Ridding, L., Nowakowski, M.
4456 and Bullock, J.M. (2015), “Wildlife-friendly farming increases crop yield:
4457 evidence for ecological intensification”, *Proceedings of the Royal Society B:*
4458 *Biological Sciences*, Royal Society, Vol. 282 No. 1816, pp. 1-8.
- 4459 Ramspek, C.L., Jager, K.J., Dekker, F.W., Zoccali, C. and van Diepen, M. (2021),
4460 “External validation of prognostic models: what, why, how, when and where?”,
4461 *Clinical Kidney Journal*, Vol. 14 No. 1, pp. 49–58.
- 4462 Random.org. (2019). *Sequence Generator*. Available: <https://www.random.org/>. Last
4463 accessed 26/12/2019.
- 4464 Razali, N.M. and Wah, Y.B. (2011), “Power comparisons of Shapiro-Wilk,
4465 Kolmogorov-Smirnov, Lilliefors and Anderson-Darling tests”, Vol. 1, pp. 21–
4466 33.
- 4467 Reid RS, Serneels S, Nyabenga M, Hanson, J. (2005), “The changing face of
4468 pastoral systems in grass dominated ecosystems of East Africa”, in Suttie Jm
4469 Reynolds Sg Batello (Ed.), *Grasslands of the World*, Food and Agricultural
4470 Organisation of the United Nations.
- 4471 Reimann, C., Filzmoser, P., Fabian, K., Hron, K., Birke, M., Demetriades, A., Dinelli,
4472 E., *et al.* (2012), “The concept of compositional data analysis in practice--total
4473 major element concentrations in agricultural and grazing land soils of Europe”,
4474 *The Science of the Total Environment*, Vol. 426, pp. 196–210.
- 4475 Reinermann, S., Asam, S. and Kuenzer, C. (2020) “Remote Sensing of Grassland
4476 Production and Management—A Review”, *Remote Sensing*, Vol.12 No. 12, p.
4477 1949.
- 4478 Ren, H. and Zhou, G. (2012), “Estimating senesced biomass of desert steppe in Inner
4479 Mongolia using field spectrometric data”, *Agricultural and Forest Meteorology*,
4480 Vol. 161, pp. 66–71.

- 4481 Ripley, B., Venables, B., Bates, DM., Hornik, K., Gebhardt, A. and Firth, D. (2019),
4482 *Package “MASS”*, available at: [https://cran.r-](https://cran.r-project.org/web/packages/MASS/MASS.pdf)
4483 [project.org/web/packages/MASS/MASS.pdf](https://cran.r-project.org/web/packages/MASS/MASS.pdf).
- 4484 Rodríguez-Ortega, T., Oteros-Rozas, E., Ripoll-Bosch, R., Tichit, M., Martín-López,
4485 B., Bernués, A. (2014) ‘Applying the ecosystem services framework to
4486 pasture-based livestock farming systems in Europe’, *Animal: an international*
4487 *journal of animal bioscience*, Vol. 8 No. 8, pp. 1361–1372.
- 4488 Rodwell, J.S. (1991), *British Plant Communities. Mires and Heaths*, No. Volume 2,
4489 Cambridge University Press.
- 4490 Rodwell, J.S. (1992), *British Plant Communities. Grassland and Montane*
4491 *Communities*, No. Volume 3. Cambridge University Press.
- 4492 Roelofsen, H.D., van Bodegom, P.M., Kooistra, L. and Witte, J.-P.M. (2014),
4493 “Predicting leaf traits of herbaceous species from their spectral
4494 characteristics”, *Ecology and Evolution*, Vol. 4 No. 6, pp. 706–719.
- 4495 Roelofsen, H.D., van Bodegom, P.M., Kooistra, L., van Amerongen, J.J. and Witte,
4496 J.-P.M. (2015), “An evaluation of remote sensing derived soil pH and average
4497 spring groundwater table for ecological assessments”, *International Journal of*
4498 *Applied Earth Observation and Geoinformation*, Vol. 43, pp. 149–159.
- 4499 Rossini, M., Migliavacca, M., Galvagno, M., Meroni, M., Cogliati, S., Cremonese, E.,
4500 Fava, F., *et al.* (2014), “Remote estimation of grassland gross primary
4501 production during extreme meteorological seasons”, *International Journal of*
4502 *Applied Earth Observation and Geoinformation*, Vol. 29, pp. 1–10.
- 4503 Roy, D.P., Zhang, H.K., Ju, J., Gomez-Dans, J.L., Lewis, P.E., Schaaf, C.B., Sun, Q.,
4504 *et al.* (2016), “A general method to normalize Landsat reflectance data to
4505 nadir BRDF adjusted reflectance”, *Remote Sensing of Environment*, Vol. 176,
4506 pp. 255–271.
- 4507 Royston, P. (1995), “Remark AS R94: A Remark on Algorithm AS181: The W test for
4508 Normality”, *Journal of the Royal Statistical Society*, Vol. 44 No. 4, pp. 547–
4509 551.
- 4510 Sakowska, K., Juszczak, R. and Gianelle, D. (2016), “Remote Sensing of Grassland
4511 Biophysical Parameters in the Context of the Sentinel-2 Satellite Mission”,
4512 *Journal of Sensors*, Hindawi, Vol. 2016, pp. 1-16. available at:
4513 <https://doi.org/10.1155/2016/4612809>.

- 4514 Salamí, E., Barrado, C. and Pastor, E. (2014), "UAV Flight Experiments Applied to
4515 the Remote Sensing of Vegetated Areas", *Remote Sensing*, Multidisciplinary
4516 Digital Publishing Institute, Vol. 6 No. 11, pp. 11051–11081.
- 4517 Schile, L.M., Byrd, K.B., Windham-Myers, L. and Kelly, M. (2013), "Accounting for
4518 non-photosynthetic vegetation in remote-sensing-based estimates of carbon
4519 flux in wetlands", *Remote Sensing Letters*, Taylor & Francis, Vol. 4 No. 6, pp.
4520 542–551.
- 4521 Schils, R., Velthof, G., Mucher, S., Hazeu, G., Oenema, O., de Wit, A. and Smit, A.
4522 (2013), *Current Methods to Estimate Grassland Production and Biological*
4523 *Fixation*, No. 2, Alterra, Wageningen.
- 4524 Schweider, M., Buddeberg, M., Kowalski, K., Pfoch, K., Bartsch, J., Bach, H., Pickert,
4525 J., Hostert, P. (2020), "Estimating Grassland Parameters from Sentinel-2: A
4526 Model Comparison Study", *Journal of Photogrammetry, Remote Sensing and*
4527 *Geoinformation Science*. Vol 88, pp. 379-390.
- 4528 Schweiger, A.K., Schütz, M., Risch, A.C., Kneubühler, M., Haller, R. and Schaepman,
4529 M.E. (2017), "How to predict plant functional types using imaging
4530 spectroscopy: linking vegetation community traits, plant functional types and
4531 spectral response", edited by Chisholm, R. *Methods in Ecology and Evolution*
4532 */ British Ecological Society*, Vol. 8 No. 1, pp. 86–95.
- 4533 Shapiro, S.S. and Wilk, M.B. (1965), "An analysis of variance test for normality
4534 (complete samples)", *Biometrika*, Narnia, Vol. 52 No. 3-4, pp. 591–611.
- 4535 Shen, L., Guo, Z. and Li, X. (2014), "Remote Sensing of Leaf Area Index (LAI) and a
4536 Spatiotemporally Parameterized Model for Mixed Grasslands", *International*
4537 *Journal of Applied Science and Technology*, Vol. 4 No. 1, pp. 46–61.
- 4538 Shipley, B. and Vu, T.-T. (2002), "Dry matter content as a measure of dry matter
4539 concentration in plants and their parts", *New Phytologist*. Vol. 153, pp. 359-
4540 364.
- 4541 Sibanda, M., Mutanga, O., Dube, T., Mothapo, M. C. and Mafongoya, P. L. (2019).
4542 Remote sensing equivalent water thickness of grass treated with different
4543 fertiliser regimes using resample HypsIRI and EnMAP data. *Physics and*
4544 *Chemistry of the Earth, Parts A/B/C*. Vol. 112, pp. 246-254.
- 4545 Silva et al. (2008), "LIFE and Europe's grasslands - restoring a forgotten habitat",
4546 *European Communities*.

- 4547 Smart, S., Goodwin, A., Wallace, H. and Jones, M. (2016), *MAVIS (Ver 1.03) User*
4548 *Manual*.
- 4549 Smart, S.M., Glanville, H.C., Blanes, M. del C., Mercado, L.M., Emmett, B.A., Jones,
4550 D.L., Cosby, B.J., *et al.* (2017), “Leaf dry matter content is better at predicting
4551 above-ground net primary production than specific leaf area”, edited by Field,
4552 K. *Functional Ecology*, Vol. 31 No. 6, pp. 1336–1344.
- 4553 Smith, M.D., Knapp, A.K. and Collins, S.L. (2009), “A framework for assessing
4554 ecosystem dynamics in response to chronic resource alterations induced by
4555 global change”, *Ecology*, Vol. 90 No. 12, pp. 3279–3289.
- 4556 Smith, P., House, J.I., Bustamante, M., Sobocká, J., Harper, R., Pan, G., West, P.C.,
4557 *et al.* (2016), “Global change pressures on soils from land use and
4558 management”, *Global Change Biology*, Vol. 22 No. 3, pp. 1008–1028.
- 4559 Souza, R., Buchhart, C., Heil, K., Plass, J., Padilla, F. M. and Schmidhalter, U.
4560 (2021), “Effect of Time of Day and Sky Conditions on Different Vegetation
4561 Indices Calculated from Active and Passive Sensors and Images Taken from
4562 UAV”, *Remote Sensing*, Vol 13, No. 9, available at:
4563 <https://doi.org/10.3390/rs13091691>
- 4564 Spagnuolo, O.S.B., Jarvey, J.C., Battaglia, M.J., Laubach, Z.M., Miller, M.E.,
4565 Holekamp, K.E. and Bourgeau-Chavez, L.L. (2020), “Mapping Kenyan
4566 Grassland Heights Across Large Spatial Scales with Combined Optical and
4567 Radar Satellite Imagery”, *Remote Sensing*, Multidisciplinary Digital Publishing
4568 Institute, Vol. 12 No. 1086, pp. 1-18.
- 4569 Stevens, C.J., Ceulemans, T., Hodgson, J.G., Jarvis, S., Grime, J.P. and Smart, S.M.
4570 (2016), “Drivers of vegetation change in grasslands of the Sheffield region,
4571 northern England, between 1965 and 2012/13”, edited by Hölzel, N. *Applied*
4572 *Vegetation Science*, Vol. 19 No. 2, pp. 187–195.
- 4573 Stewart, K.E.J., Bourn, N.A.D. and Thomas, J.A. (2001), “An evaluation of three quick
4574 methods commonly used to assess sward height in ecology”, *Journal of*
4575 *Applied Ecology*, Vol. 38, pp. 1148–1154.
- 4576 SVC. (2012), *SVC HR-1024i / SVC HR-768i User Manual*, Spectral Vista
4577 Corporation.
- 4578 Tao, X., Liang, S., He, T. and Jin, H., (2016), “Estimation of fraction of absorbed
4579 photosynthetically active radiation from multiple satellite data: Model

- 4580 development and validation”, *Remote sensing of environment*, Vol. 184, pp.
4581 539–557.
- 4582 Théau, J., Lauzier-Hudon, É., Aubé, L. and Devillers, N. (2021), “Estimation of forage
4583 biomass and vegetation cover in grasslands using UAV imagery”, *PLoS One*,
4584 Vol. 16 No. 1, pp. 1-18.
- 4585 Tilman, D., Reich, P. B. and Knops, J. M. H. (2006), “Biodiversity and ecosystem
4586 stability in a decade-long grassland experiment”, *Nature*, Vol. 441 No. 7093,
4587 pp. 629–632.
- 4588 Tucker, C.J. (1979), “Red and photographic infrared linear combinations for
4589 monitoring vegetation”, *Remote Sensing of Environment*, Vol. 8 No. 2, pp.
4590 127–150.
- 4591 Tucker, C.J. (1985), “Satellite Remote Sensing of Total Herbaceous Biomass
4592 Production in the Senegalese Sahel: 1980-1984”, *Remote Sensing of*
4593 *Environment*, Vol. 17, pp. 233–249.
- 4594 Vescovo, L., Wohlfahrt, G., Balzarolo, M., Pilloni, S., Sottocornola, M., Rodeghiero,
4595 M. and Gianelle, D. (2012), “New spectral vegetation indices based on the
4596 near-infrared shoulder wavelengths for remote detection of grassland
4597 phytomass”, *International Journal of Remote Sensing*, Vol. 33, No. 7,
4598 available at: <https://www.ncbi.nlm.nih.gov/pmc/articles/PMC3859895/>
- 4599 Veen, C.J.V.D., Van Der Veen, C.J. and Csatho, B.M. (2006), “Spectral
4600 Characteristics of Greenland Lichens”, *Géographie Physique et Quaternaire*.
4601 Vol. 59 No. 1, pp. 63-73.
- 4602 Viljanen, N., Honkavaara, E., Näsi, R., Hakala, T., Niemeläinen, O. and Kaivosoja, J.
4603 (2018), “A Novel Machine Learning Method for Estimating Biomass of Grass
4604 Swards Using a Photogrammetric Canopy Height Model, Images and
4605 Vegetation Indices Captured by a Drone”, *Collection FAO: Agriculture*,
4606 Multidisciplinary Digital Publishing Institute, Vol. 8 No. 70, pp. 1-28.
- 4607 Wang, R., Gamon, J.A., Cavender-Bares, J., Townsend, P.A. and Zygielbaum, A.I.
4608 (2018a), “The spatial sensitivity of the spectral diversity–biodiversity
4609 relationship: an experimental test in a prairie grassland”, *Ecological*
4610 *Applications*, Vol. 28 No. 2, pp. 541–556.
- 4611 Wang, R., Gamon, J.A., Schweiger, A.K., Cavender-Bares, J., Townsend, P.A.,
4612 Zygielbaum, A.I. and Kothari, S. (2018b), “Influence of species richness,

4613 evenness, and composition on optical diversity: A simulation study”, *Remote*
4614 *Sensing of Environment*, Vol. 211, pp. 218–228.

4615 Wang, R., Gamon, J.A., Emmerton, C.A., Springer, K.R., Yu, R. and Hmimina, G.
4616 (2020), “Detecting intra- and inter-annual variability in gross primary
4617 productivity of a North American grassland using MODIS MAIAC data”,
4618 *Agricultural and Forest Meteorology*, Vol. 281, pp. 1-12.

4619 Wang, S., Baum, A., Zarco-Tejada, P. J., Dam-Hansen, C., Thorseth, A., Bauer-
4620 Gottwein, P., Bandini, F. and Garcia, M. (2019), “Unmanned Aerial System
4621 multispectral mapping for low and variable solar irradiance conditions:
4622 Potential of tensor decomposition”, *ISPRS Journal of Photogrammetry and*
4623 *Remote Sensing*, Vol. 155, pp. 58-71, available at:
4624 <https://www.sciencedirect.com/science/article/abs/pii/S0924271619301583>

4625 Wang, Y., Yang, Z., Kootstra, G. and Khan, H. A. (2023), “The impact of variable
4626 illumination on vegetation indices and evaluation of illumination correction
4627 methods on chlorophyll content estimation using UAV imagery”, *Plant*
4628 *Methods*, Vol. 19, No. 1, available at: [https://doi.org/10.1186/s13007-023-](https://doi.org/10.1186/s13007-023-01028-8)
4629 [01028-8](https://doi.org/10.1186/s13007-023-01028-8)

4630 Wang, Z., Townsend, P.A., Schweiger, A.K., Couture, J.J., Singh, A., Hobbie, S.E.,
4631 Cavender-Bares, J. (2019), “Mapping foliar functional traits and their
4632 uncertainties across three years in a grassland experiment”, *Remote sensing*
4633 *of environment*, Vol. 221, pp. 405–416.

4634 Weiss, M., Baret, F., Smith, G.J., Jonckheere, I. and Coppin, P. (2004), “Review of
4635 methods for in situ leaf area index (LAI) determination: Part II. Estimation of
4636 LAI, errors and sampling”, *Agricultural and Forest Meteorology*, Vol. 121 No.
4637 1, pp. 37–53.

4638 Wellstein, C., Poschlod, P., Stefano, G.A.C., Campetella, G., Rosbakh, S., Canullo,
4639 R., Kreyling, J., *et al.* (2017), “Effects of extreme drought on specific leaf area
4640 of grassland species: A meta-analysis of experimental studies in temperate
4641 and sub-Mediterranean systems”, *Global Change Biology*, Vol. 23 No. 6, pp.
4642 2473–2481.

4643 Whitley, E. and Ball, J. (2002), “Statistics review 6: Nonparametric methods”, *Critical*
4644 *Care / the Society of Critical Care Medicine*, Vol. 6 No. 6, pp. 509–513.

4645 Wickham, H. (2016), *ggplot2: Elegant Graphics for Data Analysis*, available at:
4646 <https://ggplot2.tidyverse.org>.

- 4647 Wold, H. (1966), "Estimation of principal components and related models by iterative
4648 least squares", in Krishnaiah, P.R. (Ed.), *Multivariate Analysis*, Academic
4649 Press, New York, pp. 391–420.
- 4650 Wold, S., Sjöström, M. and Eriksson, L. (2001), "PLS-regression: a basic tool of
4651 chemometrics", *Chemometrics and Intelligent Laboratory Systems*. Vol. 58,
4652 pp. 109-130.
- 4653 Wylie, B.K., Meyer, D.J., Tieszen, L.L., Mannel, S. (2002), "Satellite mapping of
4654 surface biophysical parameters at the biome scale over the North American
4655 grasslands A case study", *Remote sensing of environment*, Vol. 79, pp. 266–
4656 278.
- 4657 Xu, B., Yang, X.C., Tao, W.G., Miao, J.M., Yang, Z., Liu, H.Q., Jin, Y.X., *et al.* (2013),
4658 "MODIS-based remote-sensing monitoring of the spatiotemporal patterns of
4659 China's grassland vegetation growth", *International Journal of Remote
4660 Sensing*, Taylor & Francis, Vol. 34 No. 11, pp. 3867–3878.
- 4661 Xu, D., Guo, X., Li, Z., Yang, X. and Yin, H. (2014), "Measuring the dead component
4662 of mixed grassland with Landsat imagery", *Remote Sensing of Environment*,
4663 Vol. 142, pp. 33–43.
- 4664 Xu, D. and Guo, X. (2015), "Some insights on grassland health assessment based on
4665 remote sensing", *Sensors*, Vol. 15 No. 2, pp. 3070–3089.
- 4666 Yang, X. and Guo, X. (2014), "Quantifying Responses of Spectral Vegetation Indices
4667 to Dead Materials in Mixed Grasslands", *Remote Sensing*, Vol. 6, pp. 4289–
4668 4304.
- 4669 Yao, X., Yao, X., Jia, W., Tian, Y., Ni, J., Cao, W. and Zhu, Y. (2013), "Comparison
4670 and intercalibration of vegetation indices from different sensors for monitoring
4671 above-ground plant nitrogen uptake in winter wheat", *Sensors*. Vol. 13 No. 3,
4672 pp. 3109–3130.
- 4673 Zaman, B., Jensen, A.M. and McKee, M. (2011), "Use of high-resolution multispectral
4674 imagery acquired with an autonomous unmanned aerial vehicle to quantify the
4675 spread of an invasive wetlands species", *2011 IEEE International Geoscience
4676 and Remote Sensing Symposium*, available at:
4677 <https://doi.org/10.1109/igarss.2011.6049252>.
- 4678 Zarco-Tejada, P.J., González-Dugo, V. and Berni, J.A.J. (2012), "Fluorescence,
4679 temperature and narrow-band indices acquired from a UAV platform for water

4680 stress detection using a micro-hyperspectral imager and a thermal camera”,
4681 *Remote Sensing of Environment*, Vol. 117, pp. 322–337.

4682 Zhang, M., Yuan, X. and Otkin, J.A. (2020), “Remote sensing of the impact of flash
4683 drought events on terrestrial carbon dynamics over China”, *Carbon Balance
4684 and Management*, Vol. 15 No. 20, pp. 1-11.

4685 Zhao, F., Xu, B., Yang, X., Jin, Y., Li, J., Xia, L., Chen, S., *et al.* (2014), “Remote
4686 Sensing Estimates of Grassland Aboveground Biomass Based on MODIS Net
4687 Primary Productivity (NPP): A Case Study in the Xilingol Grassland of
4688 Northern China”, *Remote Sensing*, Vol. 6, pp. 5368–5386.

4689 Zhao, K., Valle, D., Popescu, S., Zhang, X. and Mallick, B. (2013), “Hyperspectral
4690 remote sensing of plant biochemistry using Bayesian model averaging with
4691 variable and band selection”, *Remote Sensing of Environment*, Vol. 132, pp.
4692 102-119.

4693

4694

4695

4696

4697

4698

4699

4700

4701

4702

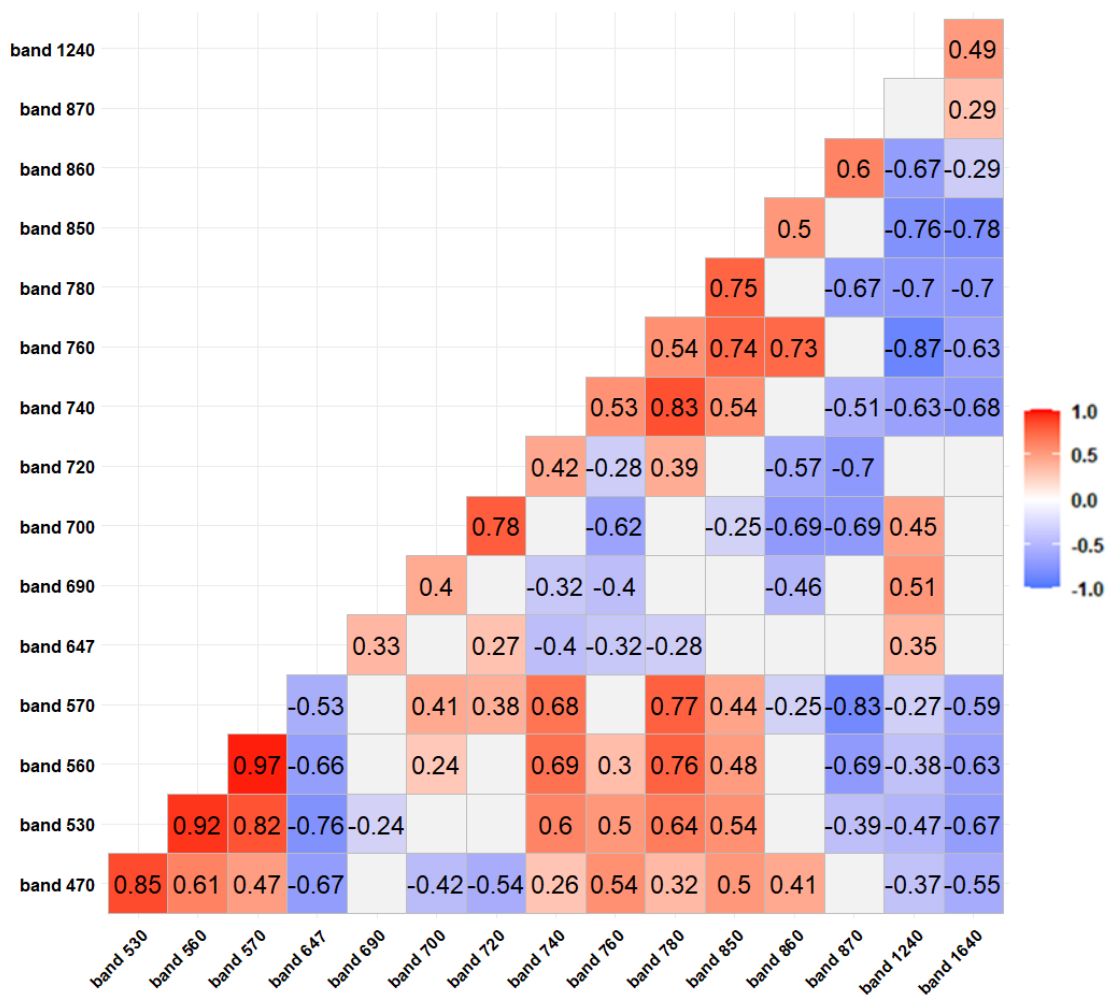
4703

4704

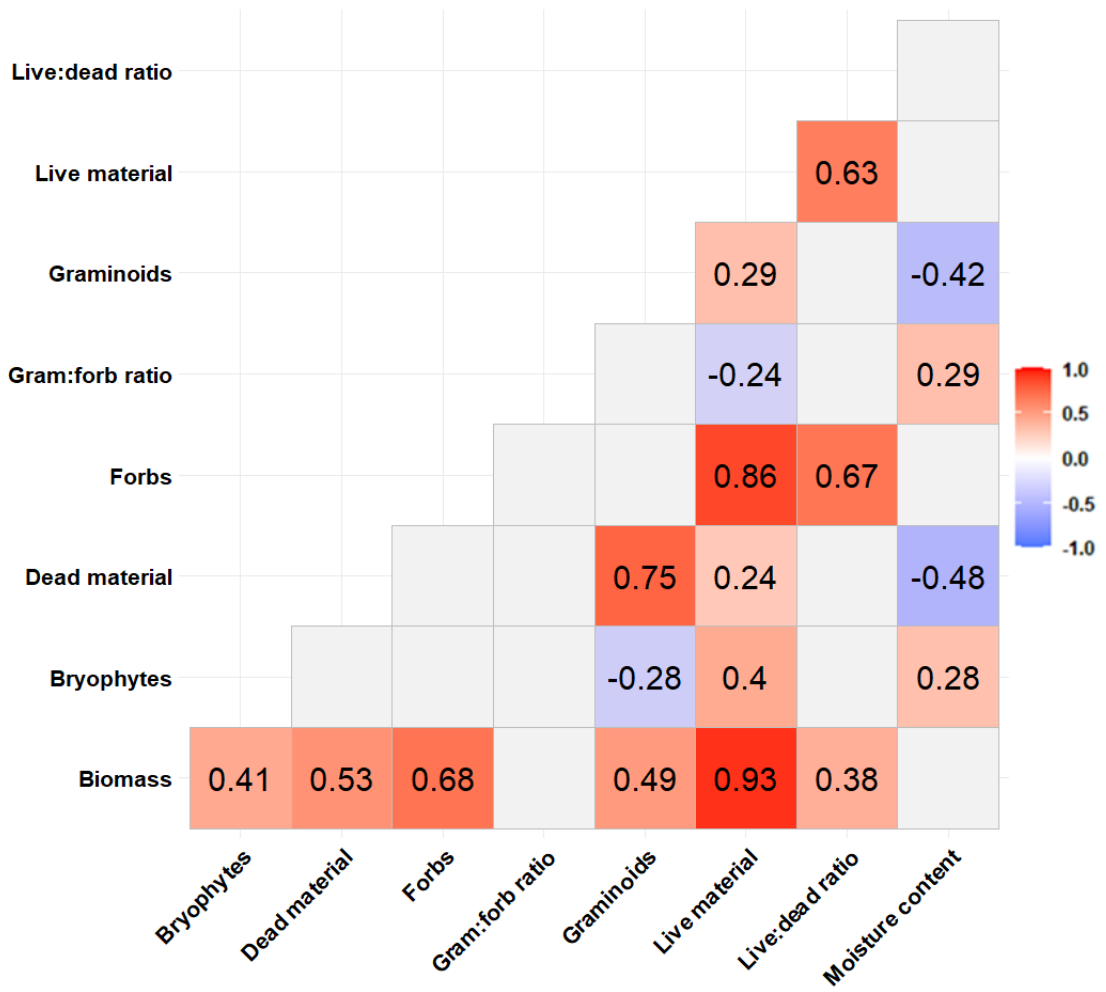
4705 **Appendix**

4706

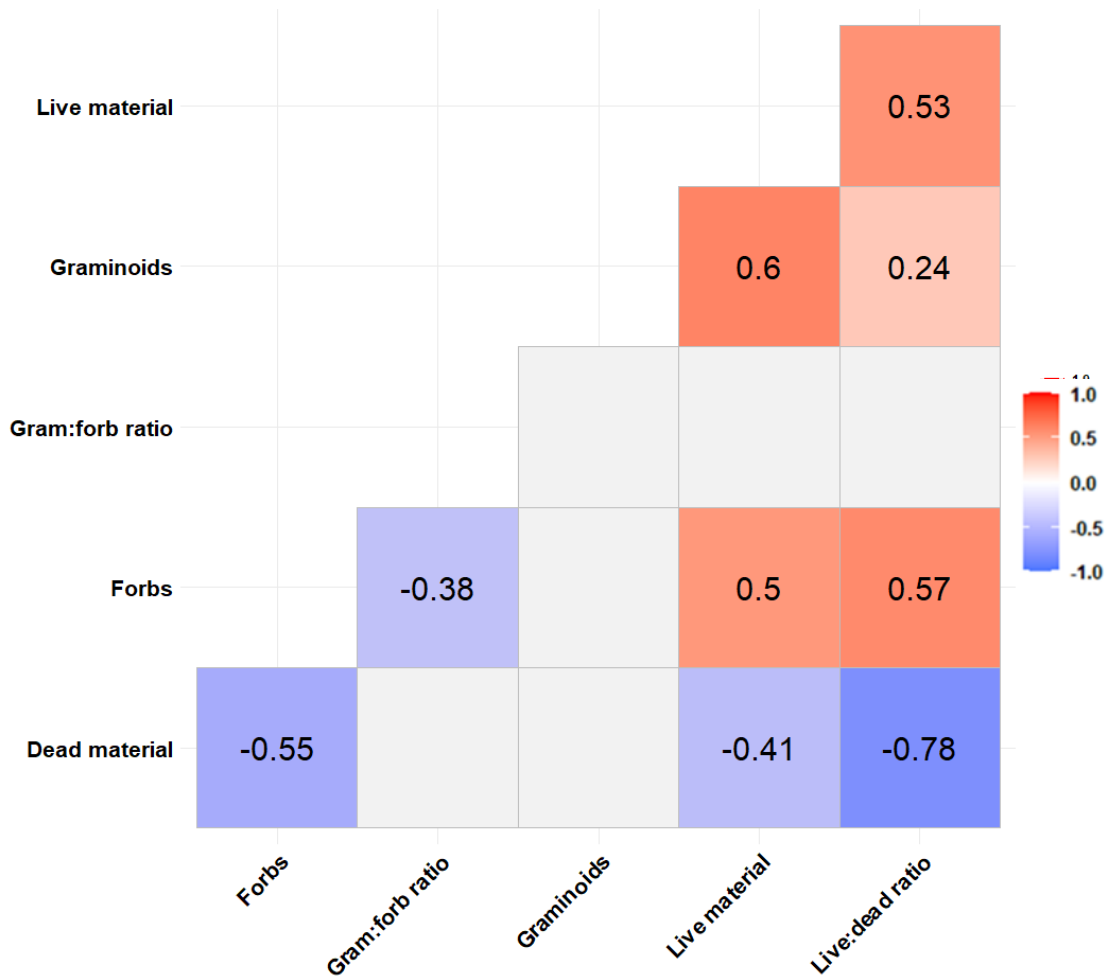
4707 **Correlation matrices**



4708



4709

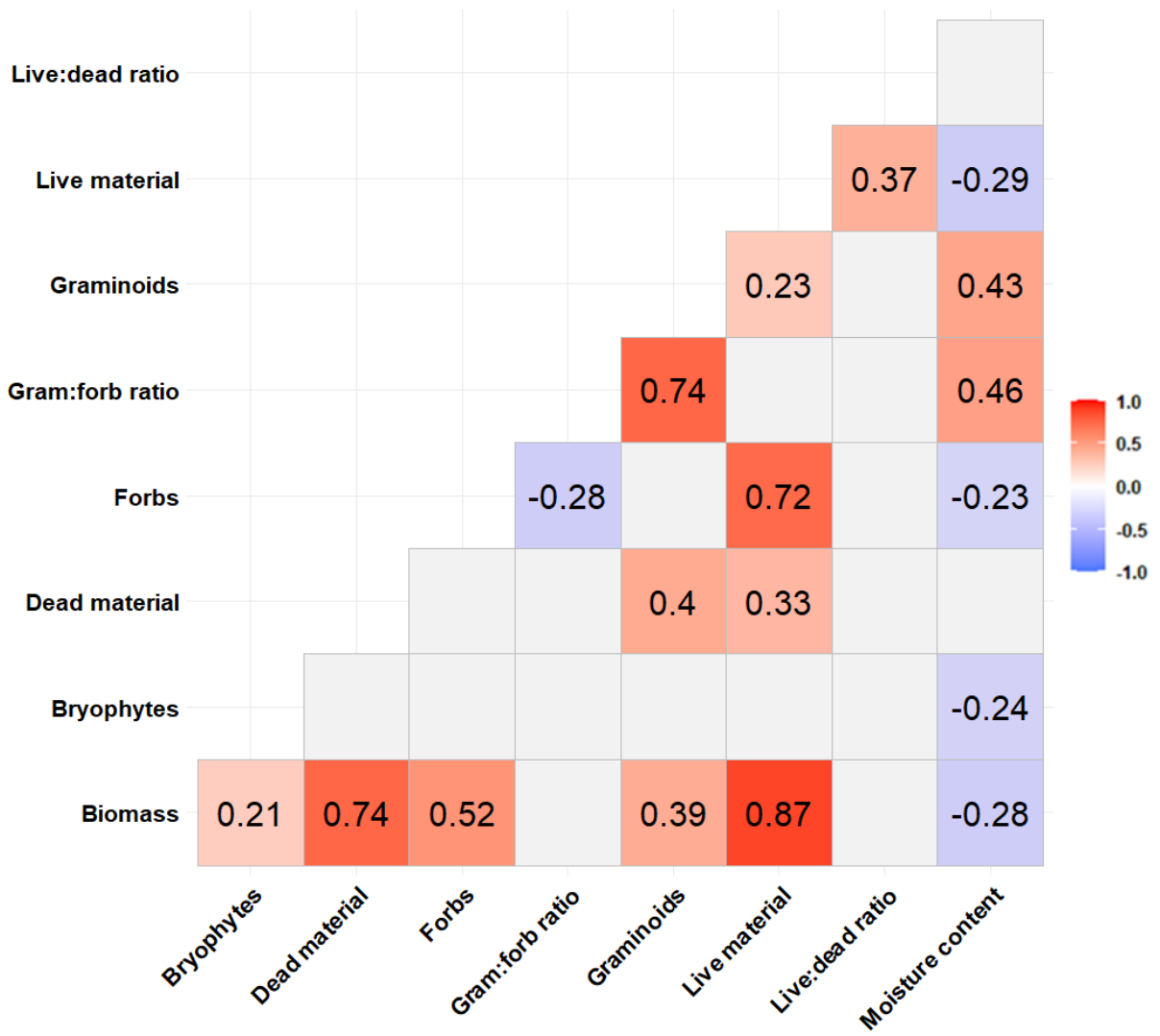


4710

4711 *Appendix Figure 1: Correlation matrices between predictors used in PLSR modelling*
 4712 *a) spectral bands, b) mass-based grassland variables and c) % cover-based*
 4713 *grassland variables. Correlation coefficients that are not statistically significant ($p >$*
 4714 *0.05) are not included. The data used to for analysis were collected across seven*
 4715 *grasslands during the summer season ($n=70$). The correlation matrix for the spectral*
 4716 *bands from the CROPSCAN (Appendix Figure 1a) indicated statistically significant*
 4717 *strong correlations between bands within each of the VIS (390-700nm) and NIR (701-*
 4718 *870nm) regions of the spectrum. There are also significant strong negative*
 4719 *correlations between NIR bands and SWIR bands (1240 and 1640nm). When using*
 4720 *mass-based grassland variables (Appendix Figure 1b), live material mass was*
 4721 *strongly correlated with biomass and forbs mass. When using % cover-based*
 4722 *variables (Appendix Figure 1c), dead material cover was negatively correlated with*
 4723 *live:dead ratio cover with a value of -0.78.*

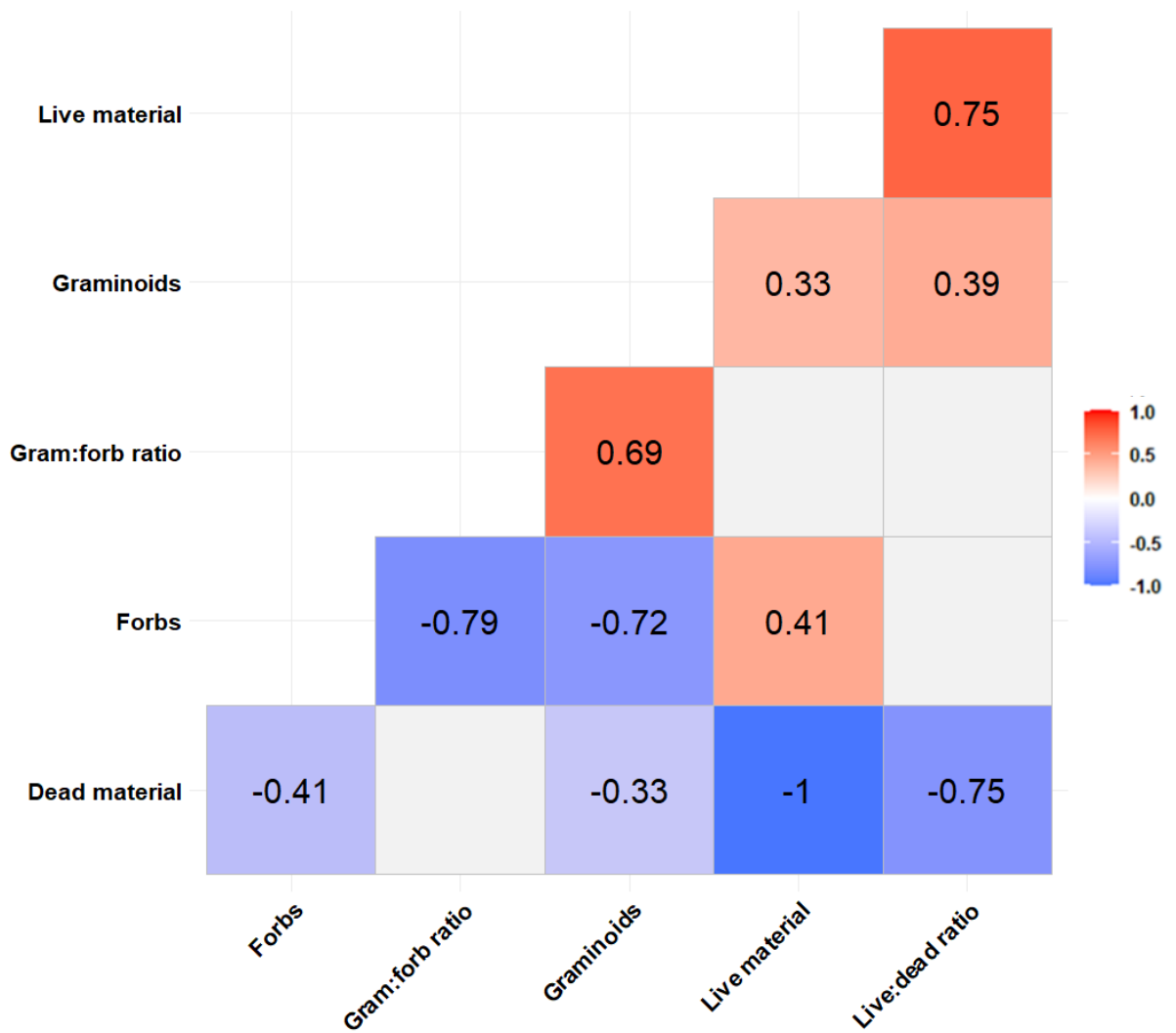
4724

4725



4728

4729

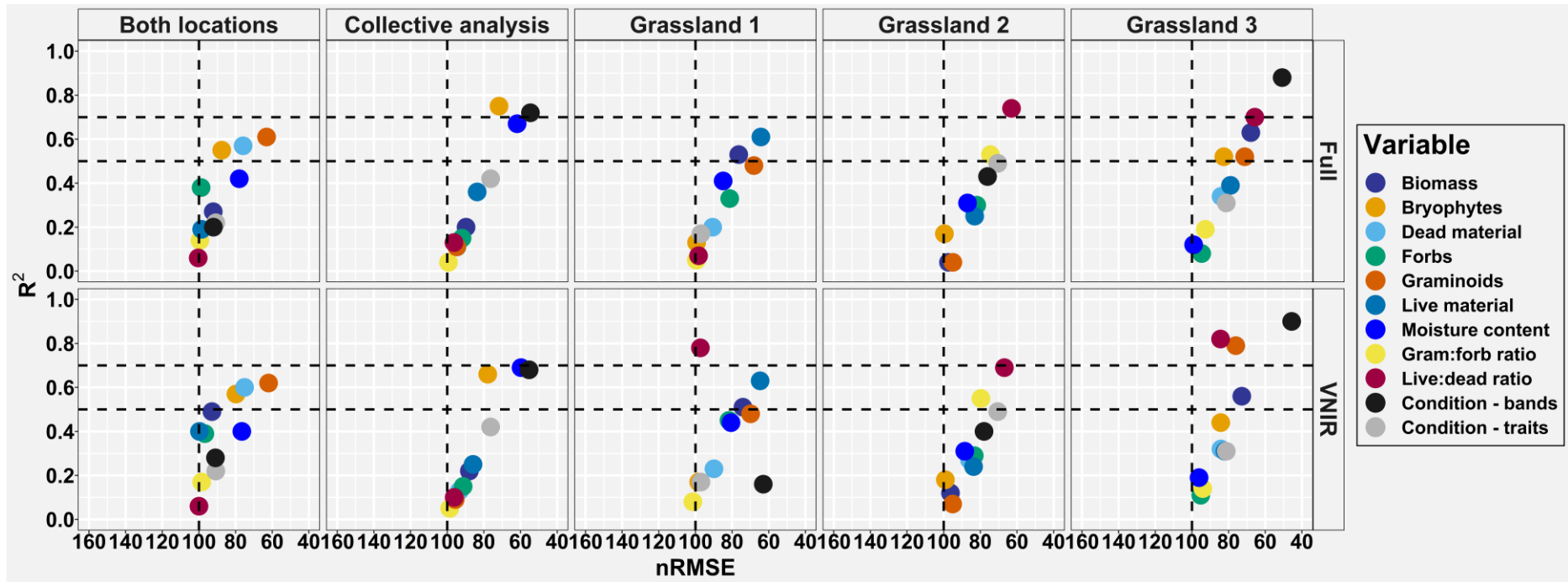


4730

4731 *Appendix Figure 2: Correlation matrices between predictors used in PLSR modelling*
 4732 *a) spectral bands, b) mass-based grassland variables and c) % cover-based*
 4733 *grassland variables. Correlation coefficients that are not statistically significant ($p >$*
 4734 *0.05) are blanked out. The correlation matrix for the spectral bands from the*
 4735 *CROPSCAN (Appendix Figure 2a) emulated those of Appendix Figure 2a; there were*
 4736 *statistically significant strong correlations between bands within the VIS and NIR*
 4737 *regions of the spectrum and there are also significant negative correlations between*
 4738 *some NIR and SWIR bands. When using grassland variables; the only significant r*
 4739 *values were between biomass and live material when using mass-based variables*
 4740 *(Appendix Figure 2b), and live material and dead material when using cover-based*
 4741 *variables (Appendix Figure 2c).*

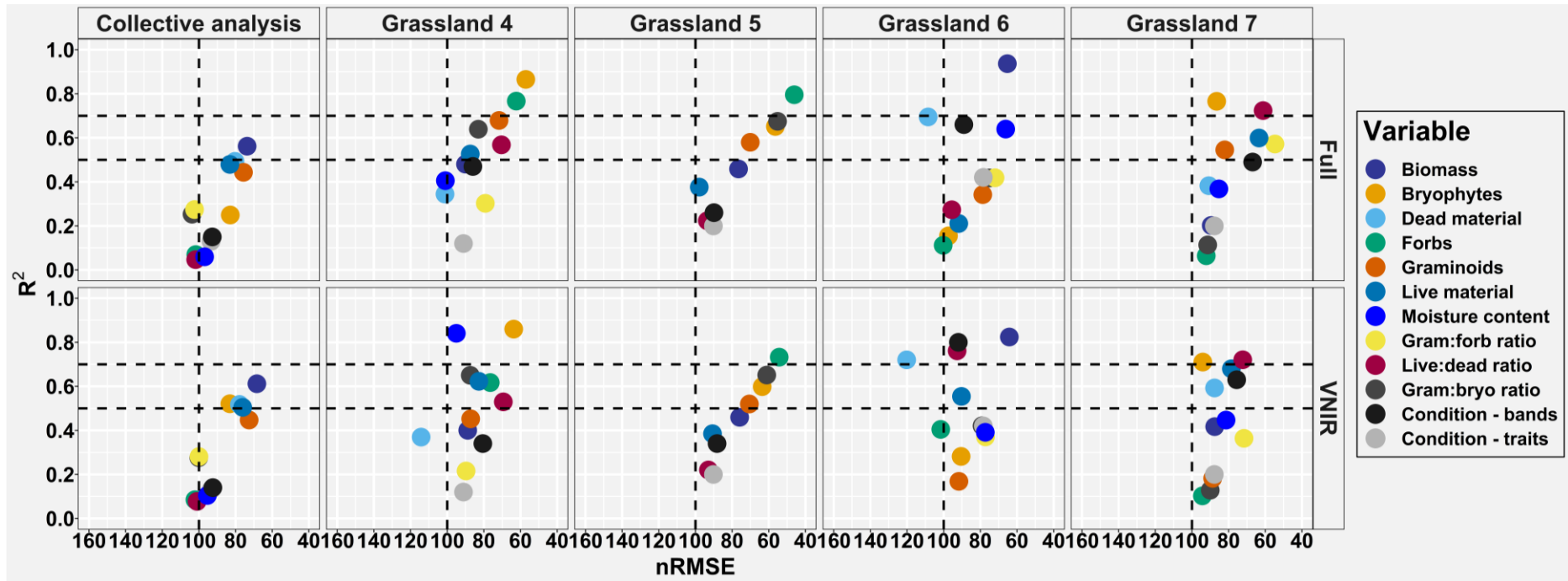
4742

4743 Chapter 4 full results

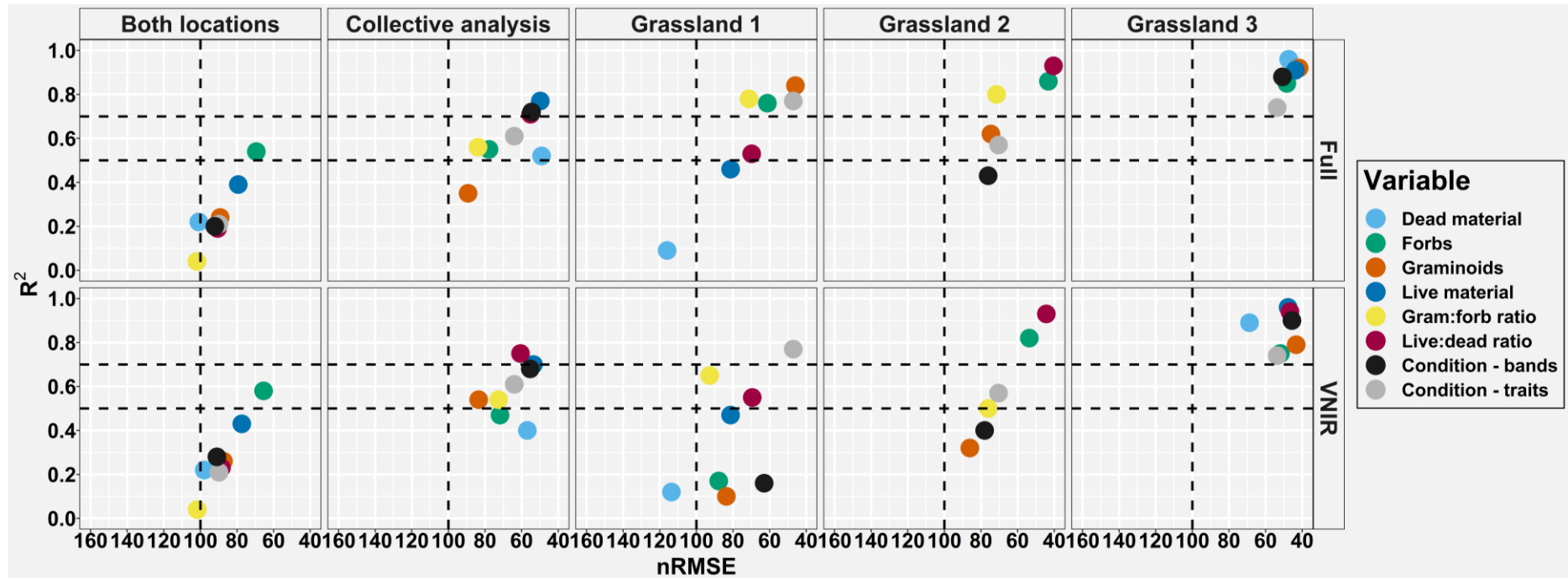


4744

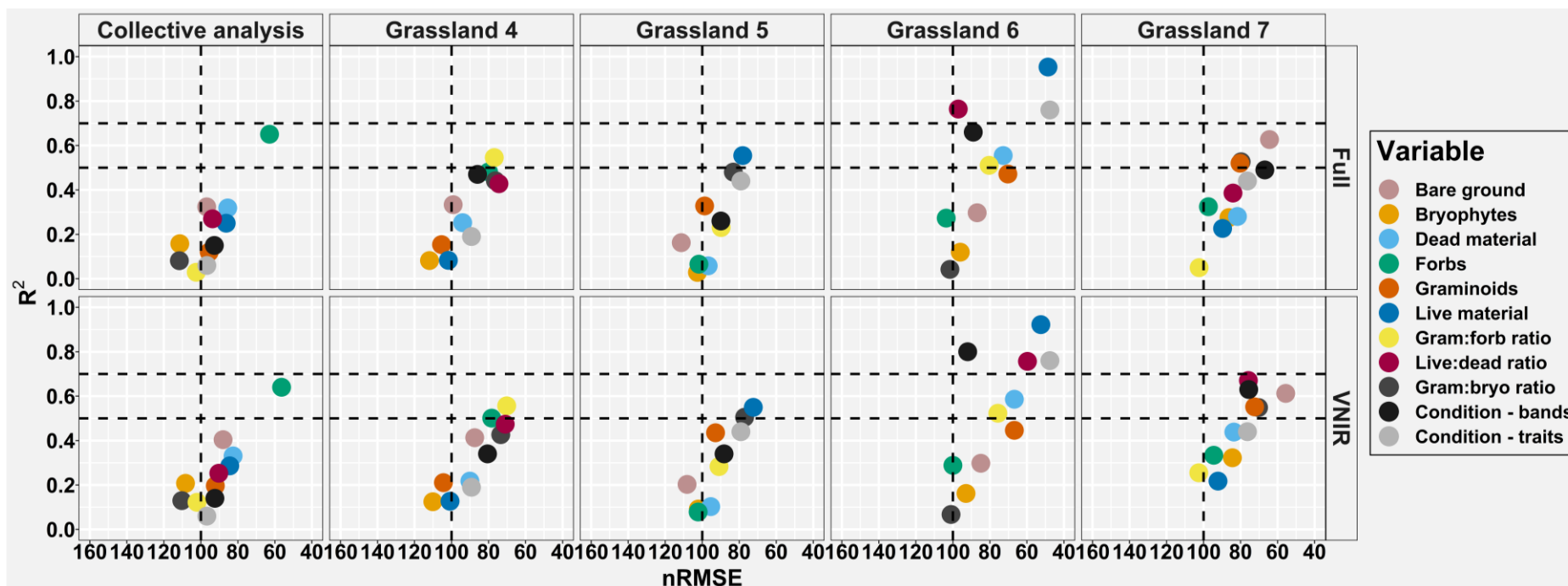
4745



4746



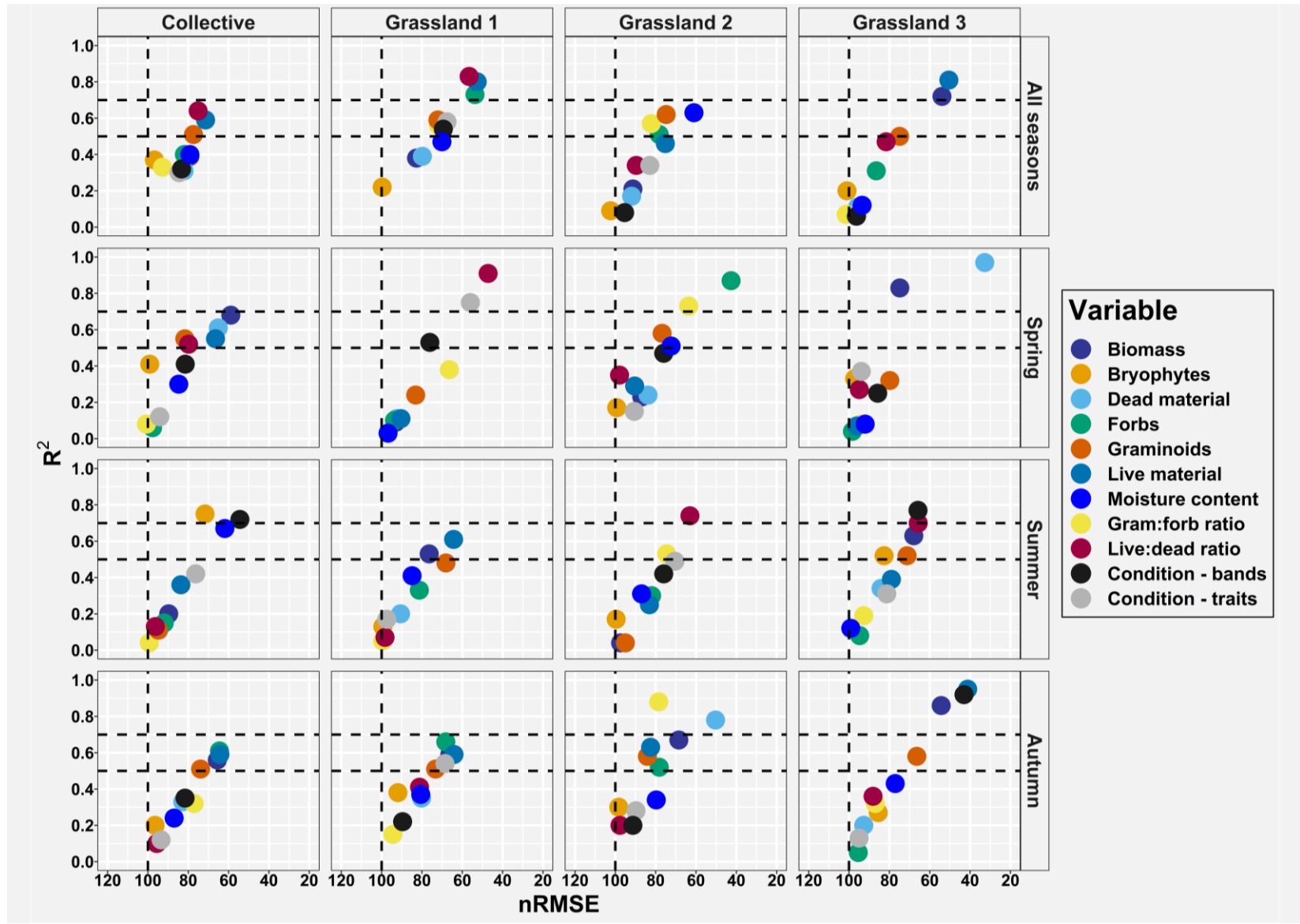
4747

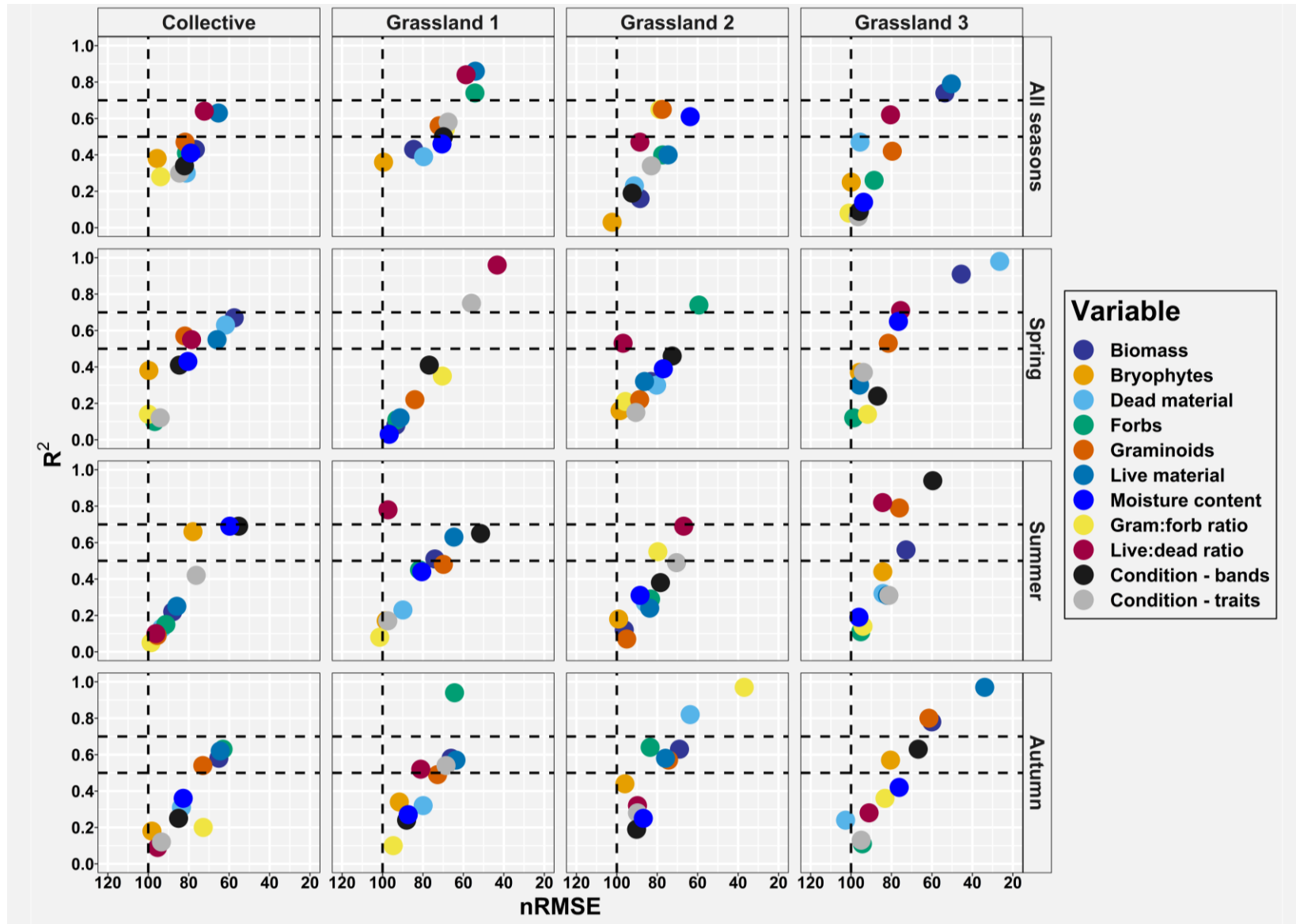


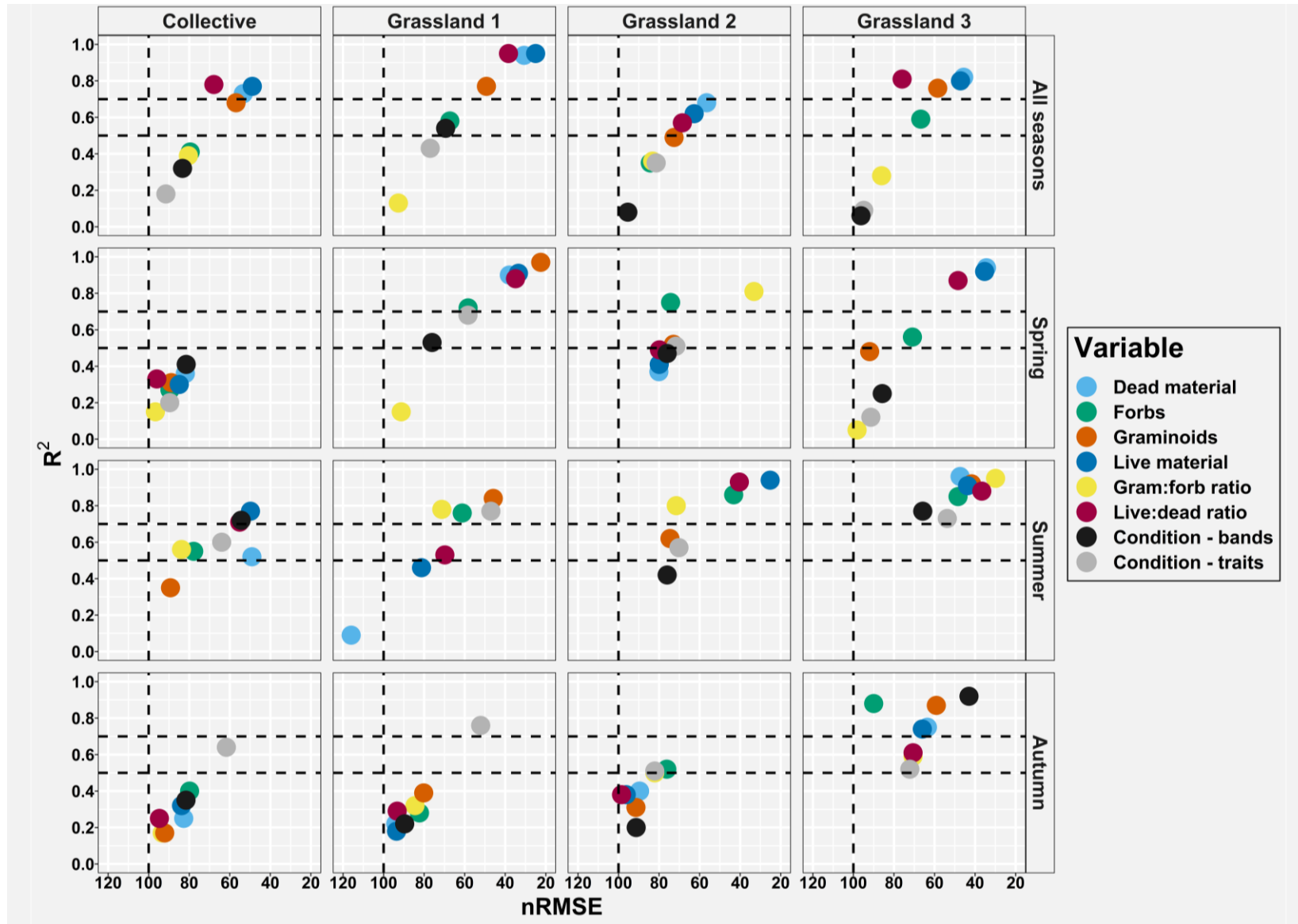
4748

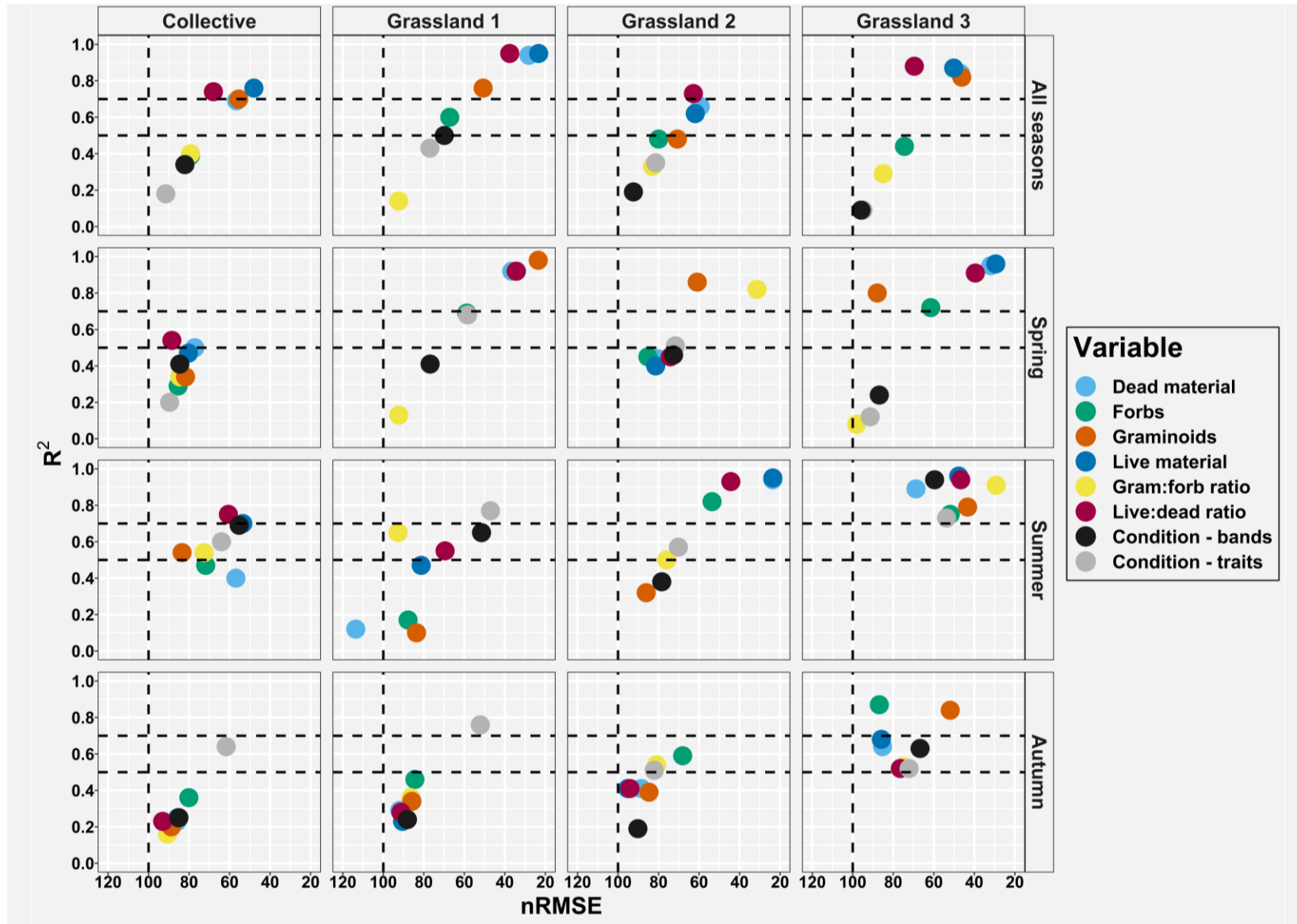
4749 *Appendix Figure 3: Plots for results of 426 PLSR regressions, each of which represent the median R^2 and nRMSE values of the iterated model*
 4750 *runs, where (i) spectral data (either FULL or VNIR) were used to predict grassland variables (coloured dots) and CSM based condition (black*
 4751 *dot) and (ii) grassland variables were used to predict CSM based condition (white dot). Panels a and b show results for mass based analysis*
 4752 *for Parsonage and Ingleborough respectively, c and d for % cover based analysis for Parsonage and Ingleborough respectively.*

4753

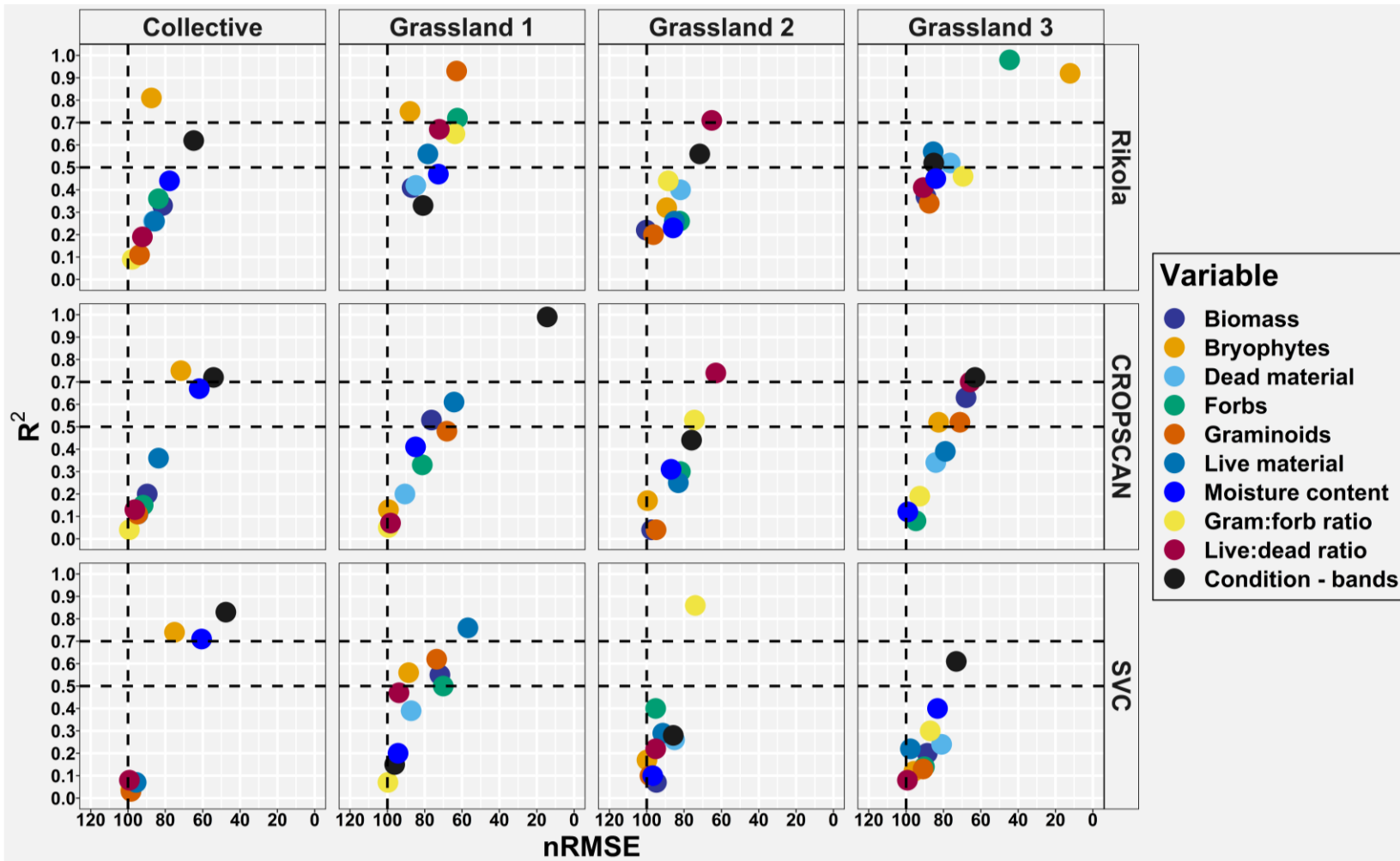


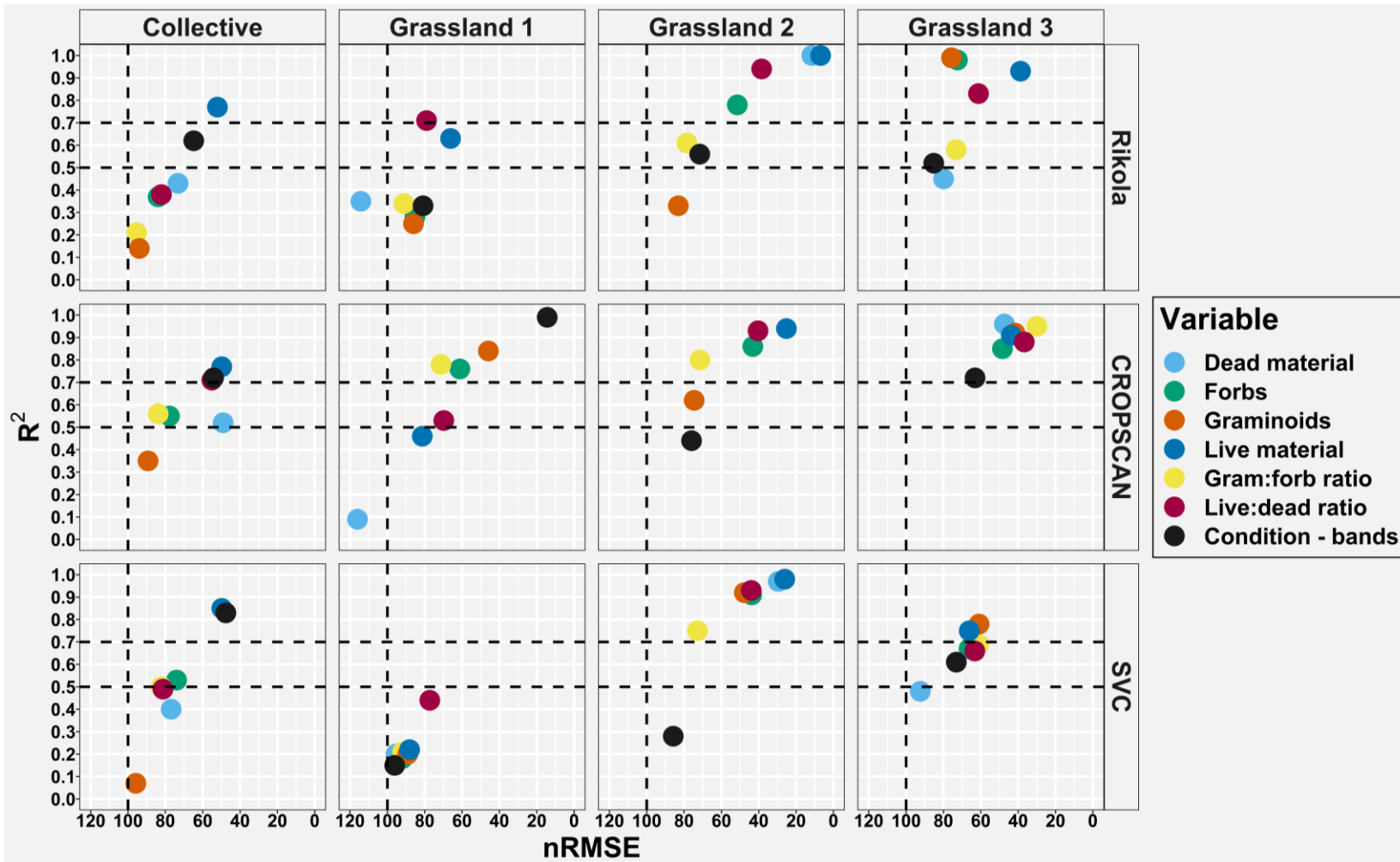






4759 *Appendix Figure 4: Median results of all iterated model runs where spectral data were used to predict CSM-condition and grassland variables*
4760 *for each of the three seasons (n = 10 or 30) and for all seasons (n = 30 or 90). Also included are the results of predicting CSM-condition using*
4761 *grassland variables as predictors. Panels a and b show results for mass based analysis (FULL and VNIR respectively), and panels c and d for*
4762 *% cover based analysis (FULL and VNIR respectively).*





4765

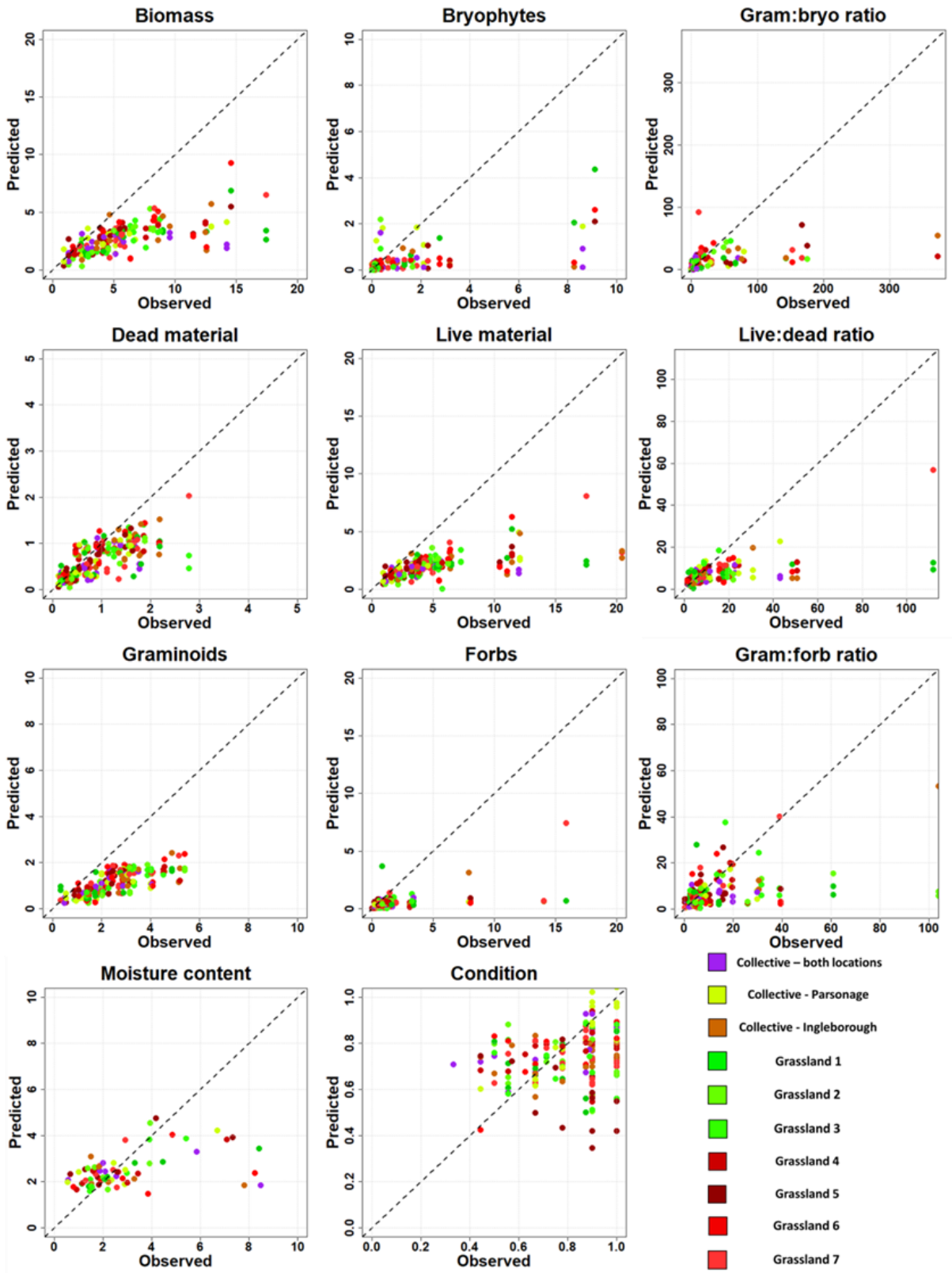
4766

4767

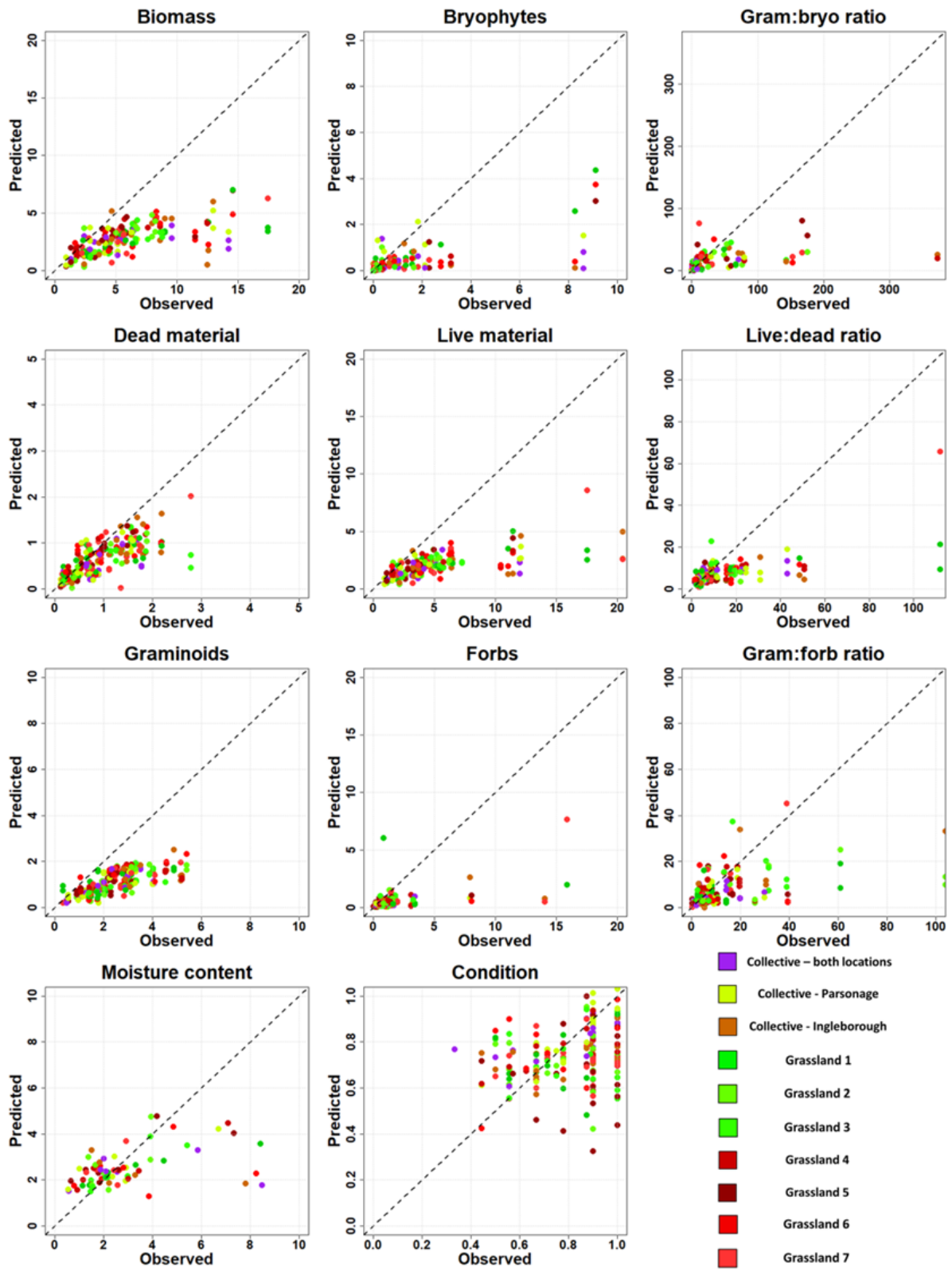
4768

4769 *Appendix Figure 5: Median results of iterated model runs where spectral data from three different devices were used to predict grassland*
4770 *variables and CSM-condition for all grasslands collectively (n = 30) or single sites (n = 10). Panel a shows results for mass based analysis and*
4771 *panel b shows results for cover based analysis.*

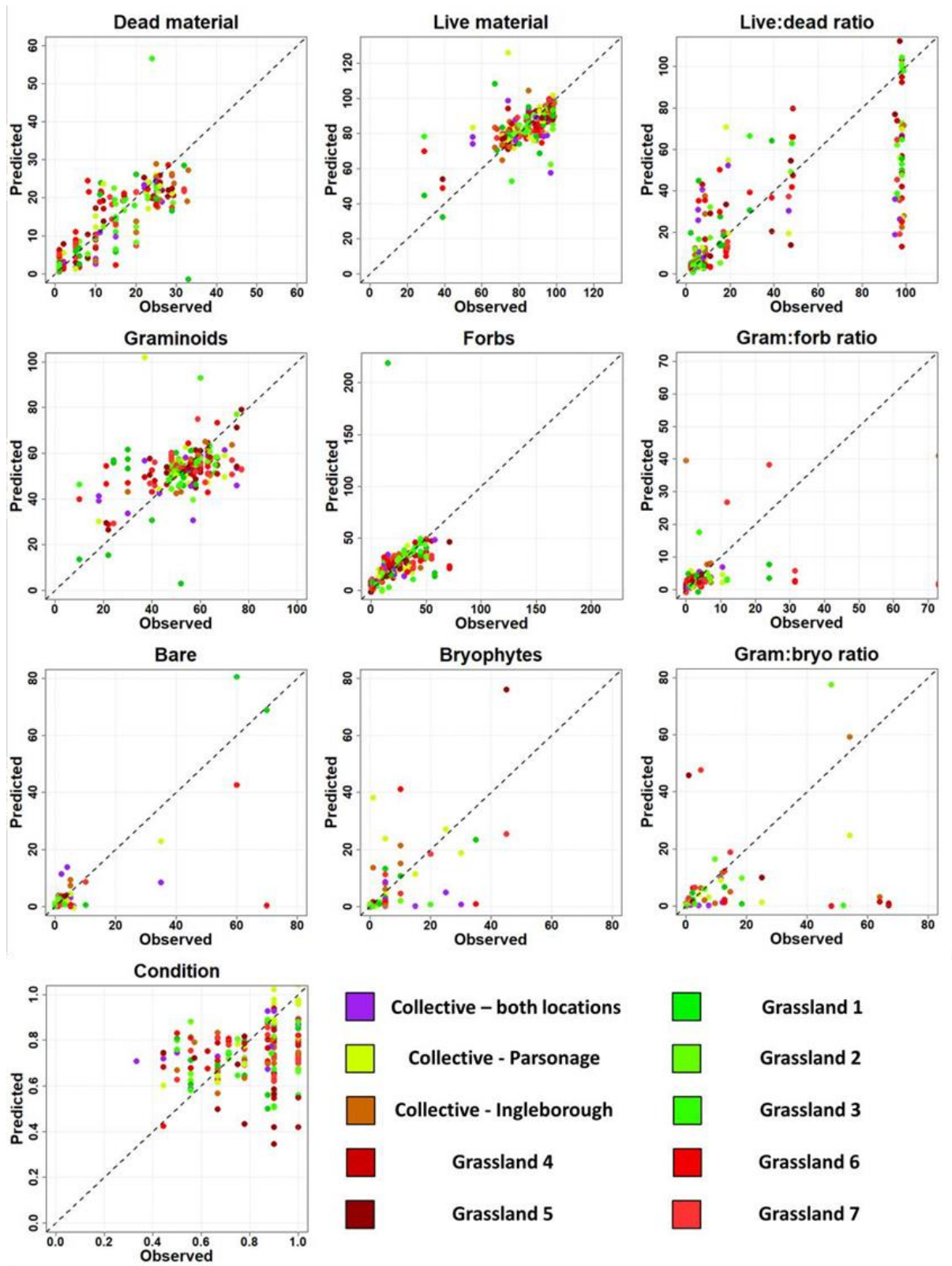
4772 Observations vs. predictions – Chapter 4



4773



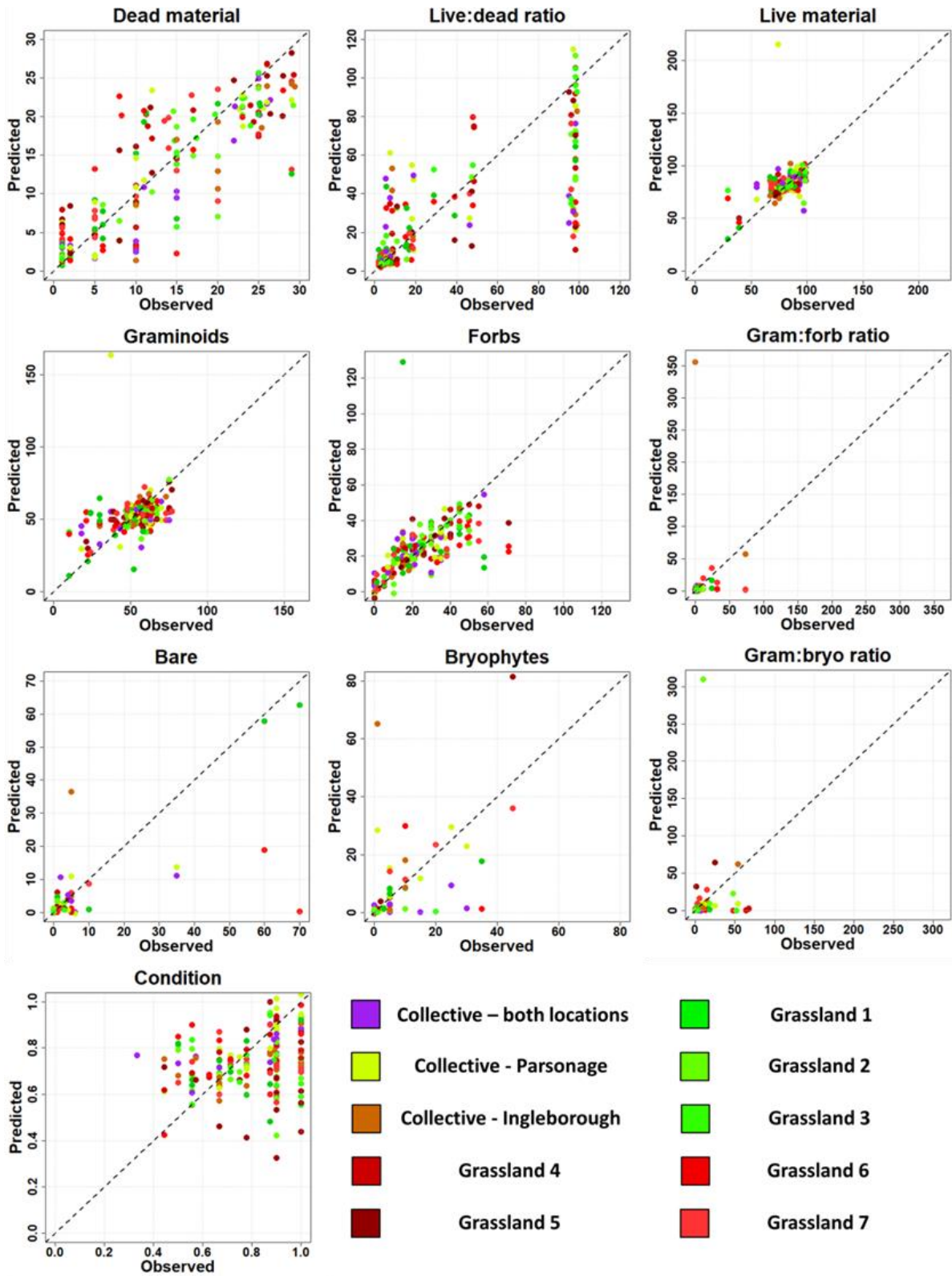
4774



4775

4776

4777



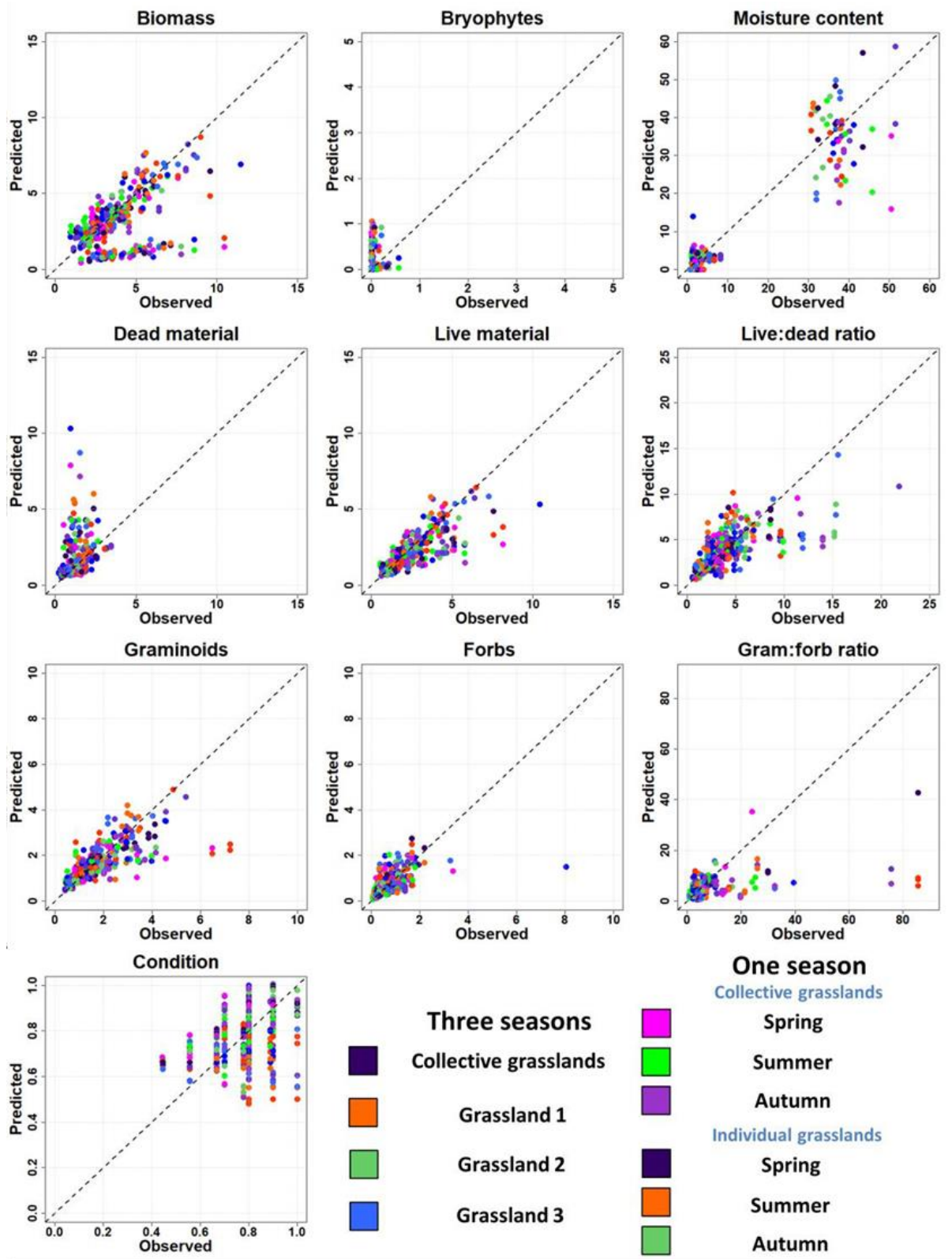
4778

4779 Appendix Figure 6: Observed and predicted values for each grassland variable and CSM-
 4780 condition where CROPSCAN spectral data were used as predictors on data collected on all
 4781 seven grasslands during the summer. The first two sets of graphs project predicted values
 4782 derived from mass data (except moisture content which is % mass) where the first set are

4783 *the results of using FULL spectral data and the second set of graphs are the result of using*
4784 *VNIR data. The next two sets of graphs are projections of predicted values derived from %*
4785 *cover data, where FULL spectral data and VNIR spectral data were used respectively.*

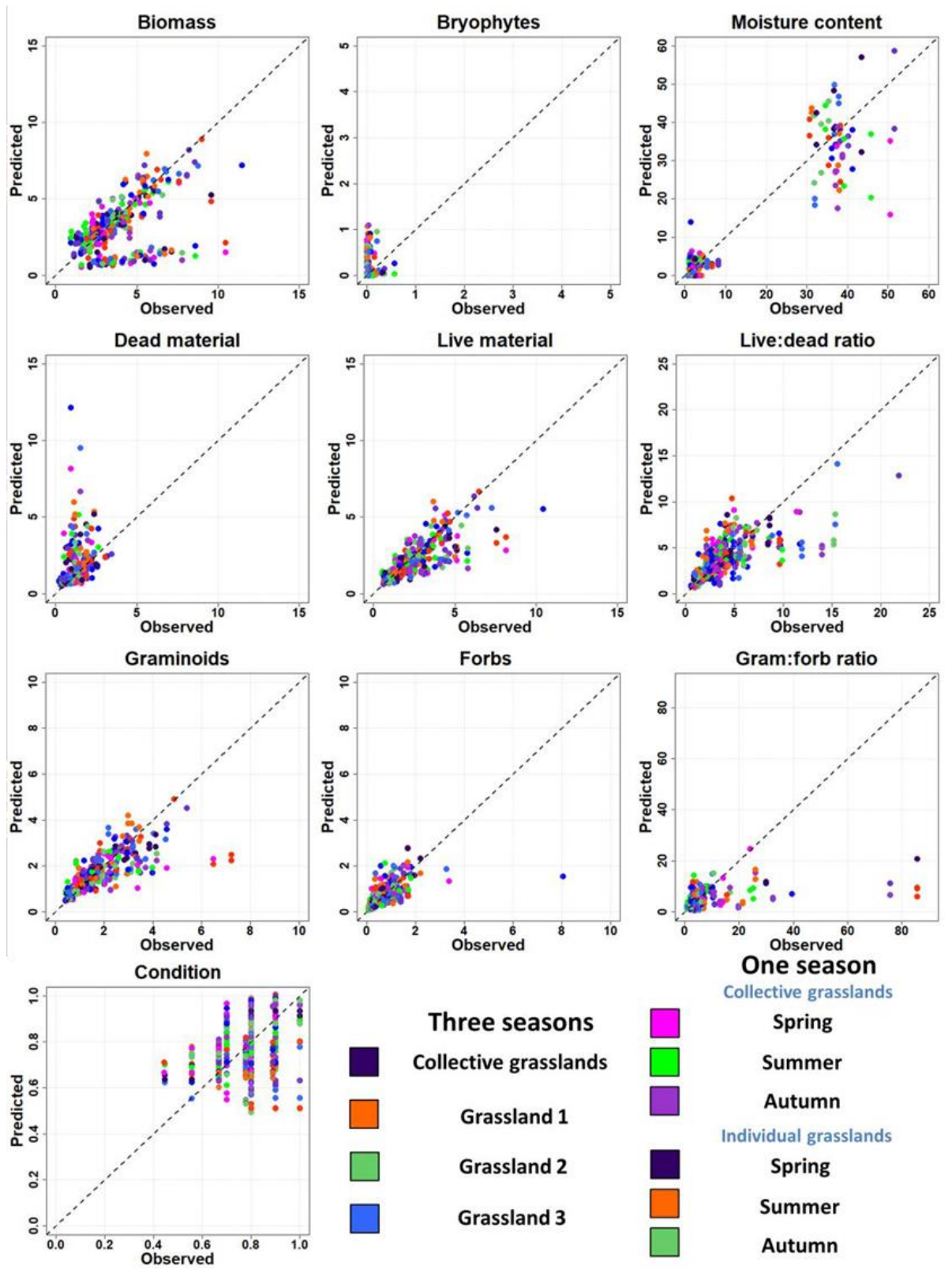
4786 **Observations vs. predictions – Chapter 5**

4787



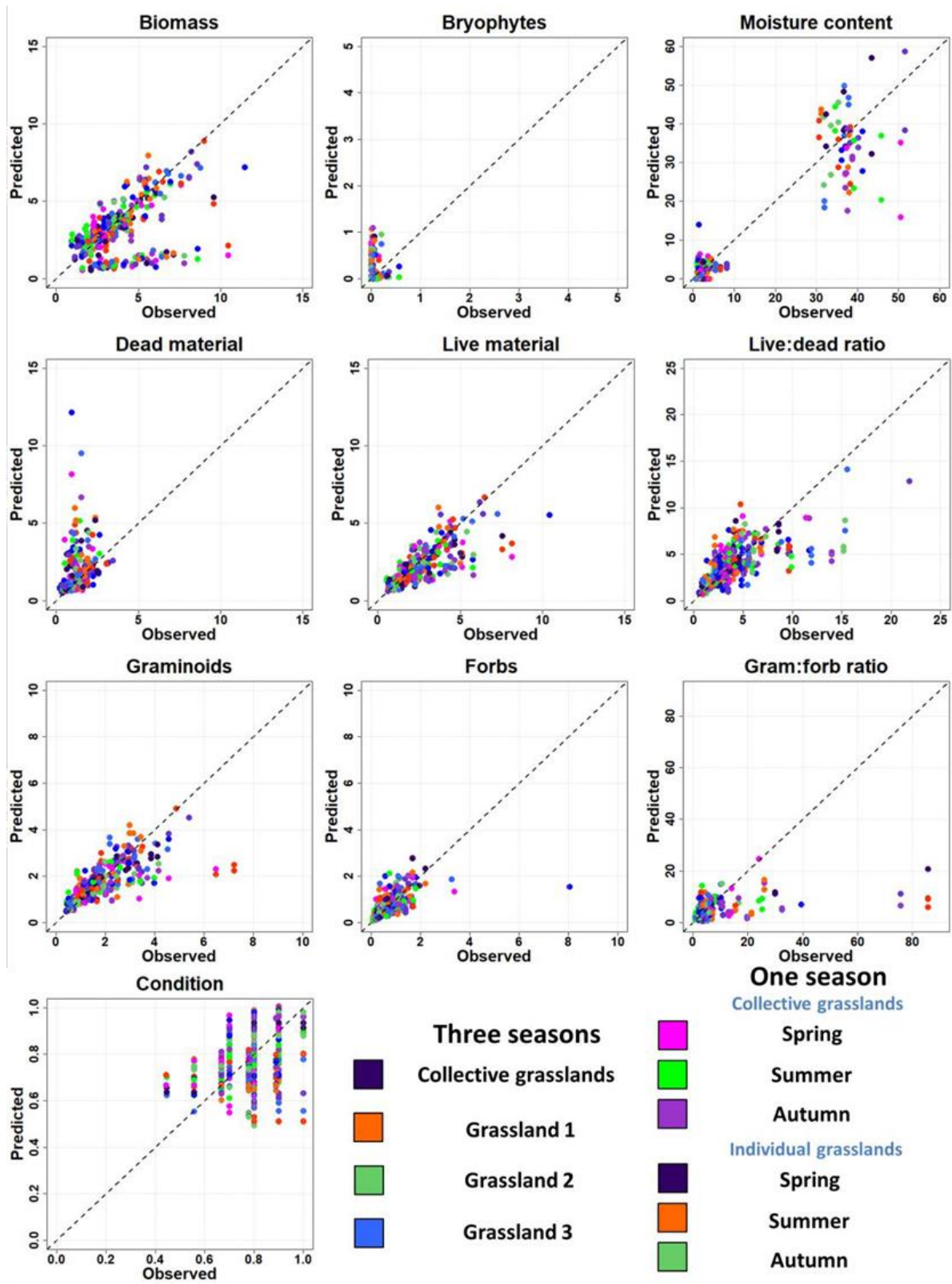
4788

4789



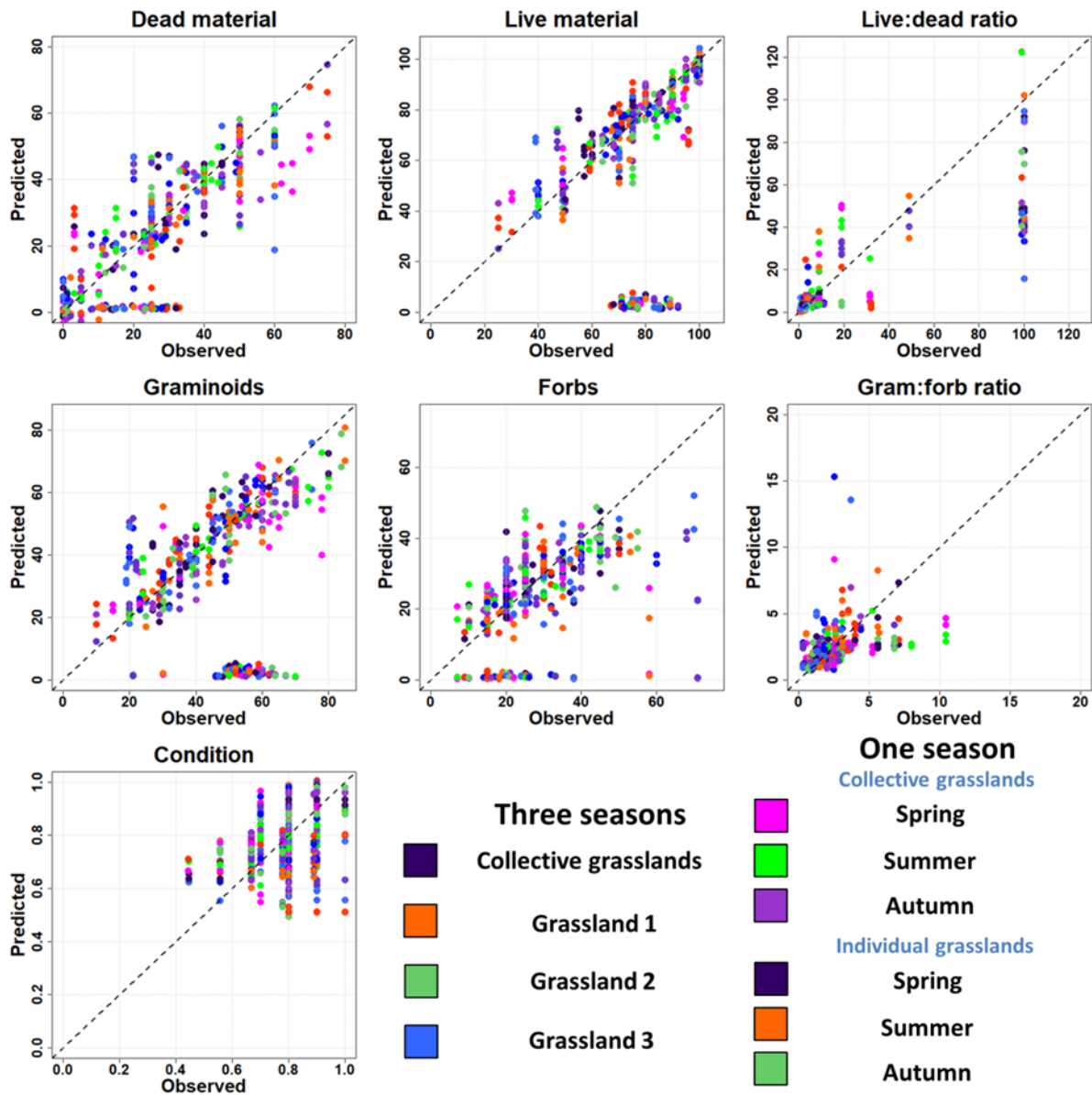
4790

4791



4792

4793

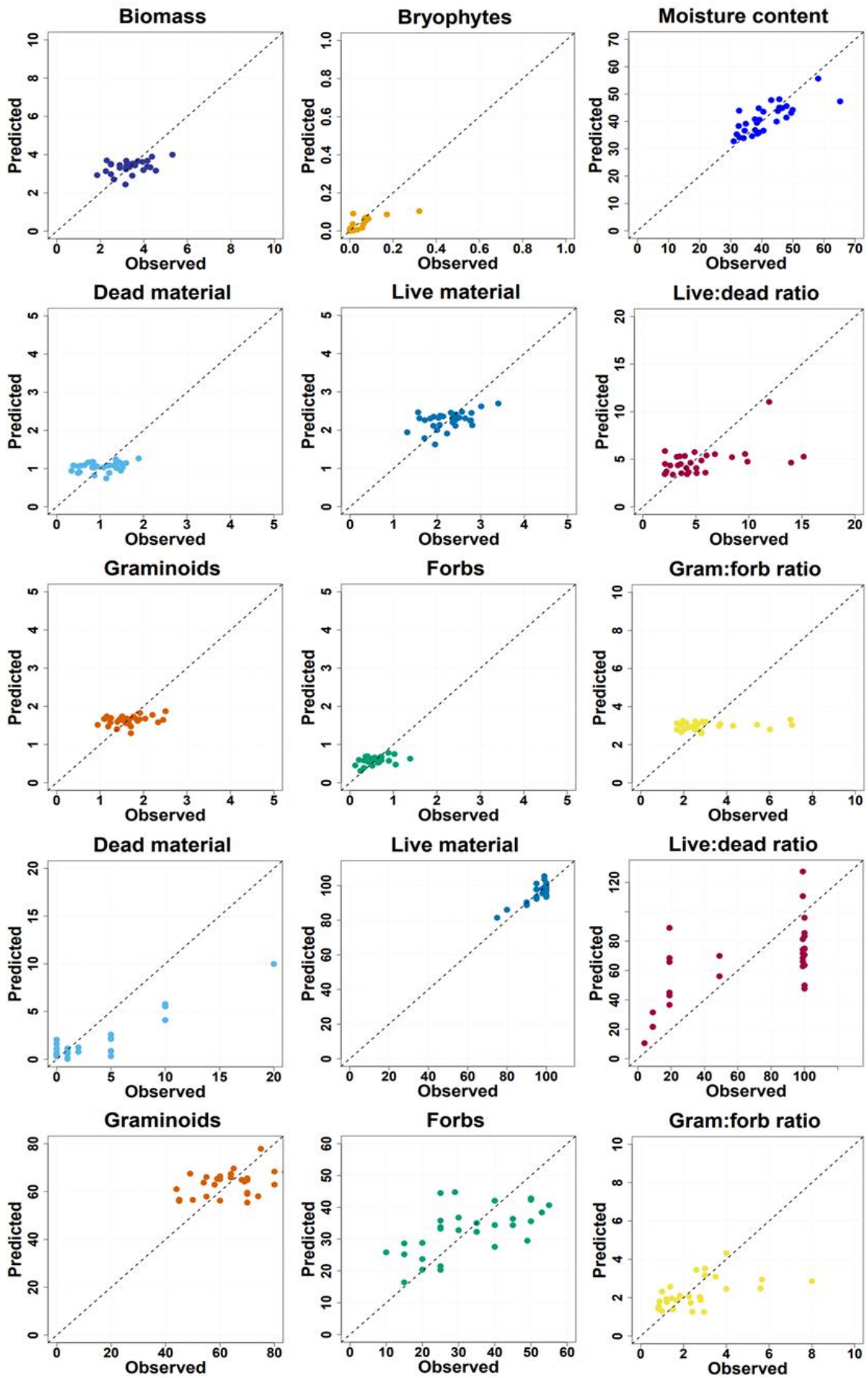


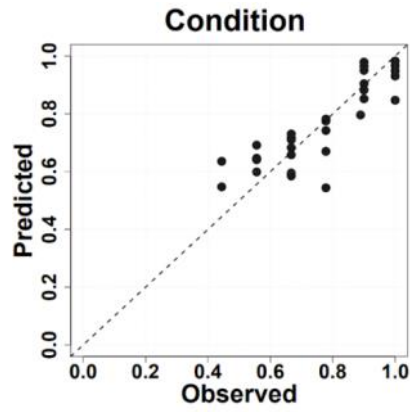
4794

4795 Appendix Figure 7: Observed and predicted values for each grassland variable and CSM-
 4796 condition where CROPSCAN spectral data were used as predictors on data collected over
 4797 three seasons on Parsonage grasslands. The first two sets of graphs project predicted
 4798 values derived from mass data (except moisture content which is % mass) where the first set
 4799 are the results of using FULL spectral data and the second set of graphs are the result of
 4800 using VNIR data. The next two sets of graphs are projections of predicted values derived
 4801 from % cover data, where FULL spectral data and VNIR spectral data were used
 4802 respectively. The data sets used include data collected on all three grasslands across three
 4803 seasons, on one grassland across three seasons, across all grasslands for one season and
 4804 on one grassland for one season.

4805 **Observations vs. predictions – Chapter 6**

4806



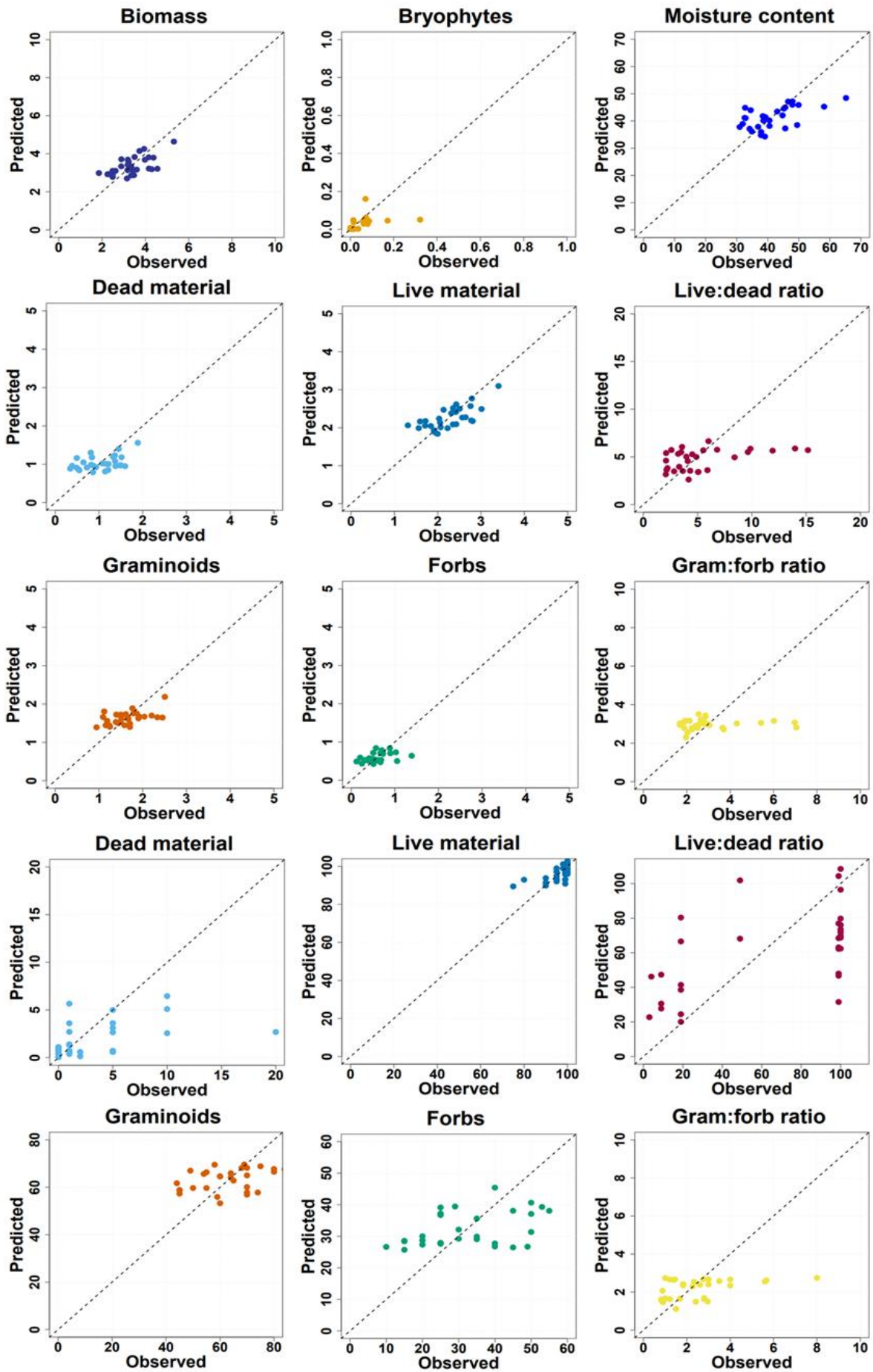


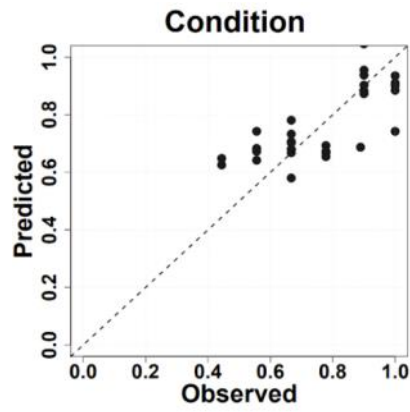
4808

4809 *Appendix Figure 7: Observed and predicted values for each grassland variable and CSM-*
 4810 *condition where CROPSCAN spectral data were used as predictors. The first three rows*
 4811 *project predicted values derived from mass data (except moisture content which is % mass)*
 4812 *and the bottom two rows project predicted values derived from % cover data.*

4813

4814





4816

4817 *Appendix Figure 8: Observed and predicted values for each grassland variable and CSM-*
 4818 *condition where Rikola spectral data were used as predictors. The first three rows project*
 4819 *predicted values derived from mass data (except moisture content which is % mass) and the*
 4820 *penultimate two rows project predicted values derived from % cover data. The bottom*
 4821 *projection shows predicted values for CSM-condition.*

4822

4823

4824

4825

4826

4827

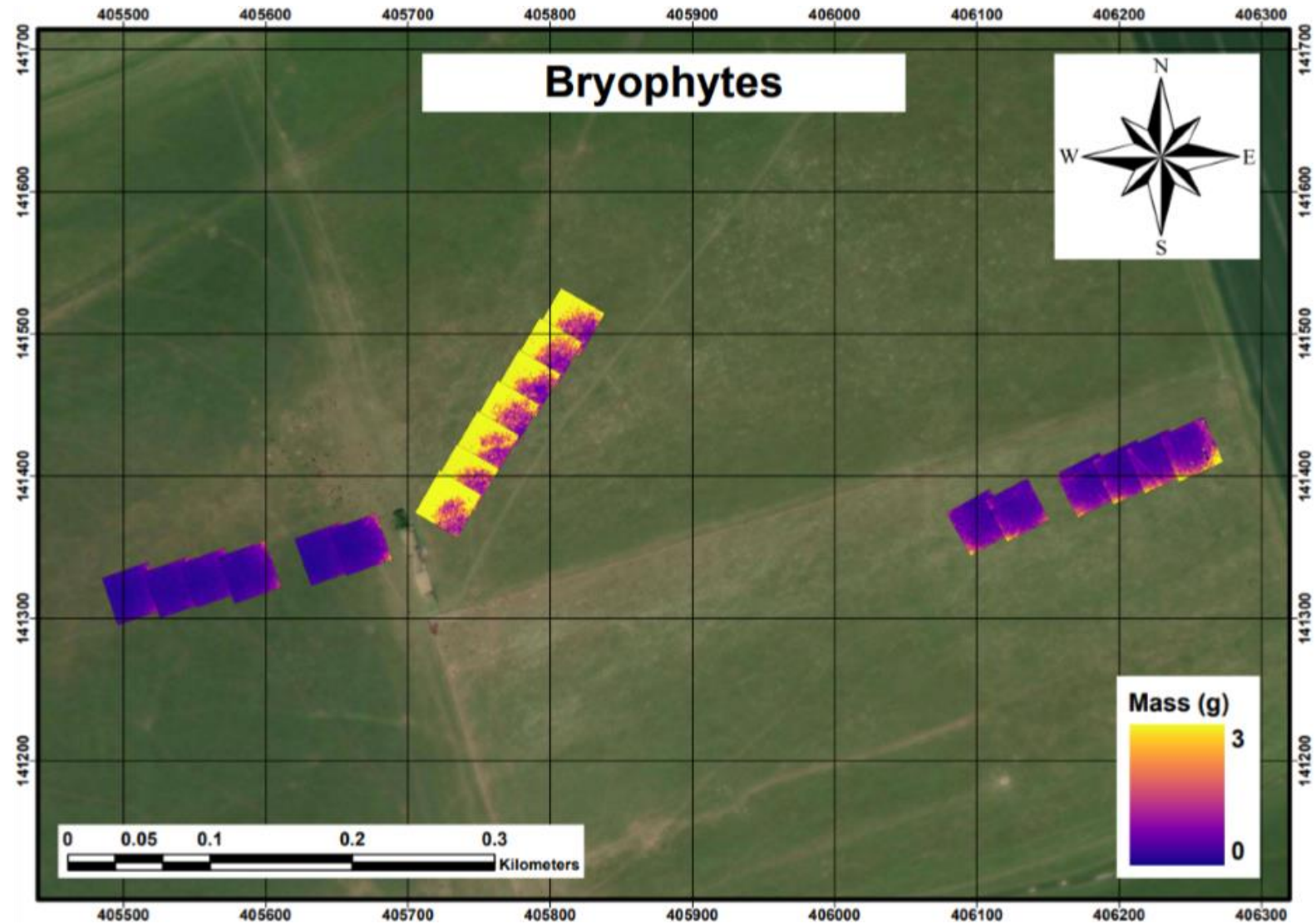
4828

4829

4830

4831 **Extrapolating predicted grassland variables and condition using Rikola data as predictors**

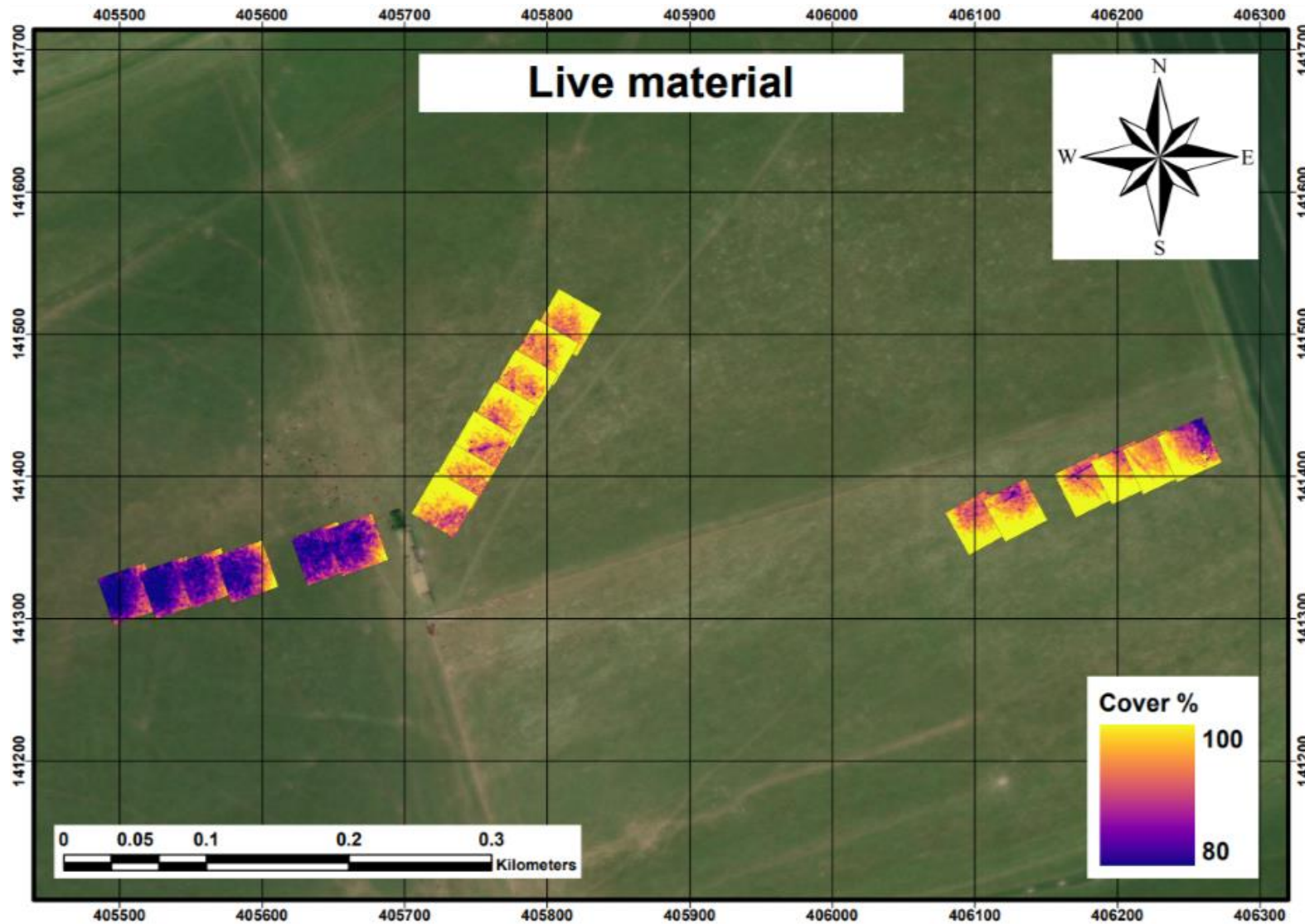
4832



4833

4834

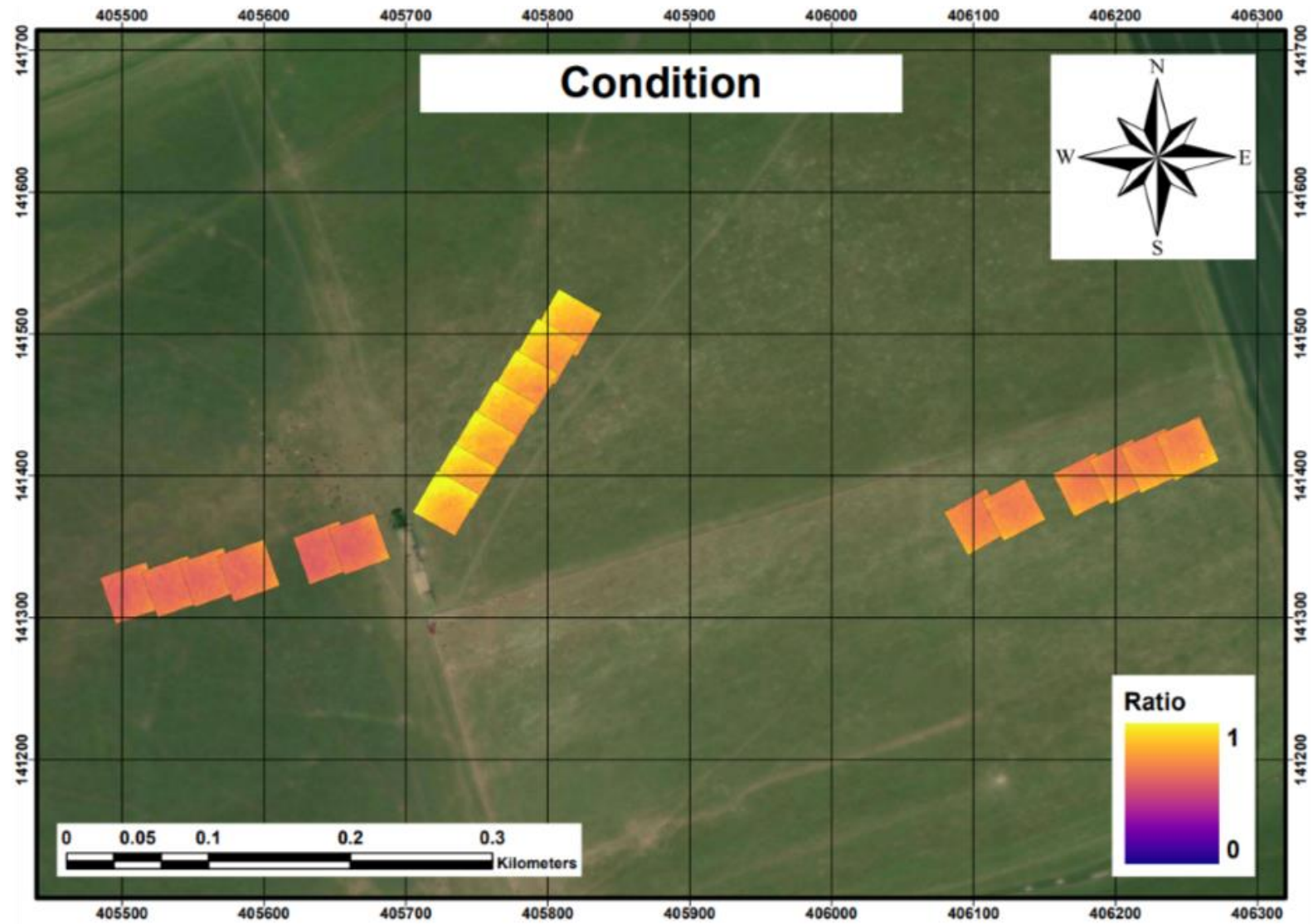
Appendix Figure 4a: Projection of predicted bryophyte mass predicted values derived from a PLSR model trained with Rikola data.



4835

4836

Appendix Figure 4b: Projection of predicted live material % cover predicted values derived from a PLSR model trained with Rikola data.



4837

4838

Appendix Figure 4c: Projection of 'condition' predicted values derived from a PLSR model trained with Rikola data.